Cherenkov and Imaging detectors for HEP and AP

ESIPAP@home - 2021

François Montanet

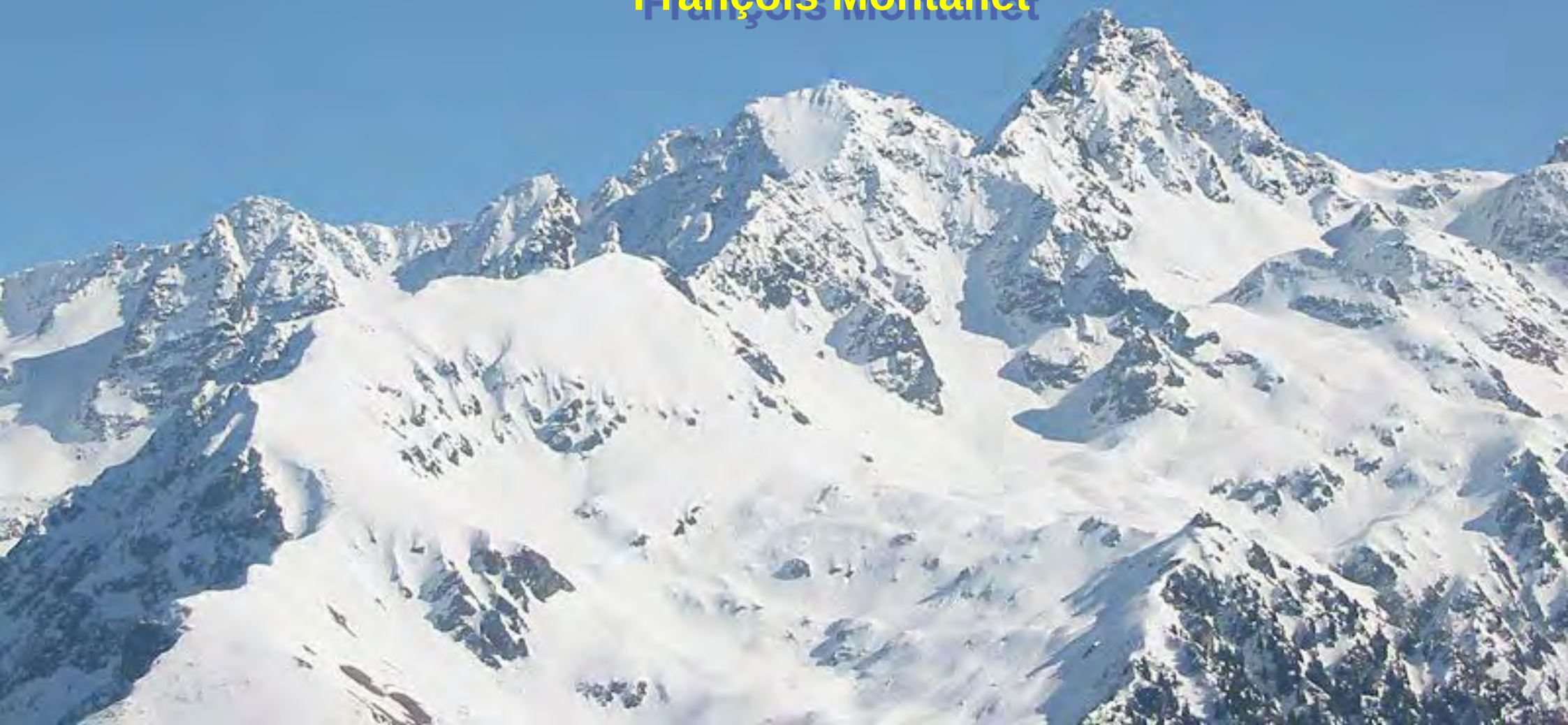

Plan of the course

- The Cherenkov effect, theory and phenomenology
- Photon detectors
- Timing and counting particles
    - The AUGER WCD as an example, plus FD
- Identifying particles
  - Threshold Cherenkov counters
    - NA9, BELLE
  - Ring Imaging Cherenkov detectors (RICH, DIRC)
    - DELPHI, LHCb, BaBar
  - Measuring charge
    - AMS, CREAM
- VHE gamma rays
    - HESS, MAGIC, CTA…
- Neutrino detectors
    - SK, Amanda, Antares, IceCube

THE CHERENKOV EFFECT

Cherenkov Radiation

Coherent emission of photons by a dielectric medium due to charged particles with velocities > local phase velocity of light in that medium.

$$\tilde{\epsilon} = \epsilon_1 + i\epsilon_2 = (n + i\kappa)^2$$

Transparent medium
=> no absorption

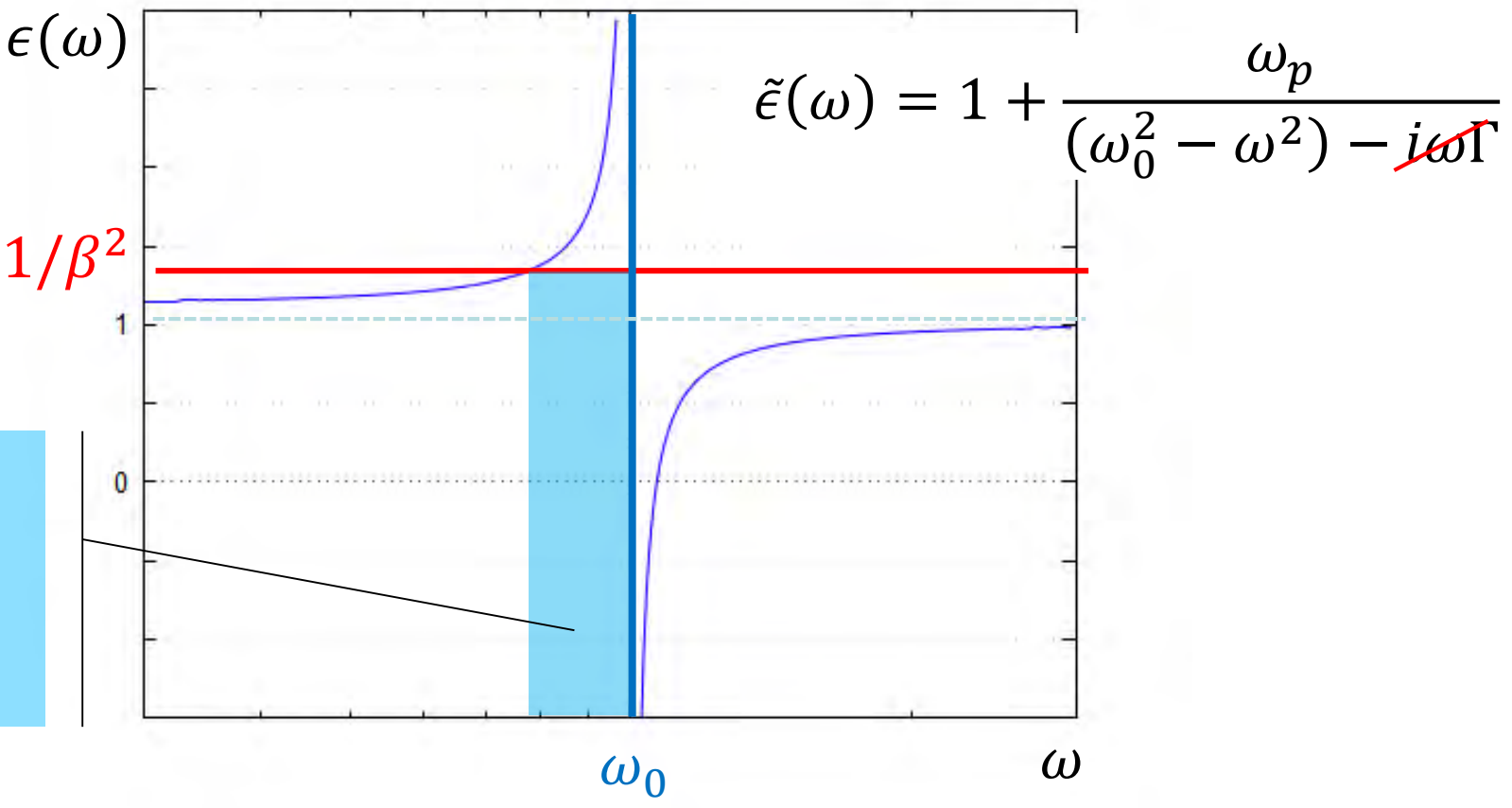

Frequency (wavelength) domain in which Cherenkov radiation occurs

Cherenkov Radiation

- Emitted on a cone whose axis is along the particle trajectory and of half opening angle θ_C such as $\cos(\theta_C) = 1/(\beta\, n)$ where β is the particle velocity/c and $n = n(\omega)$ is the frequency dependent refractive index.

- Threshold defined by the condition $\frac{1}{\beta\, n} < 1 \quad \Rightarrow \quad \beta > \frac{1}{n}$

- Emission at all frequencies with $n(\omega) > 1$ (from UV to radio), with a flat photon yield as function of $h\nu$.

- Generally detected from near UV to visible light (but not only).

$$\frac{dN^2}{dx\, d\omega} = \frac{\alpha}{c} Z^2 \sin^2\theta_C = \frac{\alpha}{c} Z^2 \left(1 - \frac{1}{\beta n}\right)$$

Cherenkov Radiation

- Allows discrimination between particles with same momentum and ≠ masses (electrons / protons / nuclei)
- Up to energies of the order of 10 GeV/nucleon if $\frac{\Delta\beta}{\beta} \approx 10^{-3}$
- Allows determining the orientation of the particle direction.
- "Ring Imaging Cherenkov" detectors or "RICH" allow a precise measurement of the velocity and charge.

RICH principle →

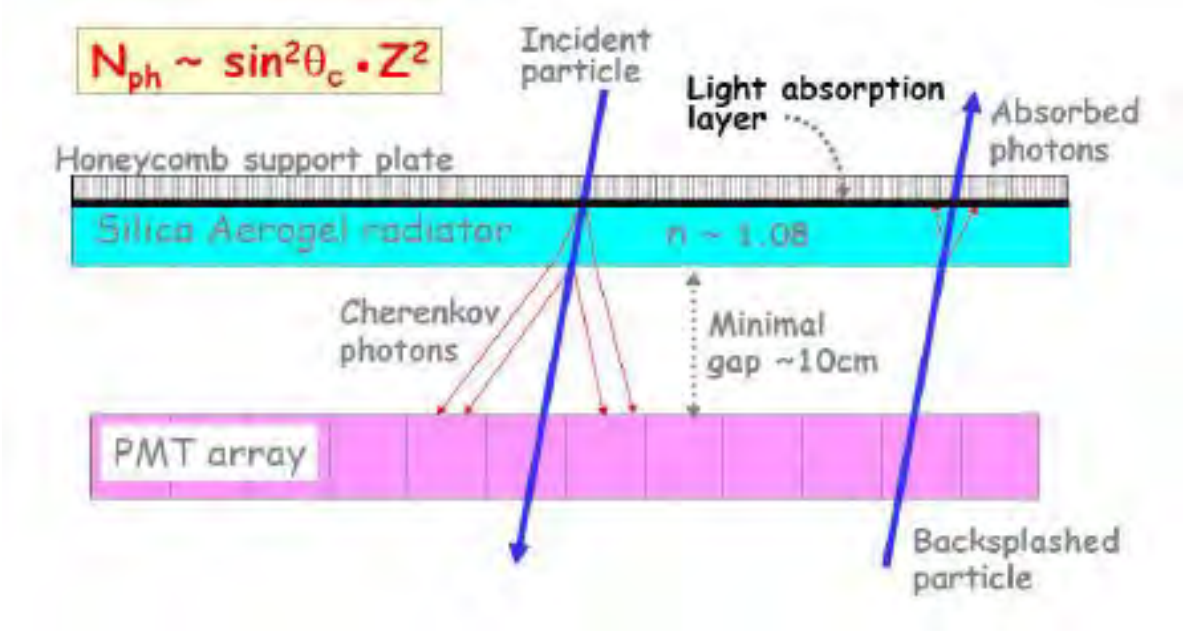

Cherenkov imaging (RICH) and charge measurement

AMS 2 Prototype

→

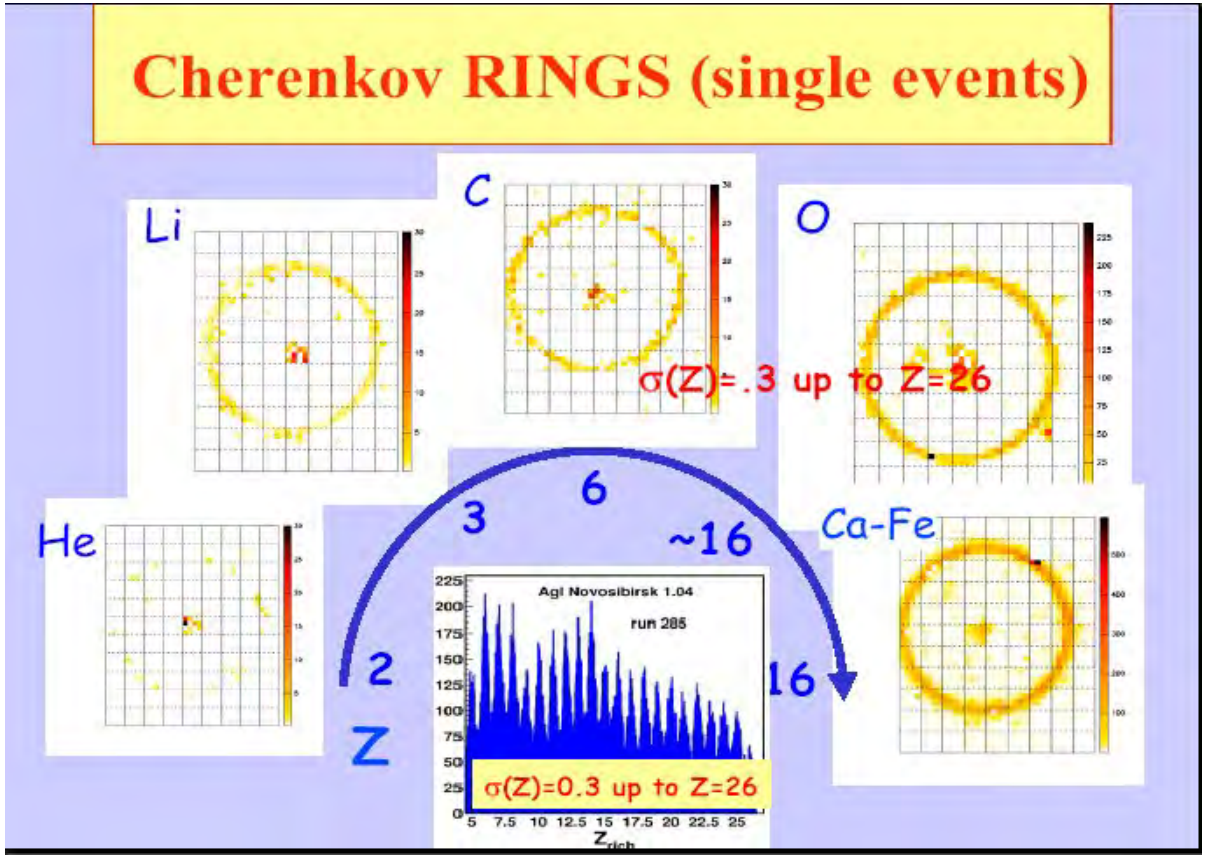

Transition radiation

- Origin: if a particle traverses the boundary between 2 ≠ dielectric media, the solution corresponding to each medium does not satisfy to the boundary condition ⇒ need for an additional "free wave".
- A dielectric medium is characterized by its "plasma" frequency ω_p (oscillation frequency of free-like electrons)

$$\omega_p = \sqrt{\frac{n_e e^2}{\varepsilon_0 m_e}} \quad \Rightarrow \quad \hbar\omega_p = 2 E_R \sqrt{4 \pi n_e a_B^3} \approx 20 \text{ eV}$$

where n_e = electron density

E_R = Rydberg energy = 13.6 eV ;

a_B = Bohr radius = 0.529×10^{-8}cm

- Roughly half of the energy is emitted in the frequency domain

$$0.1 \gamma \omega_p < \omega < \gamma \omega_p$$

- For a Lorentz factor $\gamma \approx 1000$, this is the X-ray domain (2 to 20 keV)
- Energy emitted by the interface is $I = \alpha Z^2 \gamma \hbar \frac{\omega_p}{3}$

Transition radiation (cont)

- Angular distribution peaked at small angles around particle direction:

$$\theta \approx 1/\gamma$$

- Small yield of X-photons per interface : $N \approx \alpha Z^2 \approx 10^{-2} Z^2$

  → multiply the number of interfaces

  → stack plastic sheets or fibers

- X-ray detection by photo-electric effect: proportional tubes

- Discriminates between particles with same energy and ≠ masses at high energies (100 GeV to 1 TeV) (instrumental detection threshold for X-rays).

- Can measure the Lorentz factor γ up to 10^5; In this case, choose material adequately to have a progressive threshold.

Comptes Rendus (Doklady) de l'Académie des Sciences de l'URSS
1937. Volume XIV, № 3

PHYSICS

COHERENT VISIBLE RADIATION OF FAST ELECTRONS PASSING THROUGH MATTER

By I. FRANK and Ig. TAMM, Corresponding Member of the Academy

In 1934 P. A. Čerenkov has discovered a peculiar phenomenon, which he has since investigated in detail (1). All liquids and solids if bombarded by fast electrons, such as β-electrons or Compton electrons produced by γ-rays, do emit a peculiar visible radiation, quite different from the eventual ordinary flourescence. This radiation is partially polarized, the electric oscillation vector being parallel to the electron beam, and its intensity can be reduced neither by temperature nor by addition to the liquid bombarded of quenching substances. The peculiarity of these characteristics was scrutinized by Wawilow (2) who suggested that this radiation must be connected with the «Bremsung» of fast electrons. Since then a new and undoubtedly the most peculiar characteristic of the phenomenon was discovered, namely, its highly pronounced asymmetry, the intensity of light emitted in the direction of the motion of electrons being many times larger than in the backward direction. It follows that the substance bombarded radiates coherently for the space of at least one wavelength of the visible light.

This peculiar radiation can evidently not be explained by any common mechanism such as the interaction of the fast electron with individual atom or as radiative scattering of electrons on atomic nuclei* On the other hand, the phenomenon can be explained both qualitatively and quantitatively if one takes in account the fact that an electron moving in a medium does radiate light even if it is moving uniformly provided that its velocity is greater than the velocity of light in the medium.

We shall consider an electron moving with constant velocity v along the z axis through a medium characterized by its index of refraction n. The field of the electron may be considered as the result of superposition of spherical waves of retarded potential, which are being continually emitted by the moving electron and are propagated with the velocity $\frac{c}{n}$. It is easy to see that all these consecutive waves emitted

* The intensity of visible light emitted by the last named process is about 10^4 times smaller than the intensity observed.

The Nobel Prize in Physics 1958
Pavel A. Cherenkov, Il´ja M. Frank, Igor Y. Tamm

The Nobel Prize in Physics 1958

Pavel Alekseyevich Cherenkov

Il´ja Mikhailovich Frank

Igor Yevgenyevich Tamm

The Nobel Prize in Physics 1958 was awarded jointly to Pavel Alekseyevich Cherenkov, Il´ja Mikhailovich Frank and Igor Yevgenyevich Tamm *"for the discovery and the interpretation of the Cherenkov effect"*.

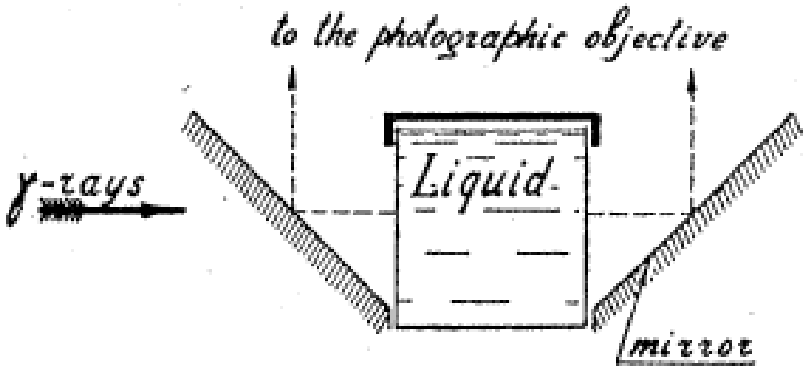

FIG. 1. Arrangement of apparatus.

All the results obtained are in good agreement with I. M. Frank and I. E. Tamm's theory of the coherent radiation of electrons moving in a medium.[6]

P. A. ČERENKOV

The Physical Institute of the Academy of Sciences of U.S.S.R.,
Moscow,
June 15, 1937.

[1] Čerenkov, C. R. Ac. Sci. U.S.S.R. **8**, 451 (1934).
[2] Čerenkov, C. R. Ac. Sci. U.S.S.R. **12** (3), 413 (1936).
[3] Čerenkov, C. R. Ac. Sci. U.S.S.R. **14**, 102 (1937).
[4] Čerenkov, C. R. Ac. Sci. U.S.S.R. **14**, 105 (1937).
[5] Wawilow, C. R. Ac. Sci. U.S.S.R. **8**, 457 (1934).
[6] Frank and Tamm, C. R. Ac. Sci. U.S.S.R. **14**, 109 (1937).
[7] Bull. Ac. Sci. U.S.S.R. No. 7, 919 (1933).
[8] E. Brumberg and S. Wawilow, C. R. Ac. Sci. U.S.S.R. **3**, 405 (1934)

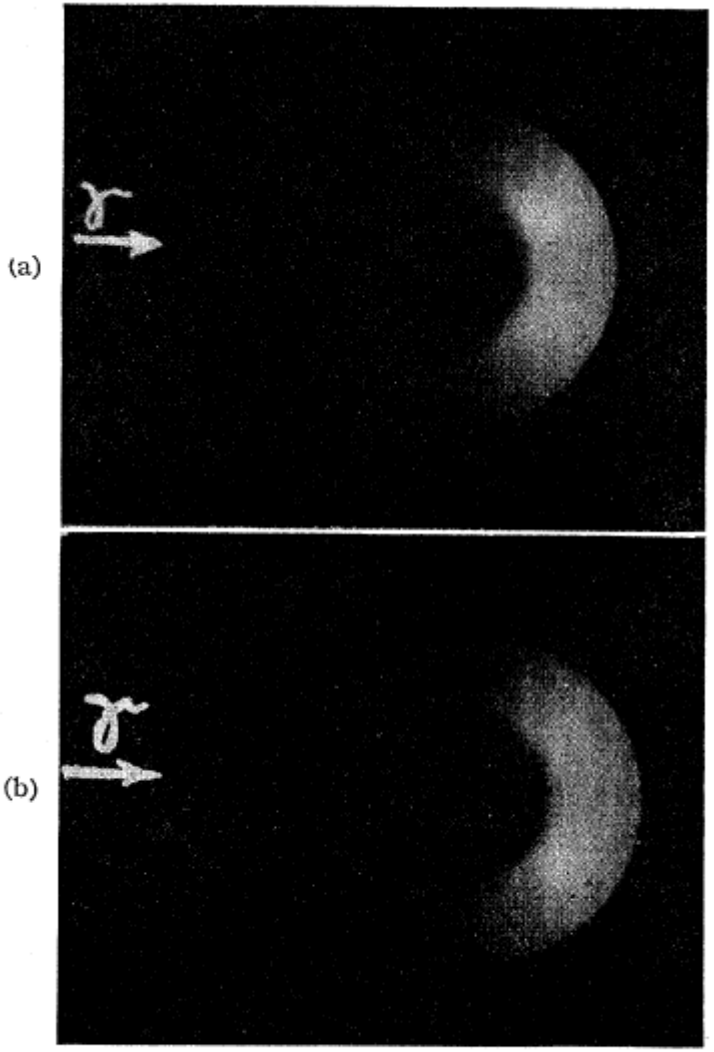

FIG. 2. Photographs showing asymmetry of luminescence. (a) water. $n = 1.337$; (b) benzene, $n = 1.513$.

P.A. Čerenkov Letter to the editor Phys.Rev 53 (1937) 378

Theory of the Cherenkov effect

- Dielectric medium electrons polarized by a moving charged particle.

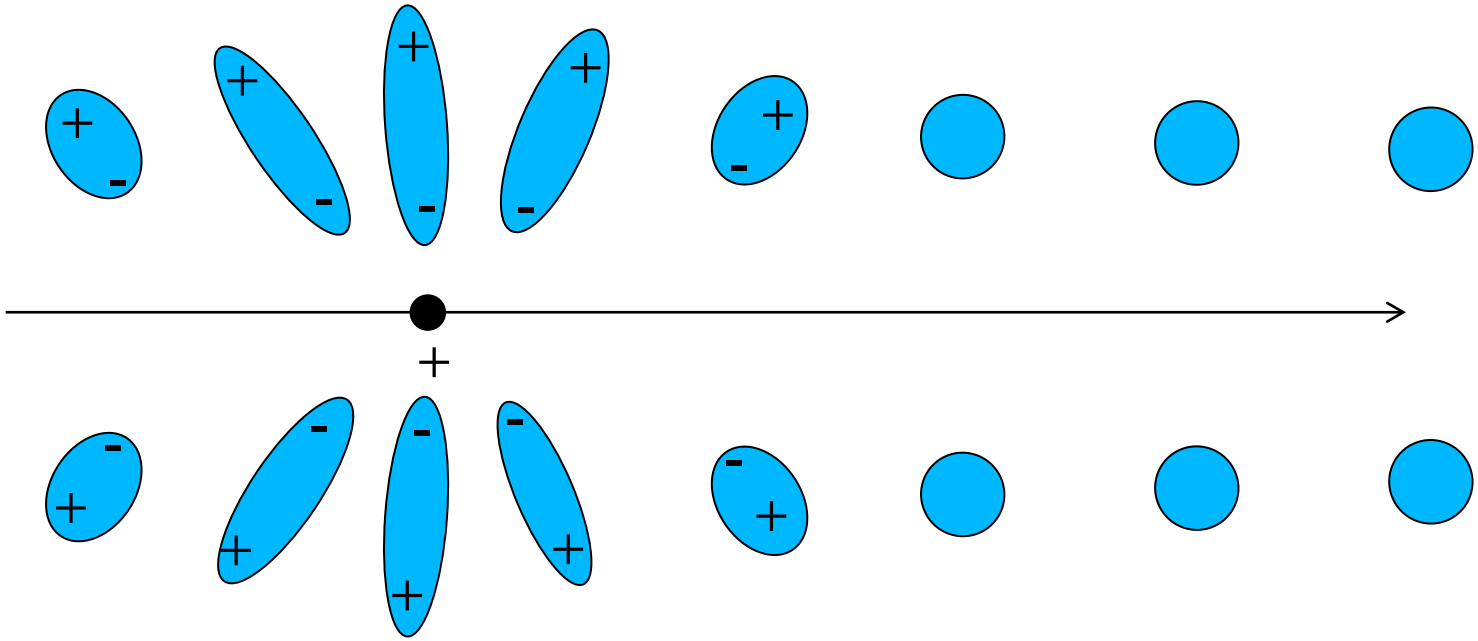

- De-exitation gives rise to a coherent radiation.
- Same basic process as energy loss (Bethe, Fermi).

The Cherenkov effect

- When a charged particle moves faster than the phase speed of light in a medium, electrons interacting with the particle can emit coherent photons while conserving energy and momentum.

- This process can be viewed as a decay.

- It is actually not the particle that emits light, but the bound electrons of the immediately surrounding (dielectric) medium.

- Emission is coherent because in phase with the particle velocity.

- Pavel A. Čerenkov and Vavilov discovered the radiation in 1934,
  Igor Tamm and Ilya Frank explained it in 1937.

Ref :
P.A. Čerenkov Letter to the editor Phys.Rev 53 (1937) 378
Frank and Tamm, C.R.Ac.Sci. U.S.S.R. 14, 109 (1937)

The theory of the Cherenkov effect

Igor Tamm and Ilya Frank

The energy emitted per unit length dx travelled by the particle per unit of angular frequency $d\omega$ is:

$$dE = \frac{q^2}{4\pi}\,\mu(\omega)\,\omega\left(1 - \frac{c^2}{v^2 n^2(\omega)}\right) dx\, d\omega$$

provided that $\beta = \frac{v}{c} > \frac{1}{n(\omega)}$

Here $\mu(\omega)$ and $n(\omega)$ are the frequency-dependent permeability and index of refraction of the medium, q is the electric charge of the particle, v is the speed of the particle, and c is the speed of light in vacuum.

Consequences:

- the **yield** of photons is **flat** versus these photons energy ($h\nu$).
- the **yield** of photons is $\propto \boldsymbol{\lambda^{-2}} \Rightarrow$ prominent at small wavelengths (UV)
- the spectrum is continuous ≠ fluorescence

The Cherenkov effect

Igor Tamm and Ilya Frank

The total amount of energy radiated per unit length is:

$$\frac{dE}{dx} = \frac{q^2}{4\pi} \int_{v>\frac{c}{n(\omega)}} \mu(\omega)\omega \left(1 - \frac{c^2}{v^2 n^2(\omega)}\right) d\omega$$

This integral is done over the frequencies ω for which the particle's velocity v is greater than speed of light in the medium $c/n(\omega)$. This integral is non-divergent because at high frequencies the refractive index becomes less than unity.

$$\frac{dE}{dx} = \frac{q^2}{4\pi} \int_{\beta n(\omega)>1} \mu(\omega)\, \omega \left(1 - \frac{1}{\beta^2 n^2(\omega)}\right) d\omega$$

Cherenkov Radiation

Coherent emission of photons by a dielectric medium due to charged particles with velocities > local phase velocity of light in that medium.

$$\tilde{\epsilon} = \epsilon_1 + i\epsilon_2 = (n + i\kappa)^2$$

Transparent medium
=> no absorption

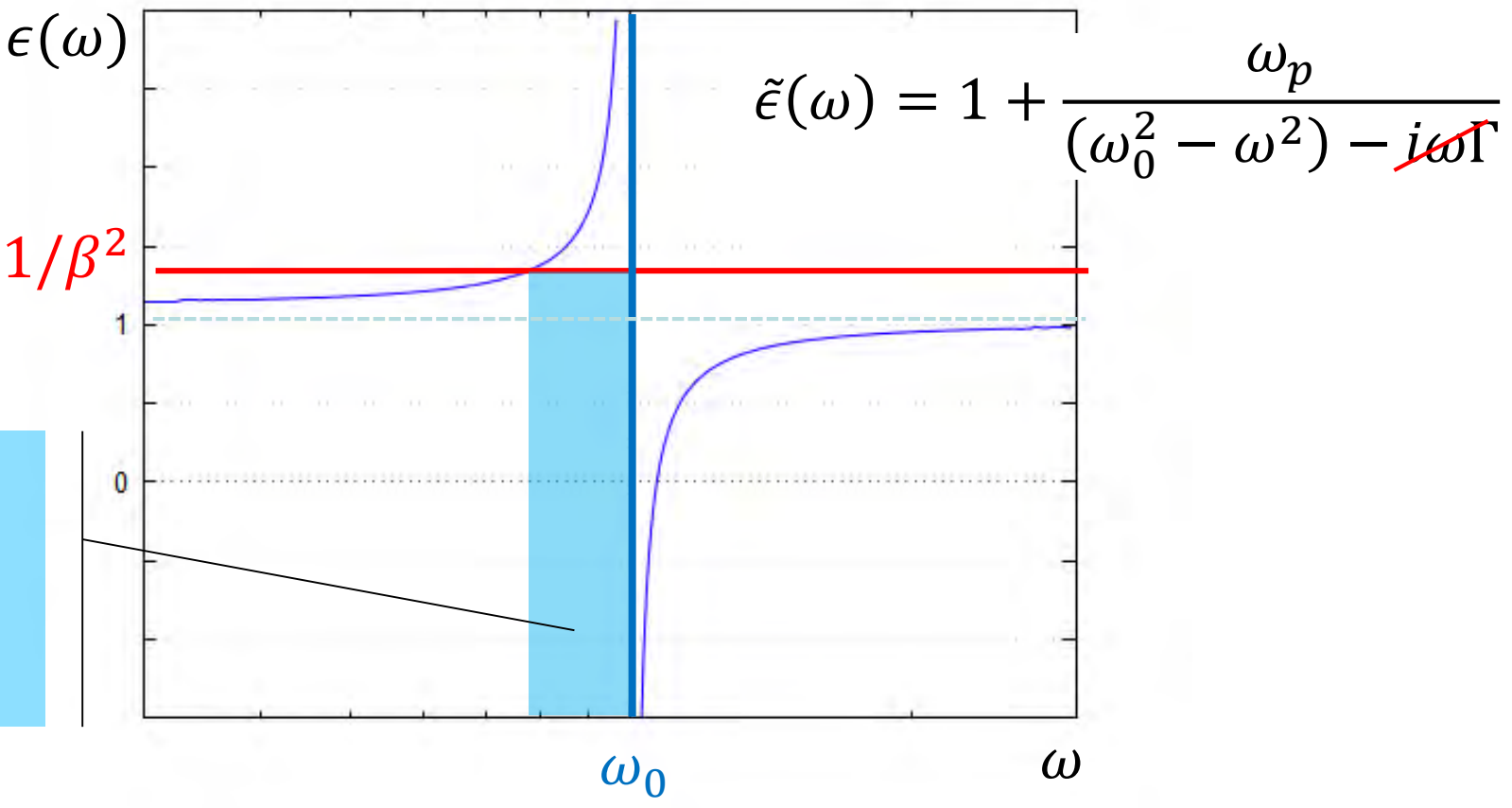

Frequency (wavelength) domaine in which Cherenkov radiation occurs

The Cherenkov effect

- Cerenkov radiation consist of a shock wave
- Similar to Doppler effect or Mach shock waves

The Cherenkov effect

- Cerenkov radiation consist of a shock wave
- Similar to Doppler effect or Mach shock waves

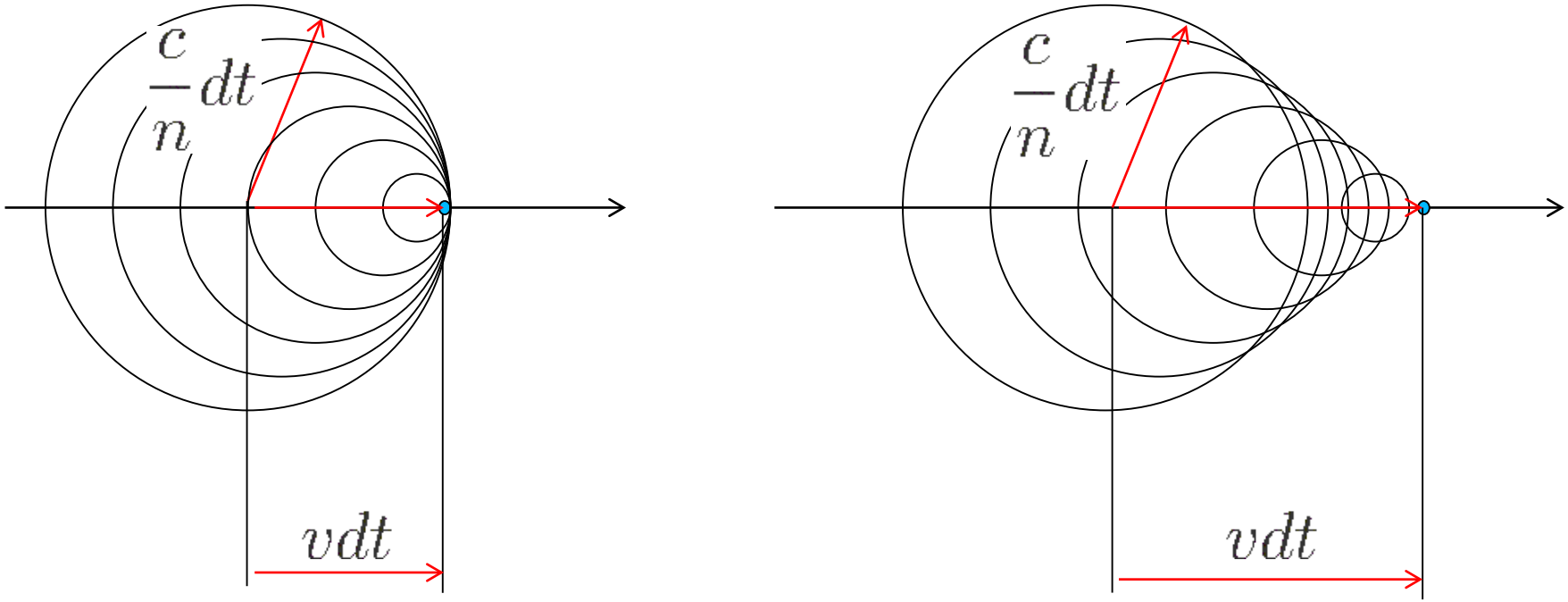

The Cherenkov effect

- Cerenkov radiation consist of a shock wave
- Similar to Doppler effect or Mach shock waves

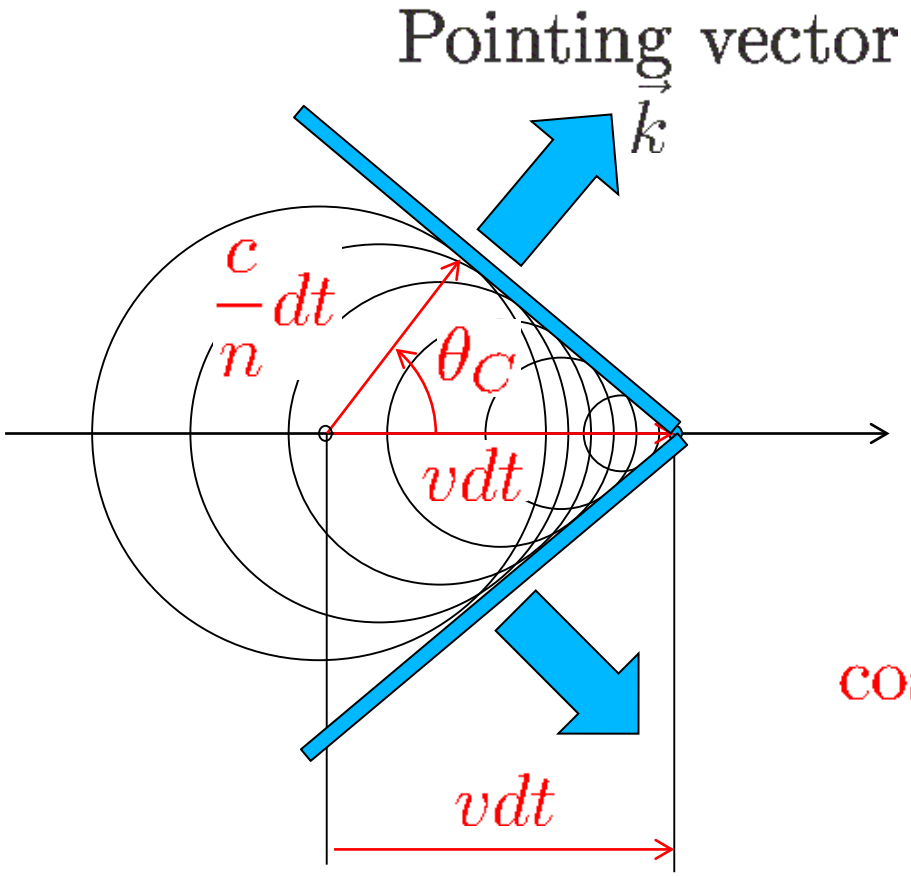

$$\cos\theta_C = \frac{c}{nv} = \frac{1}{n\beta}$$

Cherenkov effect

Relevant formulae:

The emission angle wrt particle direction

$$\theta_C = \mathrm{acos}\left(\frac{1}{n\,\beta}\right)$$

if $n\beta > 1$.

The threshold velocity:

$$\beta_{th} = \frac{1}{n}$$

thus the threshold momentum:

$$p_{th} = m\beta_{th}\gamma_{th} = \frac{m}{\sqrt{n^2-1}} \approx \frac{m}{\sqrt{2\delta}}$$

with $\delta = n - 1 \ll 1$

Cherenkov effect

Relevant formulae (cont):

The number of photons produced per unit length and unit of photon energy by a particle with charge Ze:

$$\frac{d^2N}{dEdx} = \frac{\alpha Z^2}{\hbar c}\left(1 - \frac{1}{\beta^2 n^2(E)}\right)$$
$$= \frac{\alpha Z^2}{\hbar c}\sin^2\theta_C$$
$$= 370\, Z^2 \sin^2\theta_C \ \text{eV}^{-1}\text{cm}^{-1}$$

or equivalently:

$$\frac{d^2N}{d\lambda dx} = \frac{2\pi\alpha Z^2}{\lambda^2}\sin^2\theta_C \approx 4.59\times 10^5\, Z^2 \ \sin^2\theta_C \ \ \text{nm}^{-1}\text{cm}^{-1}$$

Cherenkov effect

Photon yield for 1 cm of water ($n = 1.33$) and 1 eV spectral band.

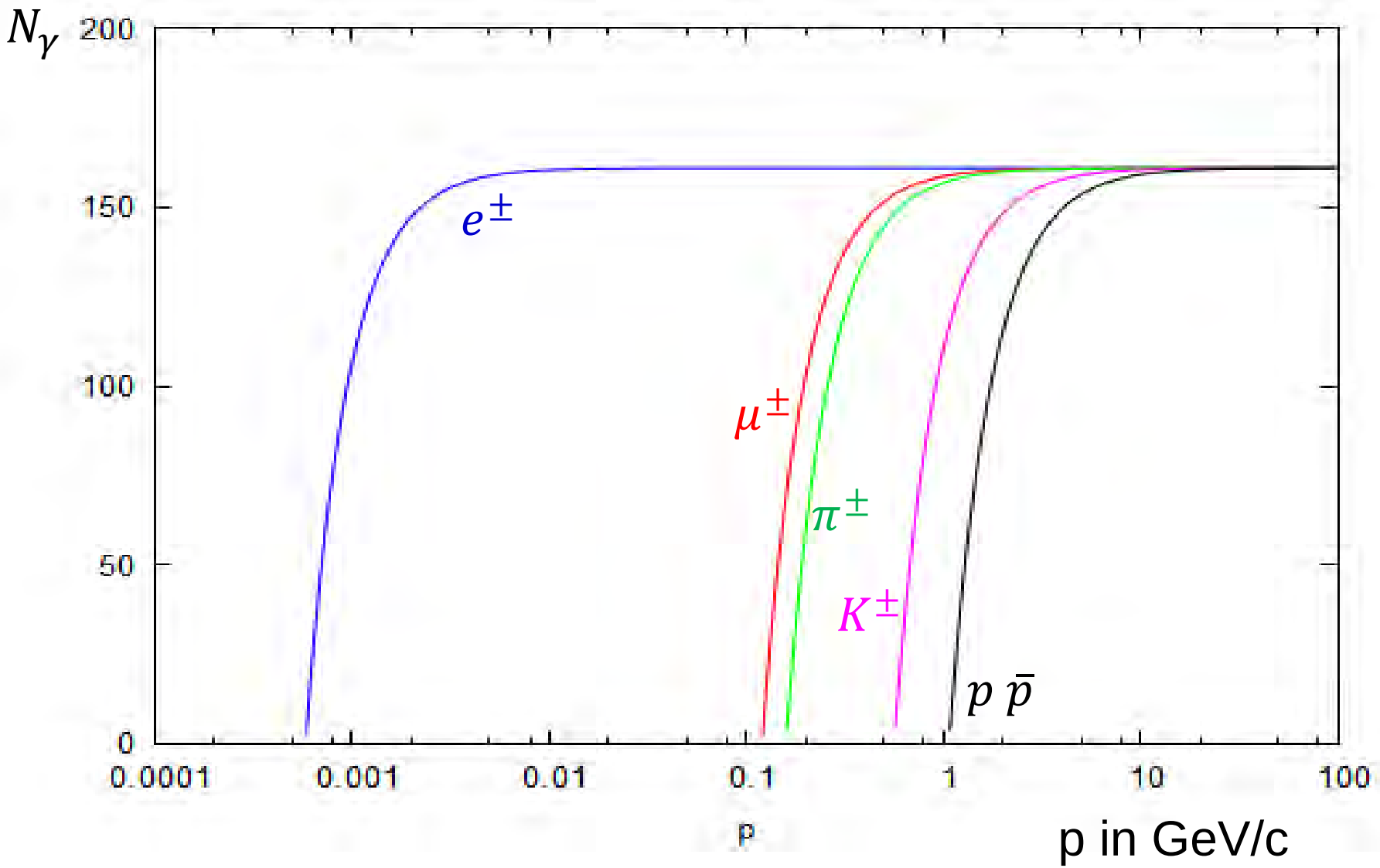

Dispersion in dielectrics

- Dielectric constant and index of refraction depending on light frequency or wavelength
  $\Rightarrow$ phase velocity and group velocity

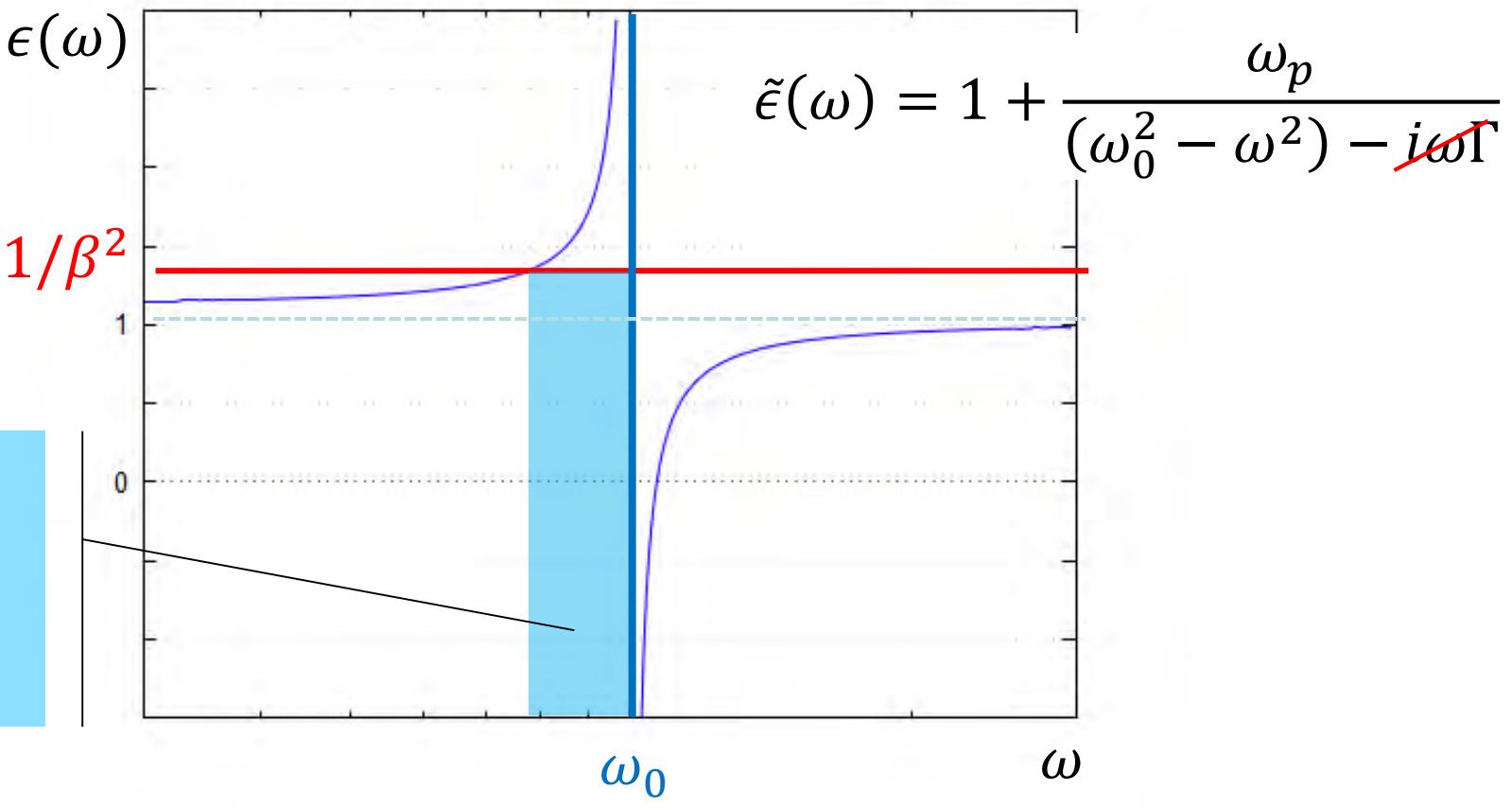

Frequency (wavelength) domaine in which Cherenkov radiation occurs

Cherenkov effect

- Dispersive material:

Indeed important for the precise timing on long distances such as in neutrino telescopes.

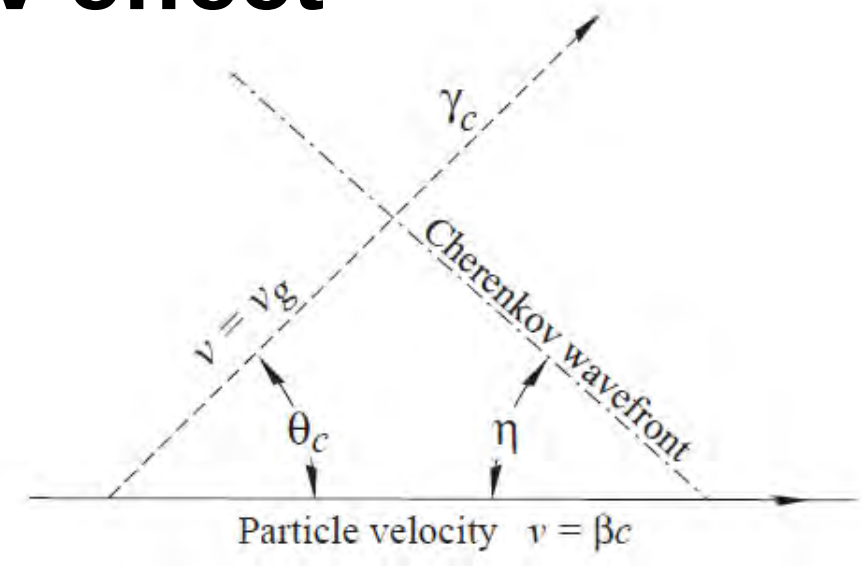

In dispersive media (where $dn/d\omega \neq 0$) one has to take into account the fact that photons propagate with the **group** velocity. Tamm showed that in that case $\theta_C + \eta \neq 90°$ with η the cone $1/2$ opening angle given by:

$$\begin{aligned} \cot\eta &= \left[\frac{d}{d\omega}(\omega \tan\theta_C)\right]_{\omega_0} \\ &= \left[\tan\theta_C + \beta^2 \omega n(\omega)\frac{dn}{d\omega}\cot\theta_C\right]_{\omega_0} \end{aligned}$$

Radiators, filling the gap between gases and liquids

- Matching refractive index to the momentum range.

Medium	$n-1$	γ_{th}	θ_C	Photons/m
He (stp)	$3.5 \cdot 10^{-5}$	120	0.48°	3
CO_2 (stp)	$4.1 \cdot 10^{-4}$	35	1.64°	40
Silica aerogel	$0.025 - 0.075$	$4.6 - 2.7$	$12.7 - 21.5°$	$2400 - 6600$
Water	0.33	1.52	41.2°	$2.1 \cdot 10^4$
Glass	$0.46 - 0.75$	$1.37 - 1.22$	$46.8 - 55.1°$	$2.6 - 3.3 \cdot 10^4$

Silica aerogel:
SiO_2 "foam" with
nano-size structure $< \lambda$

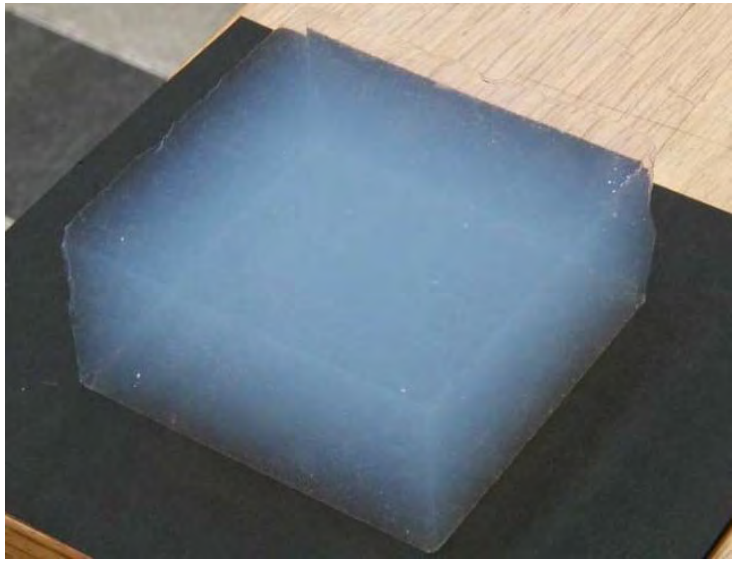

Cherenkov angle vs mass and momentum

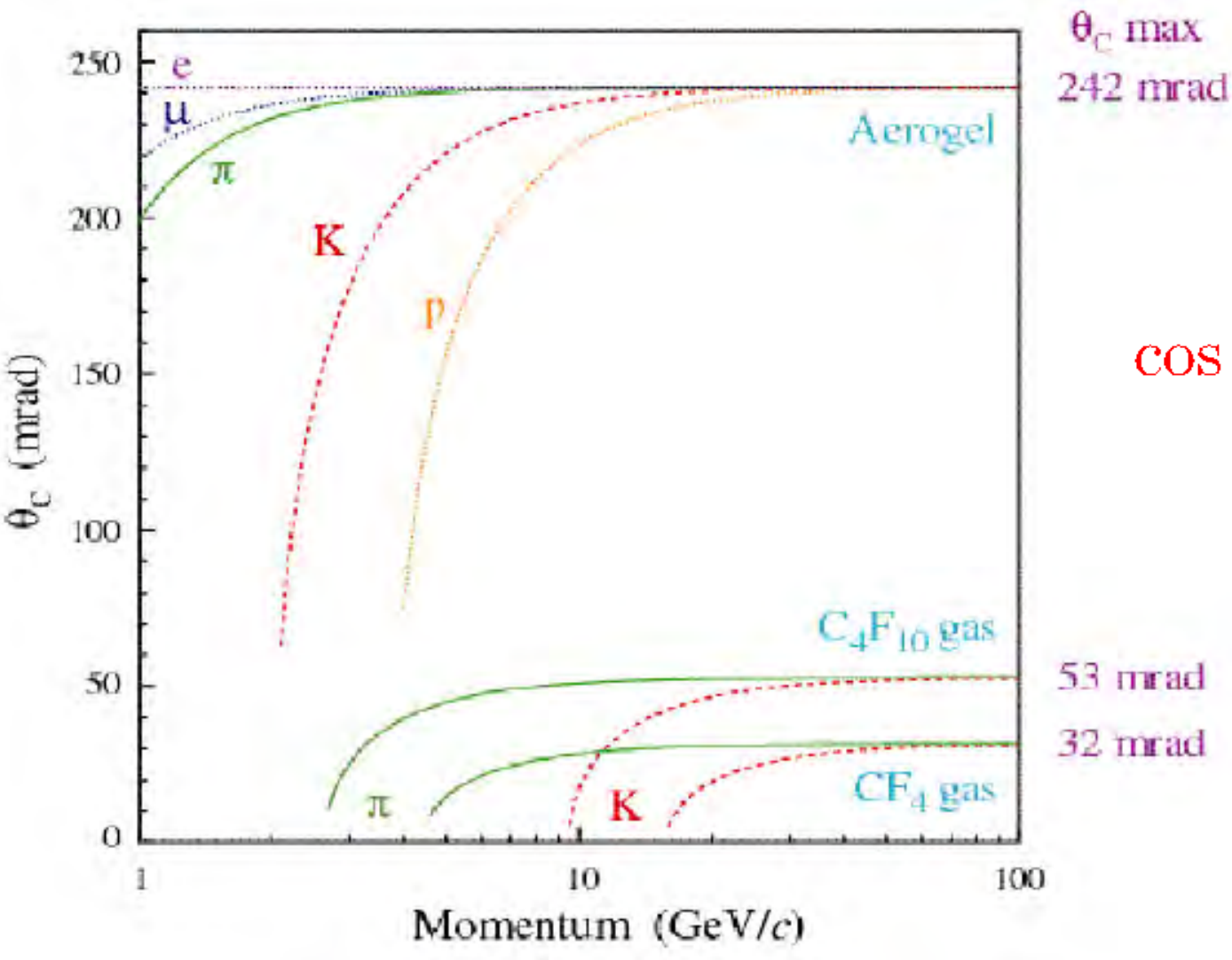

$$\cos\theta_C = \frac{c}{nv} = \frac{1}{n\beta}$$

Cherenkov not only optical

- Radio-wave Cherenkov emission (also called Askarian effect) by EM showers in dense dielectric materials (ice, salt, sand, lunar regolith …)
- Coherent Cherenkov like emission for $\lambda \gg$ shower size $\approx X_0$

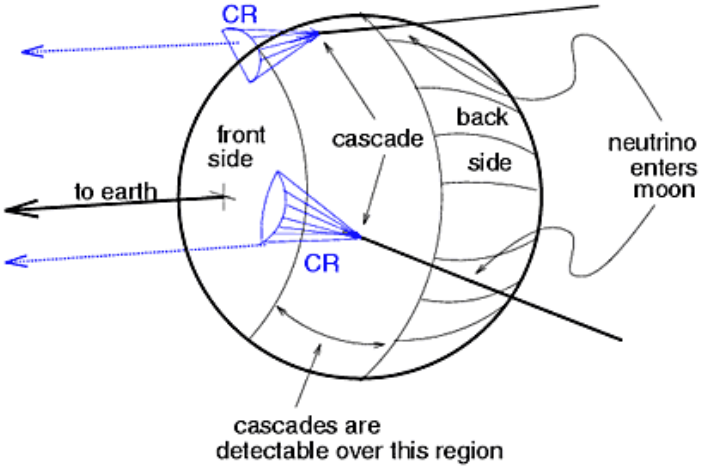

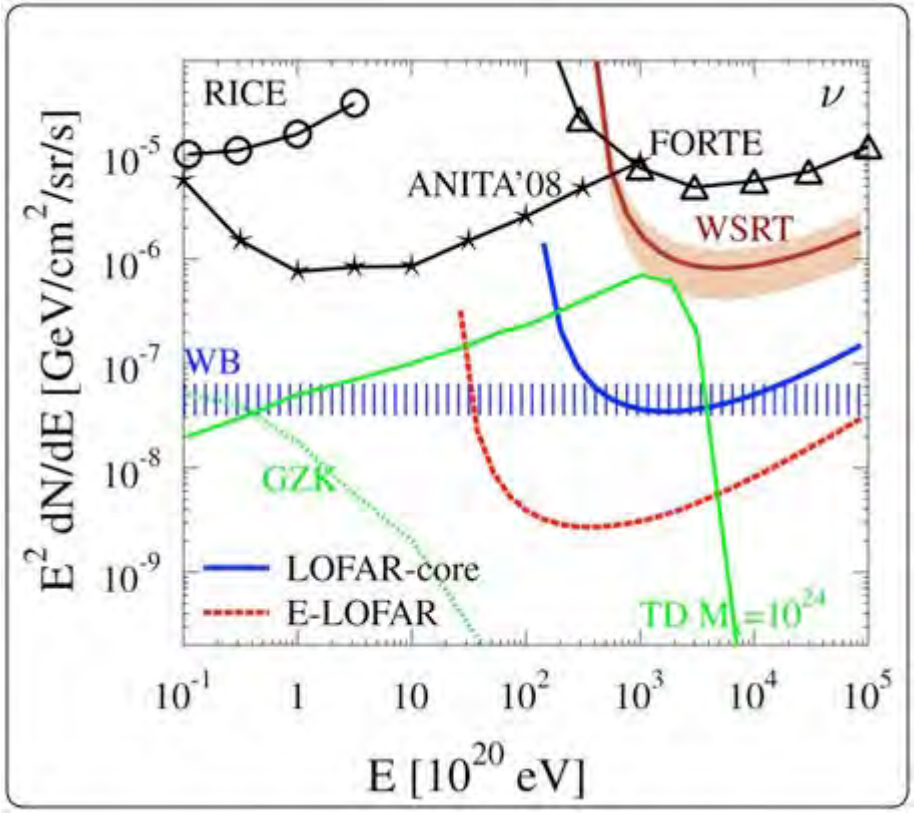

PHOTON DETECTORS

Emphasis on Cherenkov detectors so single photon sensitivities, for near UV or visible wavelengths and very short light pulses.

Photon detectors

- Main key features

- Vacuum devices:
  - Photomultiplier Tubes
  - MicroChannel Plate
  - Hybrid

- Solid State devices:
  - PhotoDiode
  - Avalanche Photo Diode : APD
  - Geiger Mode APD : Arrays of SPAD: SiPM / MPPC …
  - Imaging devices: CCD and sCMOS, EMCCD

Key features

The 4 steps of the photo-detection process:

1. **Emission** of primary charge carrier (pe, e/h)
2. **Collection** of primary charge carrier
3. **Multiplication/Amplification** of primary charge carrier (optional)
4. **Collection** and **Readout** of secondary (or primary) charges

The measurement process is modified by noise sources and by signal collection inefficiency at each step:

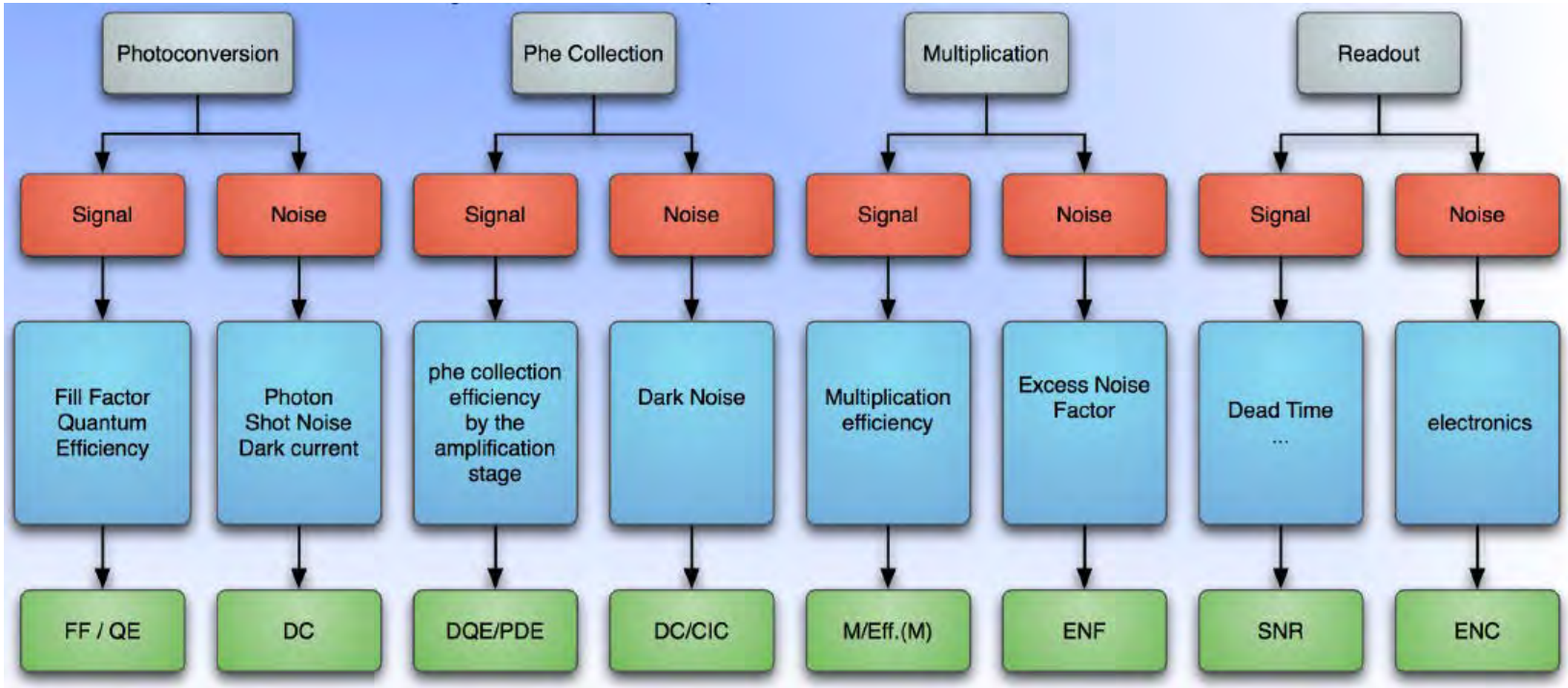

Rémi Barbier, NDIP 2011, Lyon, France

Photoelectric effect

1. **External**: the photoelectron is emitted into the vacuum from a photocathode material.

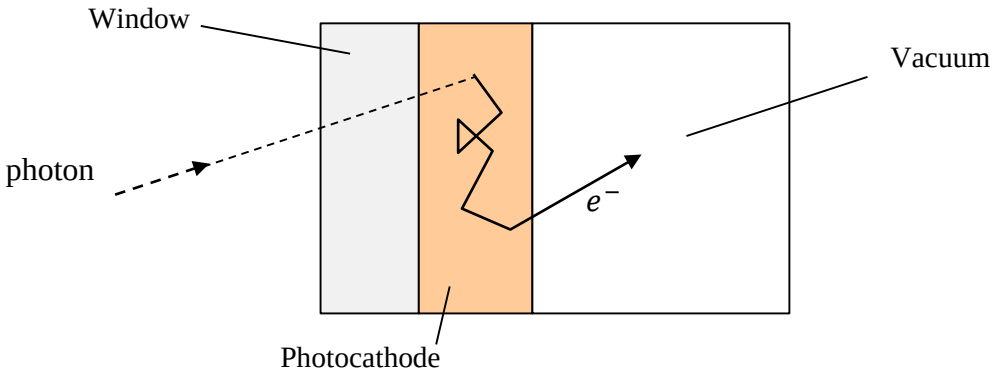

→pe = photoelectron

2. **Internal**: the pe is excited and occupies the conduction band of the semiconductor material, the photoconductive effect.

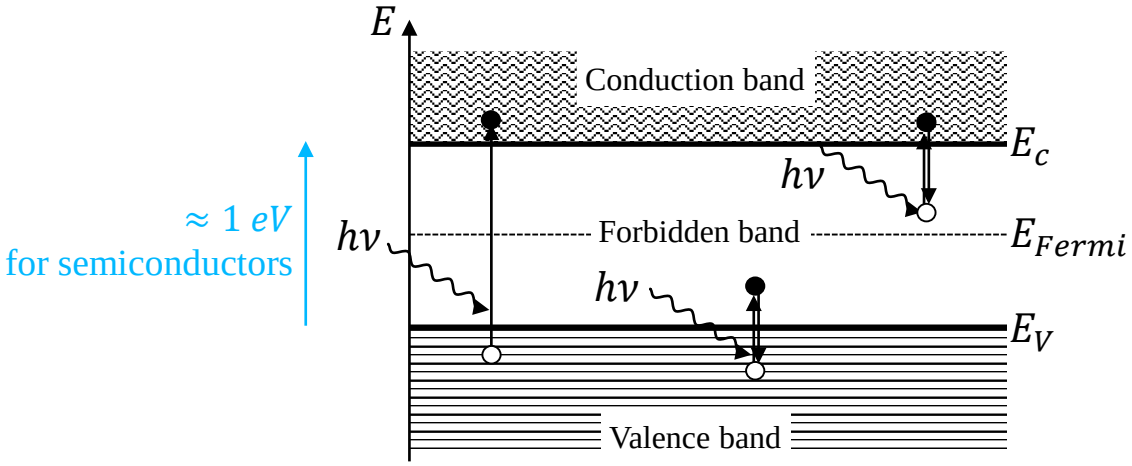

→e/h = electron/hole

Quantum efficiency

Photoelectric effect is a quantum (probabilistic) process

$$QE(\%) = \frac{N_{pe}}{N_\gamma} \times 100$$

Silicon is at least $\times 2$ better than photocathodes (but this not the end of the story).

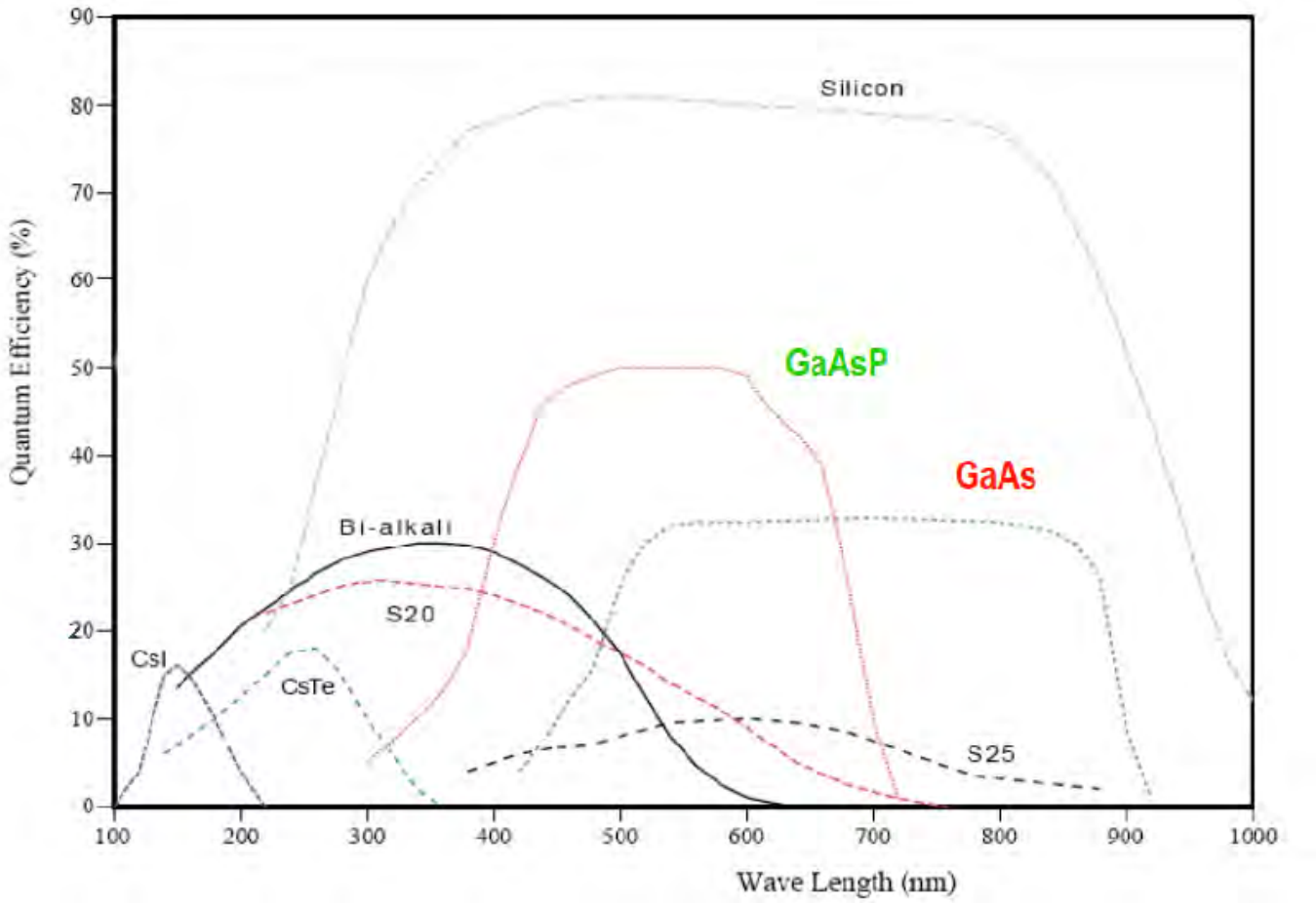

Quantum efficiency

Different definitions depending on detectors:

1. The radiant sensitivity $S[A/W]$: is the ratio between the output current and the input radiant power at a given wavelength.
   S is related to QE by: $QE(\%) \approx 124 \times \frac{S(mA/W)}{\lambda(nm)}$
2. The Fill Factor FF is the ratio between the sensitive surface and the detector surface also called geometrical efficiency (ε_{geom}).
3. Collection Efficiency CE is the probability to transfer the primary pe or e/h to the amplification stage or readout channel.
4. Multiplication Efficiency ME is the prob. that the amplification process give a detectable signal or trigger a multiplication (ε_{Geiger}).
5. Photon Detection Efficiency PDE is the probability that a single photon trigger a detectable output pulse also called the Detective Quantum Efficiency DQE.

For SiPM: $PDE = \varepsilon_{geom} \times \varepsilon_{Geiger}$

For others: $DQE = PDE = FF \times QE \times CE \times ME$

Noise in Photon Detectors

Energy = Number of collected secondary carriers:

$$E = M \times PDE \times N_\gamma$$

where M is the mean multiplication coefficient (gain). M is a stochastic variable with variance σ_M^2.

Energy resolution:

Ideal case: shot noise

$$\frac{1}{SNR} = \frac{\sigma_E}{E} = \sqrt{\frac{1}{N_\gamma}}$$

Real case:

$$\frac{1}{SNR} = \frac{\sigma_E}{E} = \sqrt{\frac{ENF}{PDF \times N_\gamma} + \left(\frac{ENC}{M \times PDF \times N_\gamma}\right)^2}$$

where ENF is the Excess Noise Factor. ENF is the noise due to the conversion, collection, multiplication processes. ENC is the Equivalent Noise Charge (readout noise from the electronics).

Excess Noise Factor 1pe:

$$ENF_{1pe} = 1 + \frac{\sigma_M^2}{M^2}$$

Excess Noise Factor for N_{pe} (assuming Poisson statistics in):

$$ENF_{N_{pe}} = M^2 \times ENF_{1pe}$$

Summary of efficiency and noise properties

	QE	CE	δ_i	ENF	G	ENC	σ/E
Ideal	1.0	1.0	1000	1.0	10^6	0	$\sqrt{1/N}$
PMT	0.5	0.8	10	1.3	10^6	200	$\sqrt{3.6/N}$
PD	0.8	1.0	-	1.0	1	200	$\sqrt{1.3/N+(300/N)^2}$
APD	0.8	1.0	2	2.0	50	200	$\sqrt{2.5/N+(5/N)^2}$
HPD	0.5	0.9	1000	1.0	10^3	200	$\sqrt{2.2/N+(1.1/N)^2}$
HAPD	0.5	0.9	1000	1.0	10^5	200	$\sqrt{2.2/N}$
CCD	0.8	1.0	-	1.0	1	50	$\sqrt{1.3/N+(60/N)^2}$
ICCD / ICMOS	0.8	0.7	-	2.0	10^4	50	$\sqrt{5.7N}$
EMCCD	0.8	1.0	2	2.0	10^3	50	$\sqrt{2.5/N}$
EBCCD / EBCMOS	0.5	0.85	1000	1.0	10^3	50	$\sqrt{2.35/N}$

K. Arisaka, NIM A 442 (2000) 80

Summary of efficiency and noise properties

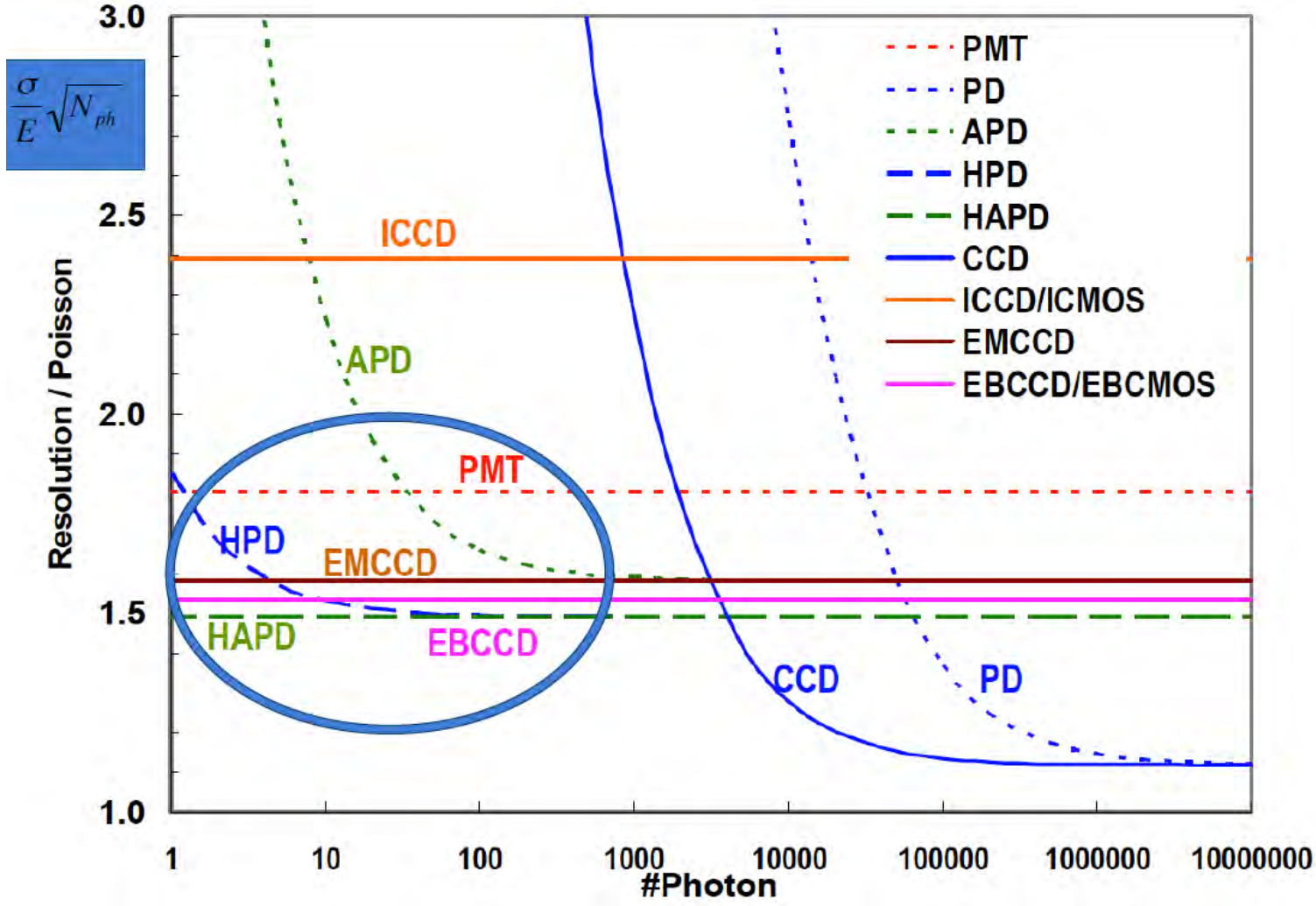

Spatial resolution (pixel size)

Pixel sizes: from large area detector PMT for Cherenkov detector to pixel array for highly resolved imaging

- Cherenkov detector : Large aperture devices
- PET scan … MaPMT or pixelAPD: Typical pixel size ~2x2mm2
- Imaging camera system : MTF (lp/mm)
  - Typical pixel size (Pitch) ~5-15 µm
  - Cellular phone 2 µm
  - DTI, doping profile, SOI

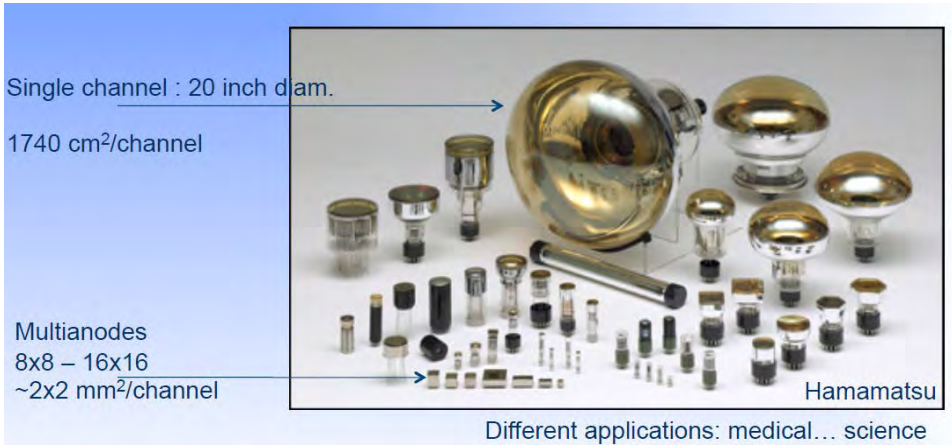

Time resolution:

- Detection process – drift of the charge – jitter …
- Front-end electronics: fast shaper
- CMOS imager CCD are extremely slow (~s-ms) compare to PMT or APD, GAPD and MCP (~ns-ps).
- MCP based devices should have the best timing resolution (10 ps)

Time resolution

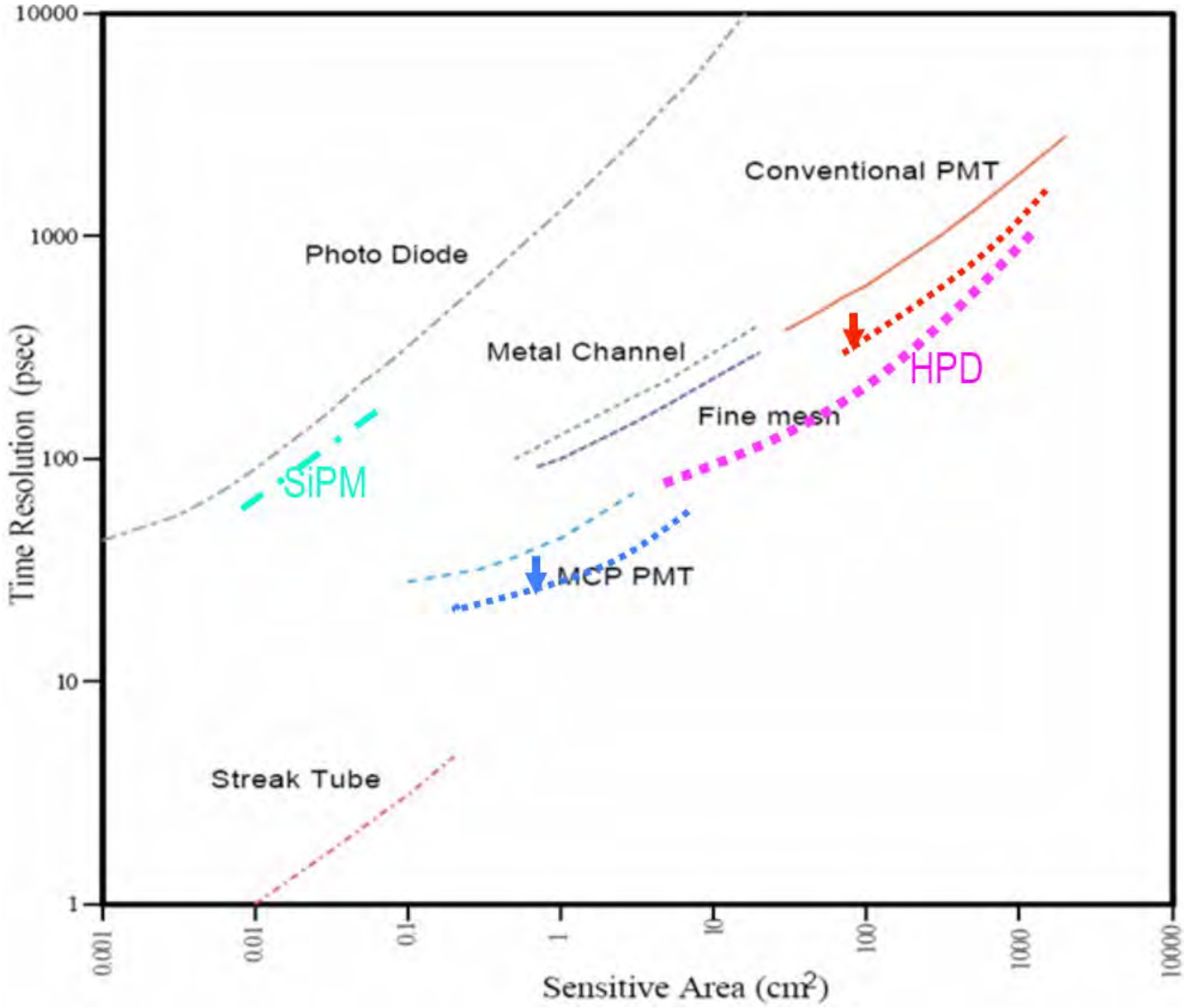

Vacuum devices

Photomultiplier Tubes: PMT

Single channel 20"
in diameter
⇒ 1740 cm²/channel

Multianodes pmts
8x8 16x16
⇒ ~2x2 mm²/channel

Photomultiplier Tubes: PMT

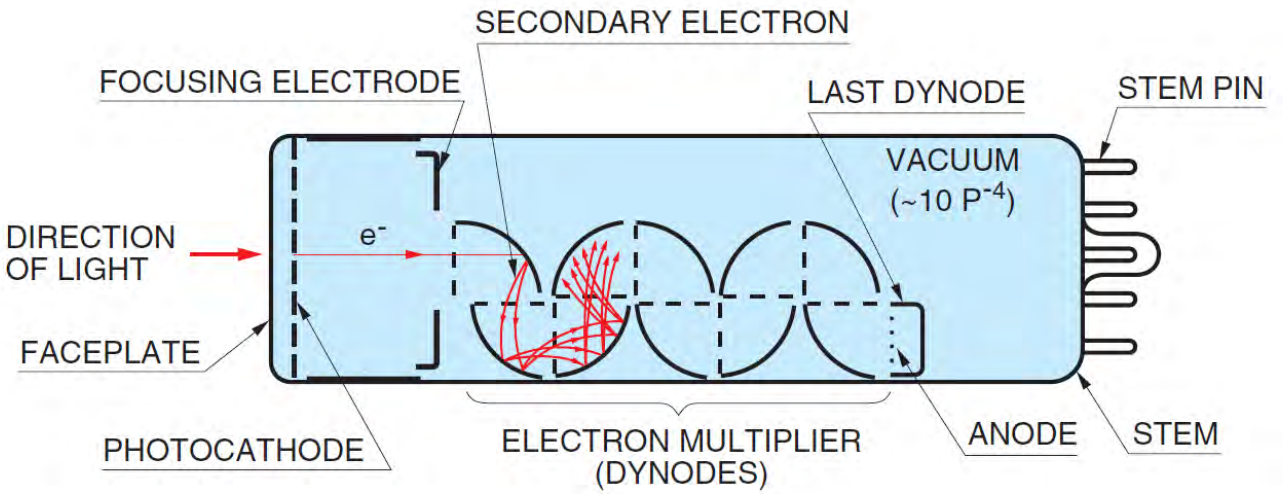

1. The photon produces a photoelectron (pe) (Quantum Eff.)
2. The pe is emitted into the vacuum (Quantum Eff.)
3. The pe is collected by the first dynode (Coll. Eff)
4. The pe is “amplified” by dynodes multiplication stages (M and ENF)
5. The secondary charges are collected by the anode
6. The anode signal is readout (Equ. Noise Charge ENC)

Photomultiplier Tubes: PMT

2021

Different photocathode sensitivities

GEN II alkali metals (Sb K Rb Cs)

GEN III IIII-V compound semiconductors GaAsP GaAs InGaAs

All are deposited via vacuum vapor deposition technics.

$QE = 20\%$ to 30% @ 400 nm

$CE = 70\%$ to 90%

Quantum efficiency is limited due to the trade off between:

Absorption ie potential barrier
→ layer thickness ↓

and

pe emission → layer thickness ↑

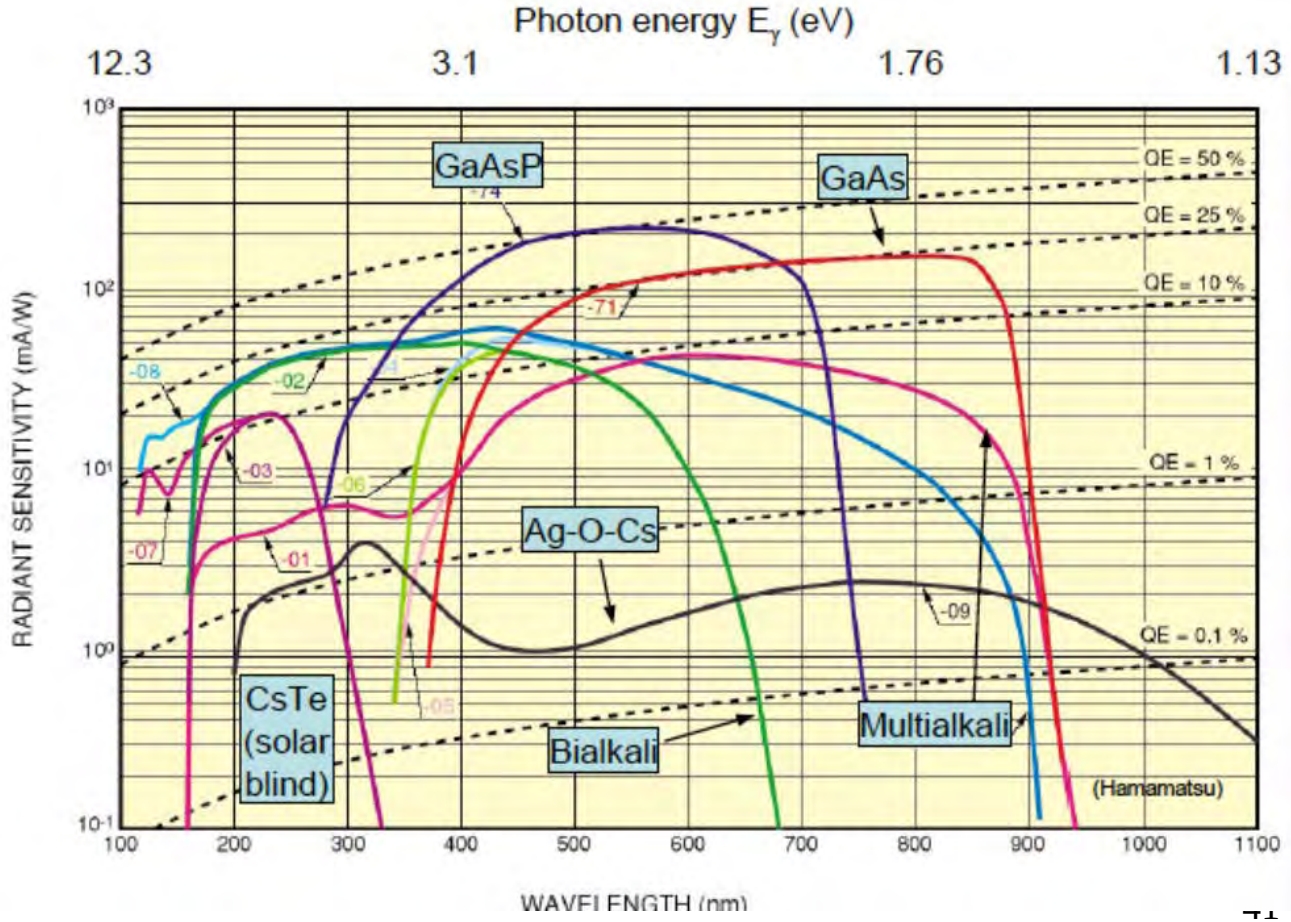

Photomultiplier Tubes: PMT

2021

Different types of multipliers.

Multiplication process:

δ_i is the secondary emission coefficient of dynode i. It depends on voltage

$\delta_i = a \times V_\delta^k$ with $a = cste$ and $k = 0.7 - 0.8$

$$M = \delta_1 \delta_2 \delta_3 \dots \delta_n = \prod_{i=1}^{n} \delta_i = \left(a \times V_\delta^k\right)^n$$

$$= a^n \times \left(\frac{V}{n+1}\right)^{kn} = A \times V^k$$

$$ENF_{1pe} = 1 + \frac{1}{\delta_1} + \frac{1}{\delta_1 \delta_2} + \frac{1}{\delta_1 \delta_2 \delta_3} + \cdots$$

$$= \frac{\delta}{\delta - 1}$$

First dynode dominates the ENF

→ single photoelectron resolution

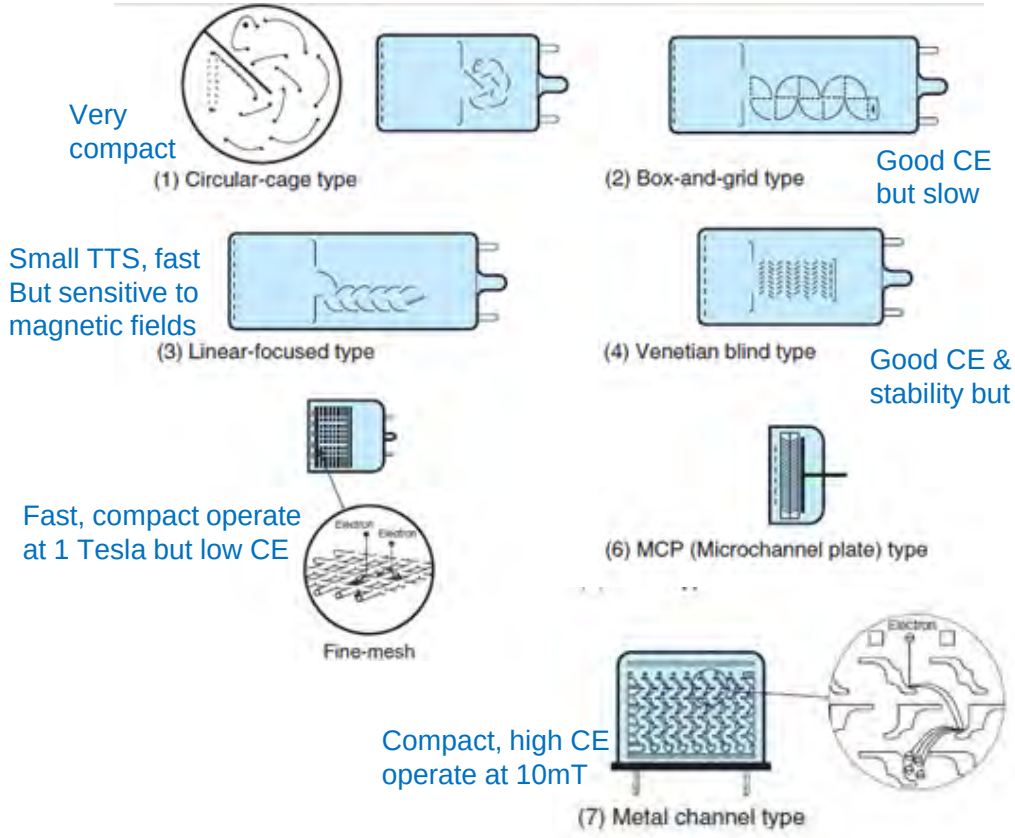

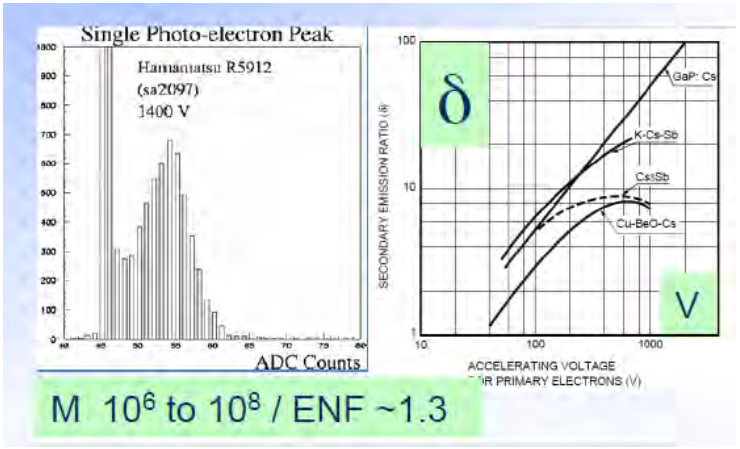

Photomultiplier Tubes: PMT

Photomultiplier Tubes: PMT

Timing properties:

Rise time (10% - 90%)

Fall time

Transit Time Spread (jitter of TT)

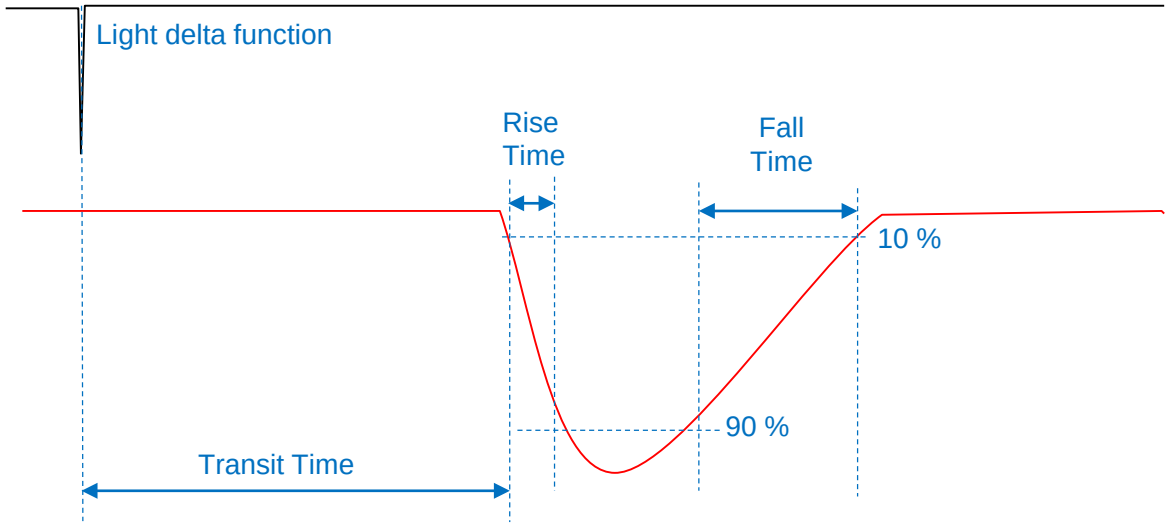

Collection efficiency and uniformity, and TTS are dominated by optimization of first stage (E field shaping).

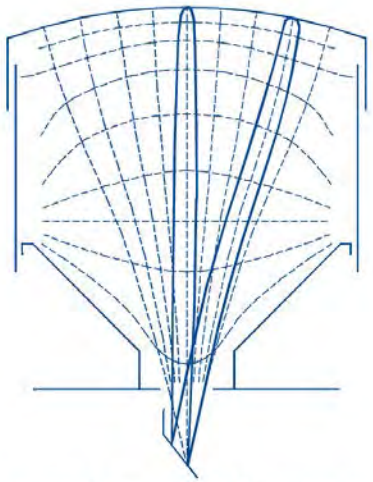

Fig.6 Example of a large, fast PMT input electron-optics.

Unit : ns

Dynode Type	Rise Time	Fall Time	Pulse Width (FWHM)	Electron Transit Time	TTS
Linear-focused	0.7 to 3	1 to 10	1.3 to 5	16 to 50	0.37 to 1.1
Circular-cage	3.4	10	7	31	3.6
Box-and-grid	to 7	25	13 to 20	57 to 70	Less than 10
Venetian blind	to 7	25	25	60	Less than 10
Fine mesh	2.5 to 2.7	4 to 6	5	15	Less than 0.45
Metal channel	0.65 to 1.5	1 to 3	1.5 to 3	4.7 to 8.8	0.4

Table 4-3: Typical time characteristics (2-inch dia. photomultiplier tubes)

Vacuum devices

2021

Multi Channel Plate MCP applied to night vision

Multi Channel PMT

MaPMT

Flat Panel H9500 Hamamatsu

- 16x16 (256) anodes
- Pixel size 2.8x2.8 mm²
- Pitch : 3.04 mm
- Effective area = 49x49 mm square
- FF = 89%
- G = $1.5\ 10^6$
- 12 Dynodes
- PC: Bialkali 24% @ 420 nm
- Transit Time 6 ns
- Transit Time Spread = 0.4 ns
- Rise Time = 0.8 ns
- Xtalk = 5%
- Anode Uniformity 1:4

MCP-PMT

PLANACON XP85022

- 32x32 (1024) anodes
- Pixel size 1.1x1.1 mm²
- Pitch : 1.6 mm
- Effective area = 53x53 mm square
- FF = 80%
- G = $1.\ 10^5$ @ 1800 V
- Dark current @ 10^5 gain = 2 (<10) nA
- 2 MCP chevron 25 micron pore 40:1 L:D ratio
- PC: Bialkali 22% @ 380 nm
- Pulse Width = 1.8 ns
- Rise Time = 0.6 ns

Micro Channel PMT

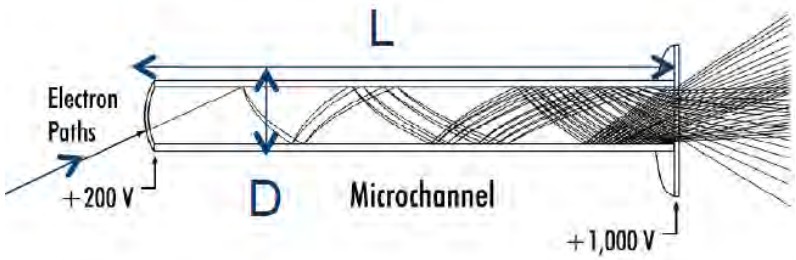

$$M = \exp(K \times \alpha)$$

$$\alpha = \frac{Length}{Diameter}$$

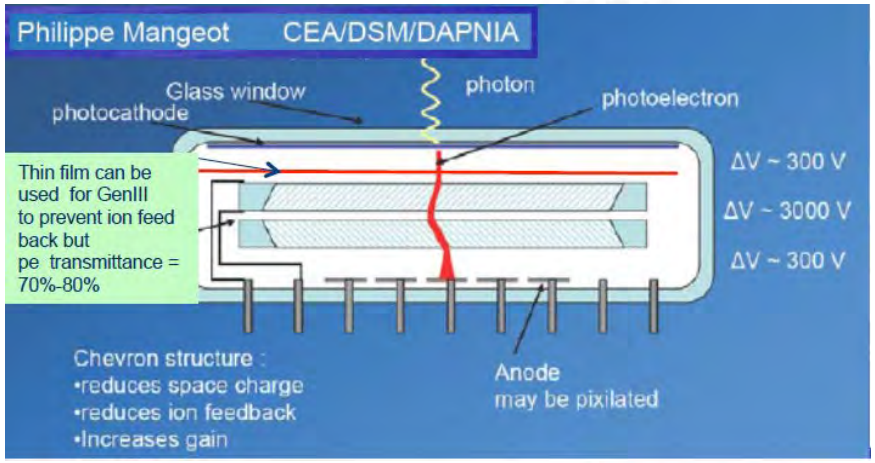

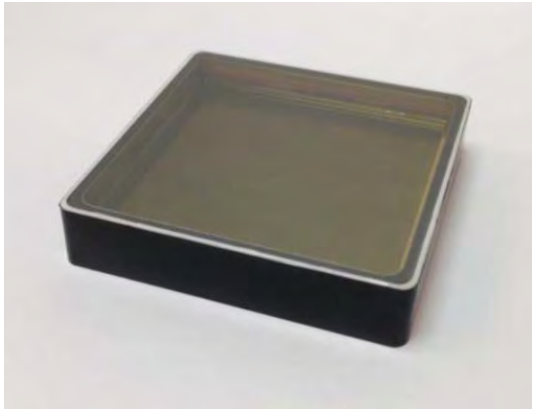

Microchannel Plate Factors

BURLE ELECTRO-OPTICS

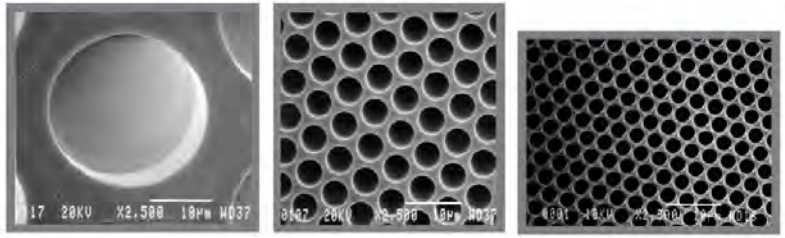

Factor	25 micron pore	5 micron pore	2 micron pore
Pulse Width	10 ns	650 ps	250 ps
Gain	10 million	5 million	2 million
Max. Ct. Rate	5 million/cm2	50 million/cm2	100 million/cm2
Noise	5 cts./cm2	5 cts./cm2	5cts./cm2
Robustness	High	Medium	Medium
Cost	Low	Medium	High

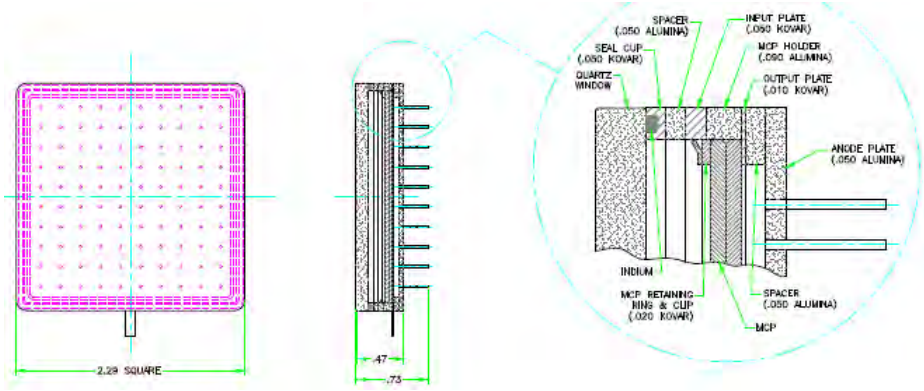

Hybrid Photon Detectors

2021

Principle:

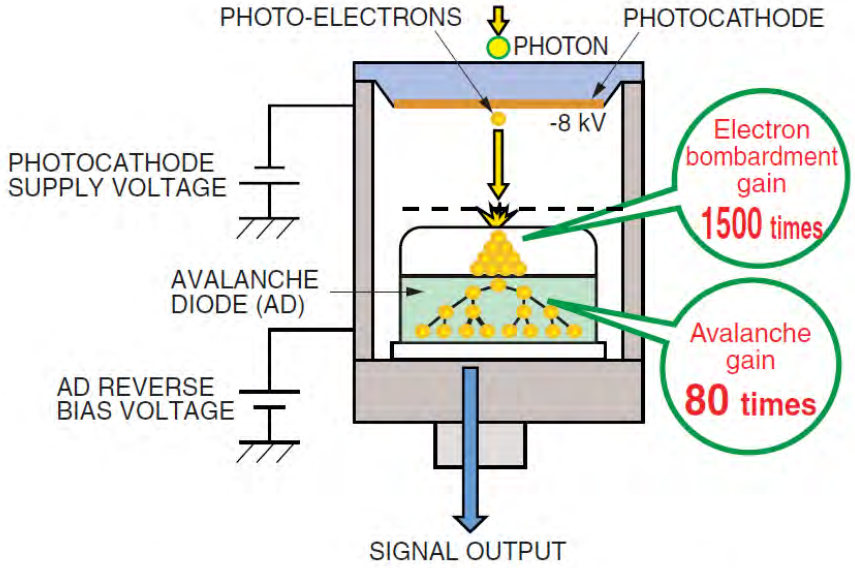

Figure 12-1: Schematic principle of an HPD

Proximity focusing

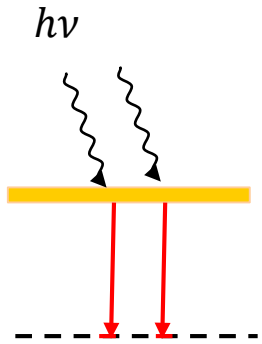

1:1 imaging

Operates in mag fields

Imaging with single photon sensitivity and spatial resolution

Electrostatic focusing

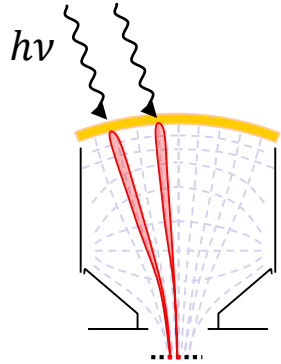

Demagnifying

Large detection aera

Large aperture & single photon sensitive

Fast : Cherenkov detectors …

Hybrid Photon Detectors

2021

1. Photocathode (Alkali / GaAs)
2. High Electric field (HV 2 to 20 kV)
3. Gain in one step by energy dissipation of keV pe's in solid-state detector. ENF ~1
4. Secondary carriers for multiplication are produced and directly readout by
   - Si-Anode+ROC = HPD / ISPA Tube …
   - APD = HAPD
   - Back thinned CCD = EBCCD
   - Back thinned CMOS = EBCMOS

Large Area HPD / Small number of pixels

LHCb CERN

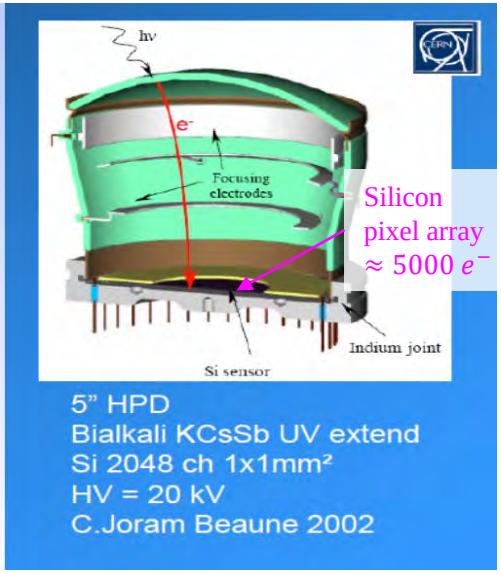

Imaging / Megapixels devices

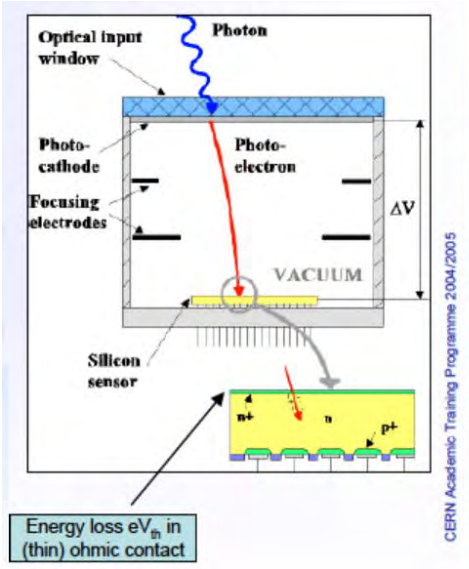

Solid State Devices

Basic works :Haitz/McIntyre (1966)

Pioneers are Russian groups: Sadygov, Golovin

- SPAD Single Photon Avalanche Diode
- SiPM Silicon PhotoMultiplier
- MRS Metallic Resistive Semiconductor
- MPGM APD Multipixel Geiger-mode Avalanche PhotoDiode
- AMPD Avalanche Micro-pixel PhotoDiode
- SSPM Solid State PhotoMultiplier
- GAPD Geiger-mode Avalanche PhotoDiod
- GMPD Geiger-Mode PhotoDiode
- DPPD Digital Pixel PhotoDiode
- MCPC MicroCell Photon Counter
- MAD Multicell Avalanche Diode
- ….

Same concept
different technological implementations

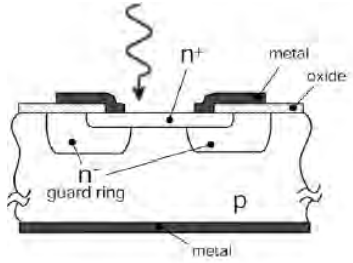

planar diode (Haitz)

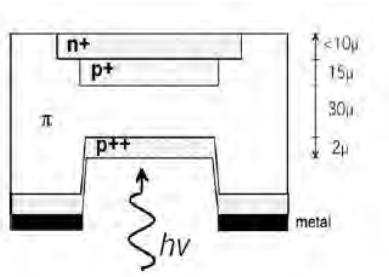

reach-through diode (McIntyre)

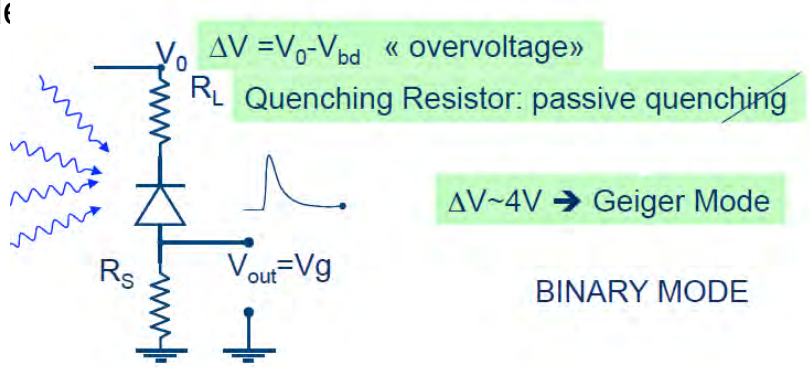

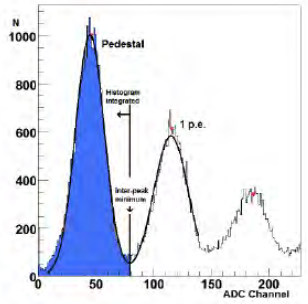

SiPM

- Each pixel works in a binary mode at single photon sensitivity
- Pixels are very small
  $\Rightarrow$ low occupancy
- Signal by counting hit pixels

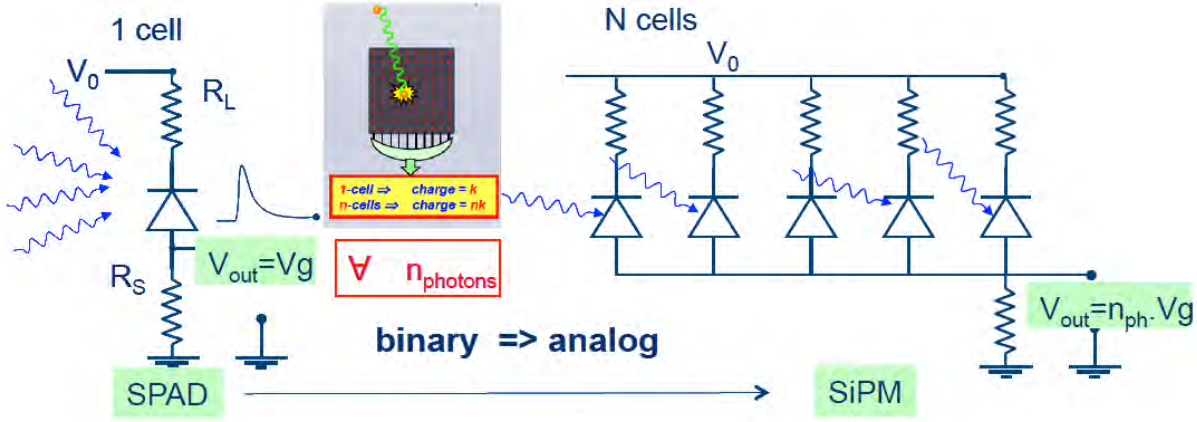

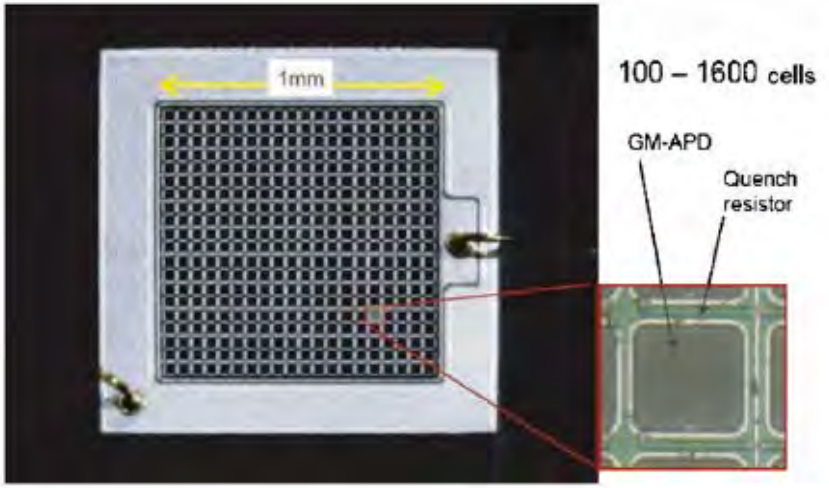

Fig. 6. Silicon photomultiplier (Hamamatsu MPPC) with a close-up of one of the cells.

Hamamatsu MPPC

$$N_{sig} = N_{cell} \times \left(1 - \exp\left(-\frac{PDE \times N_\gamma}{N_{cell}}\right)\right)$$

Gain: $G = 2 \times 10^6 \ @ \ \Delta V \approx 6V$

Photon Detection Efficiency:

$PDE = QE \times FF \times GE$

GE = Geiger efficiency

FF = Geometrical efficiency

$PDE \approx 20\%$

Other Solid State PD

Many other aspect of photon detectors not covered here:

- Pinned Diodes
- Avalanche Photo Diode
- CCD
- ICCD
- CCD
- ICMOS
- sCMOS
- EMCCD
- pnCCD
- EBCCD
- EBCMOS

TIMING AND COUNTING: THE AUGER DETECTOR EXAMPLE

Counting particles or timing measurements

- Example : the Auger Water Cherenkov Tanks

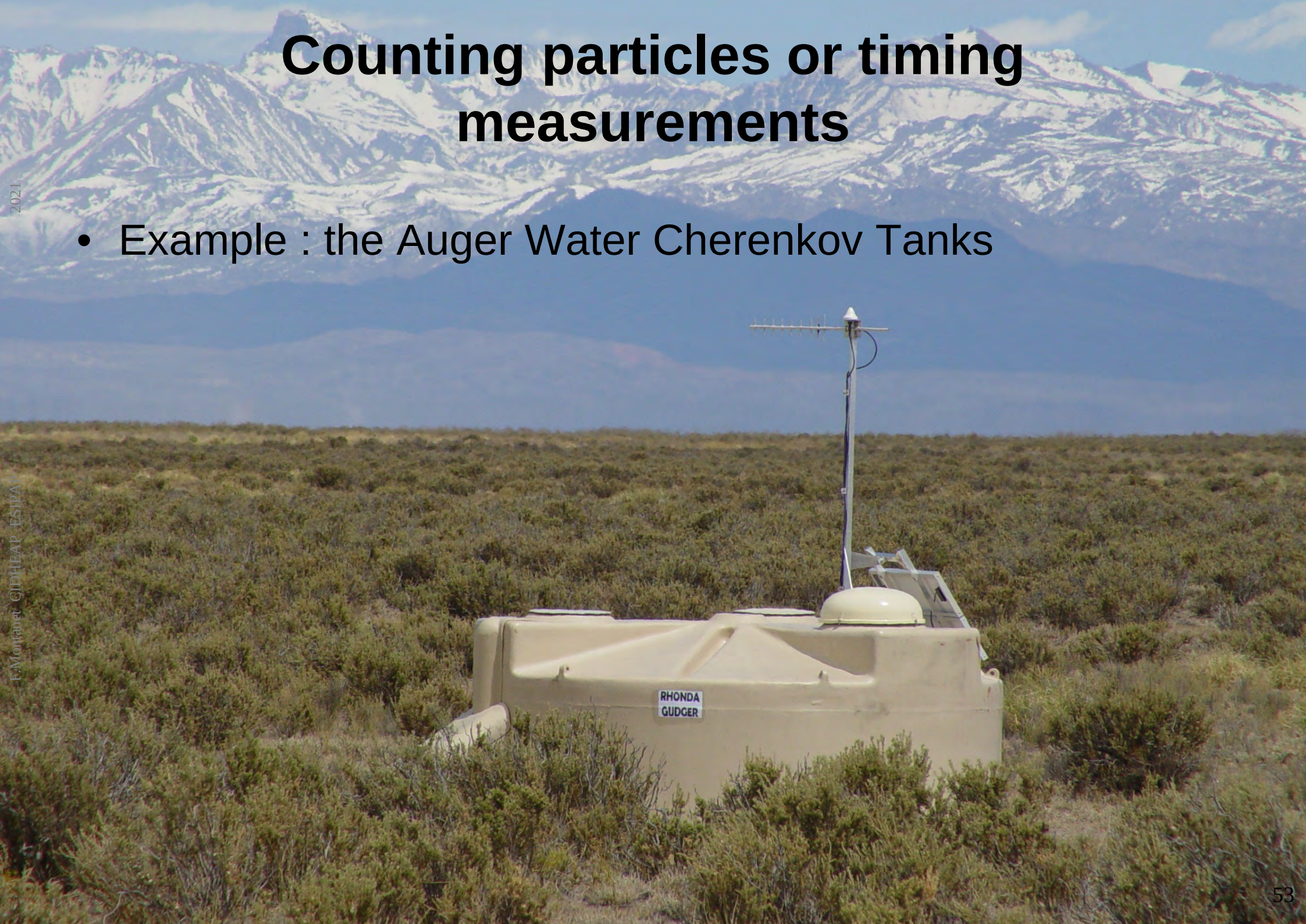

Pierre Auger observatory

Timing

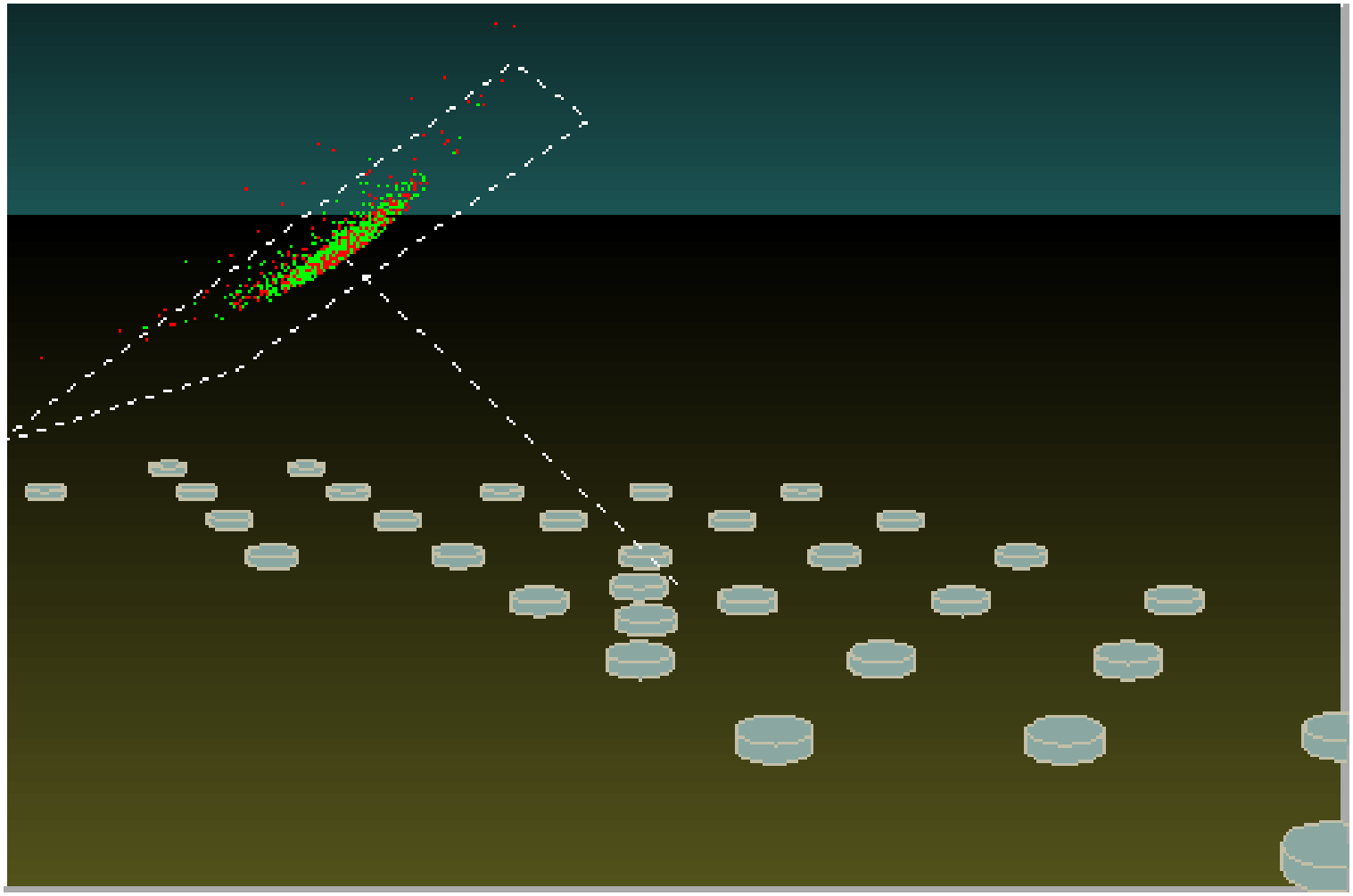

Thin pancake (few tens ns) of particles traveling at speed $v \sim c$.
Spacing is 1.5 km $\Rightarrow$ few 10 ns relative timing to achieve 0.1° angular resolution for vertical showers. Acheivable with GPS + flash ADCs.

From EAS footprint and LDF to primary CR energy estimator

AUGER

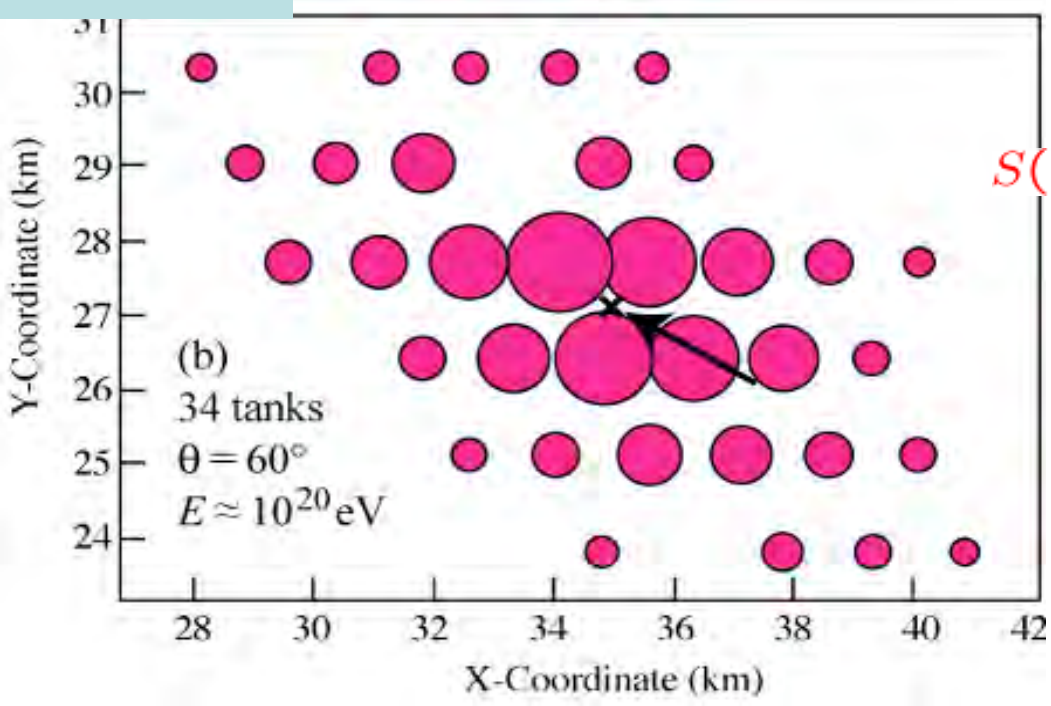

$S(1000)$

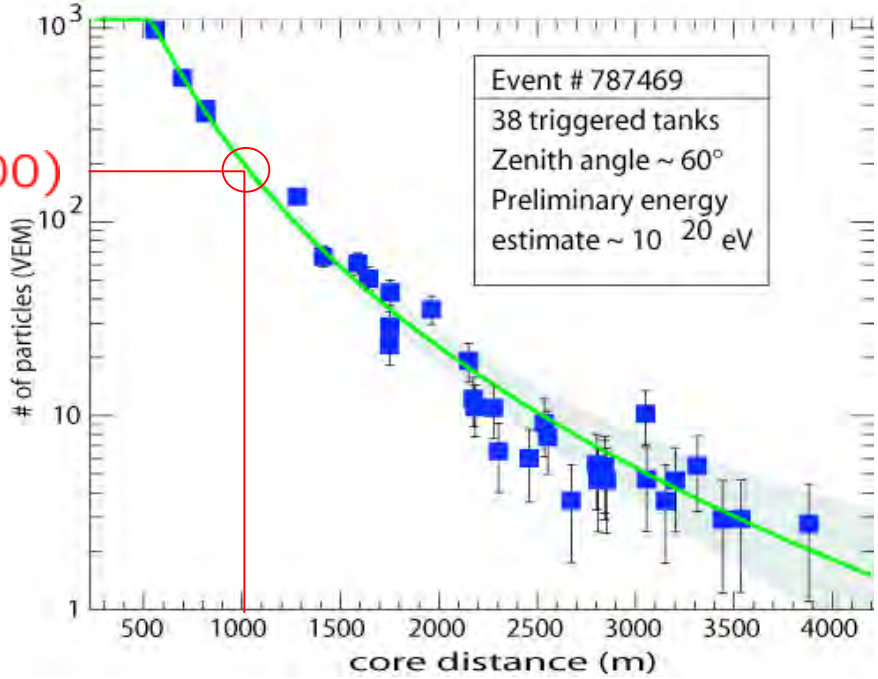

Idea from Hillas 1970 (pioneered by Haverah Park and Agasa)

- energy estimator: signal at fixed (large) core distance S(R)
- small shower-to-shower fluctuations, depends on primary E only
- Determination of particle density → LDF -> S(R)
- Largest uncertainty: converting estimator to energy (see later)

The surface array detectors

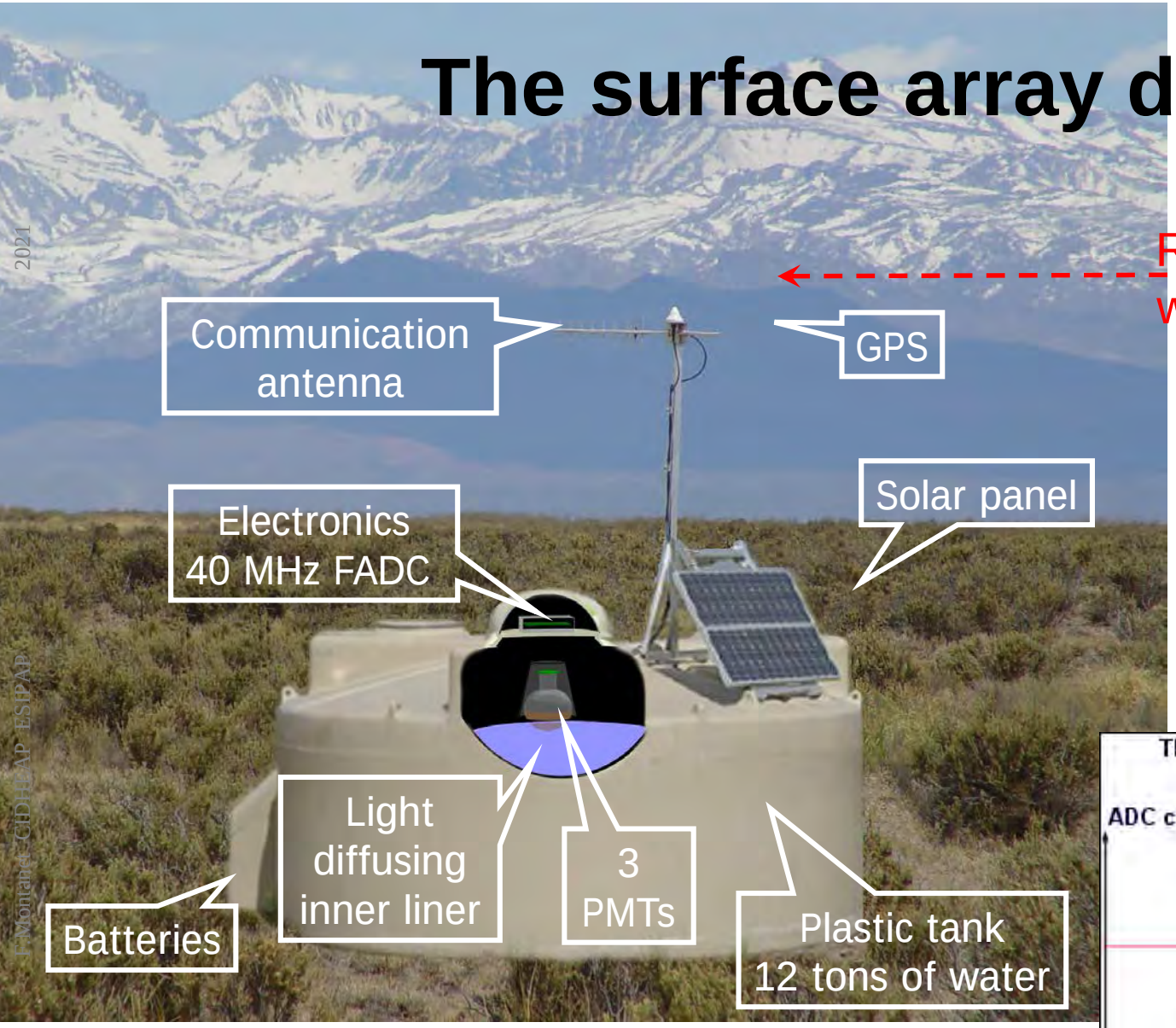

Radio waves

Central DAQ

Local trigger

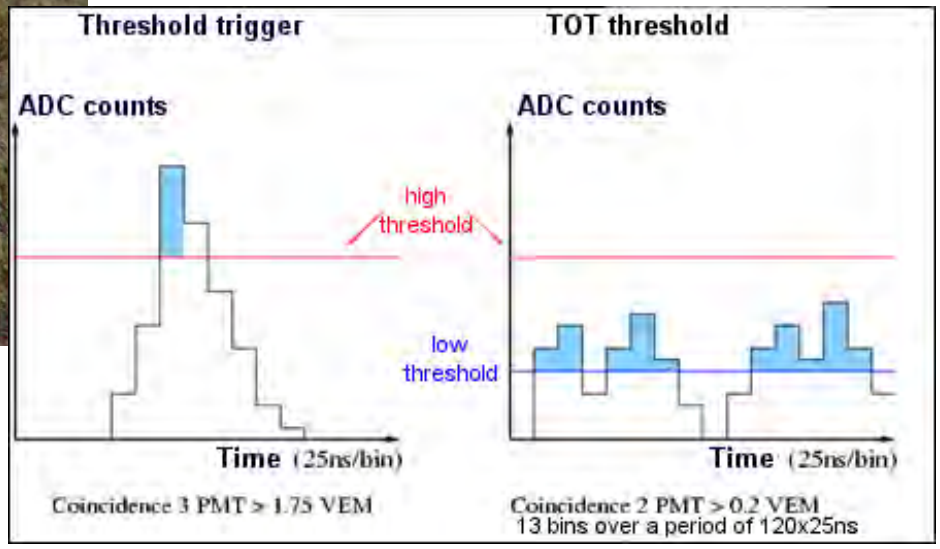

Self-calibration:
1 VEM = average signal from vertical through going muons.

Installing the world largest particle detector

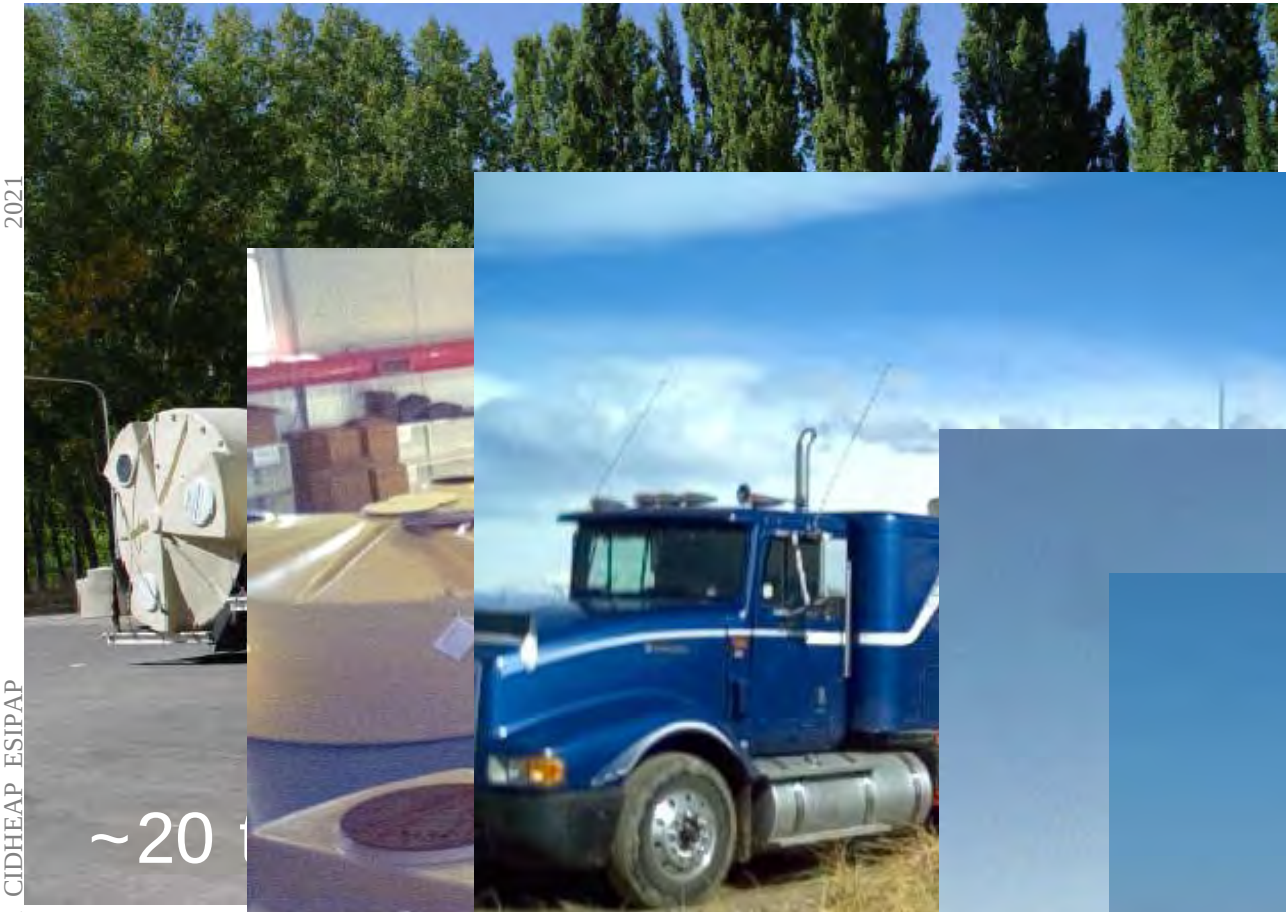

~20 t

Moving to

W

Installing the world largest particle detector

Pierre Auger Observatory surface detectors

UHECR event

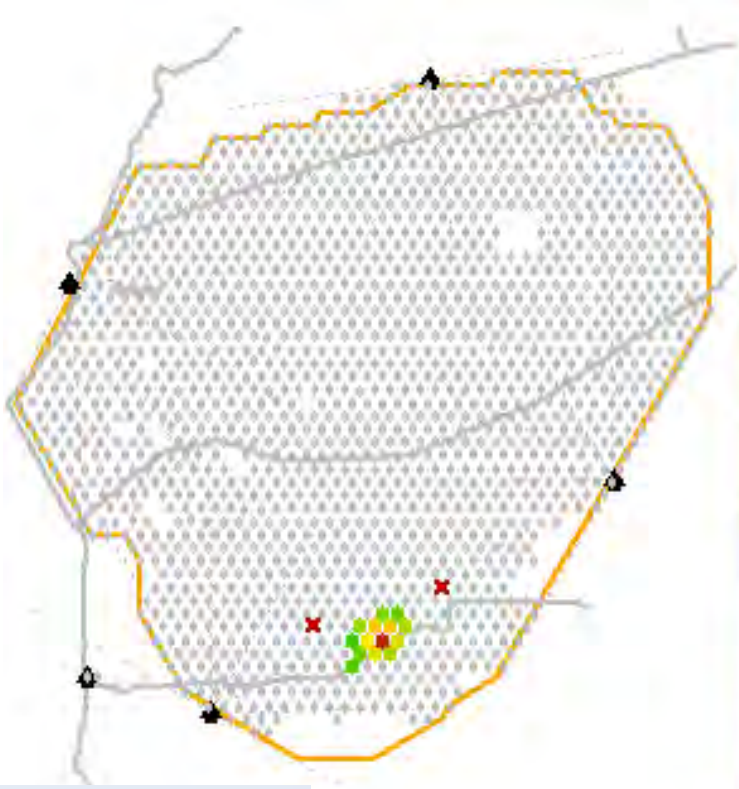

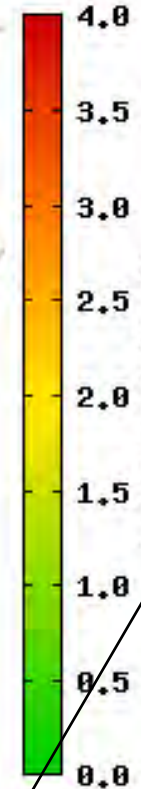

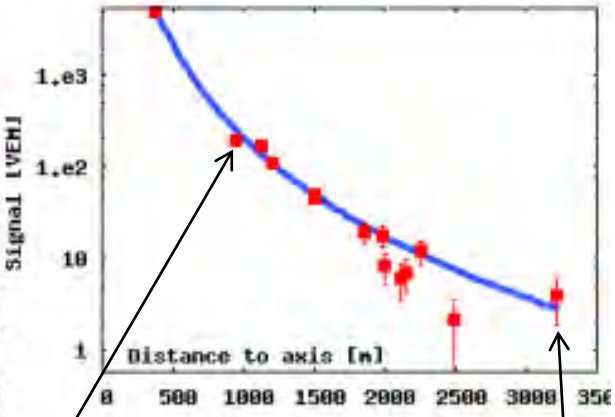

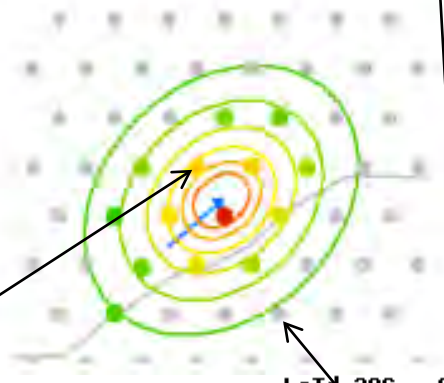

Generic Information	
Id / Date	10485600 / Tue Oct 26 17:39:16 2010
Nb. of stations	14
Energy	49.7 ± 1.9 EeV
Theta	40.2 ± 0.2 deg
Phi	-139.2 ± 0.2 deg
Curvature	10.9 ± 0.5 km
Core Easting	476053 ± 19 m
Core Northing	6079248 ± 12 m
Reduced Chi^2	8.36

LsId 266 - Lina

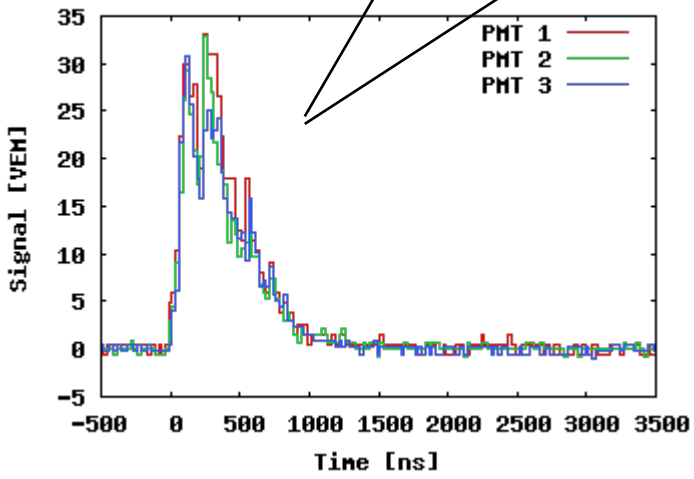

LsId 326 - Agostina

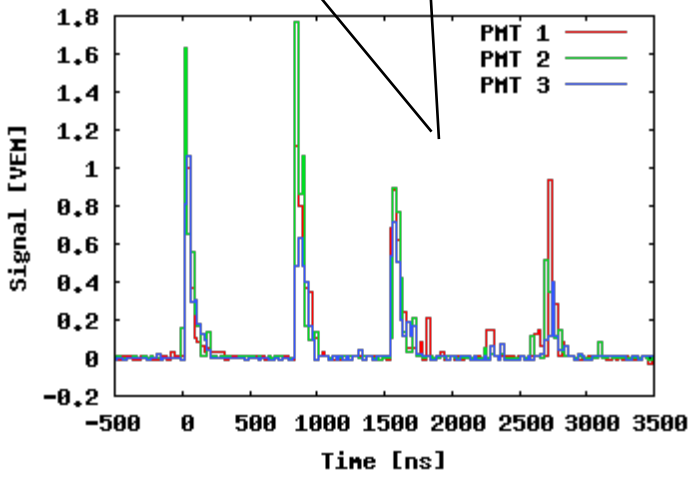

Fluorescence in air

- Charge particles (mostly e^+e^-) excite N_2 molecules that de-excite via molecular fluorescence emitting rays in UV (along with other wavelength)

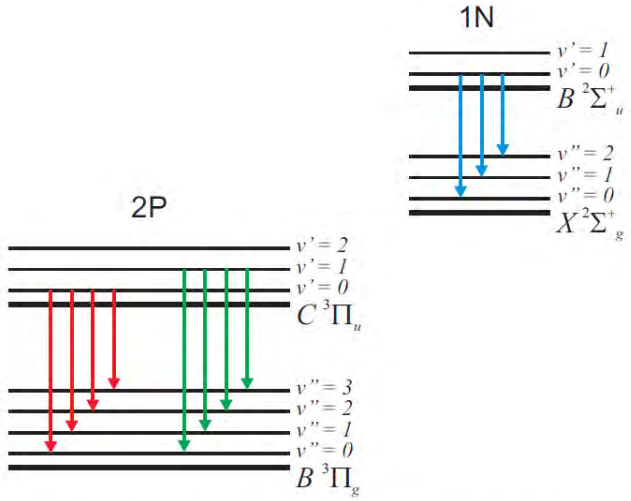

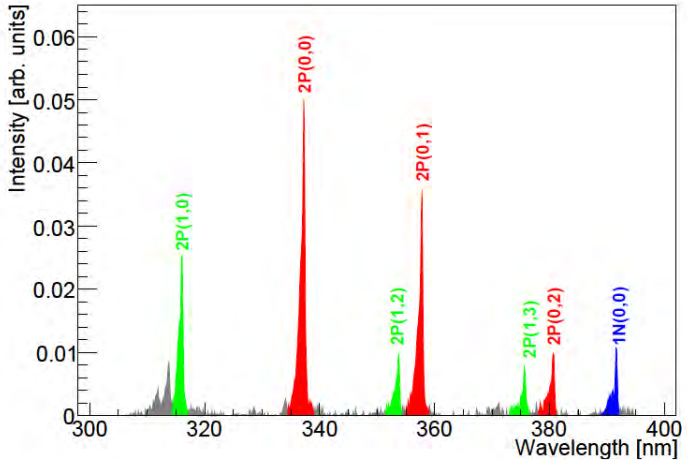

- Light yield measured in lab experiments with a 15% accuracy.
- 28 photons / MeV ⇒ ~4 photons / meter
- 4π emission
- Detectable at UHE ($> 10^{17}$ eV) at > 20 km
- Moonless, clear sky nights ⇒ ~10% duty cycle

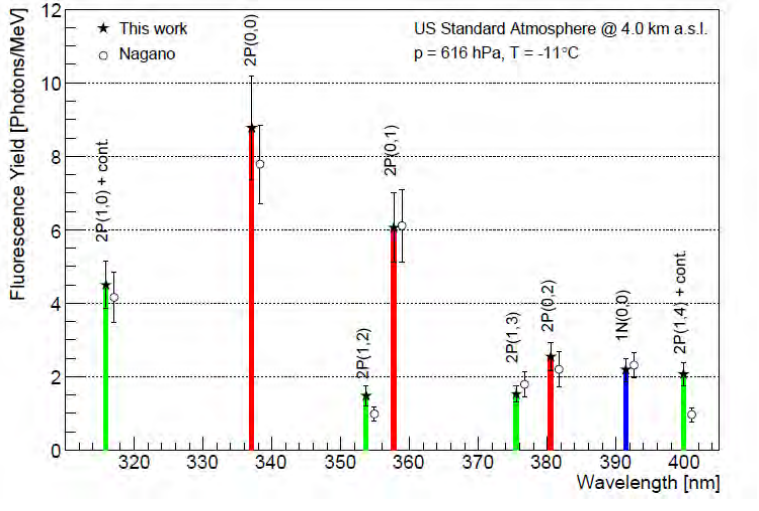

FD at 4 sites:
each 6 telescopes 30°x30° field of view each

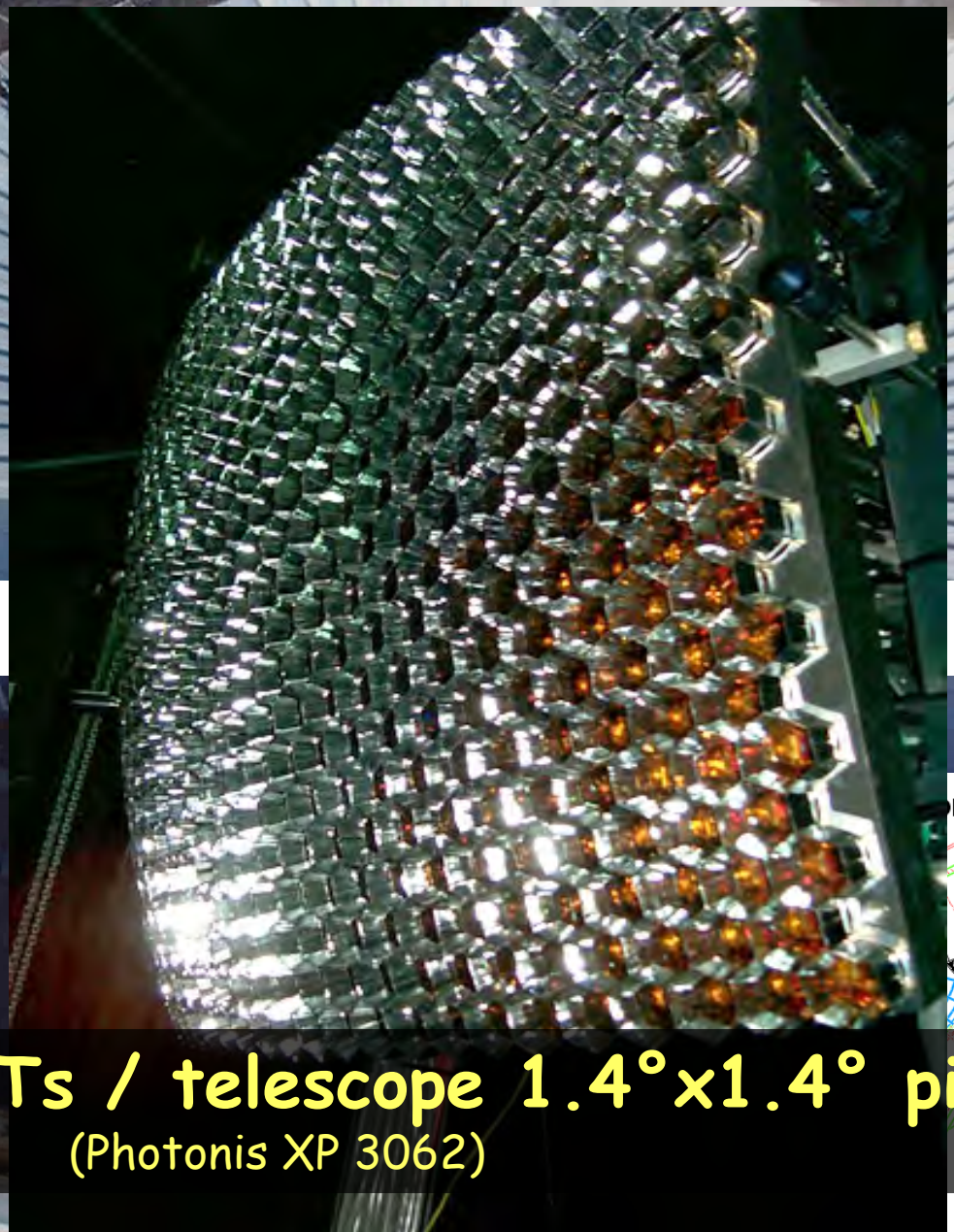

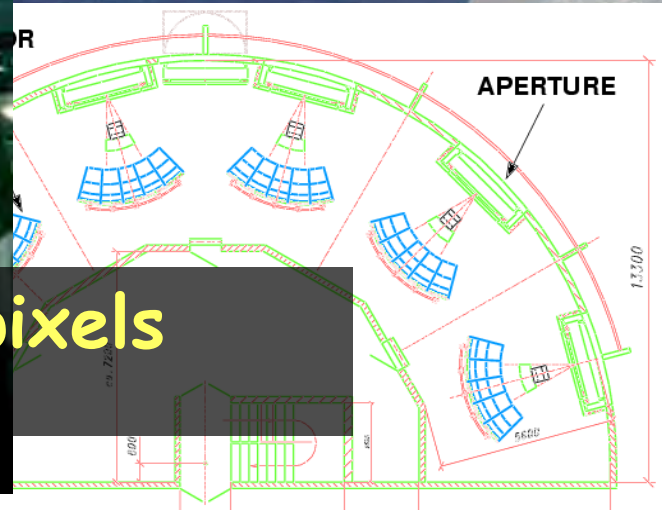

440 PMTs / telescope 1.4°x1.4° pixels

(Photonis XP 3062)

Pierre Auger Observatory fluorescence detectors

F.Montanet CIDHEAP ESIPAP 2021

Pierre Auger Observatory fluorescence detectors

F.Montanet CIDHEAP ESIPAP 2021

From EAS longitudinal profile to primary CR energy

The Hybrid “image” of the same shower, pioneered by Auger, increases as well the accuracy of the profile measurement.

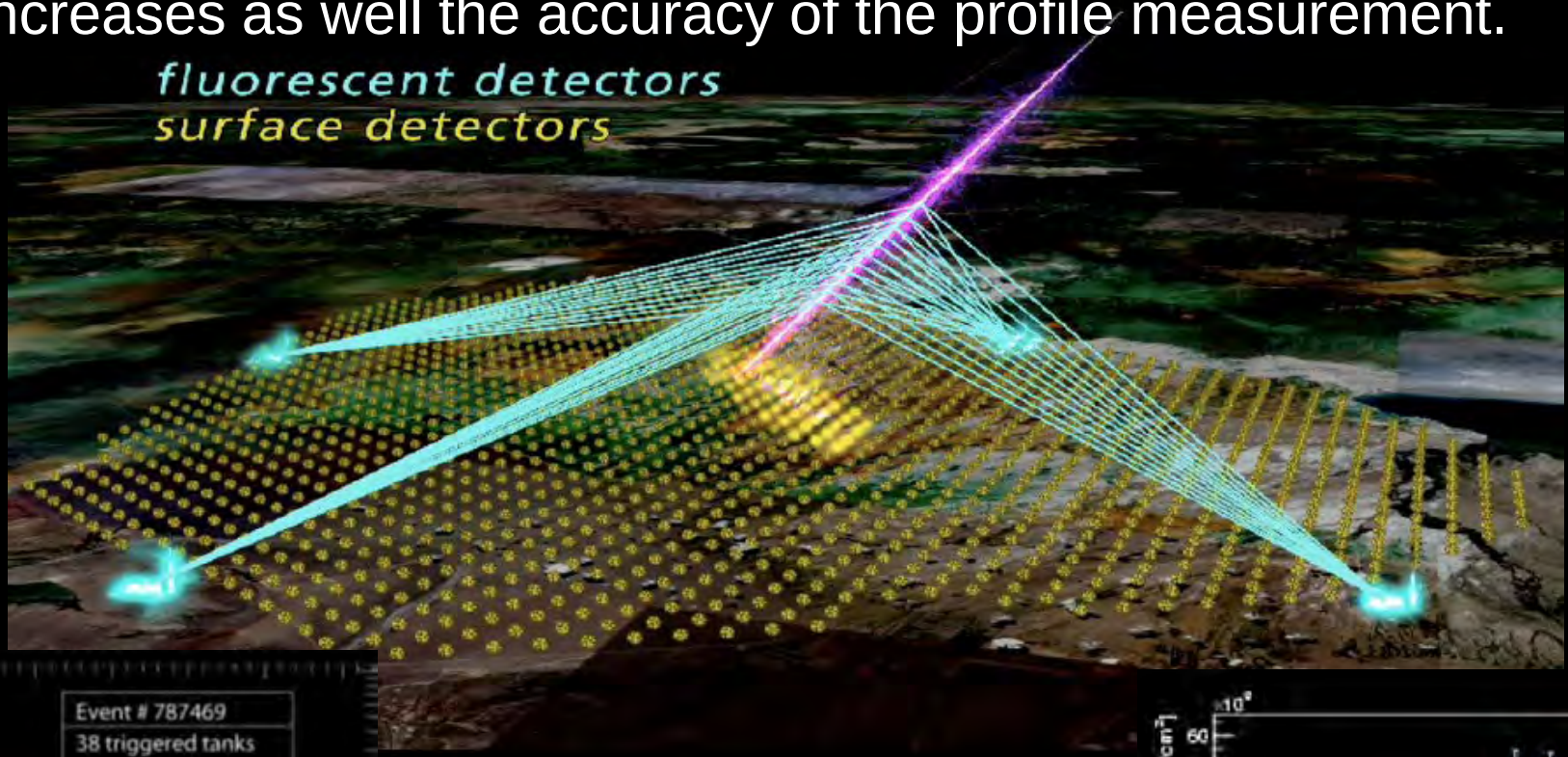

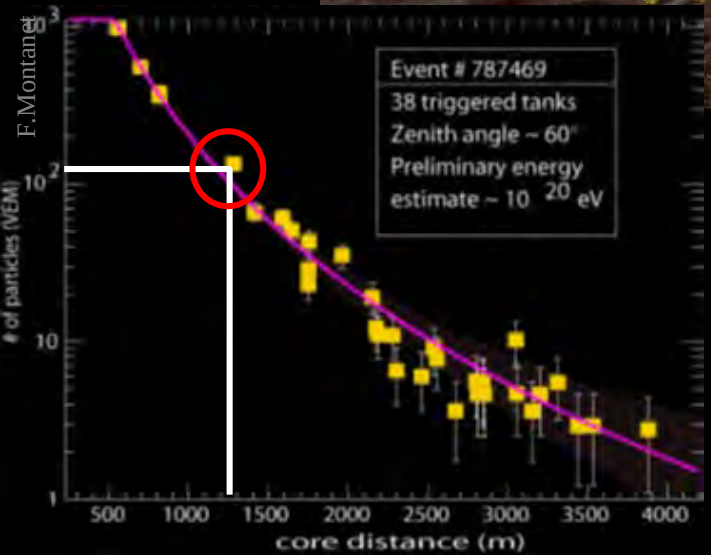

PROGRESS:
Calibration of SD energy estimator through FD

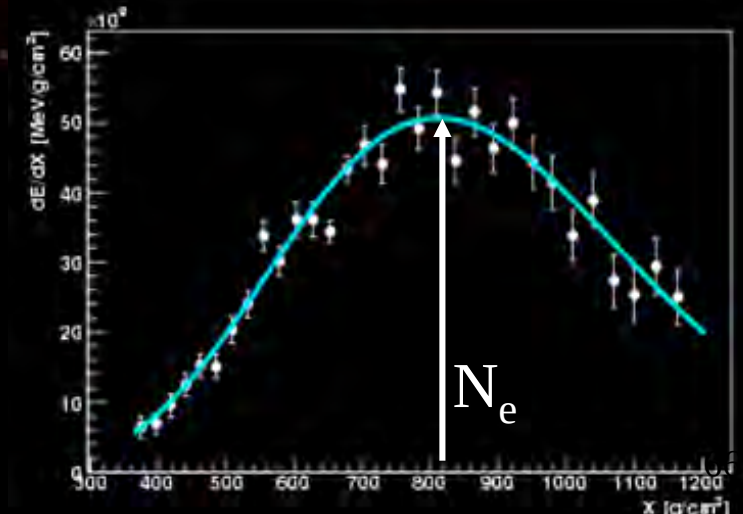

Improving measurements

Fluorescence vs Hybrid techniques :

	Hybrid	SD only	FD only
Angular resolution	0.2°	1-2°	3-5° (0.5° stereo)
Aperture	Independent on E, mass, models.	Independent on E, mass, models.	Dependent on E, mass, models, spectral shape.
Energy	Independent on mass, models.	Dependent on mass, models.	Independent on mass, models.

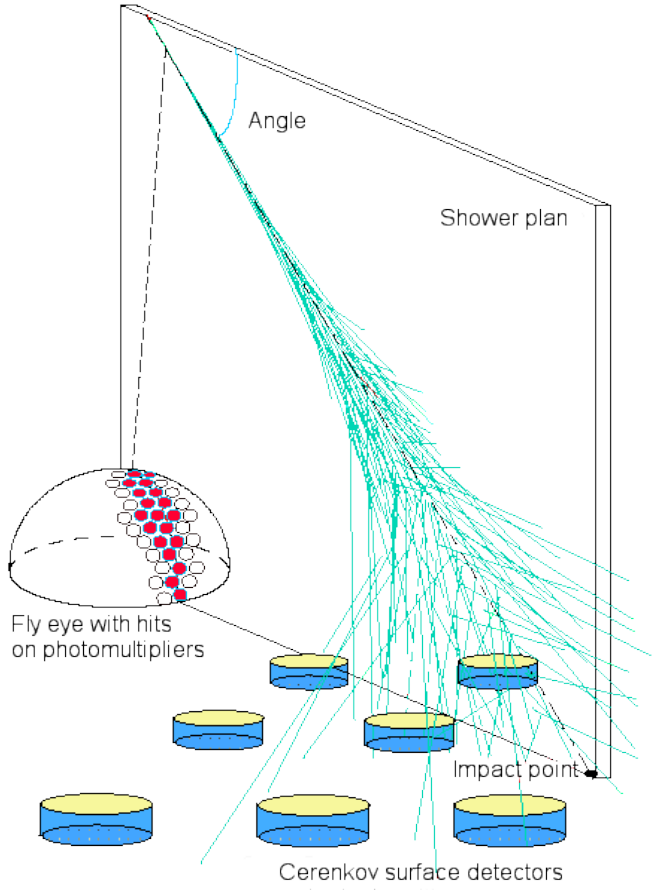

From EAS longitudinal profile to primary CR mass composition

Average depth of shower maximum $<X_{max}>$;

Width of distribution RMS(X_{max}) at a certain E

sensitive to primary composition

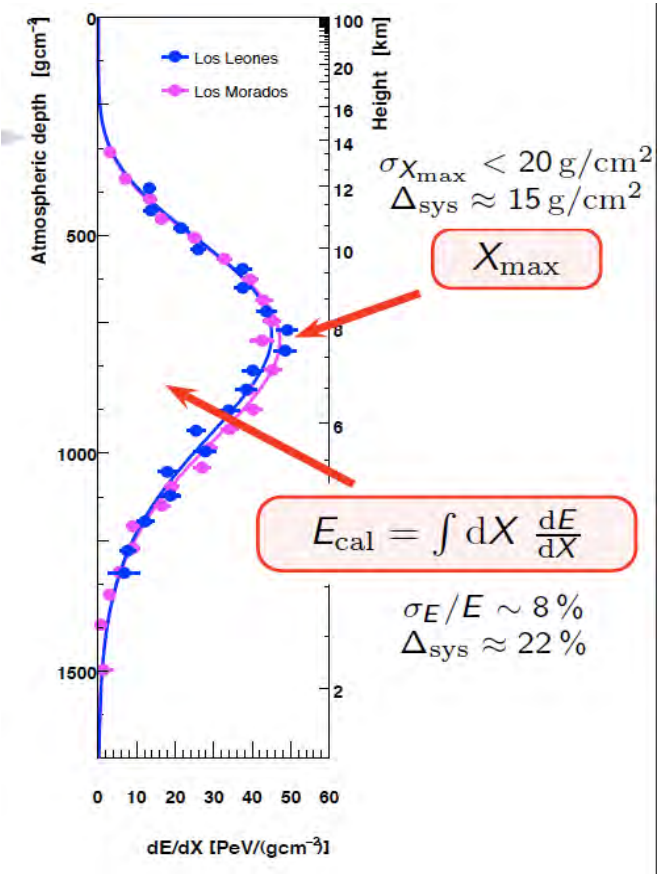

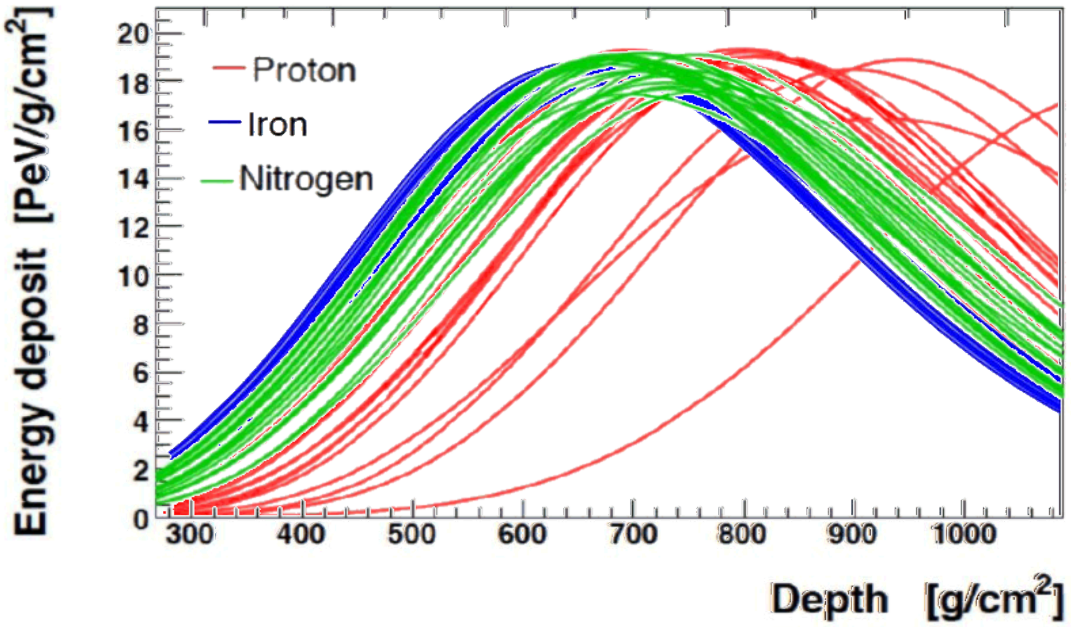

$$X_{max} \propto \log(E_0) - \log(A) \text{ (MC Sim.)}$$

From EAS longitudinal profile to primary CR mass

$\sigma(X_{max}) \approx 60$ g/cm^2

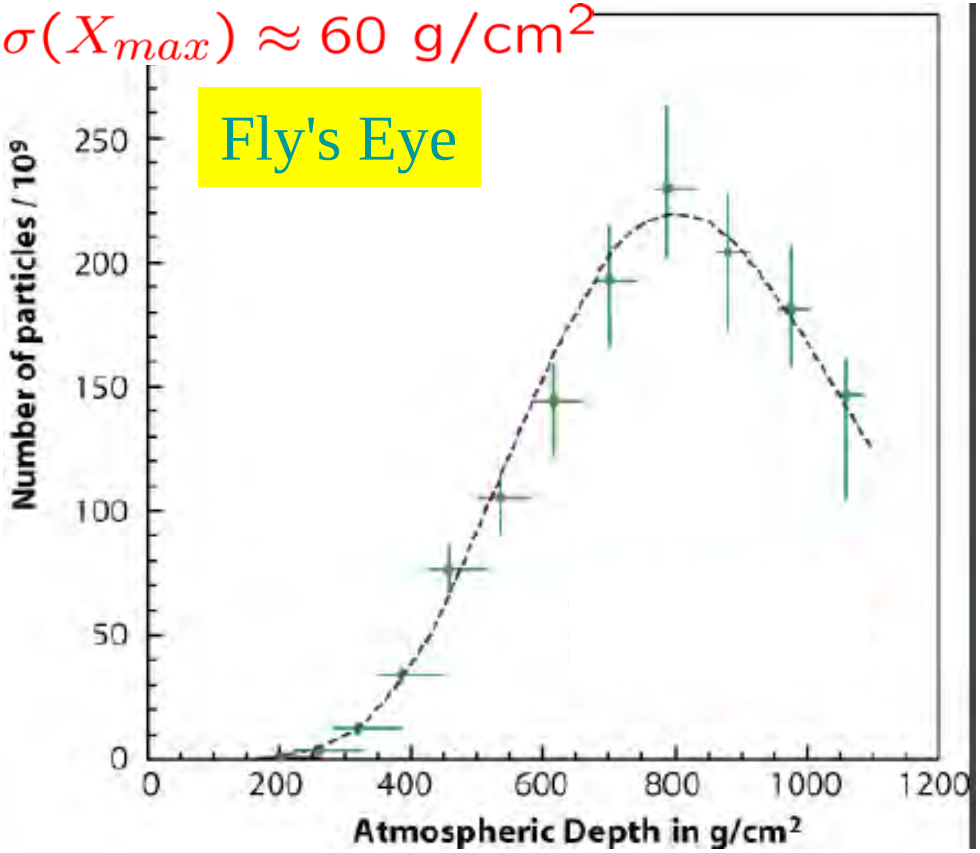

$\sigma(X_{max}) \approx 20$ g/cm^2

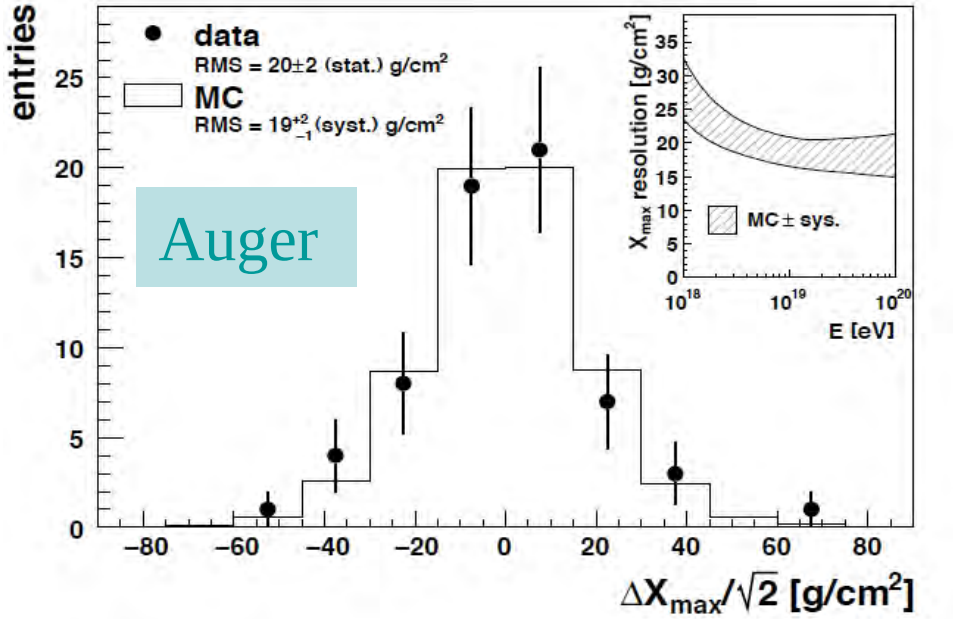

PROGRESS:

Fly's Eye showed experimental access to X_{max} through fluorescence

High precision now possible through higher resolution + stereo and hybrid measurements (around 20-25 g/cm^2)

N.B. : $< X_{max} >_{proton} - < X_{max} >_{iron} \approx 150$ g/cm^2

Delicate issues: great care in event selection (possible biases)

Important drawback: strong need for models in the interpretation

From EAS longitudinal profile to primary CR energy

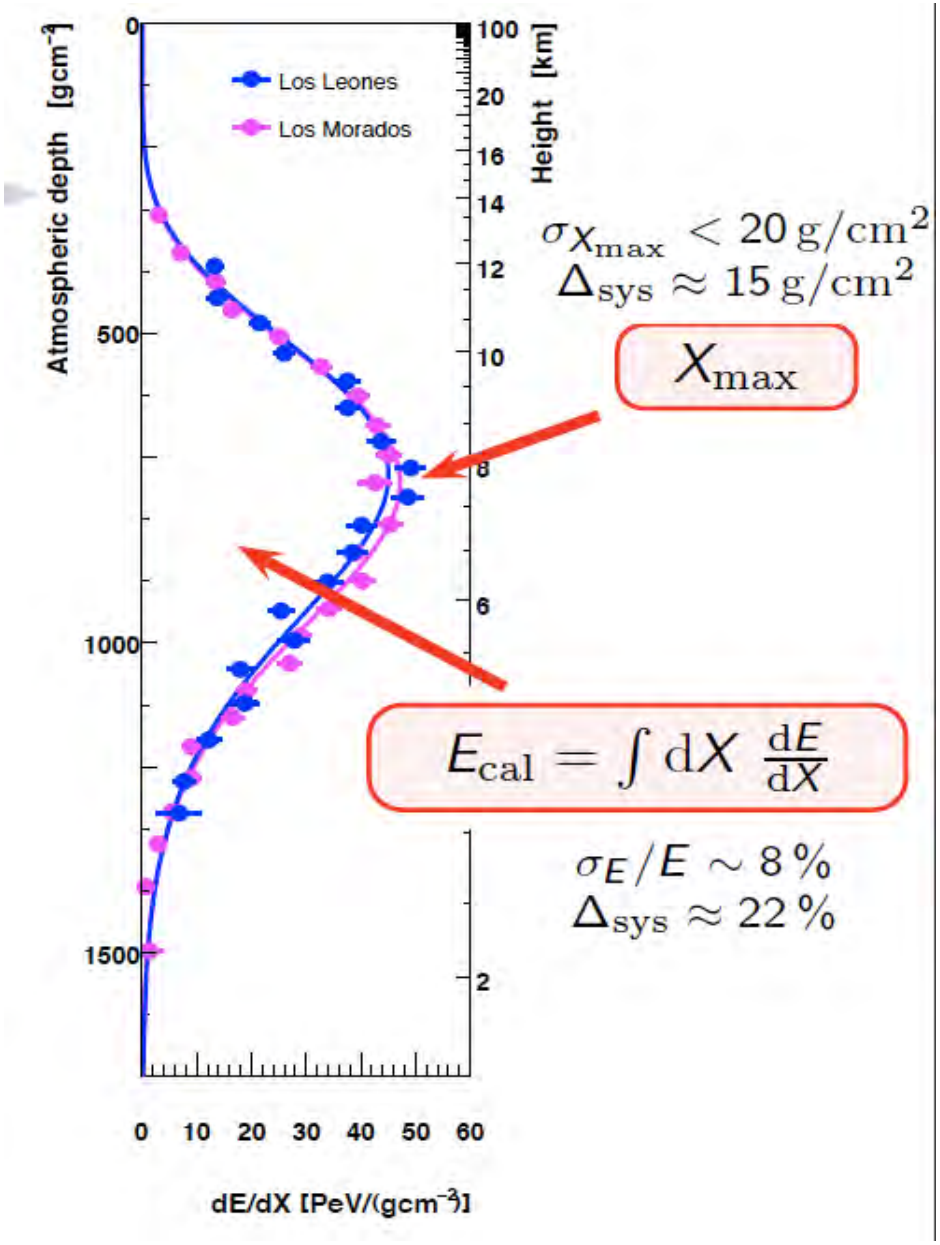

PROGRESS:

Calorimetric measurement of E with :

- Fluorescence technique
- Validated by Fly's Eye
- Largest uncertainty: fluorescence yield,
- Atmosphere, "missing" energy
- No hadronic model dependence

Fly's Eye

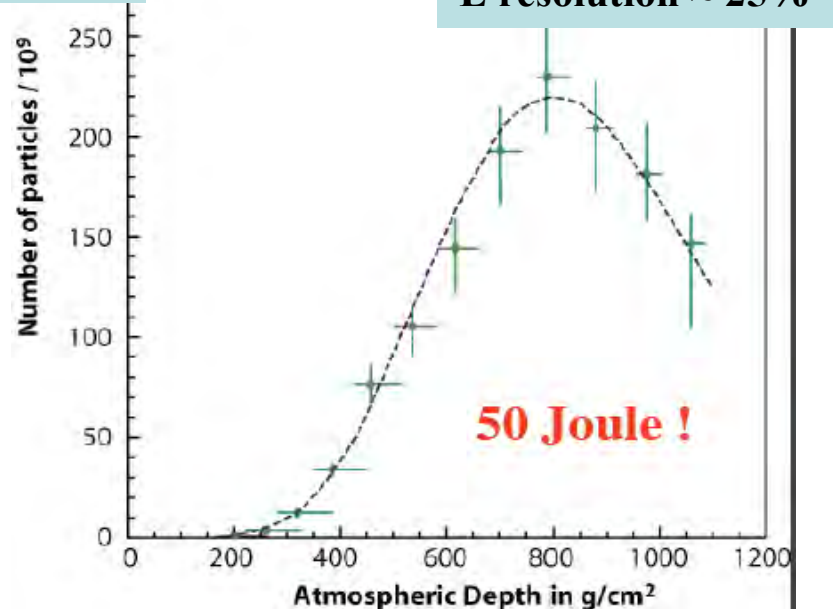

IDENTIFYING PARTICLES CONSTRAINING PARTICLE VELOCITY

Threshold Cherenkov counters

- Hundredth of examples on fix target experiments, where different threshold Cherenkov can be used to separate particle masses over a large range of momentum and over large solid angles.
- for example NA9 at CERN in the eighties, studying hadronic final state in deep inelastic scattering of 250GeV muons on H_2 target

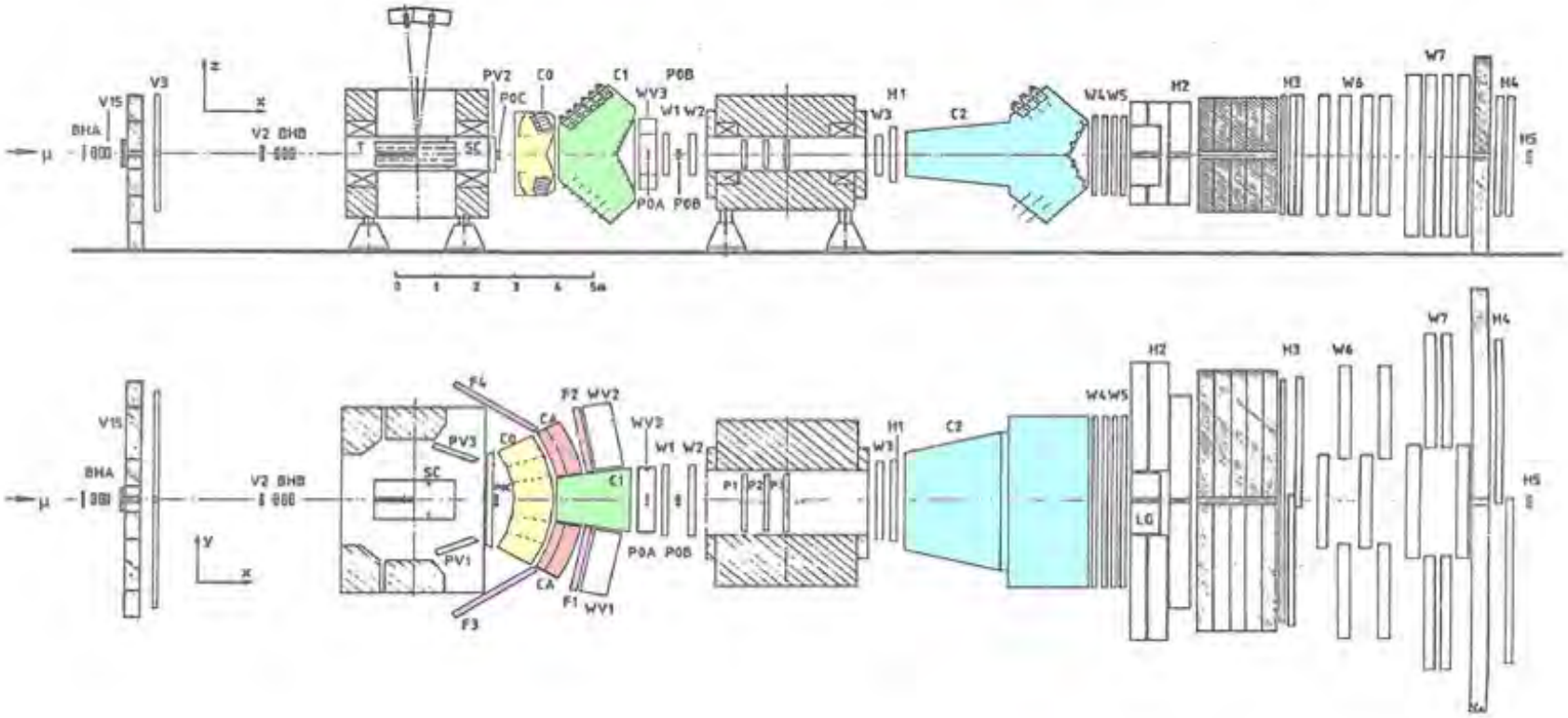

Threshold Cherenkov

- NA9:

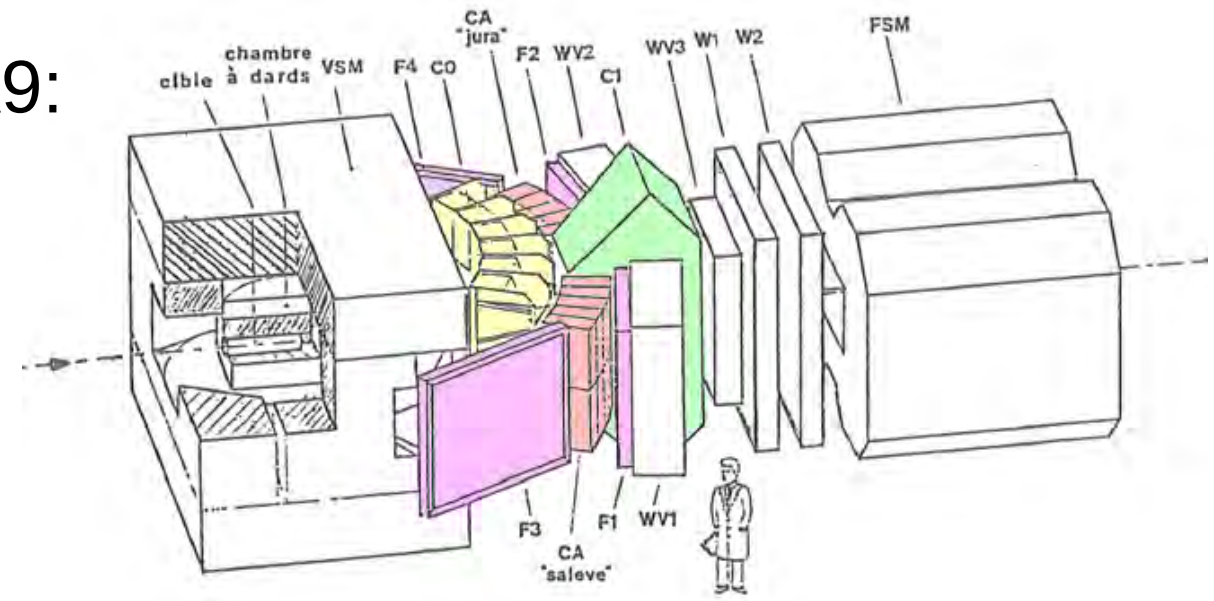

Detector	Angular range	Radiator type and index (n-1)	Thresholds for π , K , p [GeV/c]
TOF F1 F2 TOF F3 F4	$\pm(10-34)°$ $\pm(32-60)°$	Scintillator NE110	π / K < 1.5 π / K < 2.5
CA	$\pm(10-32)°$	SiO_2 silica aerogel 3×10^{-2}	0.6 , 2 , 3.8
C0	$\pm32°$	Neo-pentane 1.5×10^{-3}	2.6 , 9.1 , 17
C1	$\pm9°$	Nitrogen 3×10^{-4}	5.6 , 2 , 38
C2	$\pm7°$	Neon 6×10^{-5}	12 , 42 , 79

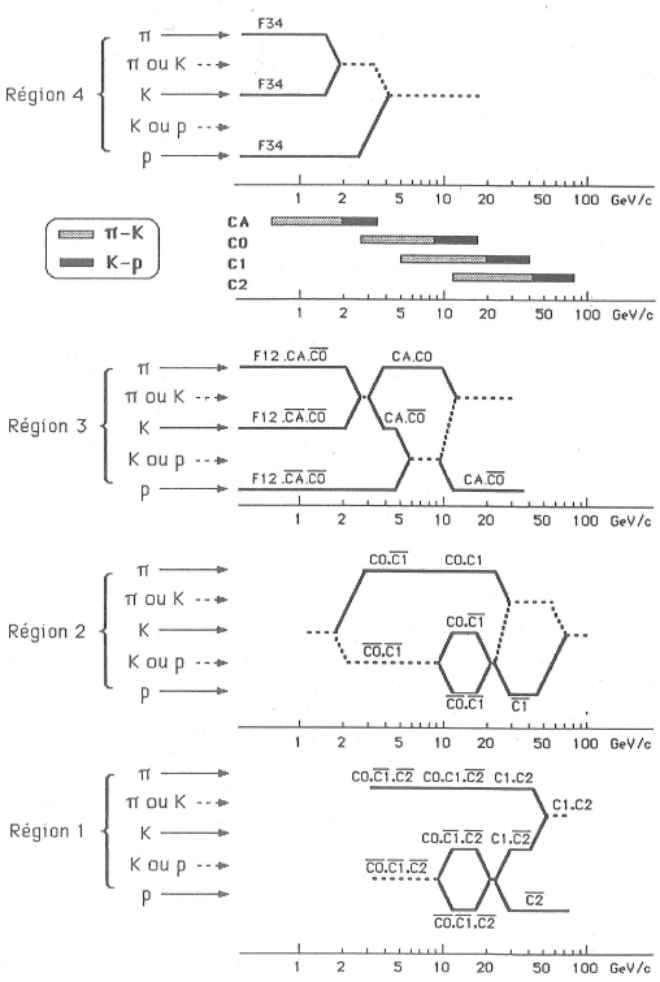

Threshold detectors

- A more recent example BELLE at KEKB
- CP violation in B mesons at e+e- collider.
- Current design: threshold aerogel Cherenkov counters to help discriminate π from K

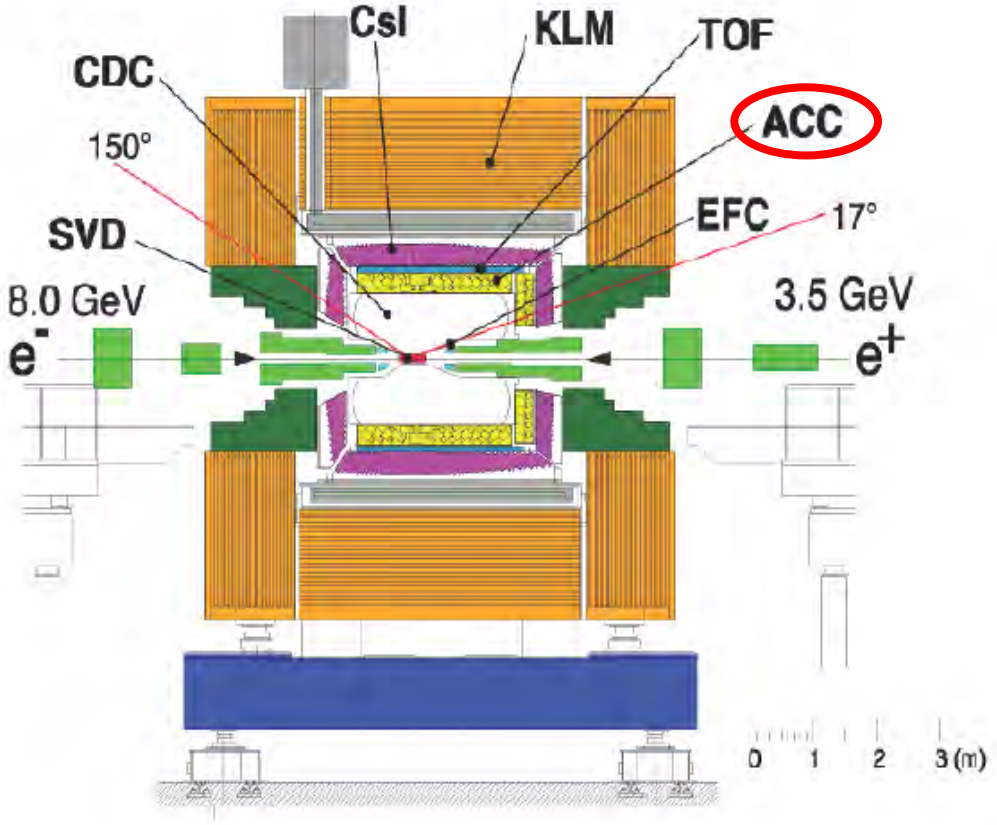

Threshold detectors

- A more recent example BELLE at KEKB

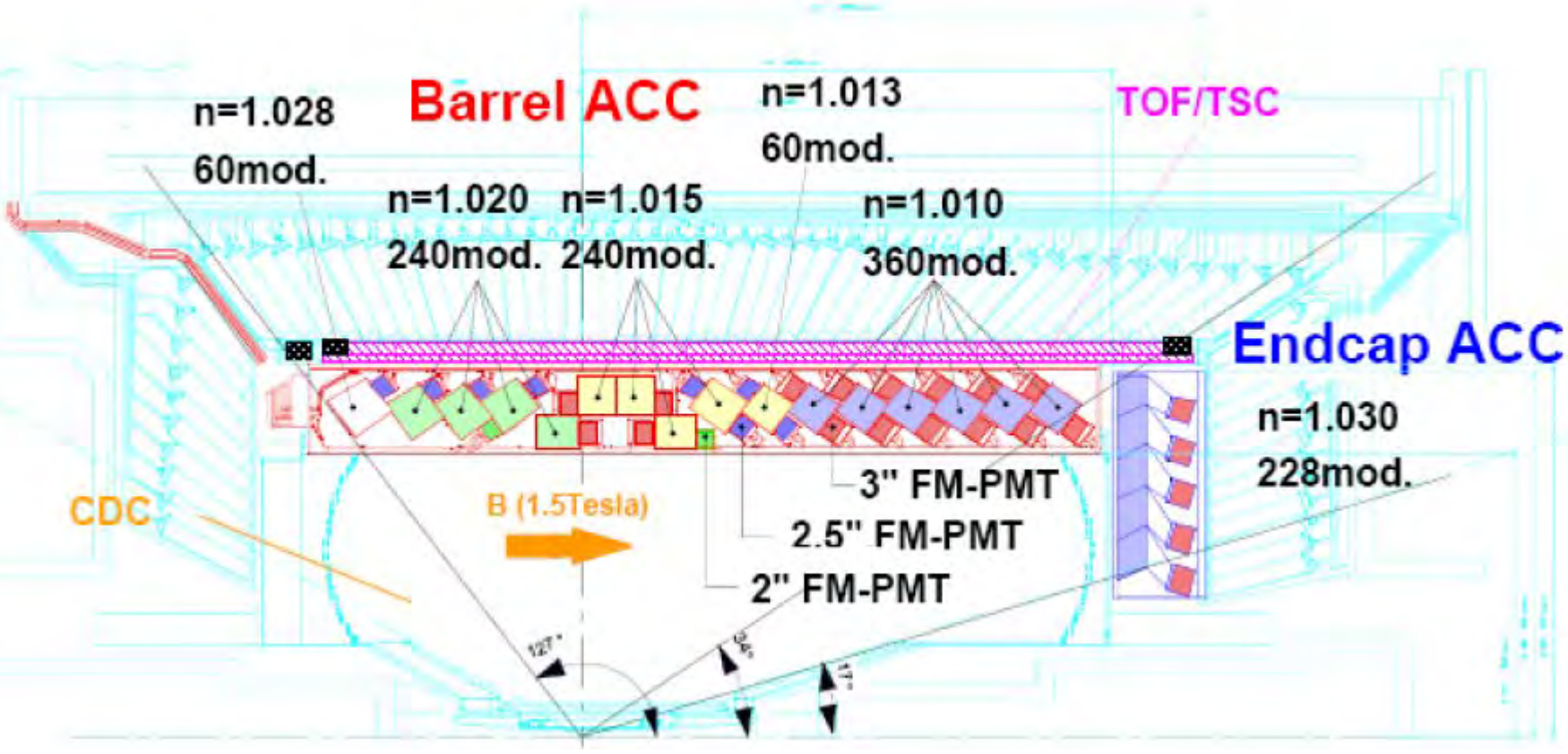

5 aerogel tiles inside a boxed lined with white reflector

Threshold detectors

- A more recent example BELLE at KEKB

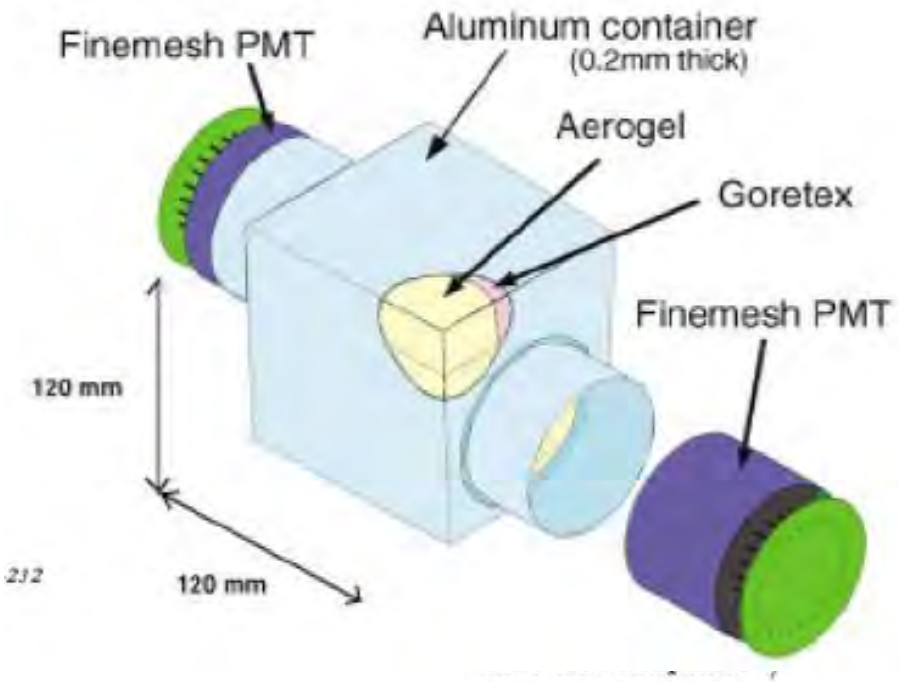

- Approx . 20 photoelectrons per Pion detected at 3.5 GeV/c
- More than 3σ separation

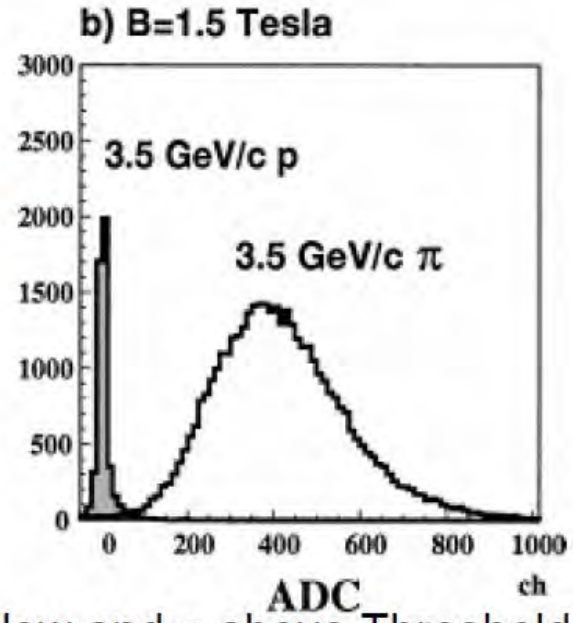

p below and π above Threshold

IDENTIFYING PARTICLES
MEASURING THE CHERENKOV ANGLE: DIFFERENTIAL, RICH, DIRC,

Differential Cherenkov Counters

- Used along beam lines to discriminate masses.
- Mesons beams ($\pi^{\pm}, K^{\pm}$), hyperon beams etc…
- Example: CEDAR at CERN, used since 70^{ies}

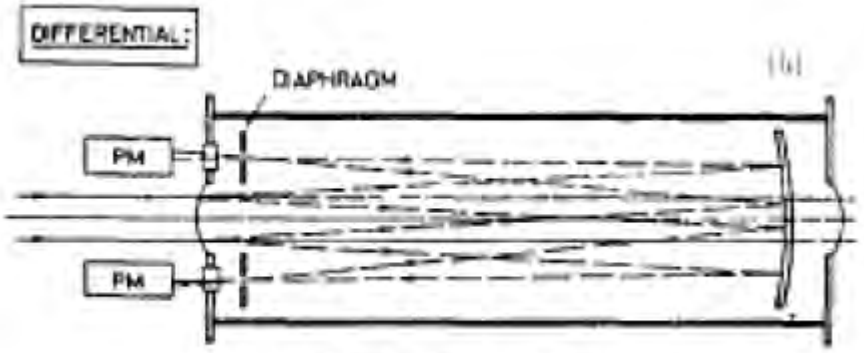

With a Gas radiator

			CEDAR - W	CEDAR - N
Velocity resolution		$\Delta\beta$	$5 \cdot 10^{-6}$	10^{-6}
Radiator	gas		N_2	He
	length	L	5.8 m	5.8 m
	pressure	P	1.6 - 8 bar	10 - 14 bar
	C angle	θ	30.8 mrad	25.8 mrad

RICH detectors

- Ring Imaging Cherenkov detectors
- First used on a fix target experiment, the OMEGA spectrometer at CERN (J. Séguinot & T. Ypsilantis)
- Major breakthrough with the DELPHI RICH
- Liquid and gas fluorocarbon radiators (2 detectors in //)
- Optimized for π, K, p separation up to 30 GeV/c

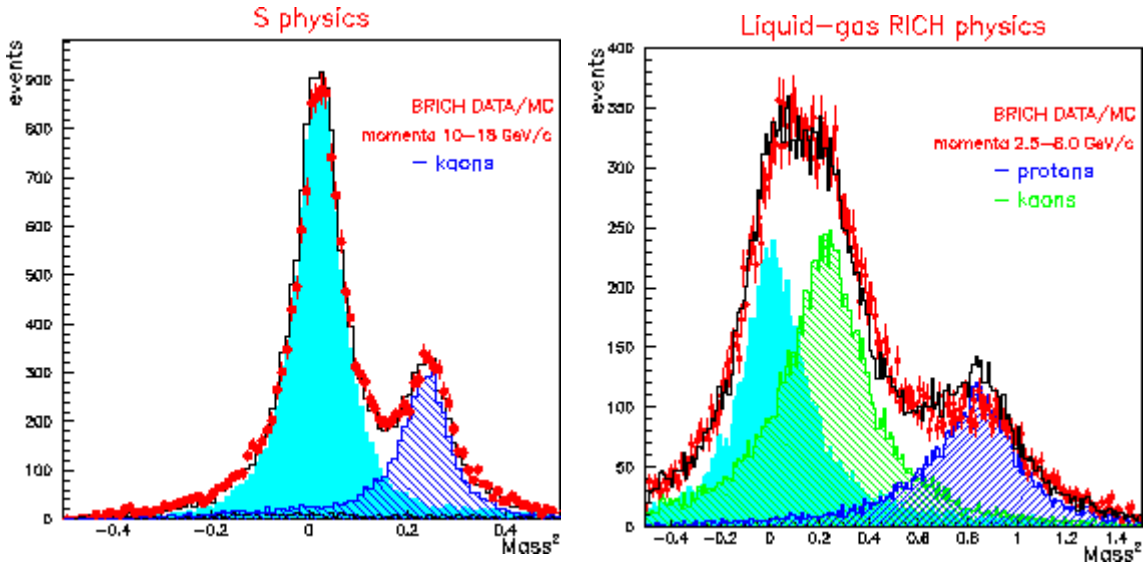

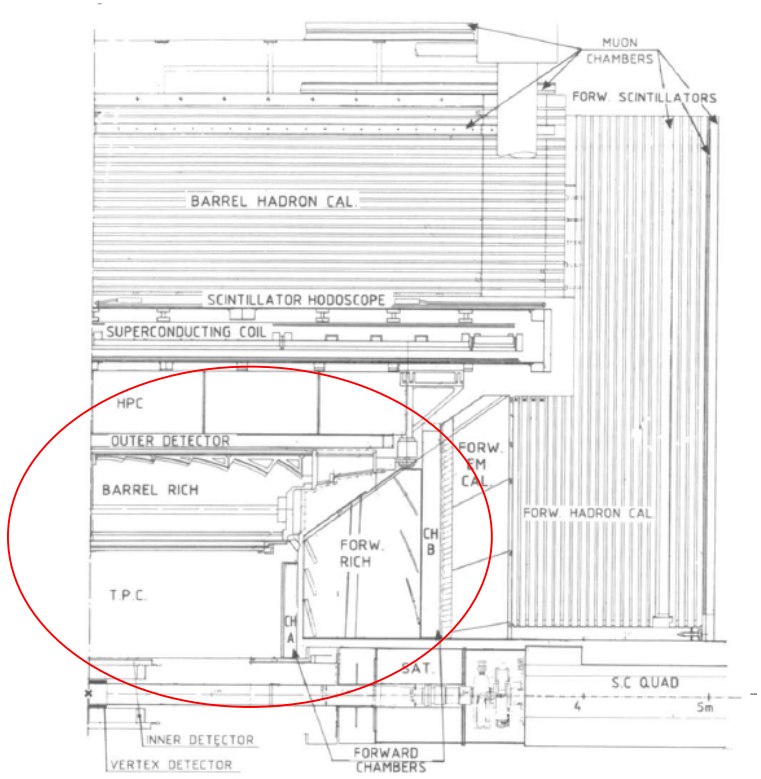

RICH detectors

- Ring Imaging Cherenkov detectors: measure both μ_C and N_{ph}

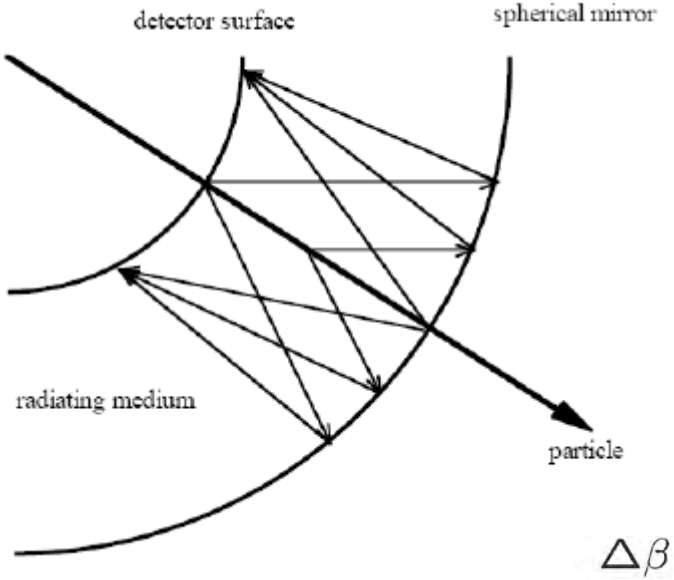

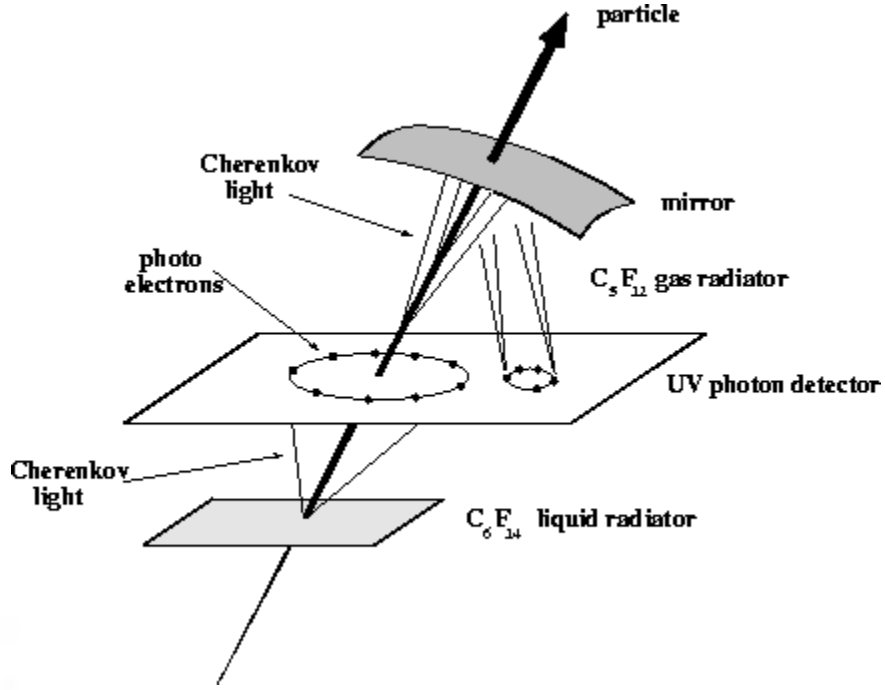

$$\frac{\Delta\beta}{\beta} = \tan(\theta)\Delta\theta_C$$

where $\Delta\theta_C = \langle\Delta\theta\rangle/\sqrt{N_{\text{ph}}} + C$

For 1.4m long CF_4 gas radiator at stp and $N_0 = 75\text{cm}^{-1}$,
$\frac{\Delta\beta}{\beta} = 1.6 \cdot 10^{-6}$

RICH also for astroparticles

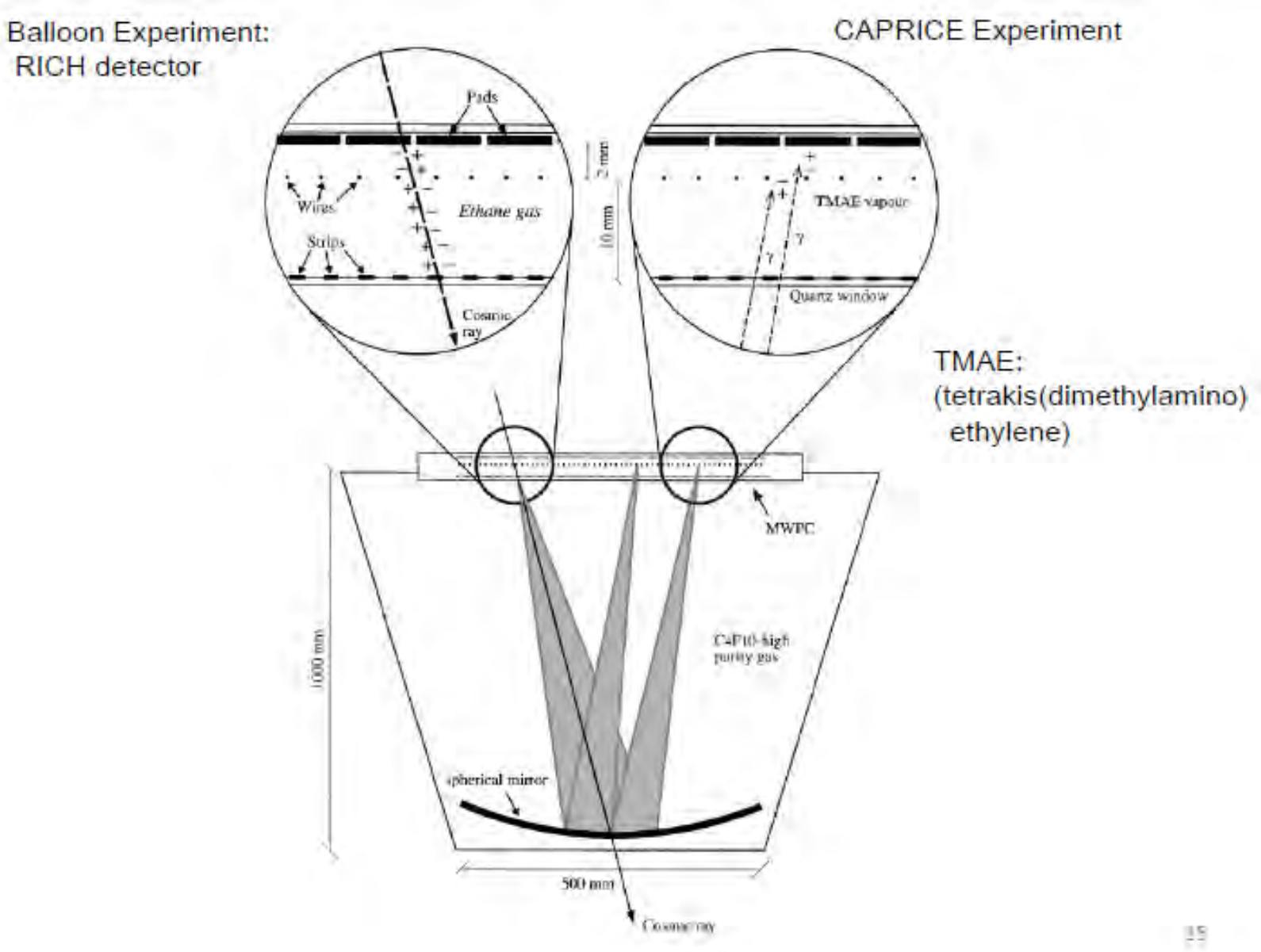

LHCb RICH

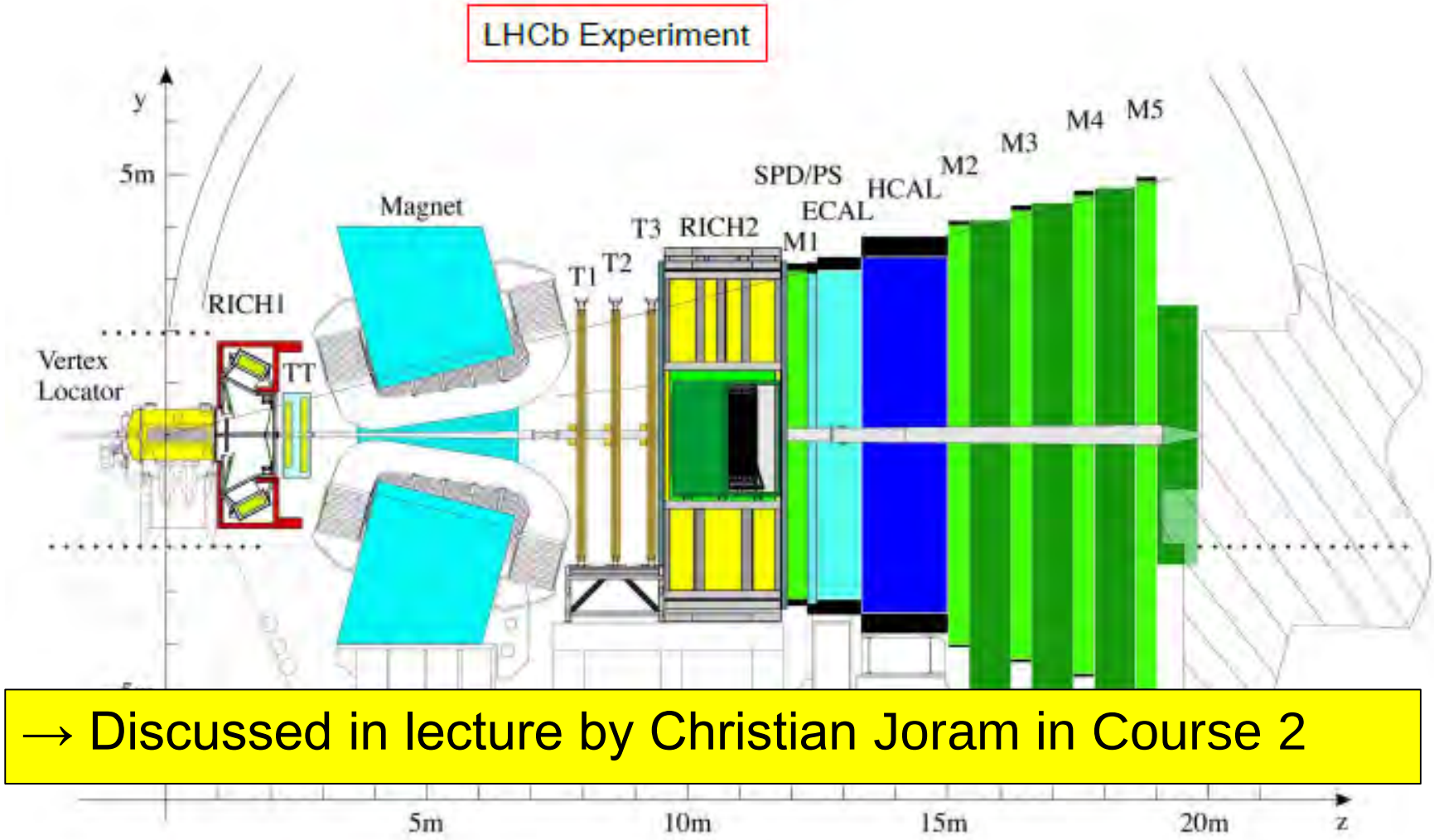

→ Discussed in lecture by Christian Joram in Course 2

- Precision measurement of B-Decays and search for signals beyond standard model.
- Two RICH detectors covering the particle momentum range 1→100 GeV/c using aerogel, C_4F_{10} and CF_4 gas radiators.

A strange idea: the DIRC

- Detection of Internally Reflected Cherenkov light
- DIRC used at BaBar
- Turned out to be successful and robust for $\pi - K$ separation.

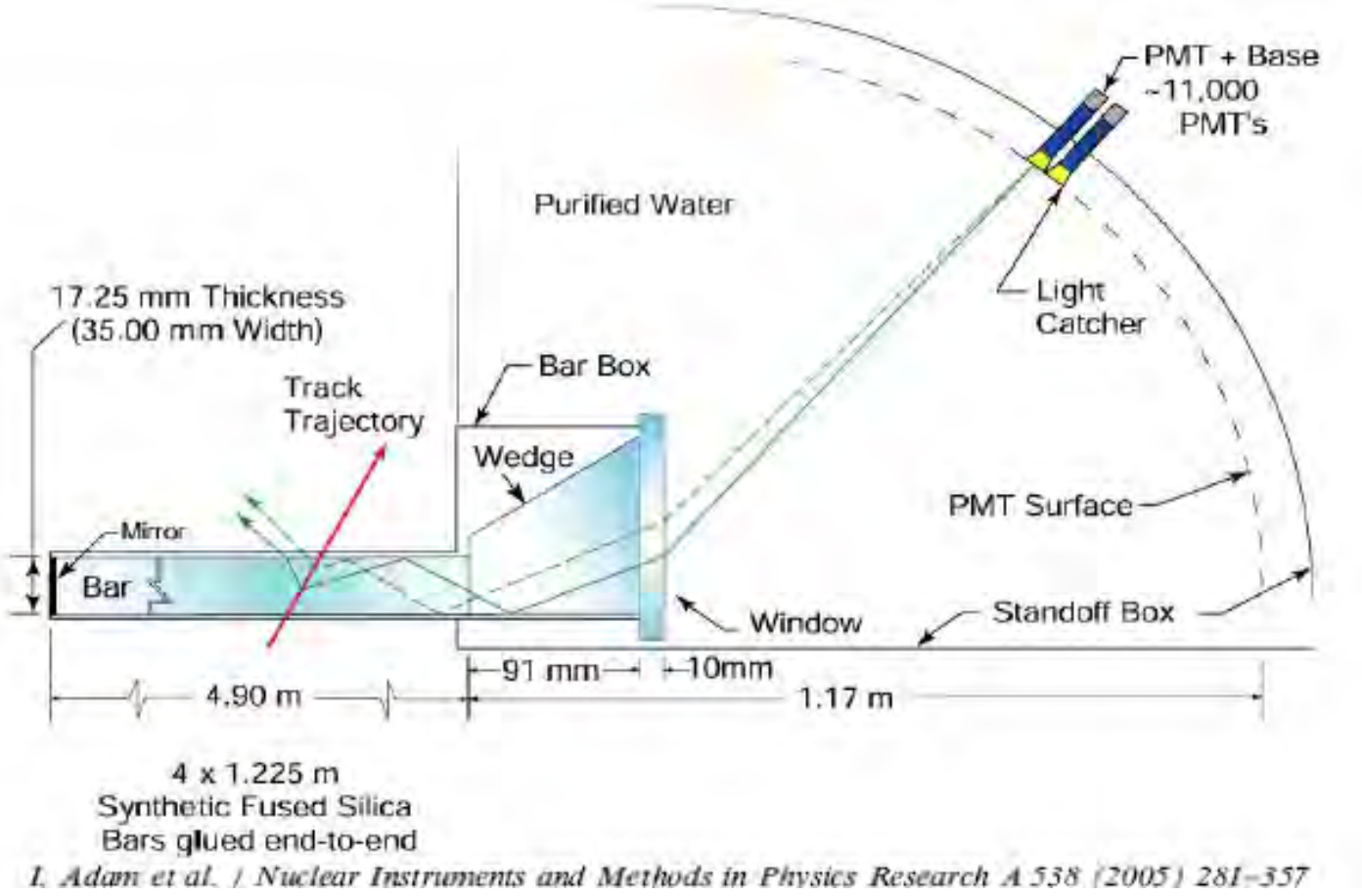

I. Adam et al. / Nuclear Instruments and Methods in Physics Research A 538 (2005) 281–357

A strange idea: the DIRC

- Detection of Internally Reflected Cherenkov light
- DIRC used at BaBar
- Turned out to be successful and robust for $\pi - K$ separation.
  - Material is actually synthetic fused silica (Spectrosil)
  - Cross section 17.25 mm x 35.0 mm.
  - Four 1.225 m long bars glued together with Epotek 301-2 optical epoxy to make one 4.9 m long DIRC bar.
  - 99.9±.0.1% transmission per meter at 442 nm
  - 98.9±.0.2% transmission per meter at 325 nm

IDENTIFYING PARTICLES CHARGE MEASUREMENT OF PRIMARY CR

How to characterize the primary particle?

- Mass m
- Electric charge Ze
- Velocity $v = \beta c$
- Lorentz Facteur $\gamma = E/mc^2$
- Momentum $p = mc\beta\gamma$
- Kinetic energy $T = mc^2(\gamma - 1)$

How to characterize the primary particle?

Detector	Observable	Link with the particule
Magnetic spectrometer	Rigidity & Sign of Z	pc/Ze
Time of flight	Velocity/c	β
Proportionnal counters Scintillators Ionisation chamber	Ionisation	$dE/dx = Z^2 f(\beta)$
Čerenkov effect	Č photons density	$dN/dx = Z^2 g(\beta)$
Transition radiation	Number of photons X	$N = Z^2 h(\gamma)$
Calorimeter	Deposited energie	$mc^2(\gamma - 1)$

Two important radiations for particle identification

Two effects of the polarization induced by charged particles in dielectric medium

Proportionnal to Z^2

- Čerenkov radiation : si $v > c/n$
  Sensitive to $\beta = v/c$

- Transition radiation : at the interface of $\neq$ dielectric media
  Sensitive to $\gamma = E/(mc^2)$

Cherenkov imaging (RICH) and charge measurement

RICH principle →

AMS 2 Prototype →

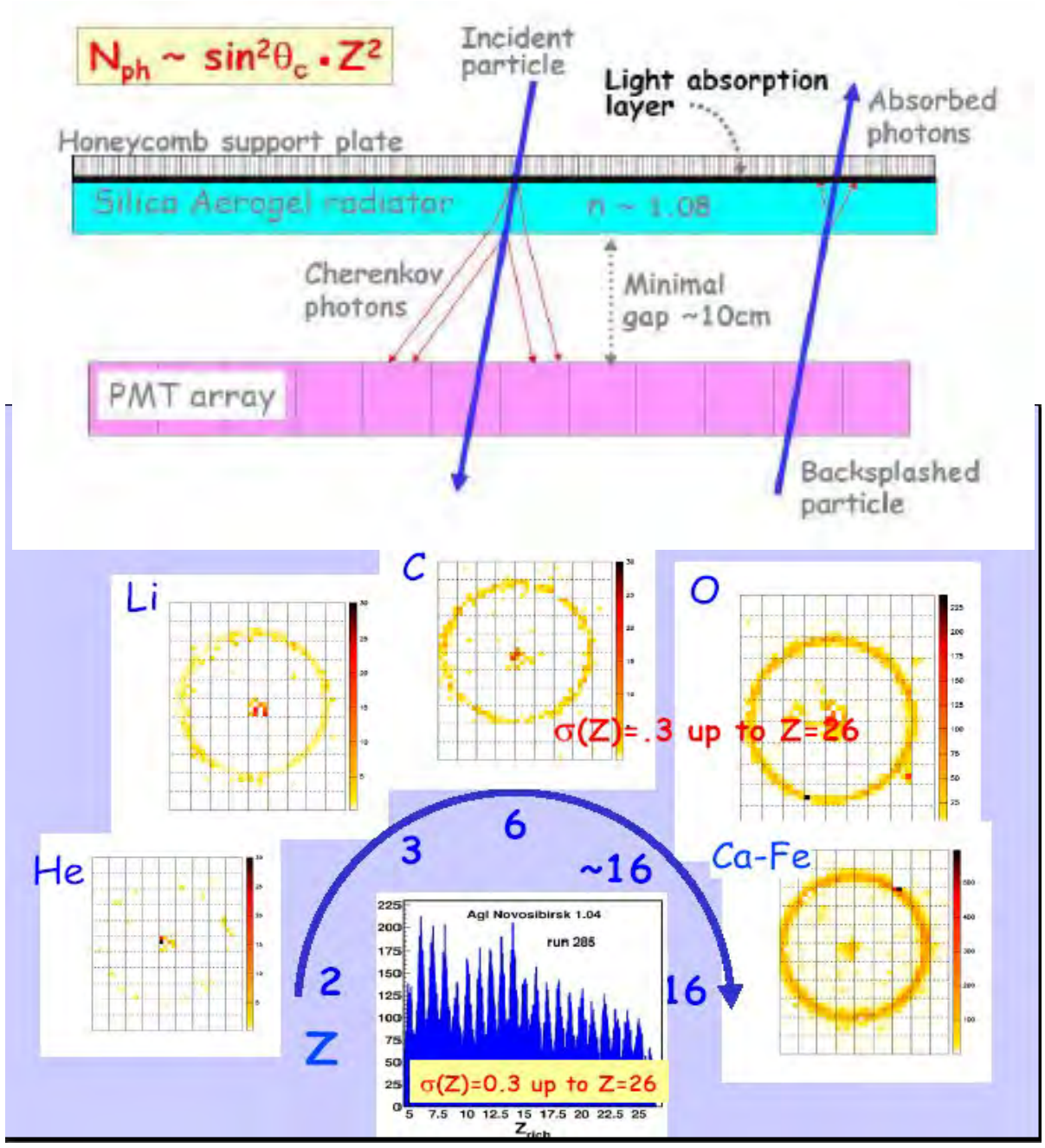

AMS-2 On Board ISS

Mission Number: STS-134
Launch: **May 19, 2011**
Orbiter: Endeavour

Space spectrometers

	AMS-1 (June 1998)	PAMELA (June 2006 - ...)	AMS-2 (May 2011 - ...)
Spectrometer Acceptance	0.82 m^2 sr	20.5 cm^2 sr	0.82 m^2 sr
Spectrometer	Permanent magnet Nd Fe B 0.15 T BL^2 = 0,15 T m^2 6 plans (Si)	Permanent magnet Nd Fe B 0.48 T BL^2 = 0,10 T m^2 6 plans (Si)	Permanent magnet Nd Fe B 0.15 T BL^2 = 0,15 T m^2 6 plans (Si)
Time of Flight	yes	yes	yes
Cherenkov	Aerogel (threshold)	-	Ring Imaging Ch.
Transition rad	-	yes	yes
Neutrons det.	-	^3He	-
Anticoincidence	-	yes	yes
Calorimeter	-	16,3 X_0 W+22 plans (Si)	16 X_0 Pb+fibers sc.

A precision, multipurpose spectrometer up to TeV

TRD
Identify e^+, e^-

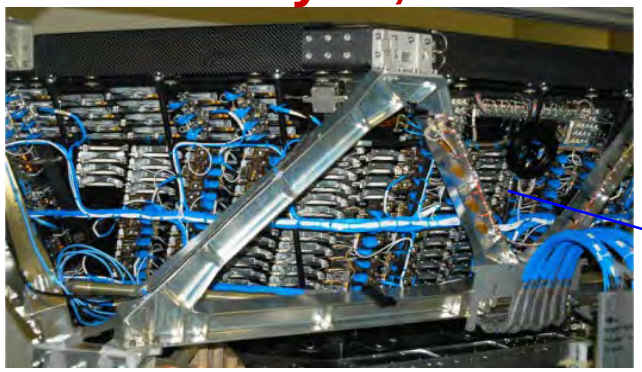

Silicon Tracker
Z, P

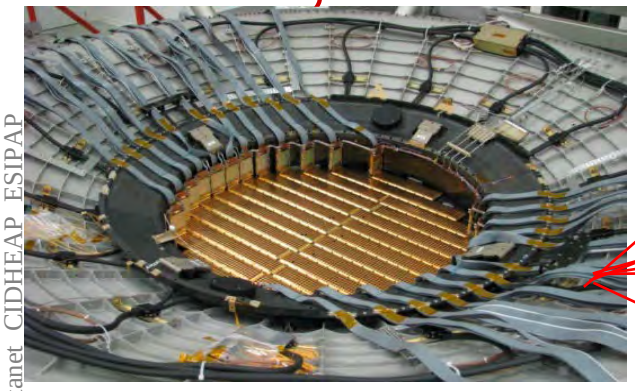

ECAL
E of e^+, e^-, γ

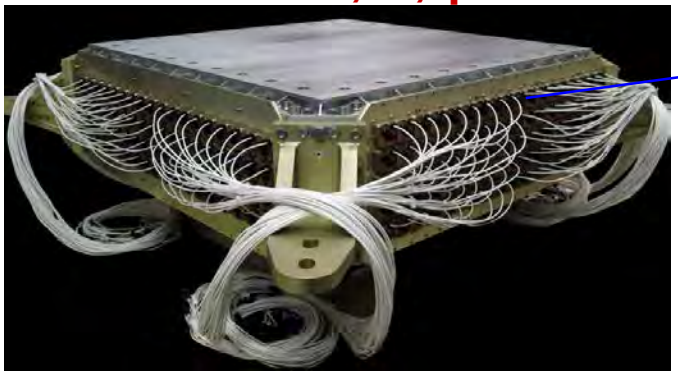

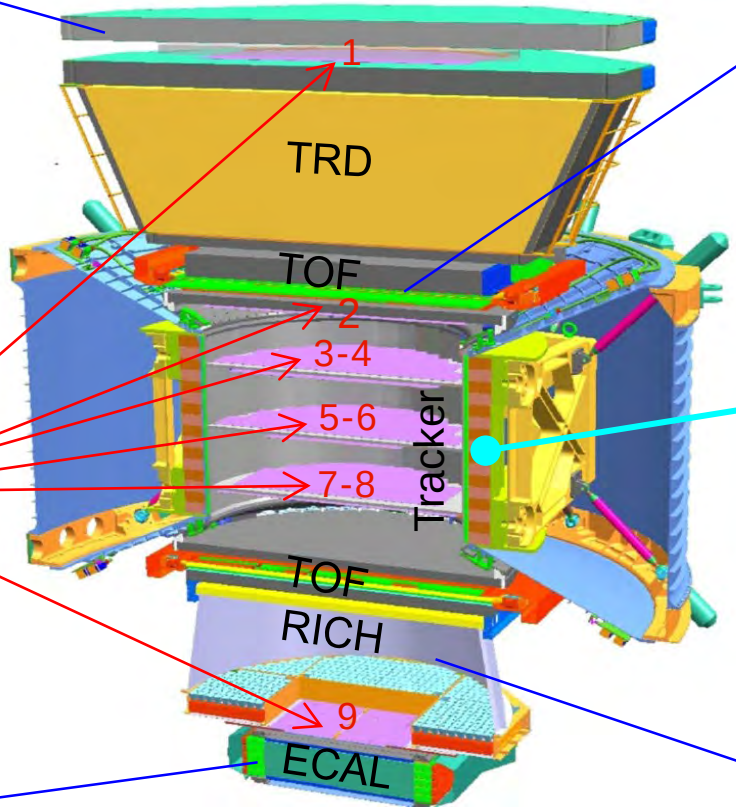

***Z, P** are measured independently by the Tracker, RICH, TOF and ECAL*

TOF
Z, E

Magnet
±Z

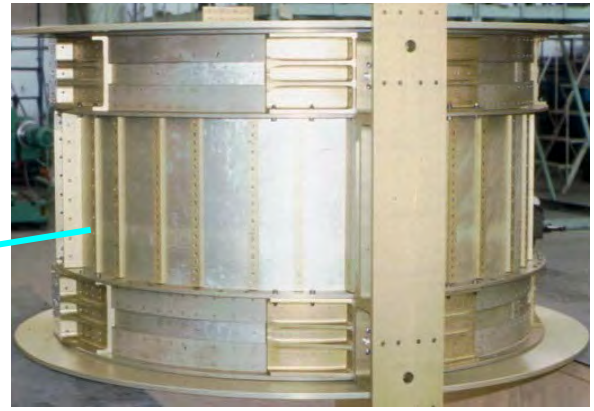

RICH
Z, E

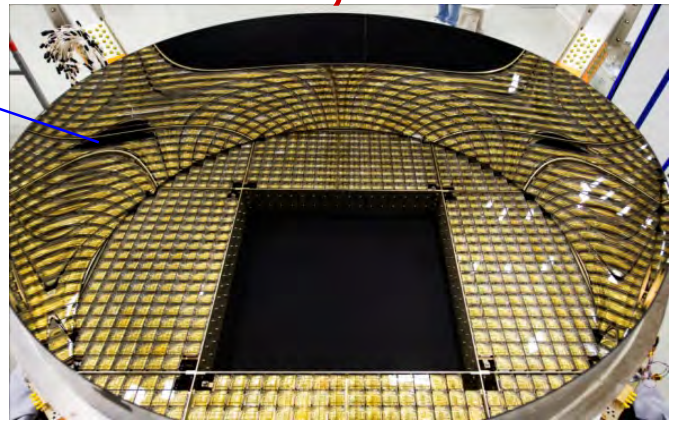

AMS charge identification

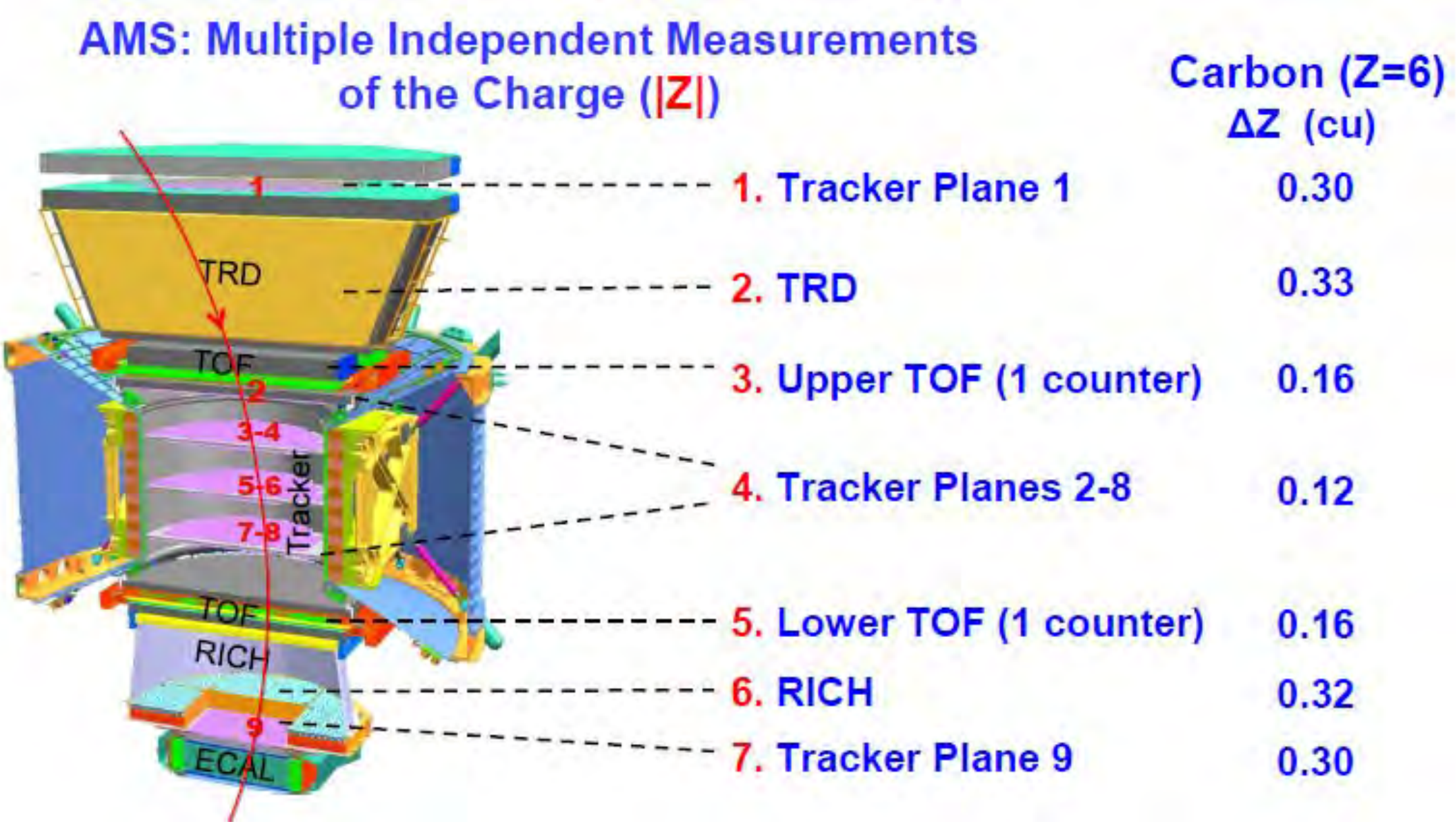

Full coverage of anti-matter & CR physics

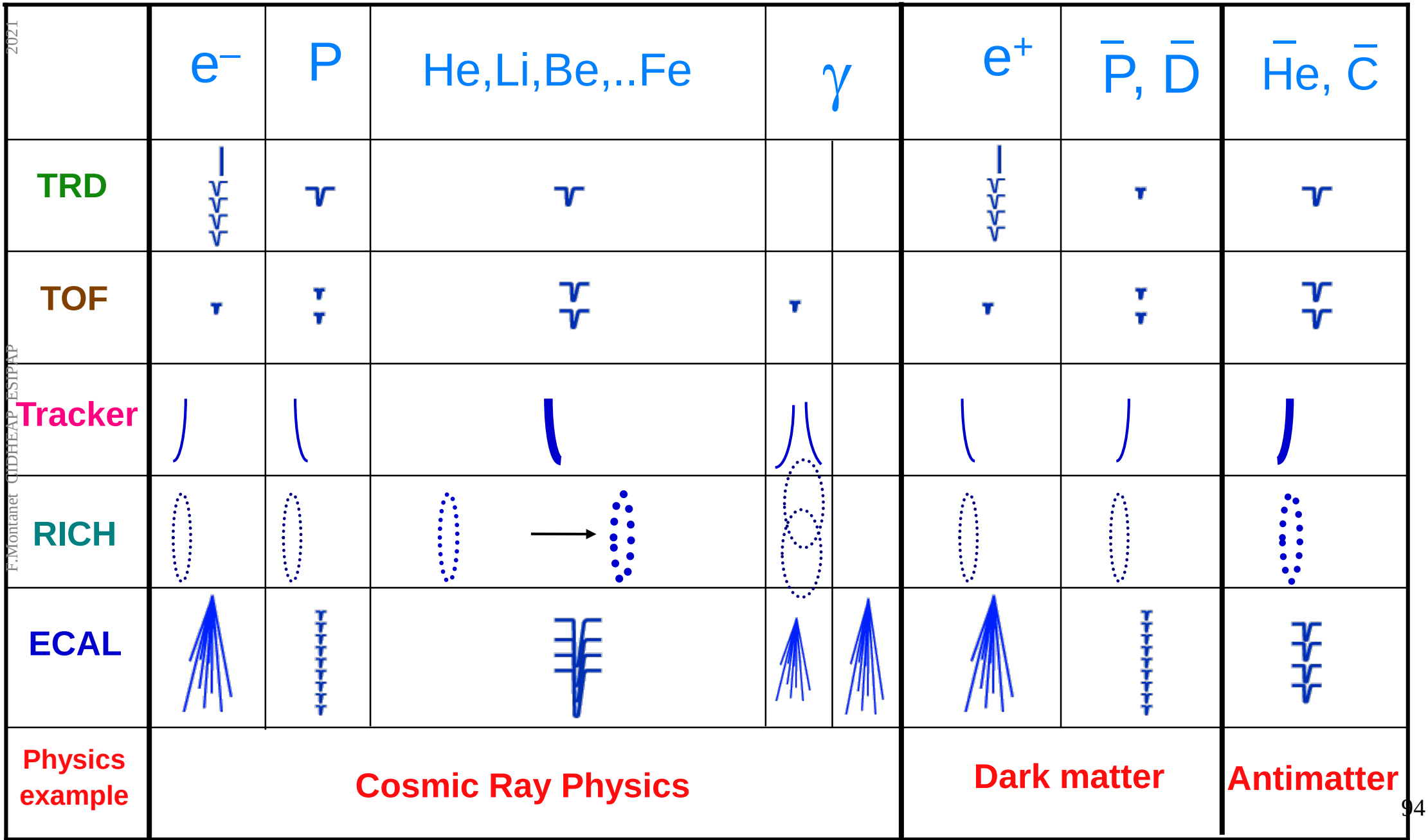

AMS Nuclei Measurement on ISS

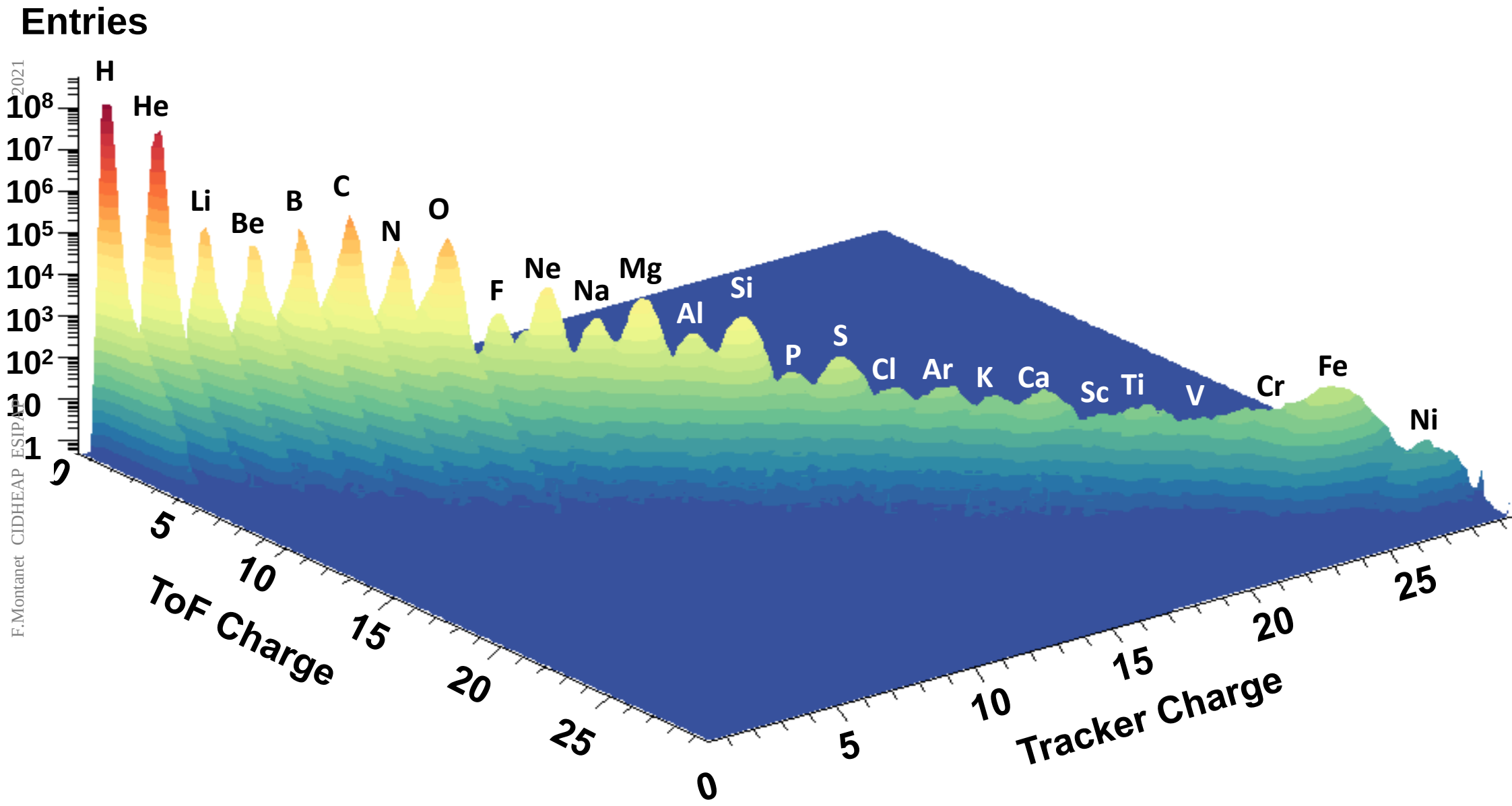

CREAM

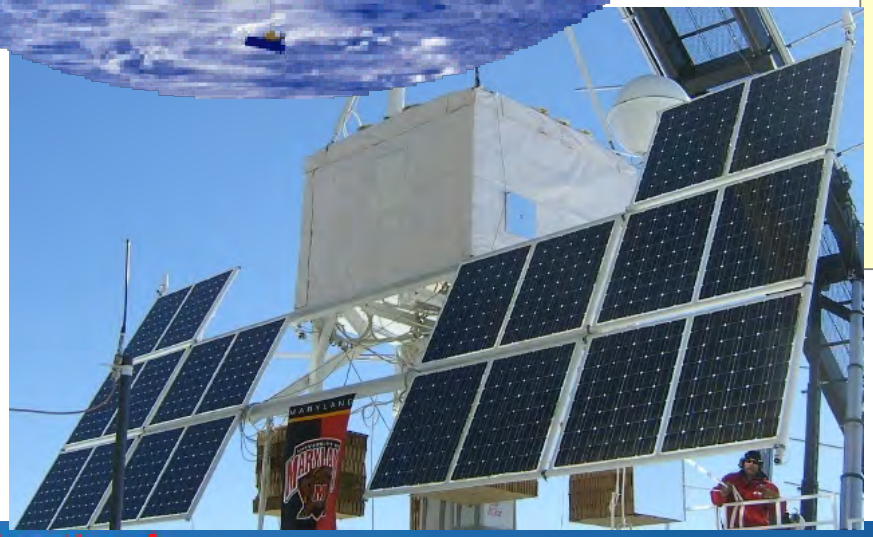

Ultra Long Duration Balloon

ULDB Proj., Adv.Sp.Res33,1633(2004) :

NASA project to develop

- Flight of < 100 days
- Payload · 2 tons
- Alt 33000 meter
- CREAM n° 1 : 2006 (2005/LDB)

F.Montanet CIDHEAP ESIPAP

CREAM

Cosmic Ray Energetics and Mass

- Objectives :
  CR composition and spectrum of the different elements
  (from TeV to ~500 TeV)
- Acceptance : 2,2 m^2 sr
- Energy measurement:
  - Calorimeter 20 X_0 (W + scint. fibres)
  - Transition Radiation Detector
- Identification :
  - TRD
  - Cherenkov detector "CHERCAM" similar to AMS-2

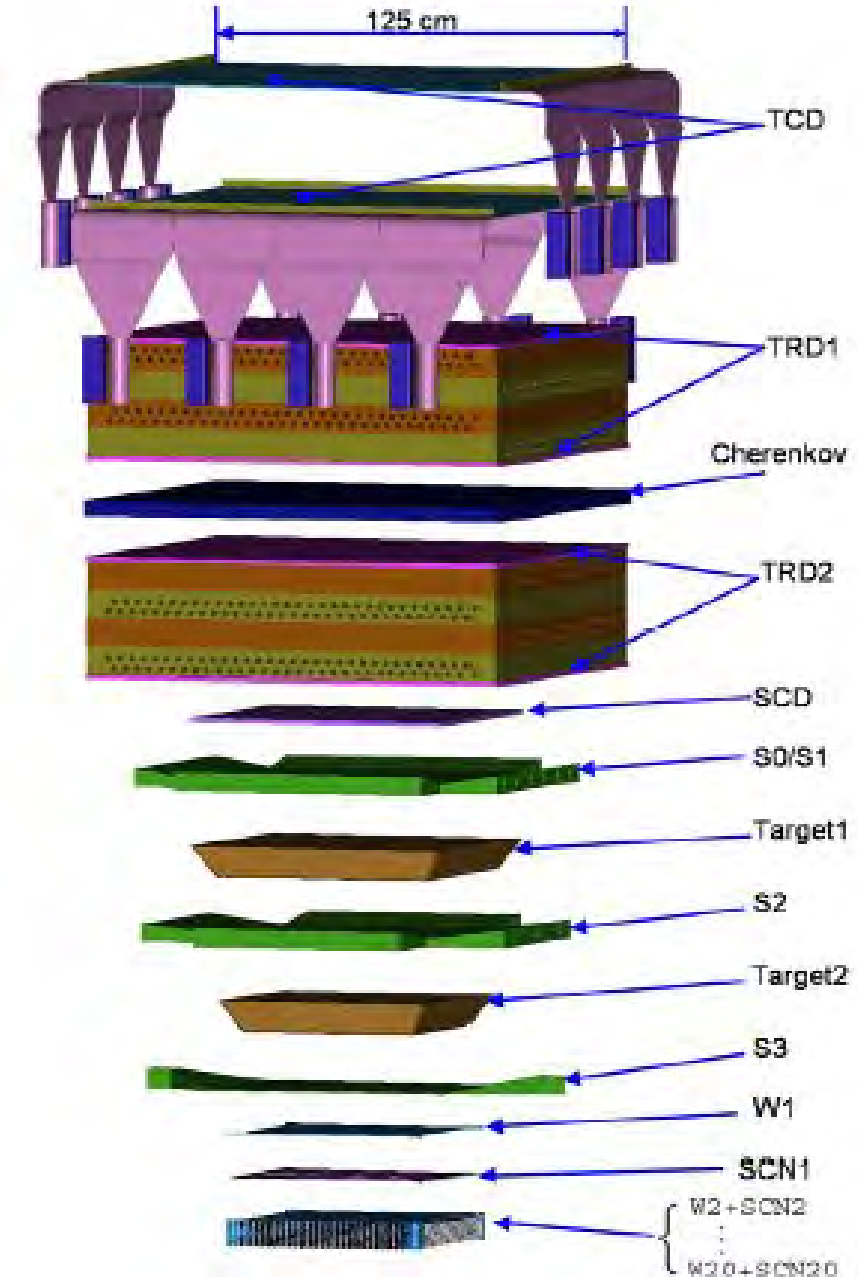

CREAM experiment

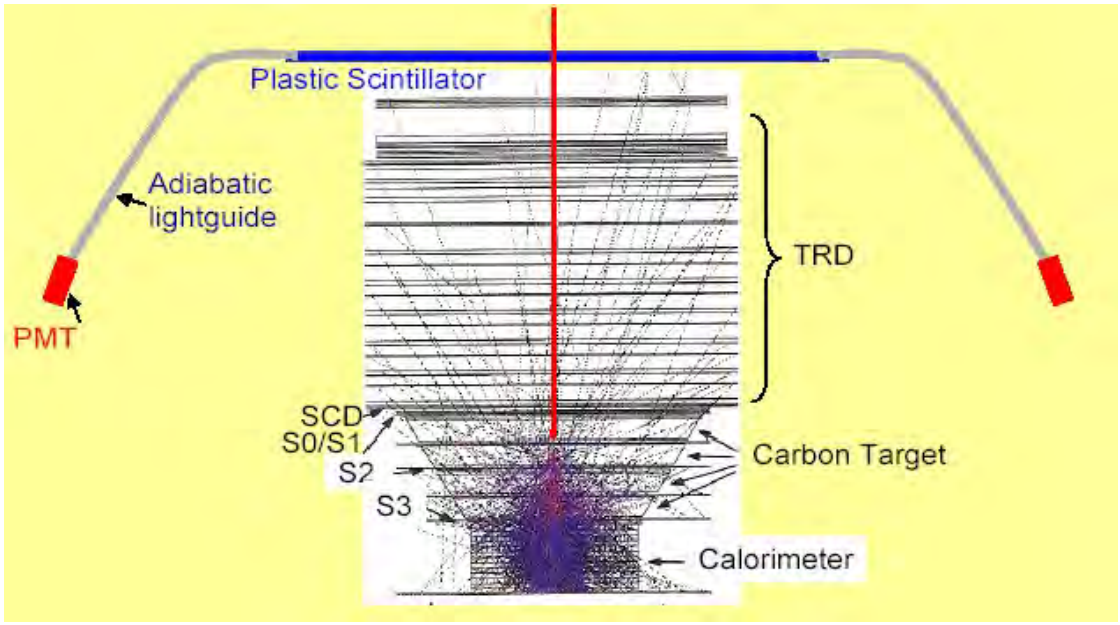

- At TeV energies, the interaction of CR in the calorimeter induces many backscattered secondary particles that one have to veto.

- The "CHERCAM" cherenkov solves this problem by measuring accurately the time of any through going particle as well as achieving a precise charge measurement (± 0,3 e)

CREAM experiment

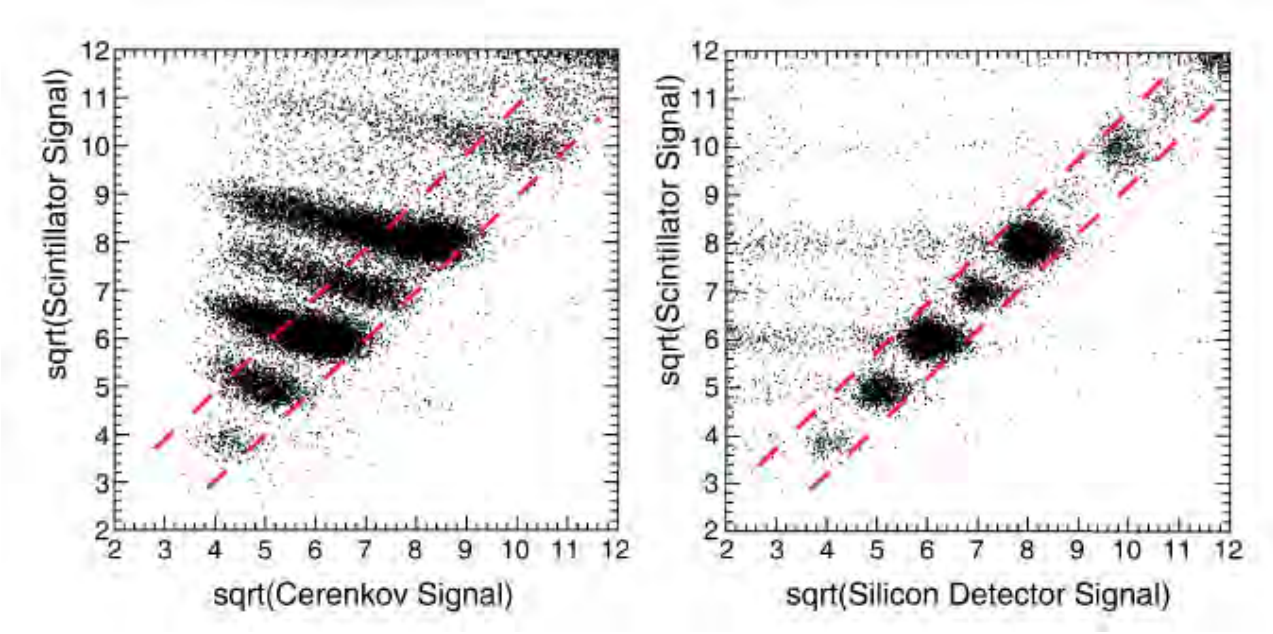

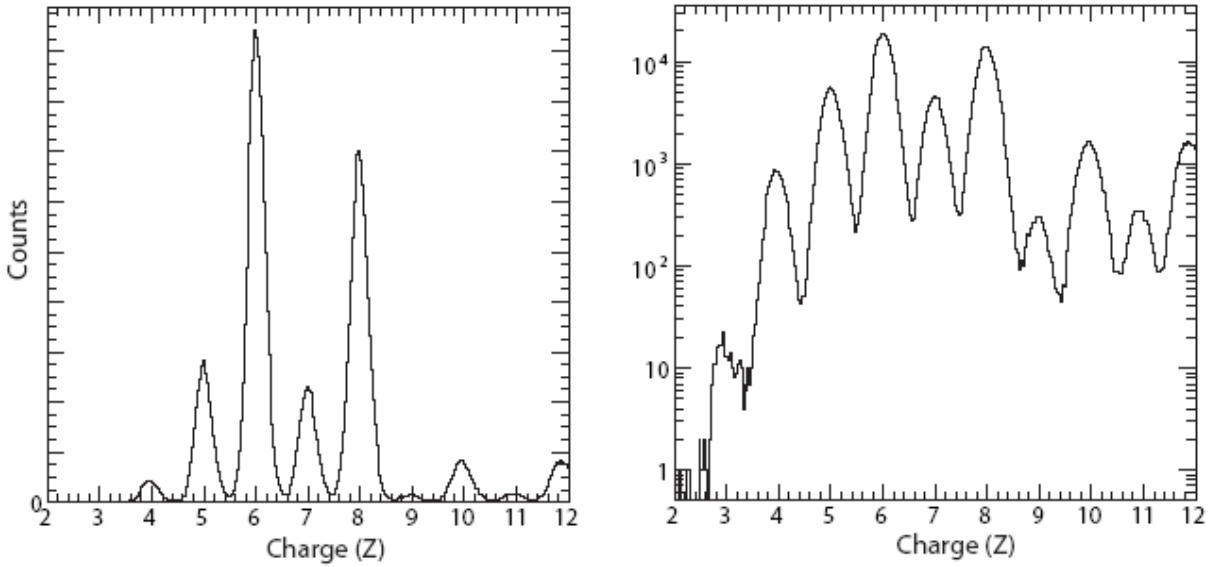

ATMOSPHERIC GAMMA-RAY SHOWERS BY CHERENKOV TELESCOPES

10 γ
300 GeV

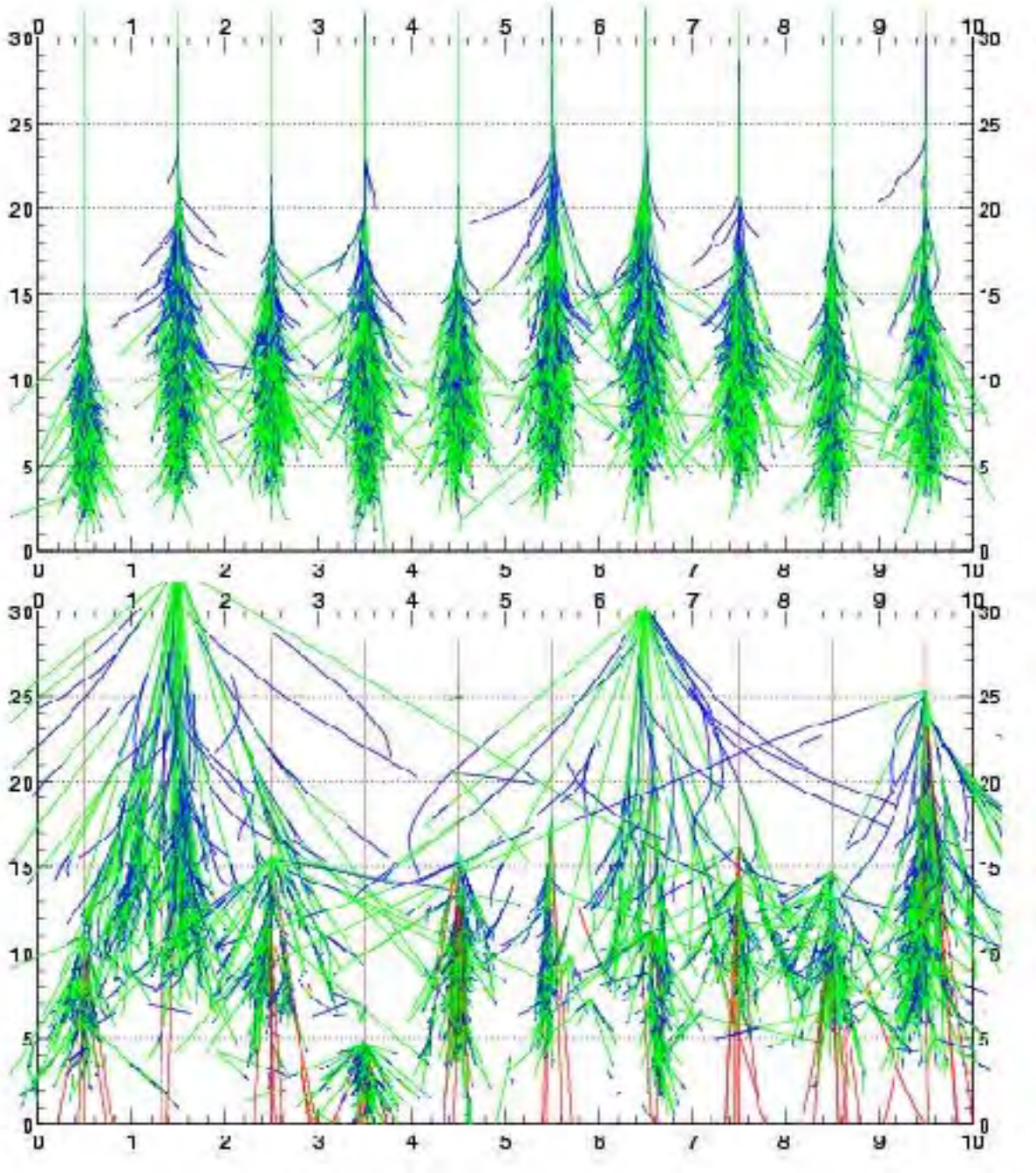

10 protons
300 GeV

Simulations de

M. de Naurois

Electromagnetic showers ($e^{\pm}$ or γ primary)

Dominating phenomena

- Radiation processes:
  - Bremsstrahlung of $e^{\pm}$
  - Pair production (>MeV) pairs $e^{+}e^{-}$
- Multiple scattering (small angular deflections) of $e^{\pm}$
- Energy losses by $e^{\pm}$
  - ionization
  - Atoms excitation

In the coulombian field of nuclei

γ induced
shower 300 GeV

Roughly
symmetric
around the axis

Small transverse
dispersion
(multiple scattering)

(almost) no muons
unless E_0>1 PeV

Essentially

e+ e- and γ
secondaries

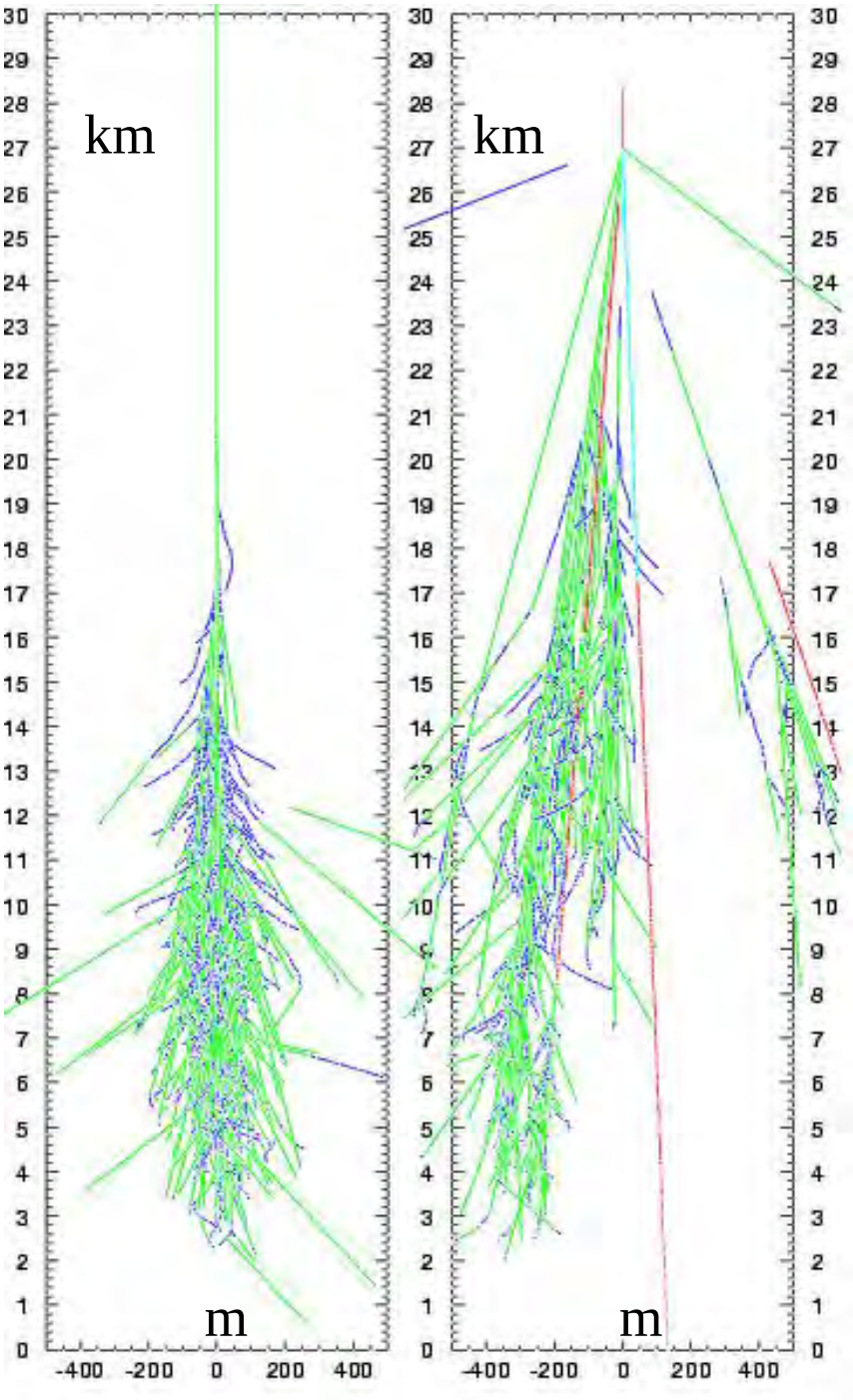

proton induced
shower 300 GeV

Large transverse
momentum

Muon component
(from mesons decays)

A hadronic shower
does contain
EM sub-showers

Optical photon emission by showers

- Showers charged particles emit light:
  - Cherenkov light : very collimated along the shower axis (Cherenkov angle at 1 Atm. ≈ 1°) threshold depending on the altitude : at ground 22 MeV for $e^{\pm}$ et 4.5 GeV for $\mu^{\pm}$

    (≈ 20 photons per m per β≈1 charged particle at 1 atm)

    Essentially used for gamma-ray astronomy
  - Nitrogen fluorescence: isotropic emission

    (≈ 4 photons per electron per m)

    Essentially used at UHE ≥ 10^{17}eV.
- This light detected by ground telescopes provides very rich information on the 3D development of the showers.
  It give a quasi calorimetric reliable measurement of the energy.

… but optical detectors can only work during moonless clear sky nights (≈ 10% duty cycle).

Cherenkov light from VHE gamma rays showers

Shower front ≈ conical at energies > TeV, very well defined in time (few nanoseconds)

… ground enlightened area of 150 m radius at 1800 m asl for TeV showers.

Any large acceptance telescope in this area receive enough photons
→ effective detection area ~ 10^5 m^2

With an array of such telescopes,
3D reconstruction of showers (stereoscopy) → total number of Cherenkov photons as an energy estimator).

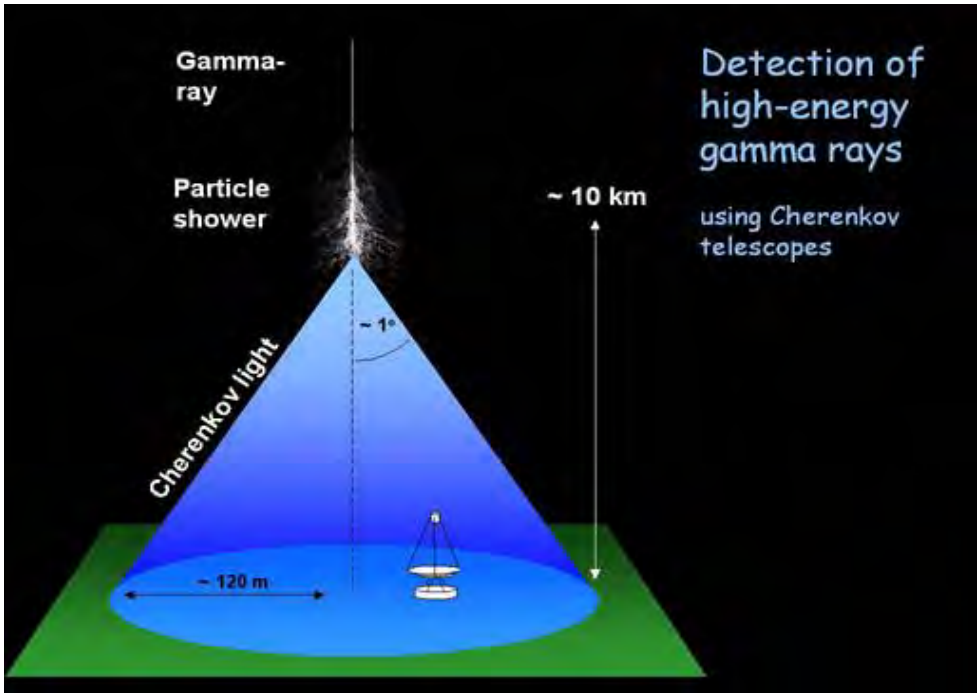

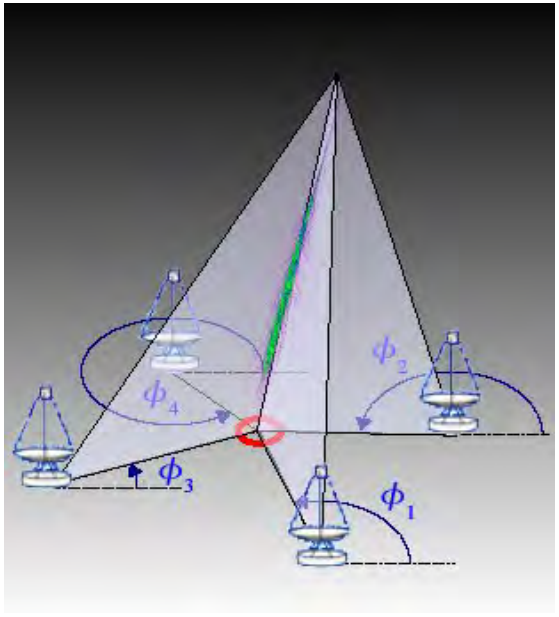

Showers Cherenkov light

- Longitudinal profile: similar to the particle density profile with a slight shift towards ground of 0.3 X_0 due to the variation of the Cherenkov threshold with altitude.

- Transverse profile: much narrower than that of charged particles ($\sigma_T \approx$ 10 to 15 m at 10 km altitude), threshold effect + energy of particles decreasing further away from axis.

- The Cherenkov « photosphere » (origin of photons distribution of EM showers) can be approximated by a 3D gaussian distribution, with axial symmetry for EM showers.

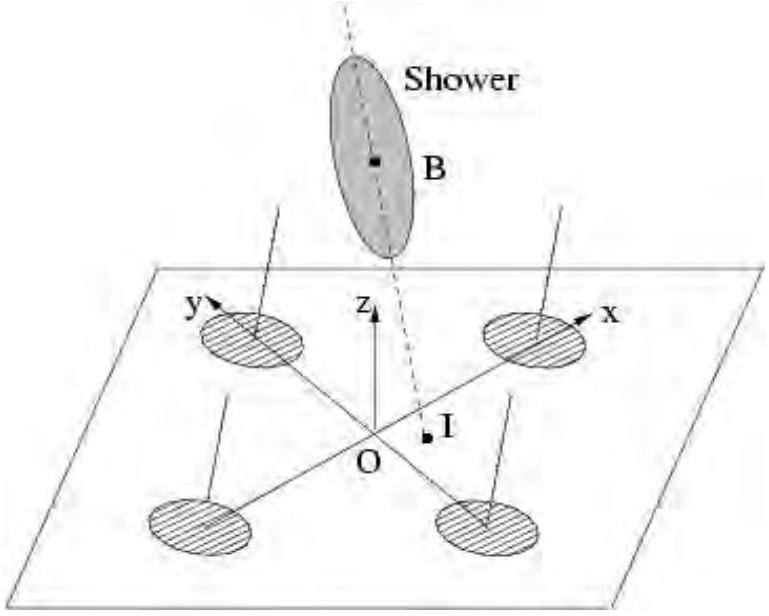

- The measurement of the transverse standard deviation σ_T allows distinguishing narrow EM showers from much wider hadronic showers, (transverse momentum of nuclear interactions ≫ QED radiative processes).

Cherenkov transverse profiles: EM versus hadronic showers

- « OFF » data: showers detected by 3 or 4 telescopes in a zone without γ sources
  $\rightarrow \sigma_T$ distribution for hadronic showers

- « ON » data : showers detected by 3 or 4 telescopes in the direction of the γ source PKS2155-304 (a blazar).

- « ON-OFF » distribution :
  $\rightarrow \sigma_T$ distribution for γ showers as seen by 3 or 4 telescopes.

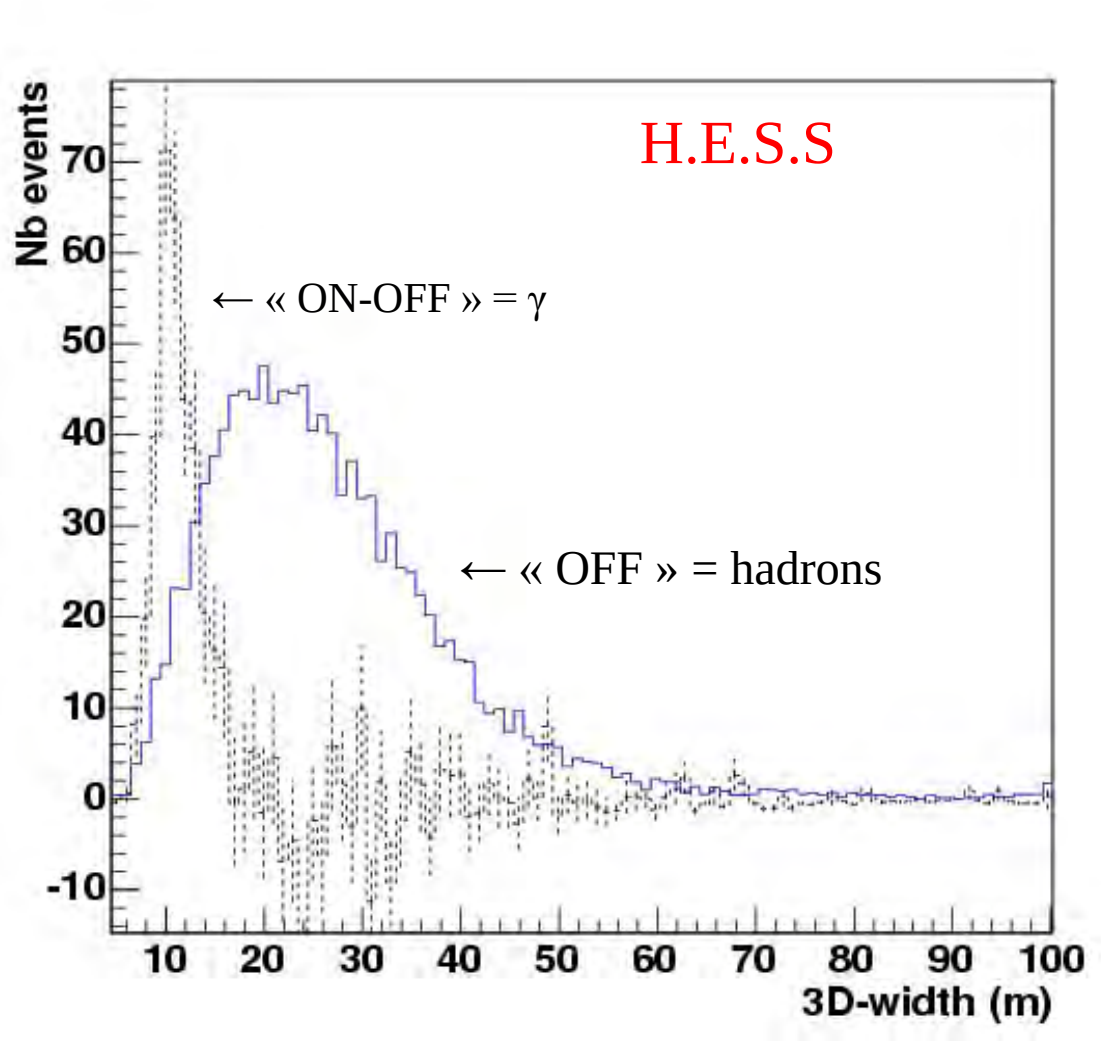

VHE gamma-ray observation

- IACT, detection principle:
  - Imagers : WHIPPLE, CANGAROO, HEGRA,CAT
    Hess, Magic, Veritas
  - Samplers :ASGAT,THEMISTOCLE,
    HEGRA-AIROBICC, CELESTE, SOLAR2

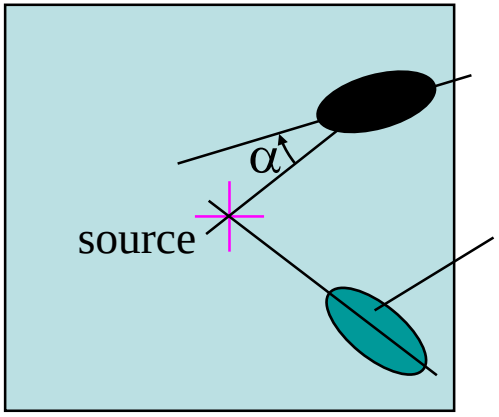

Shower pointing back at the source

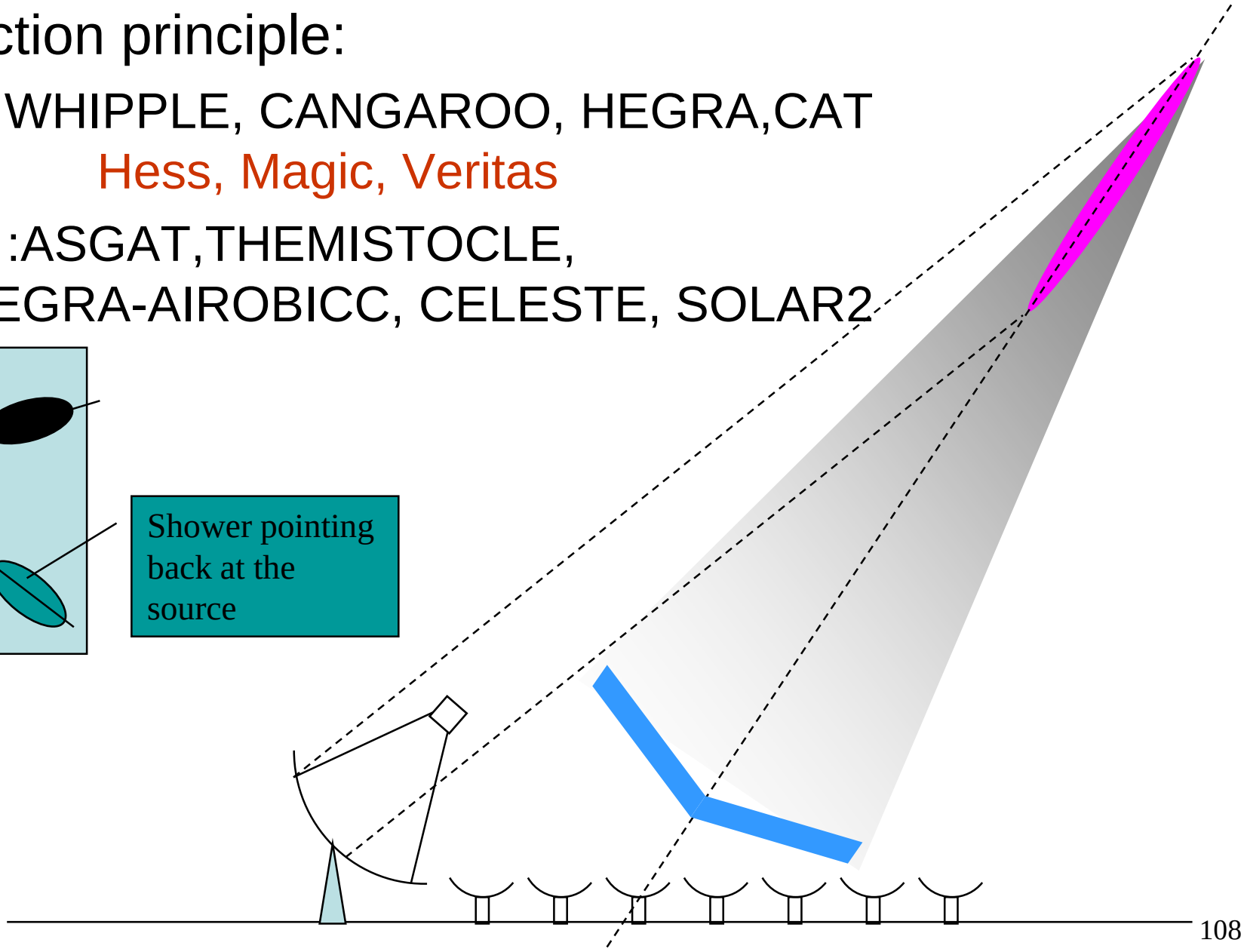

Gamma-ray astronomy above 100 GeV

- Atmospheric Cerenkov Detectors (IACTs) "imagers"
  - Limited field of view instruments (5° for H.E.S.S.),
    $\Rightarrow$ must follow the source apparent displacement on the sky.
  - Can follow only one source at the time.
  - Only work at clear sky m oonless nights.
  - Great γ-hadron discriminating power $\rightarrow$ most of the TeV sources discoveries.

- Surface particle detectors "samplers"
  (charged particles and γ secondaries at ground level)
  - Large field of view ($\approx$ steradian) instrument
  - High duty cycle
  - Low γ - hadron discrimination power $\rightarrow$ limited sensitivity.

Atmospheric Cerenkov Detectors

Imagers

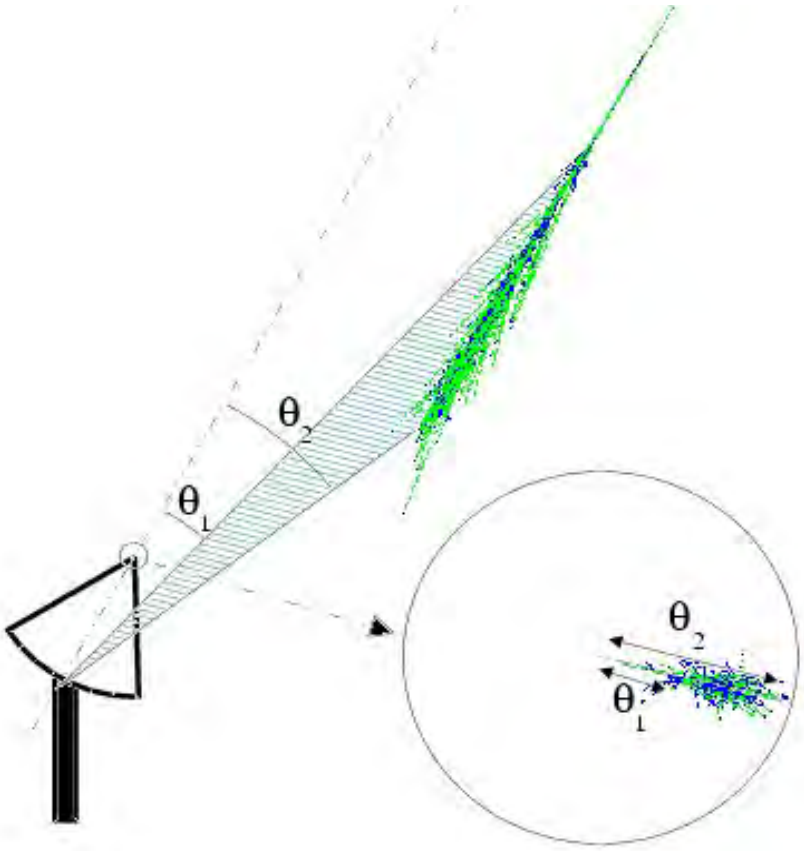

Form the shower image in the focal plane

IACT

Samplers

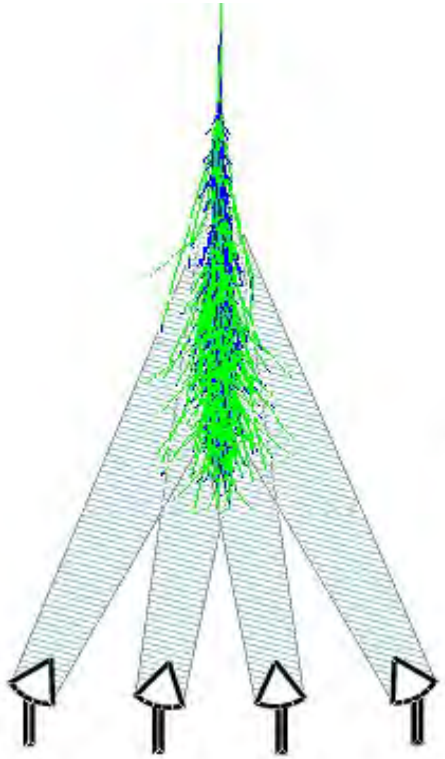

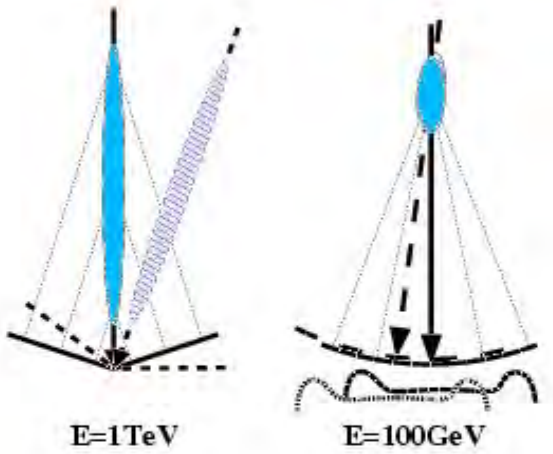

Arrival time + amplitudes on a large number of stations

IACTs in stereoscopic mode

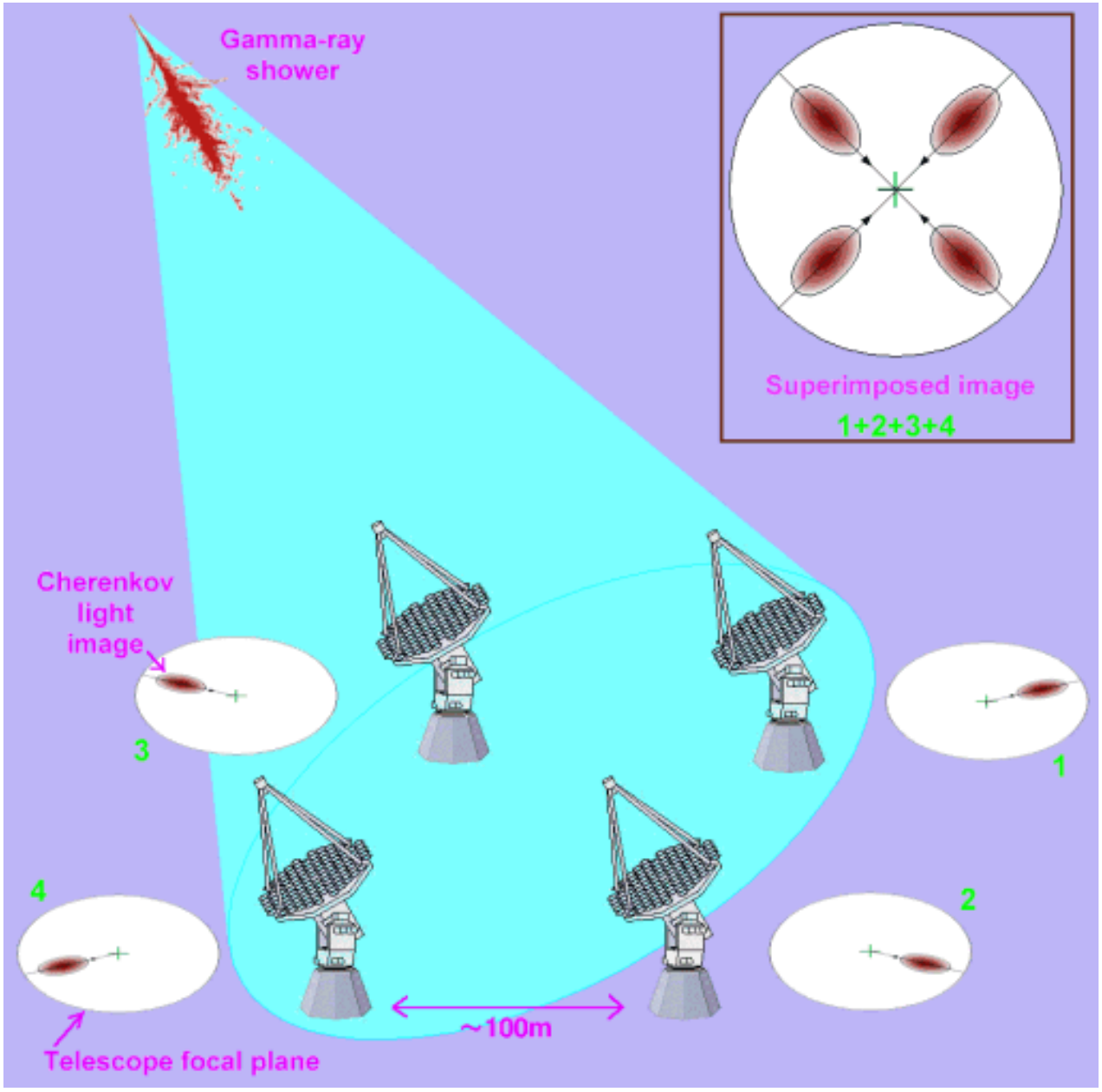

Former IACT

WHIPPLE

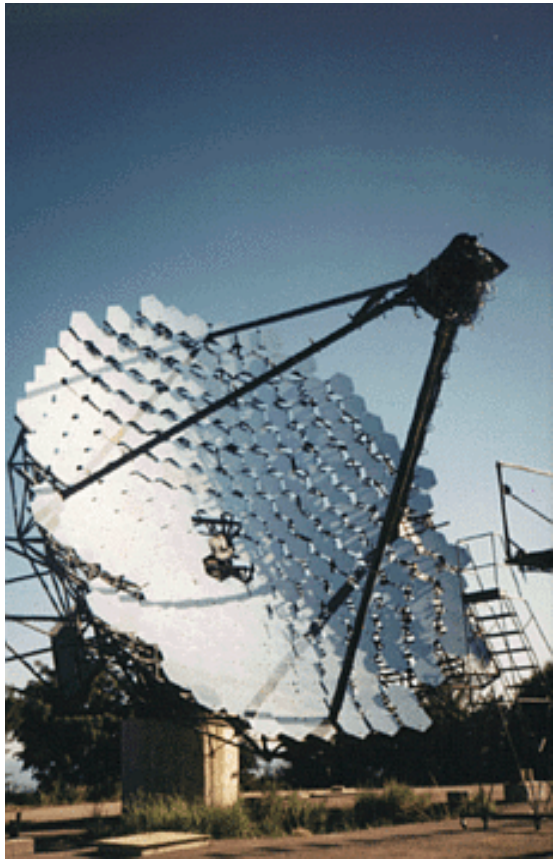

CAT

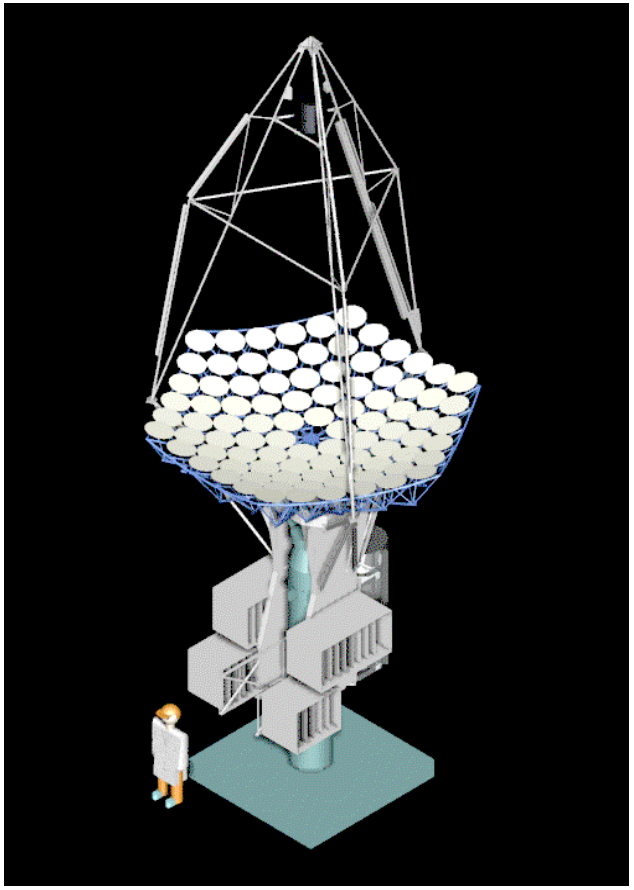

ACTs:
Lowering the energy threshold

Sky background ~ 10^{12} photons m^{-2} sr^{-1} s^{-1}

$$\frac{\text{Signal}}{\sqrt{\text{sky bg}}} \propto \frac{A_{\text{col}}\ \tau\ \Omega_g\ \epsilon}{\sqrt{A_{\text{col}}\ \Delta t\ \Delta\Omega\ \epsilon}} \propto \sqrt{\frac{A_{\text{col}}\ \epsilon}{\Delta t\ \Delta\Omega}}$$

- Increase the photons collection area ≈ reflector area A_{col}
- Increase the photon detection efficiency (mirror reflectivity, light funnels, PMTs quantum efficiency)
- The coincidence time gate Δt should not exceed by much the Cherenkov characteristic time ($\tau \approx 3$ ns) → isochrones mirror, fast triggering
- The solid angle ΔΩ within which the photon signal is integrated should not exceed much the angular size of the shower Ω_g
  → small pixels, triggering by fraction of the field of view or using nearby pixel patterns.

Current ACTs : large mirrors

Observatory	# of telescopes	Reflector diameter (m)	Site
CANGAROO III	4	10	Australia
HESS I	4 → 4+1	12 (28)	Namibia
MAGIC	1→2	17	Canaries
VERITAS	2→ 4	12	Arizona


VERITAS


CANGAROO III


MAGIC

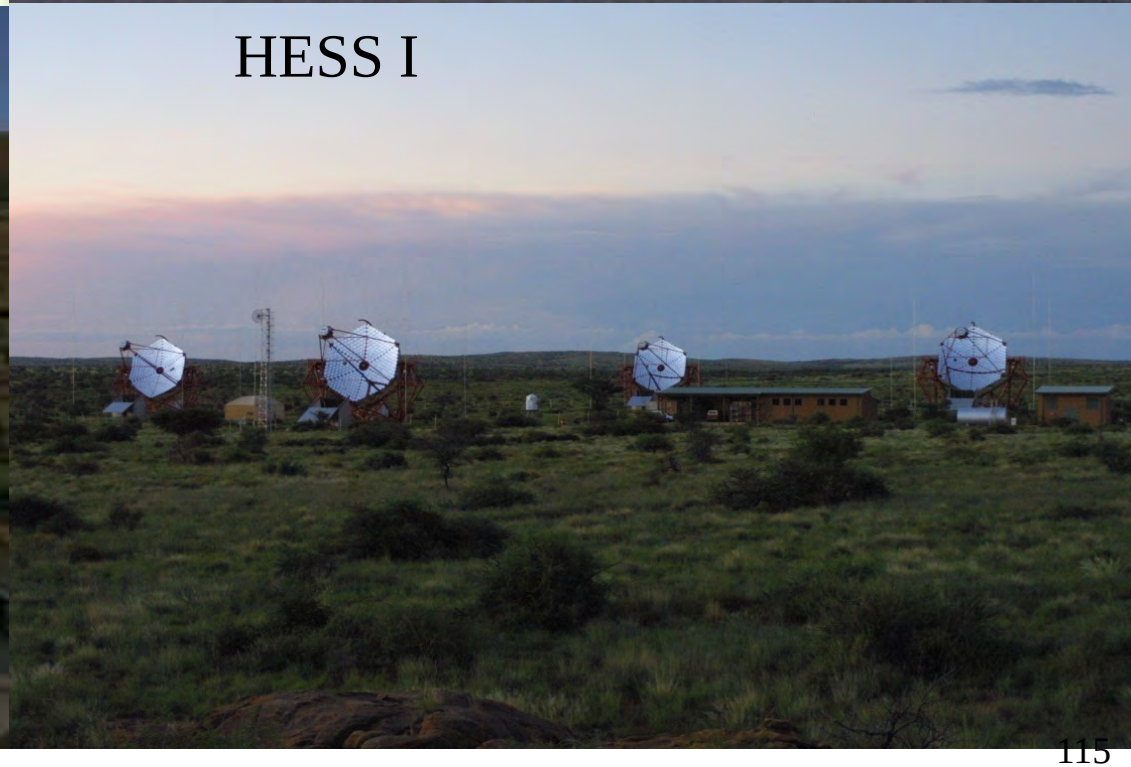
HESS I

Hess 2004 : x4 telescopes

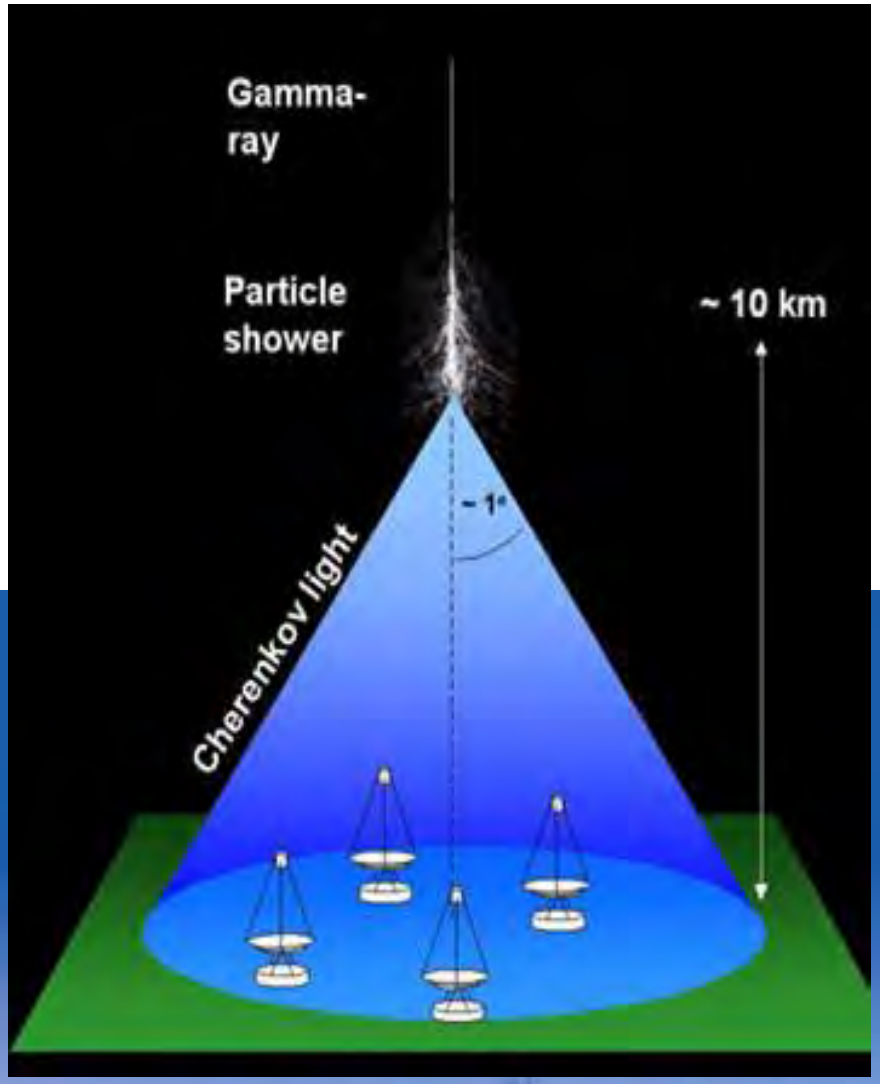

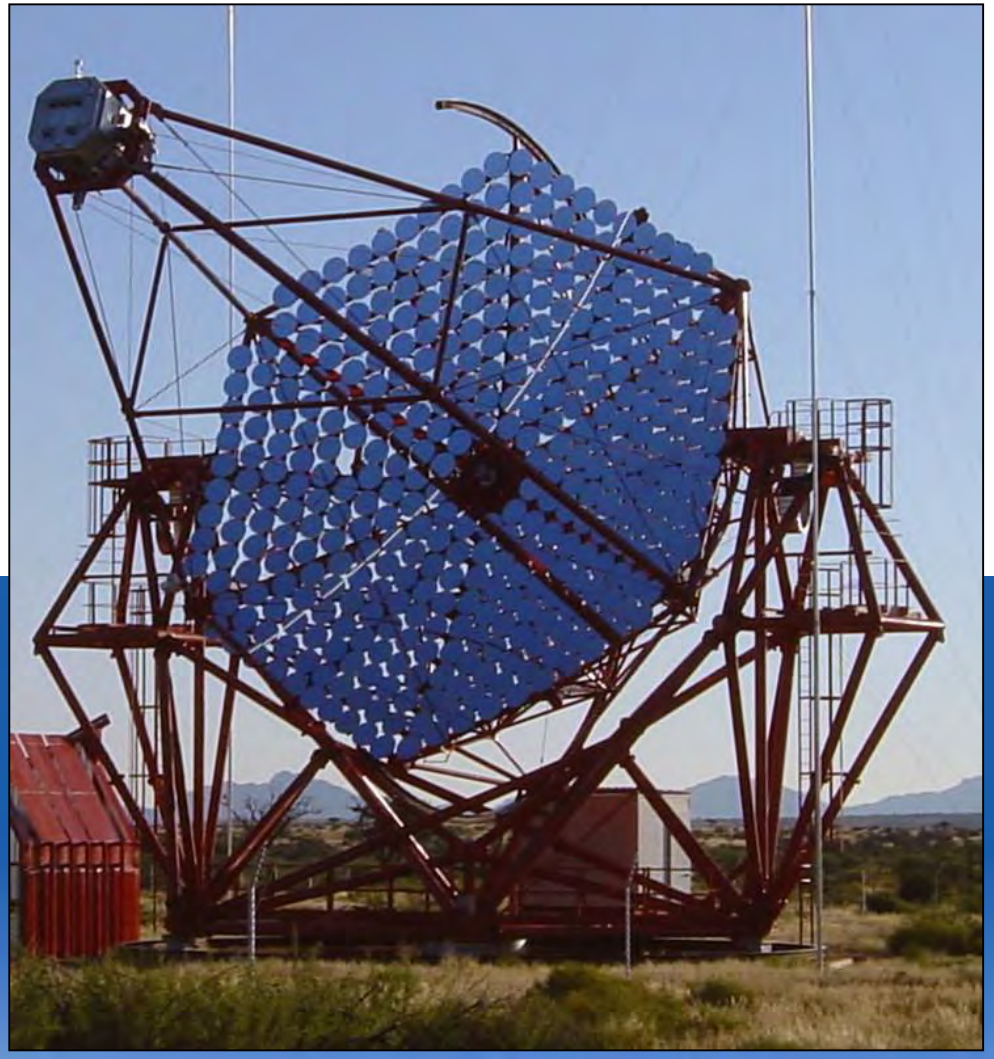

Imaging telescopes: higher resolution cameras

Experiment	# pixels	Pixels size	Field of view
CANGAROO III	552	0.115°	3°
HESS I	960	0.16°	5°
MAGIC	396+180	0.08°-0.12°	4°
VERITAS	499	0.15°	3.5°

Imaging telescopes: high resolution cameras

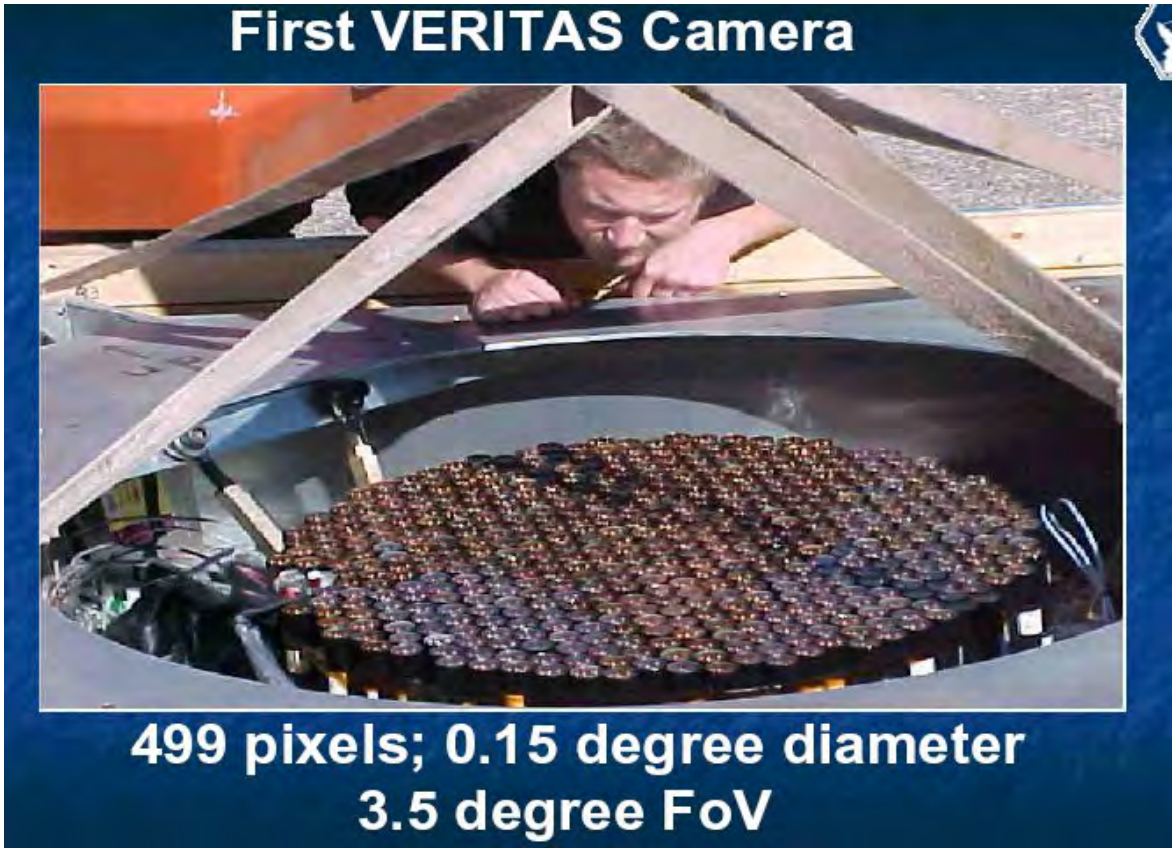

VERITAS

MAGIC

Imaging telescopes: high resolution cameras (H.E.S.S.)

- 960 phototubes equipped with light funnels (Winston cones).
- On board trigger electronics (partially overlapping sectors)
- On board continuous analog memory and fast (Ghz) sampling (Analog Ring Sampler) + integrated signal 12 ns → ADC

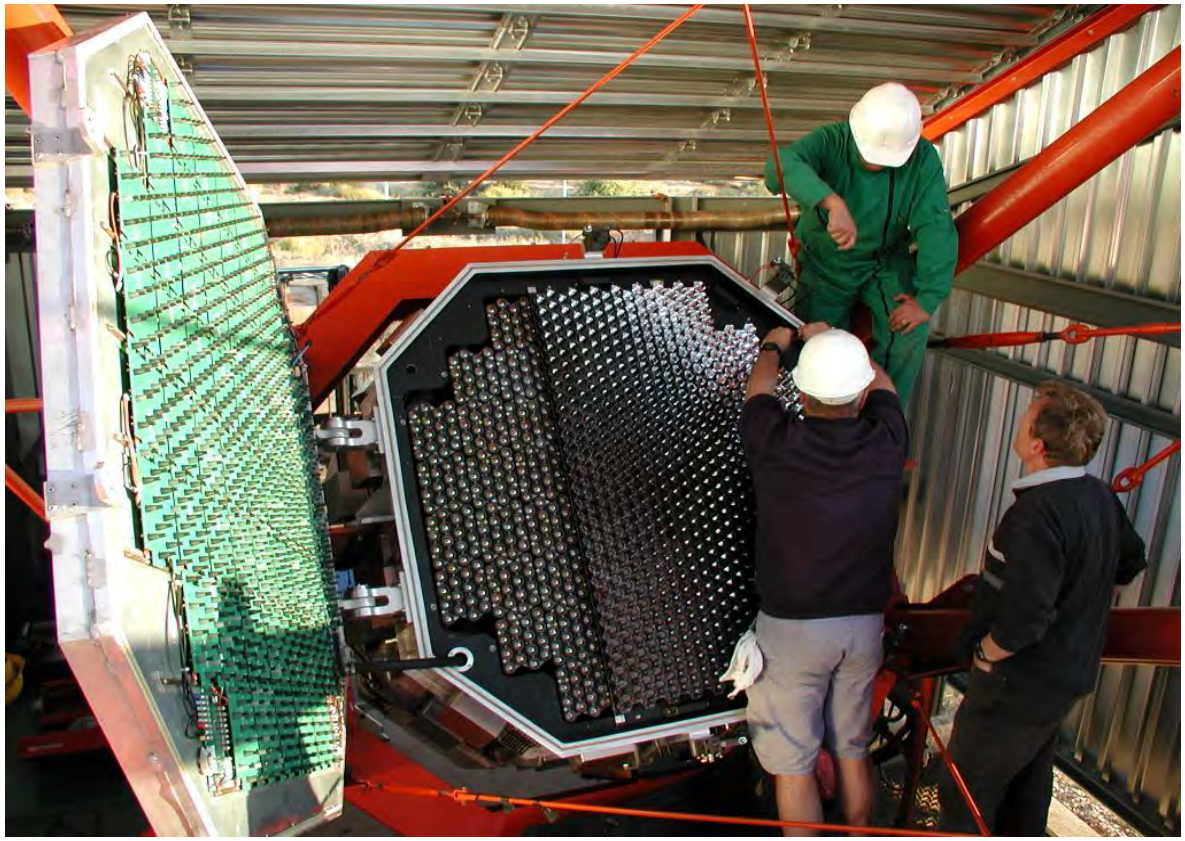

VERITAS Movie Camera

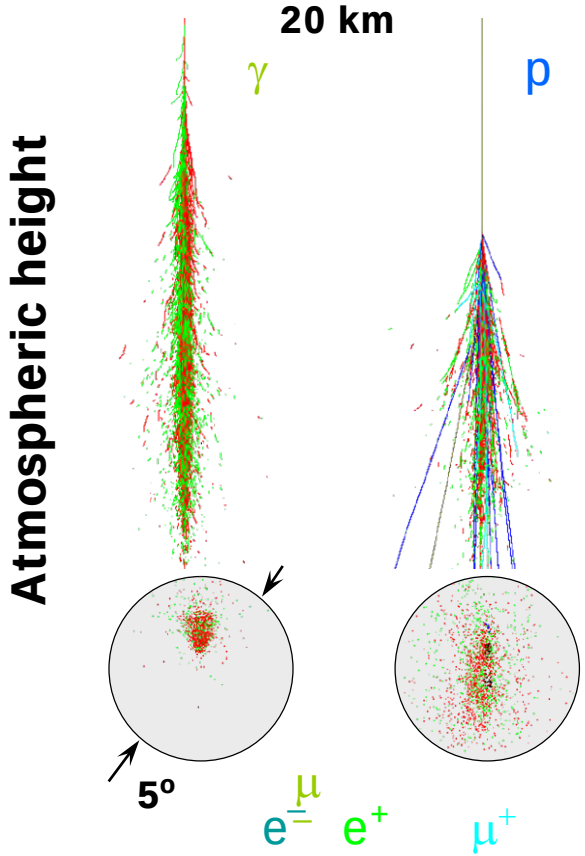

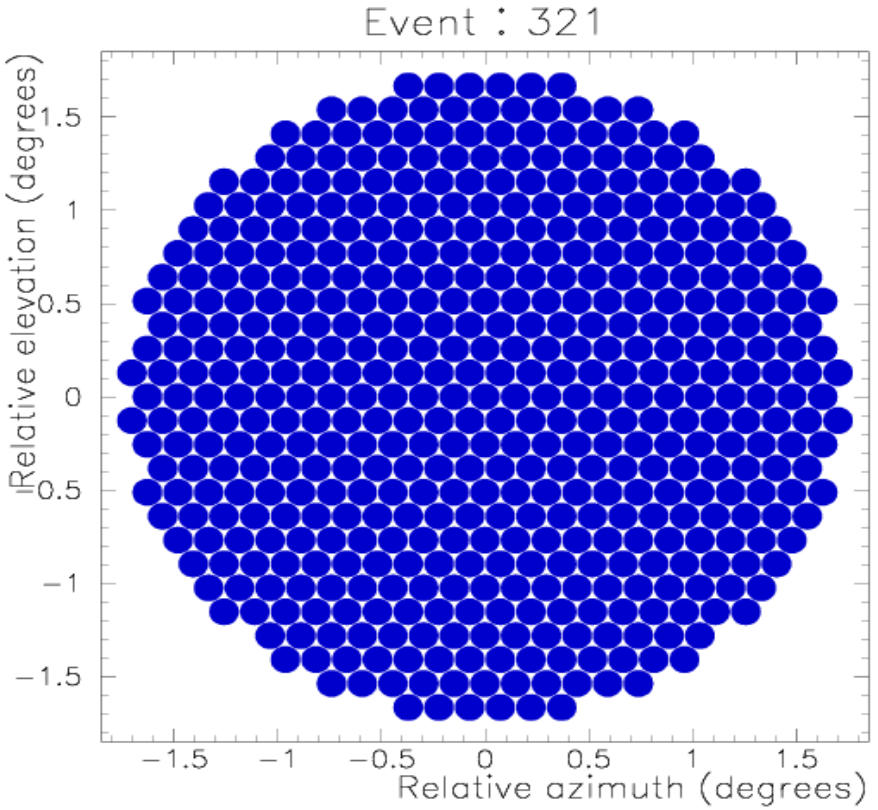

An effective detector monitoring: muon rings

- Muons through the mirror produce a perfect ring image whose light content is completely computable.
- Comparing measured signals with estimations ⇒ global efficiency including effects such as:
  - near atmosphere absorption;
  - mirror reflectivity;
  - light collection;
  - PMTs quantum efficiency .
- The detector monitoring is then automatically taken into account in the data analysis.

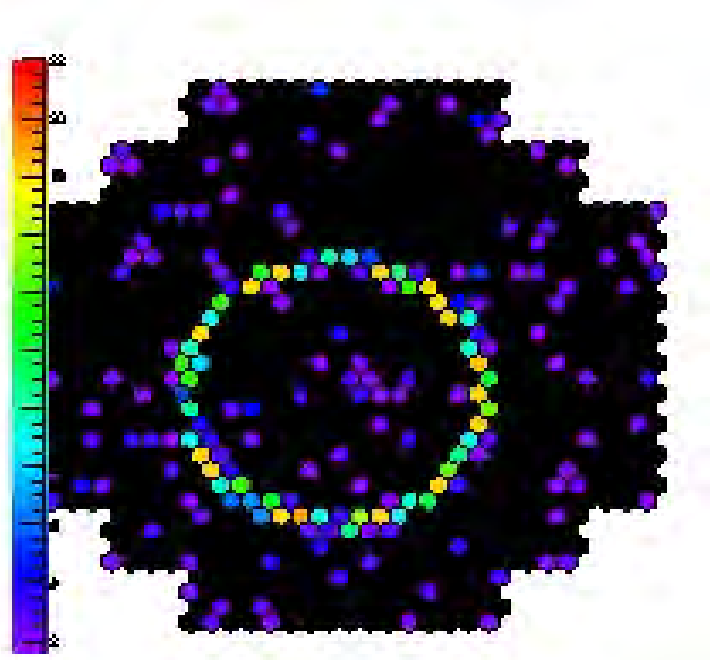

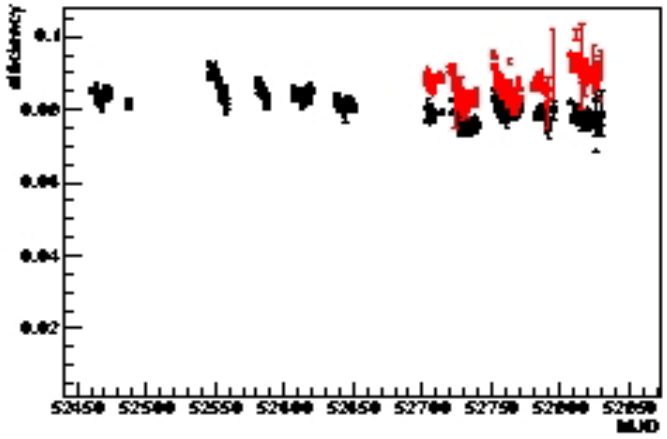

Stereoscopic IACTs

- Each showers is seen by many telescopes
- Very high hadron shower rejection factor (> 1000)

  axial symmetry + narrow 3D width

  + punctual source pointing
- Much improved angular resolution wrt 1 telescope

  (≈ 4' with 4 telescopes)
- Better energy resolution

  (≈15%)

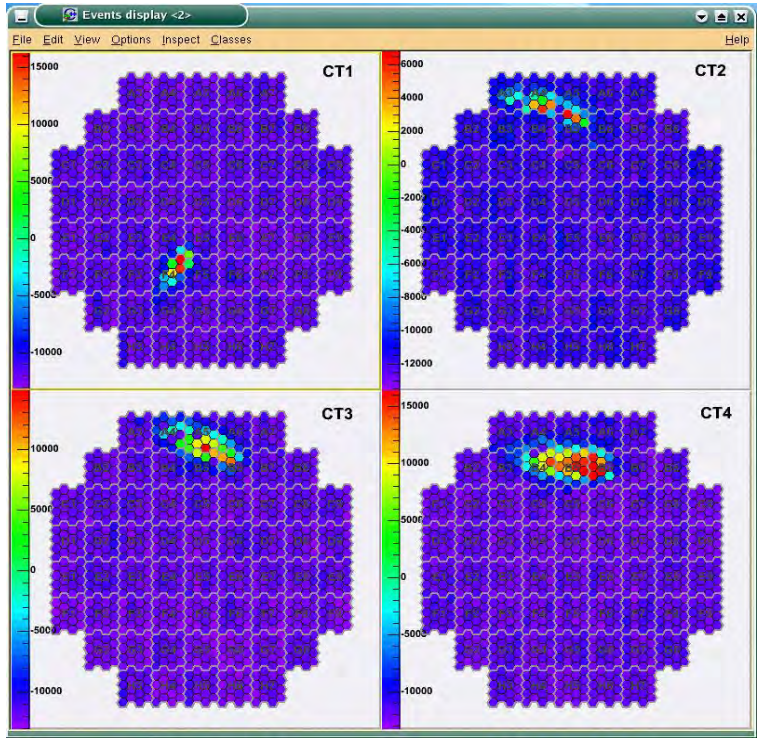

Stereoscopic IACTs

- Direct measurement of the origin of the gamma-ray in the field of view (important for extended sources)
- Direct measurement of the ground impact point (important for the determination of the energy)

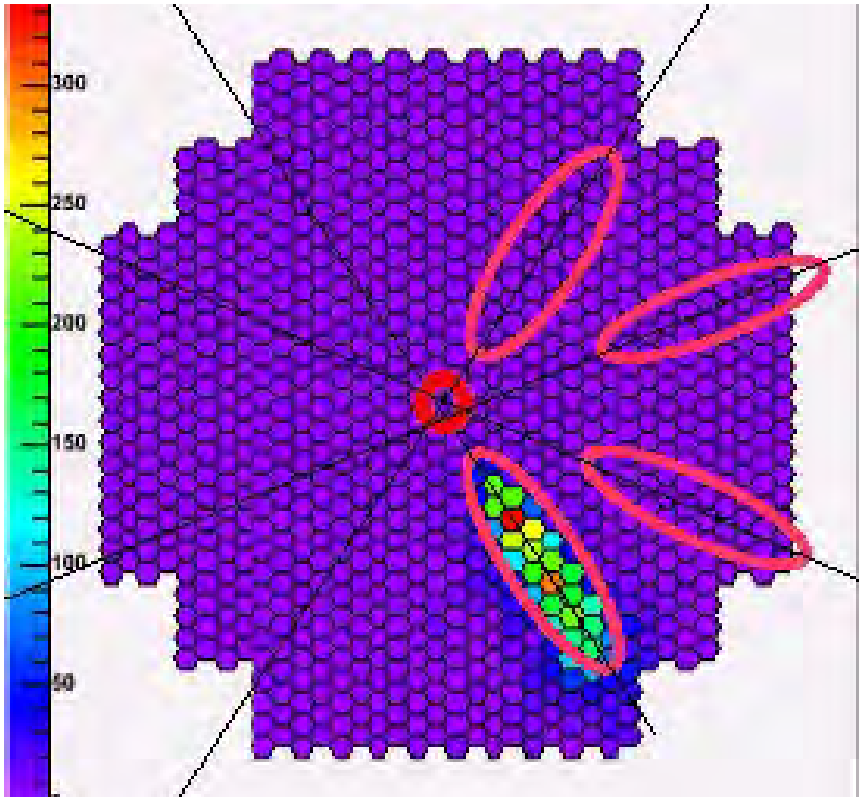

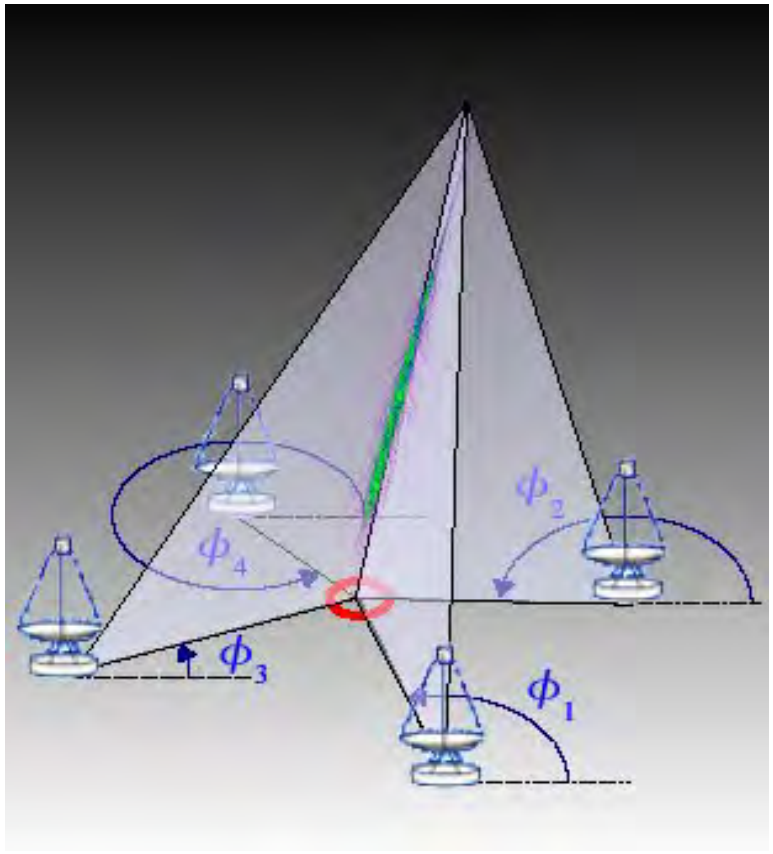

Sensitivity to gamma-ray sources: H.E.S.S.

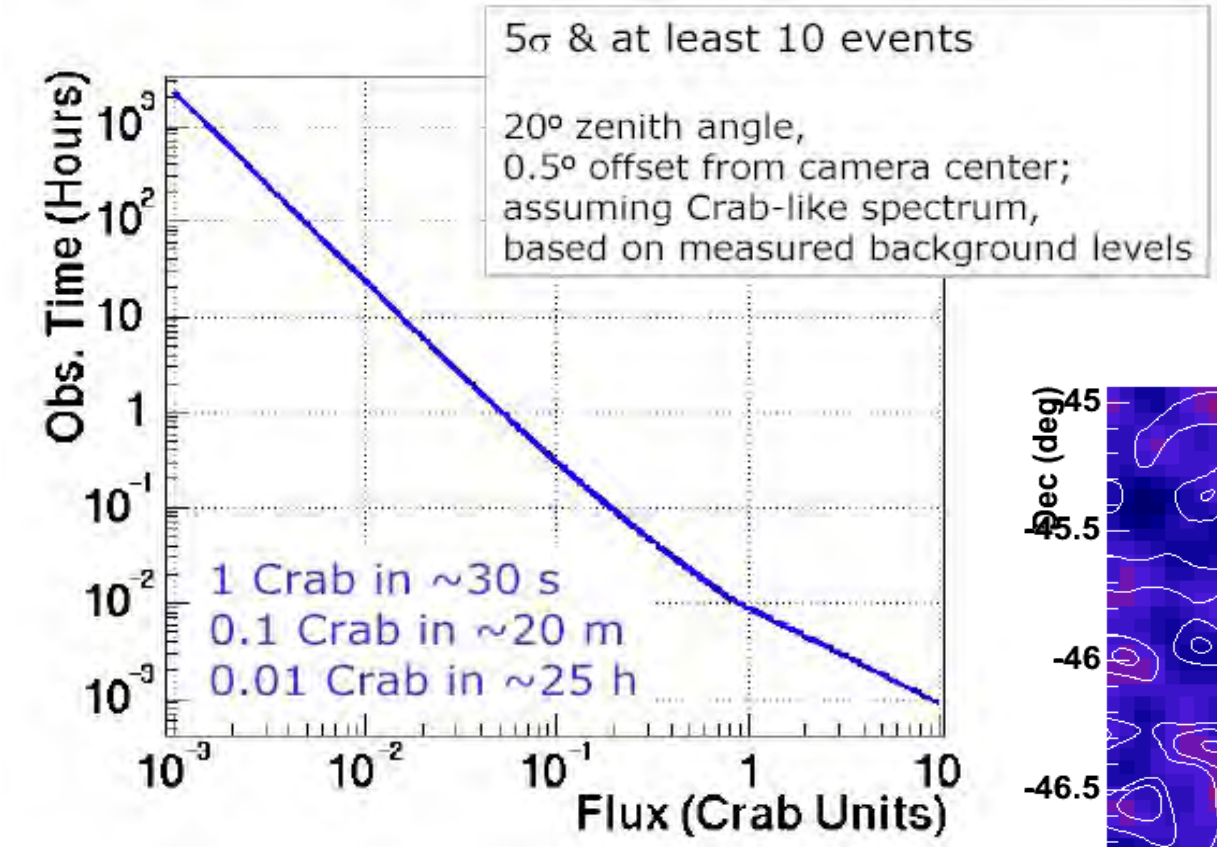

More than hundred TeV-sources

Extended sources capability e.g. Vela Junior (2° in diameter)

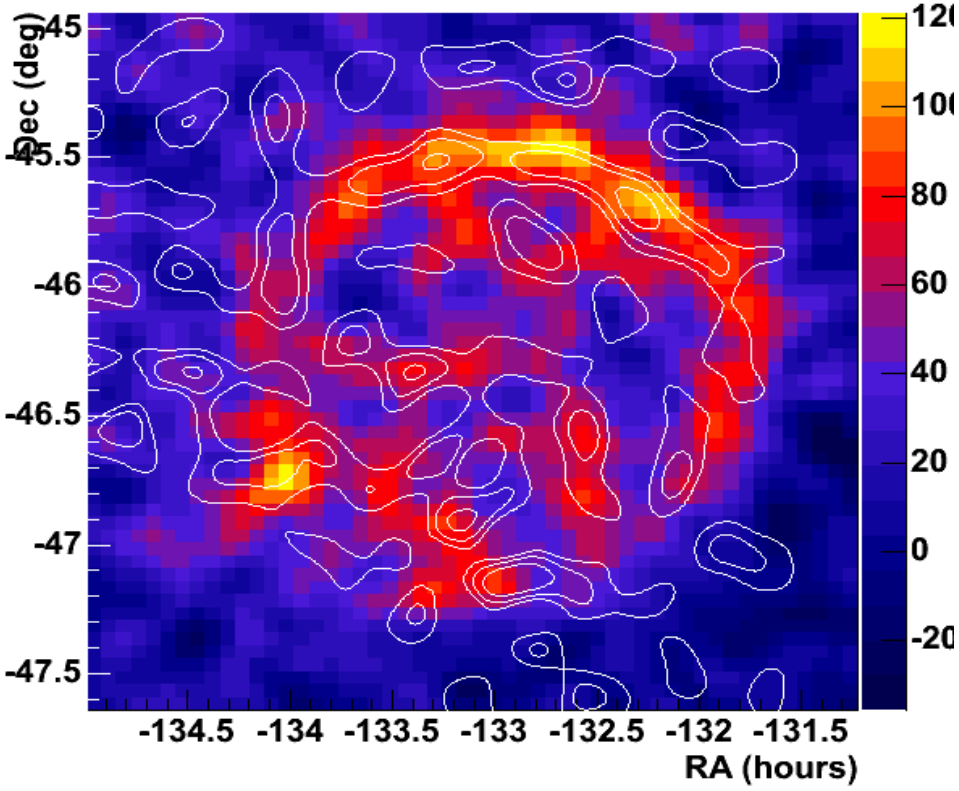

M. Lemoine-Goumard 2006

Galactic Plane Survey with H.E.S.S.

- **~2800 hr of observations of the inner Galaxy (2004–2012)**
  - ~100 sources above the H.E.S.S.-I sensitivity ~1% of Crab
  - Large variety of source types & ~1/3 of unidentified sources

  - 5 resolved shell-type SNRs

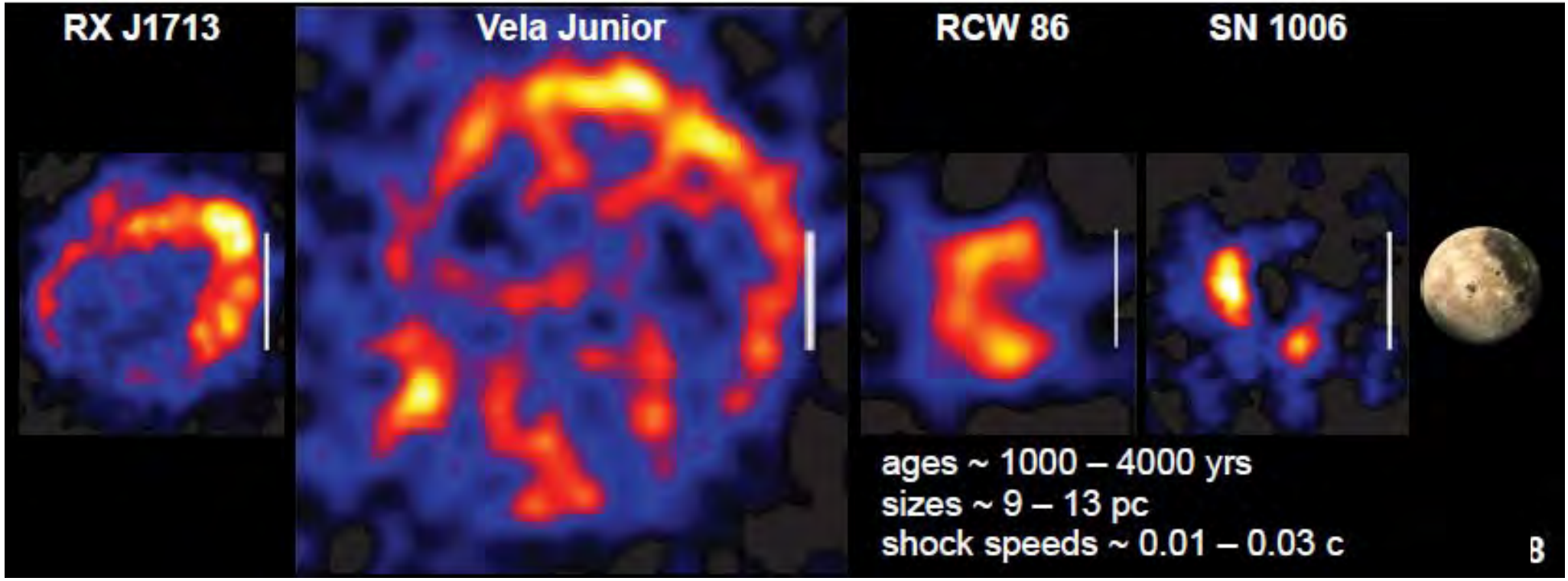

Energy threshold

- The threshold depends on the zenith angle

- Typically 120 GeV
  at the zenith for H.E.S.S.
  and comparable stereoscopic systems.
- MAGIC II (2 identical large telescopes)
  down to 50 GeV.
- Started in 2012 : H.E.S.S. II
  - 50 GeV with a very large telescope
    + les 4xHESS I in stereo
  - 20 GeV expected in « mono »
    with HESS II large telescope
    and a second level trigger.

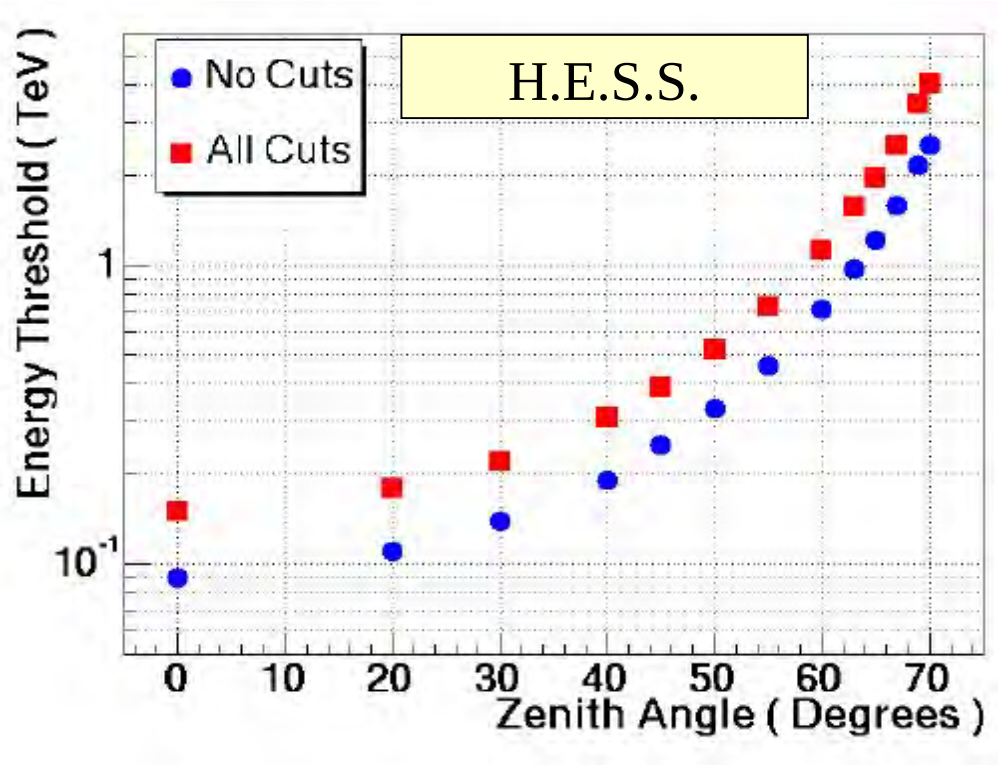

Sensitivity of current imaging telescopes

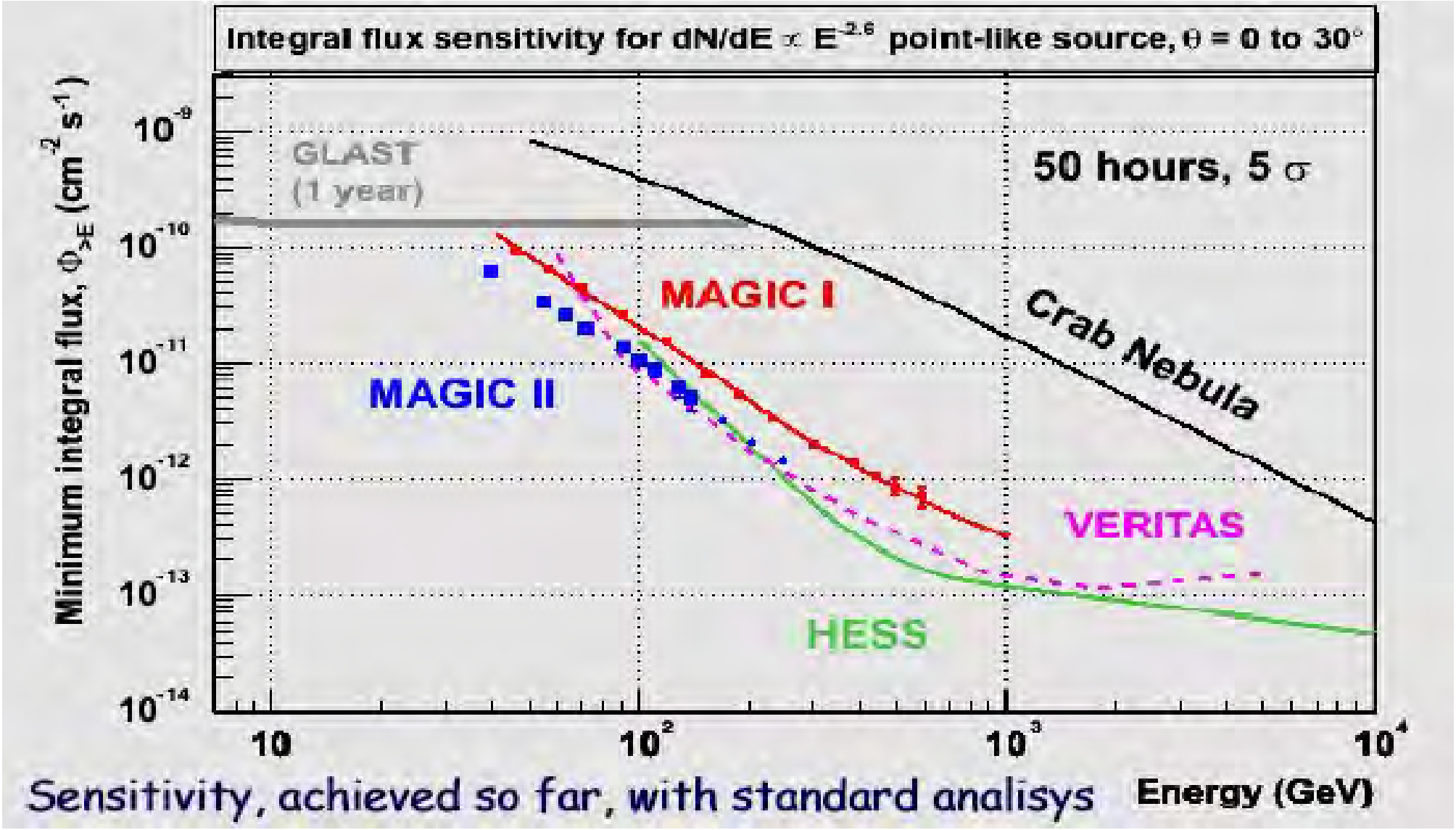

Down to 20 et 50 GeV with H.E.S.S. II

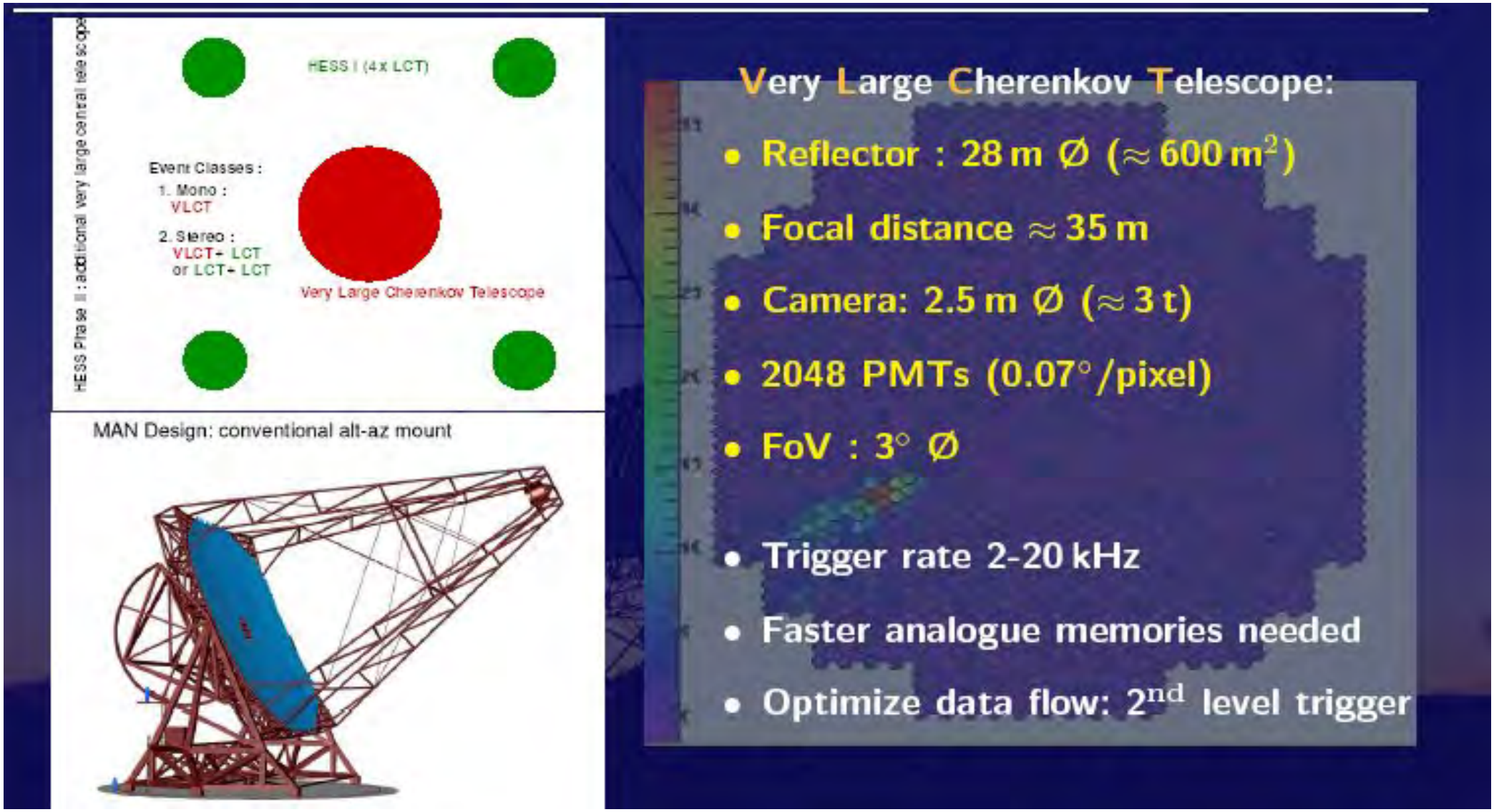

HESS II

- First light July 2012

The FERMI, MAGIC , H.E.S.S. II and CTA era

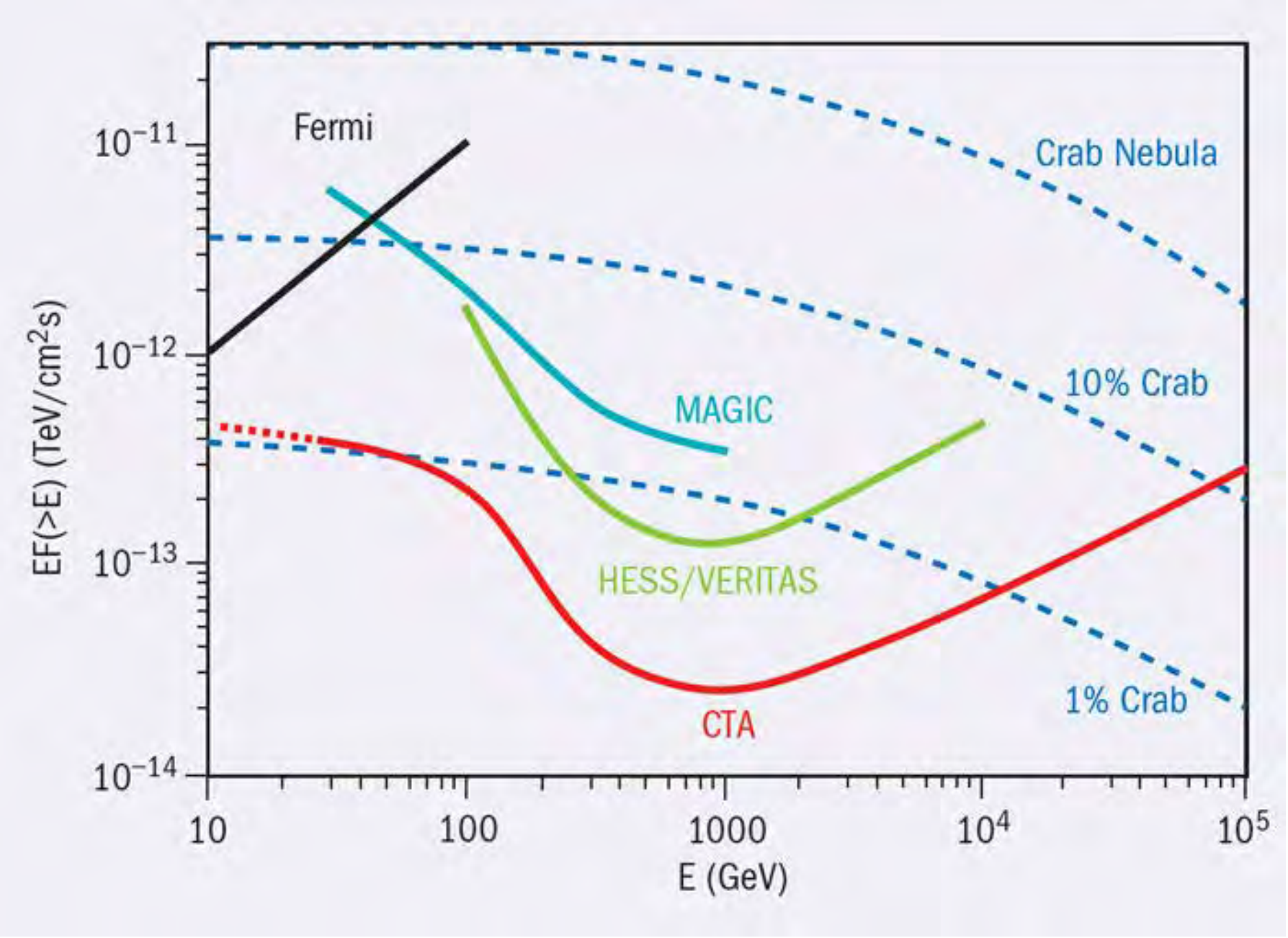

Toward a large array of IACTs : CTA

- Goal : a milli-Crab sensitivity at the TeV
- This could be achieved with 20 to 30 imaging telescopes (HESS-I type)
- The sensitivity is not only increased because of the covered area, but also due to improved stereoscopic quality (improved hadron rejection factors and angular resolution) : 56% of the showers seen by at least 4 tel with 16 in total, up to 2/3 with 36 tel.
- International consortium HESS-MAGIC-VERITAS, 2 sites one north one south: CTA = Cherenkov Telescope Array.

A (once favored) alternative solution: sampling arrays

- To lower threshold, benefit of the very large mirror area from experimental solar power plants ~ 2000 - 6000 m^2

- Need to split the beam from the different heliostats

  → Secondary optics

- One PMT per heliostat.

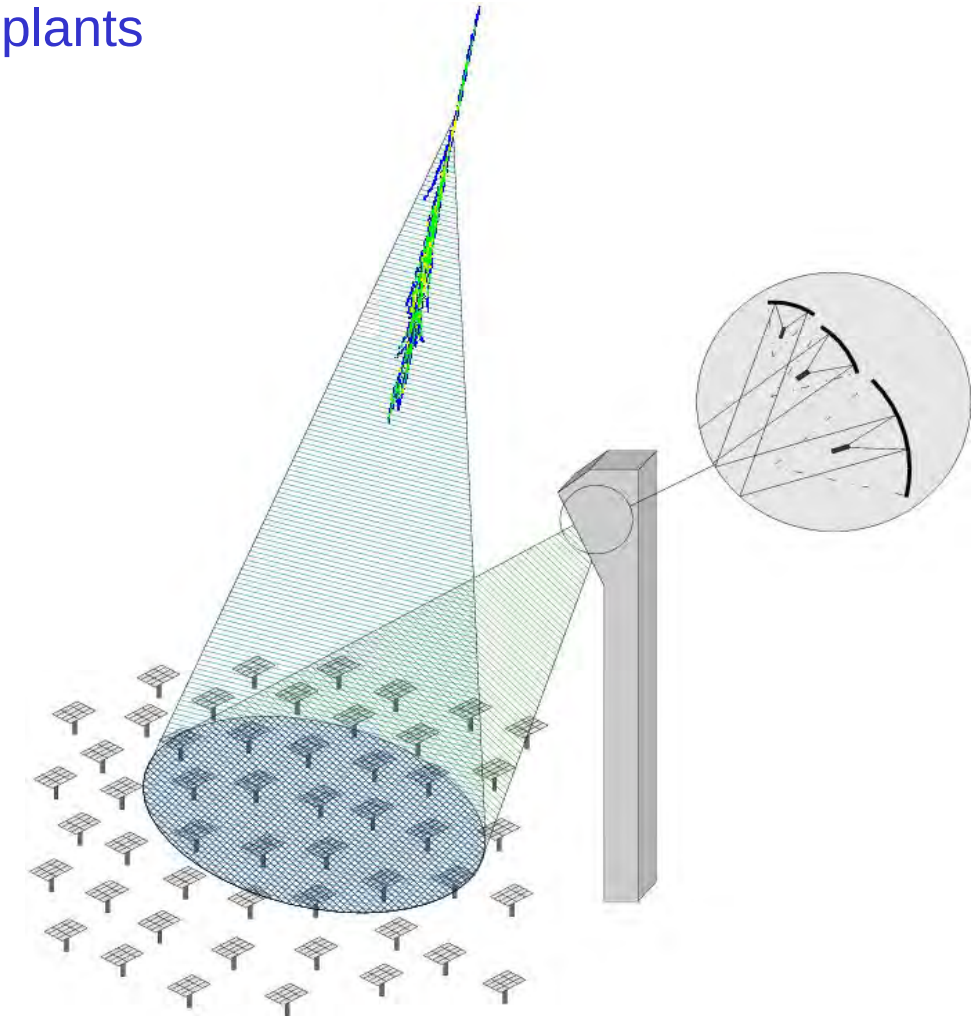

CELESTE (France)

53 ×54 m²

STACEE (USA)

64 × 40 m2

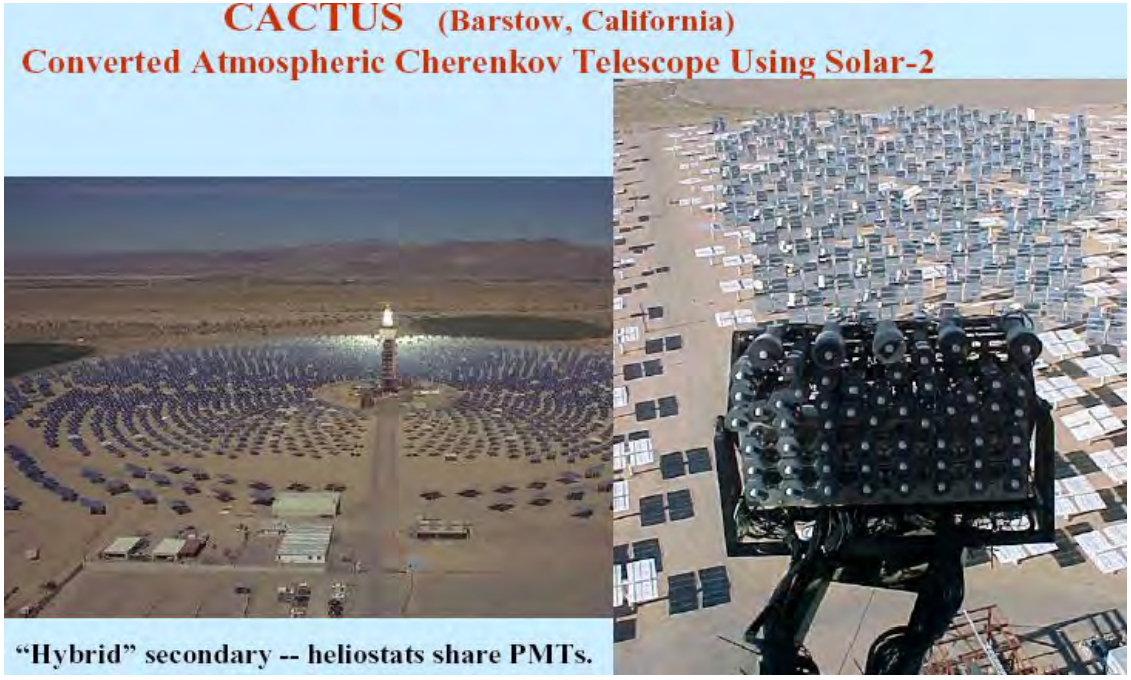

CACTUS (USA)

160 × 40 m2

Large field of view gamma-ray detectors

- Detect the shower particle reaching ground (at high altitude) (scintillateurs, RPCs or water Cherenkov detectors)
- Large duty cycle ≈ 90%
- Large solid angle ~ steradian
- Well suited to look for unpredictable transient phenomena (ex: gamma-ray burst)
- … BUT small sensitivity (~0.5 Crabe) because of rather poor hadron shower rejection factor and limited angular resolution (0.5° to 1°) ; (measured from timing in different detectors).
- … as well as rather high threshold (~ 1 TeV)

Large field of view gamma-ray shower detectors

Tibet

- 4300m asl
- Scintillator array
- 497 detectors
  - 0.5m^2 each
  - 5mm lead on each
- 5.3x10^4 m^2 (phys. area)
- 680 Hz trigger rate
- 0.9^o resolution

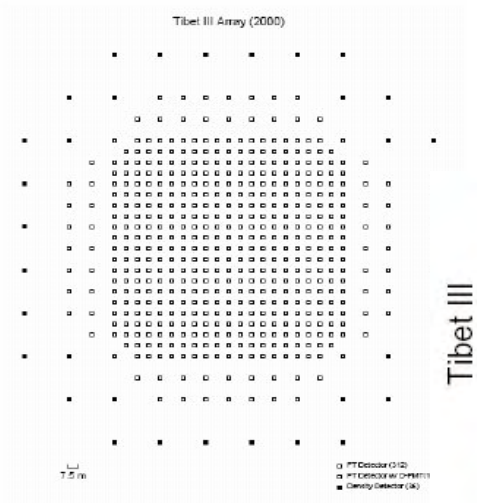

Milagro

- 2600m asl
- Water Cherenkov Detector
- 898 detectors
  - 450(t)/273(b) in pond
  - 175 water tanks
- 3.4x10^4 m^2 (phys. area)
- 1700 Hz trigger rate
- 0.5^o resolution
- 90% proton rejection

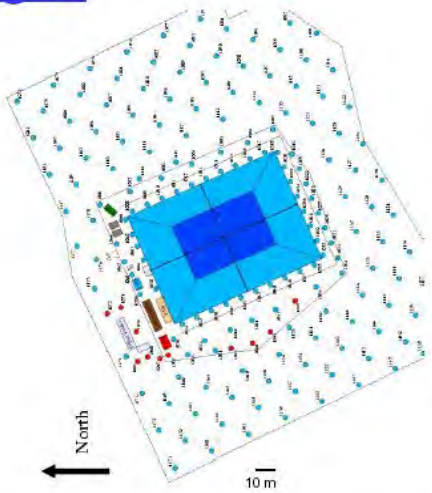

Scintillators

Tibet III

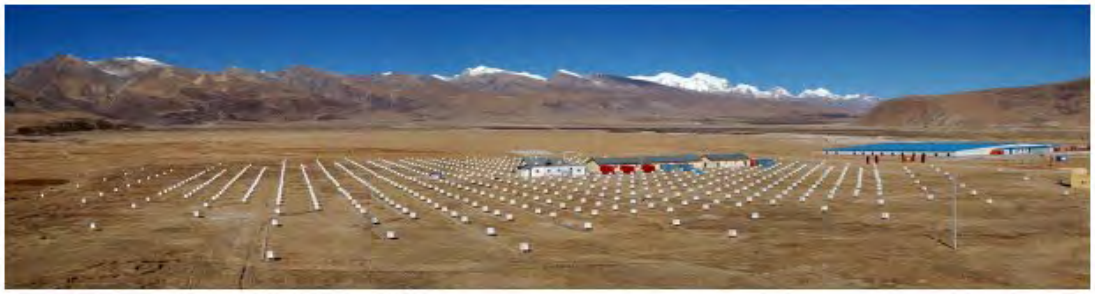

Milagro

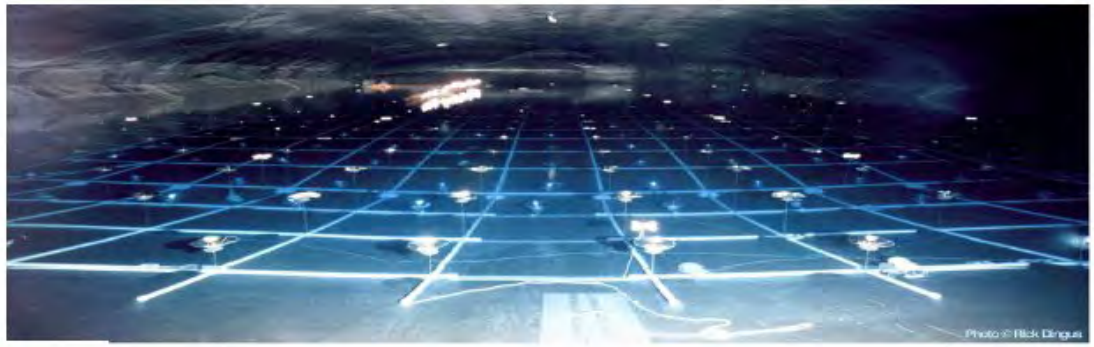

« water pool »

(water Cherenkov detectors)

Hadronic background rejection by MILAGRO

- Cherenkov light in the deeper PMTs → hadrons
  (cf. muons that traverses completely the pool).
- Hadronic showers: irregular light distribution → less PMTs hit but larger signal each
- EM showers: more regular light distribution → many more PMTs hit with small signal each PMT.

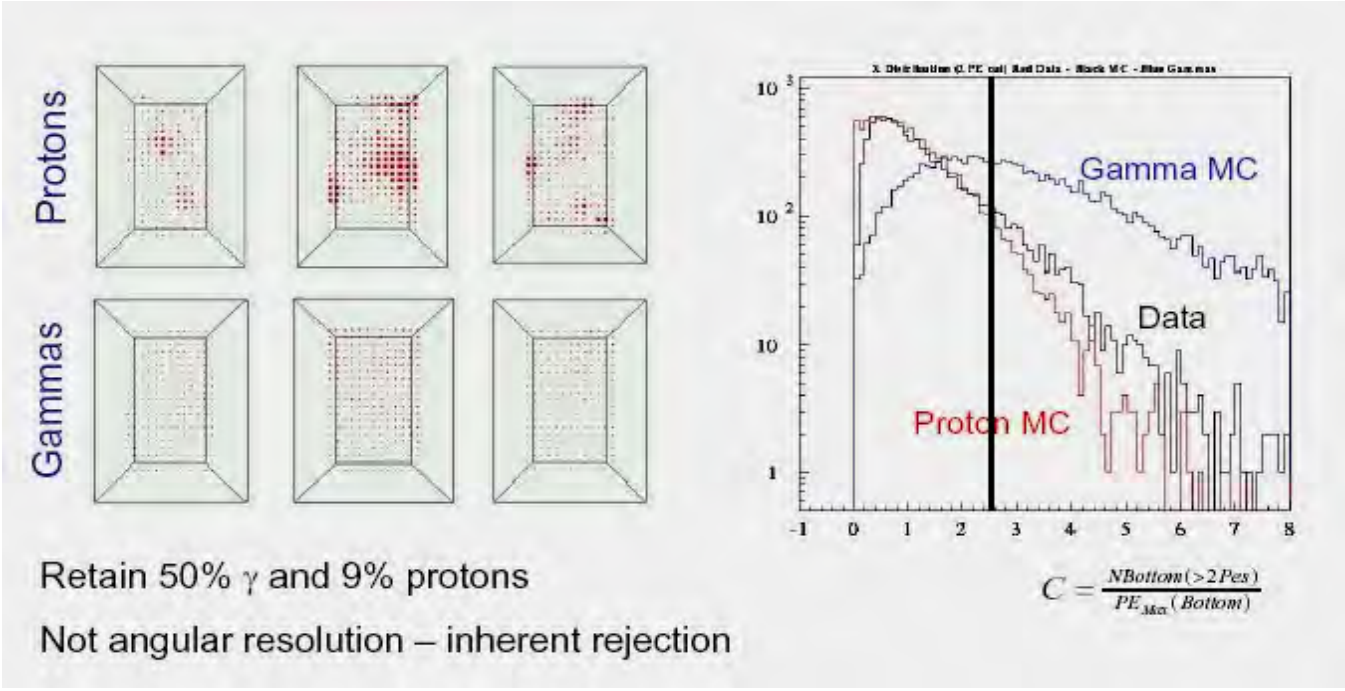

Proton rejection factor ~ 10


HAWC
High Altitude Water Cherenkov
Gamma-Ray Observatory
F.Manganet CIDHEAP ESIPAP
300 tanks completed in Dec.2014
Sierra Negra volcano near Puebla, Mexico.
at an altitude of 4100 meters

HAWC
High Altitude Water Cherenkov
Gamma-Ray Observatory

2021

Gamma/Hadron rejection

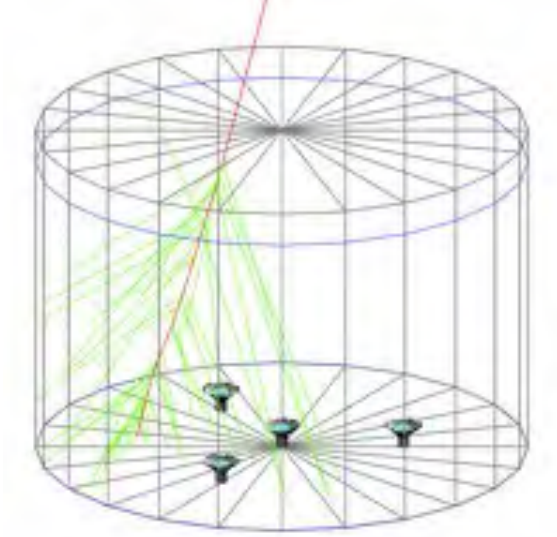

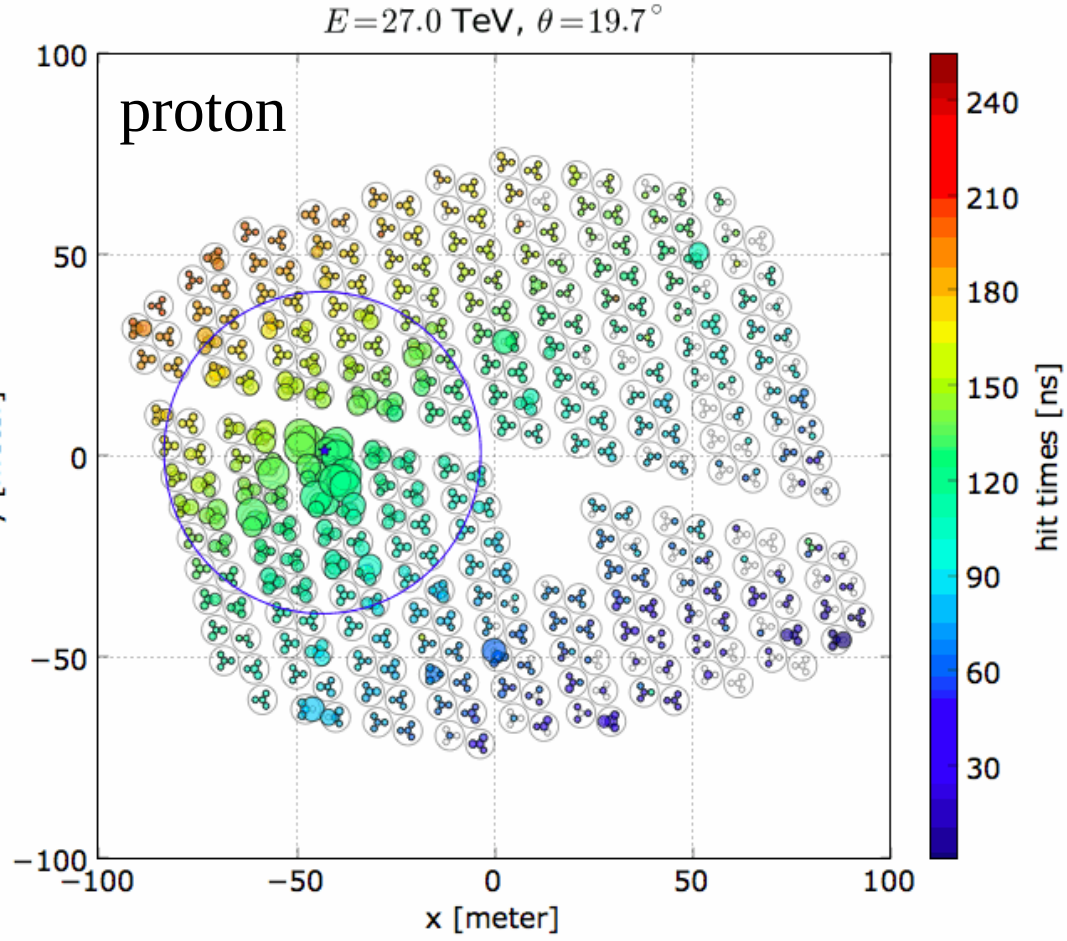

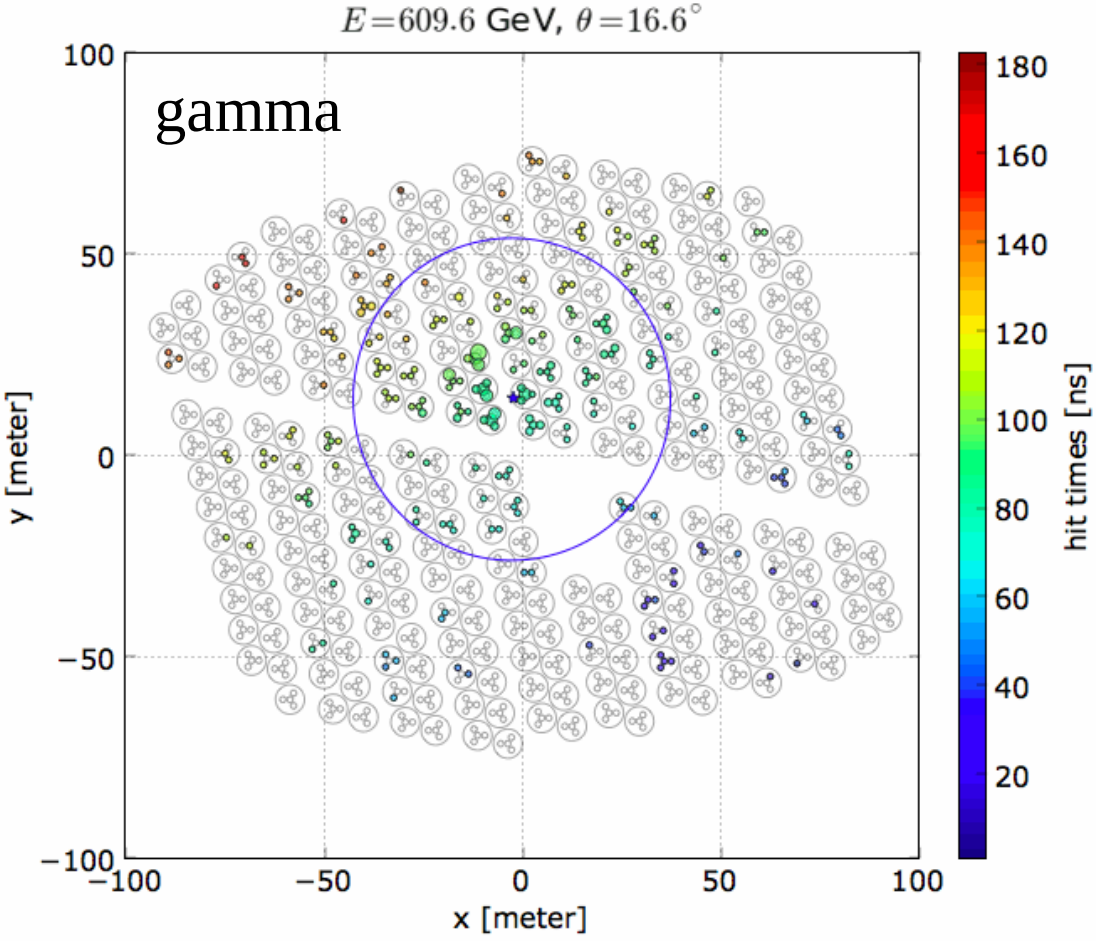

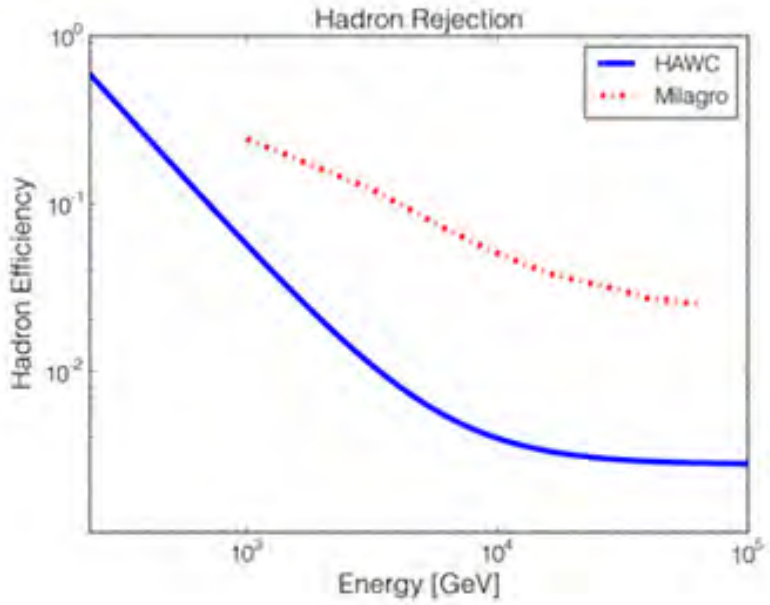
Hadron Rejection
HAWC
Milagro
Hadron Efficiency
Energy [GeV]

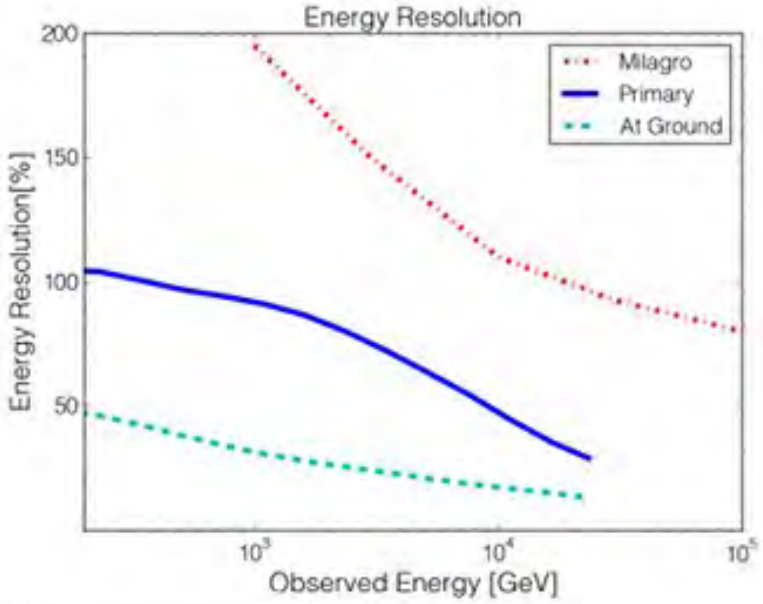
Energy Resolution
Milagro
Primary
At Ground
Energy Resolution[%]
Observed Energy [GeV]

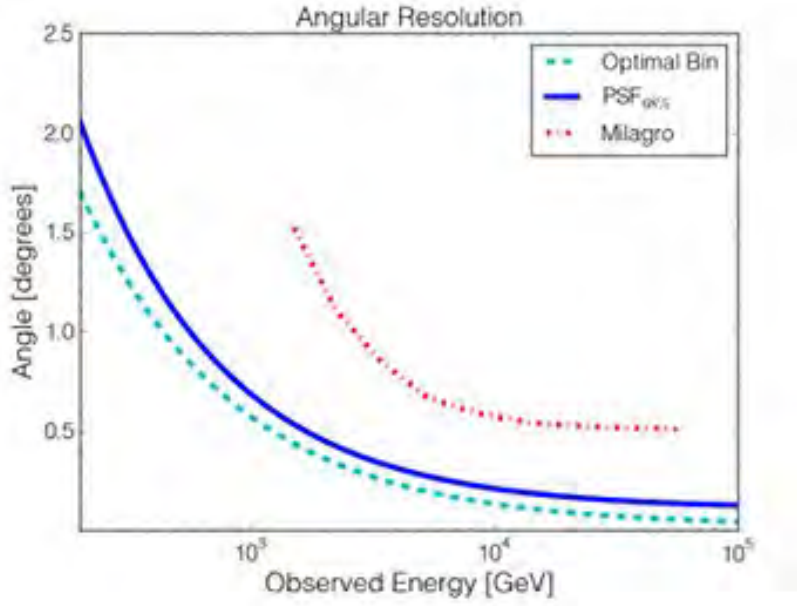
Angular Resolution
Optimal Bin
Milagro
Angle [degrees]
Observed Energy [GeV]

LHAASO

- Project being set up in China, using a complexe setup of different detectors, including Water Cherenkov detectors, IACT etc…

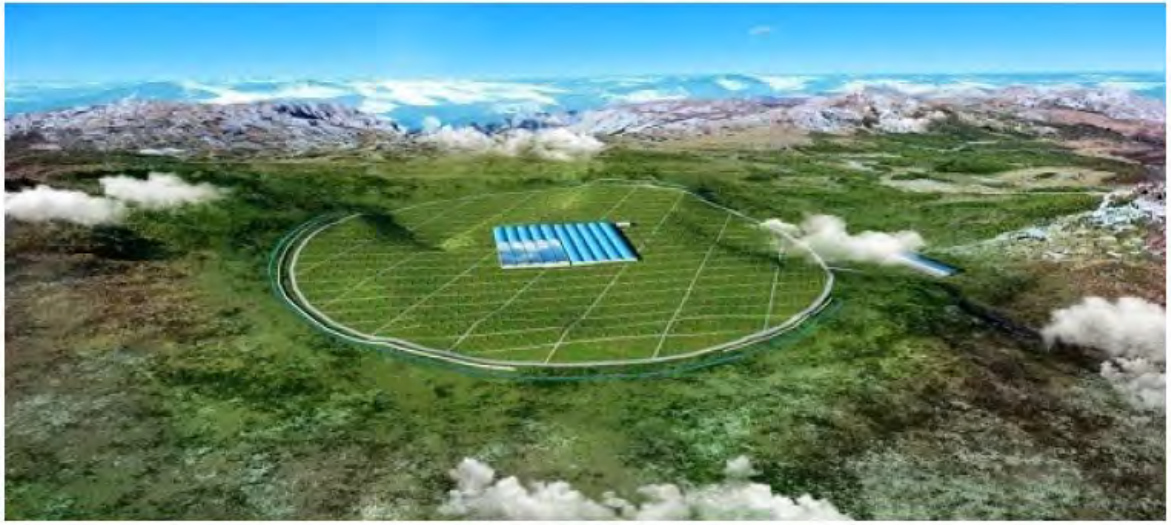

(a)

(b)

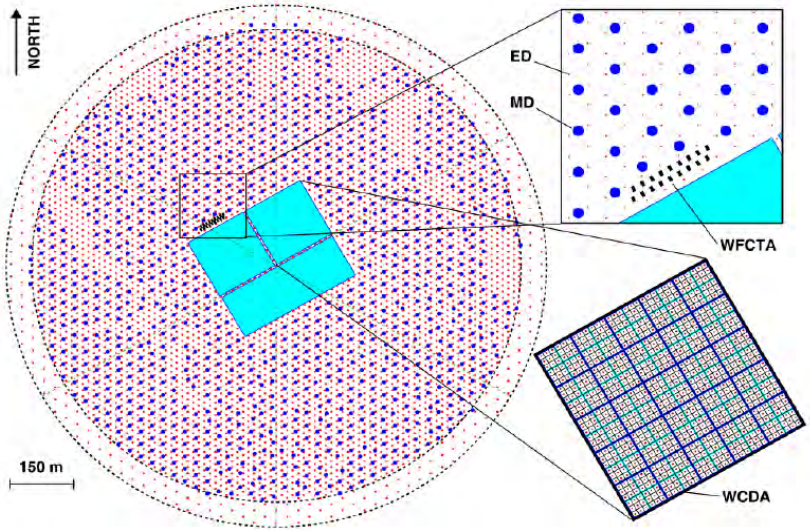

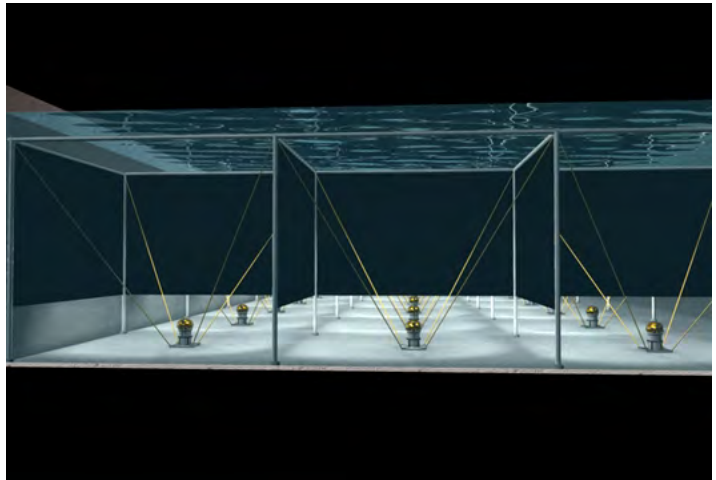

New and future generation of space and ground γ-telescopes

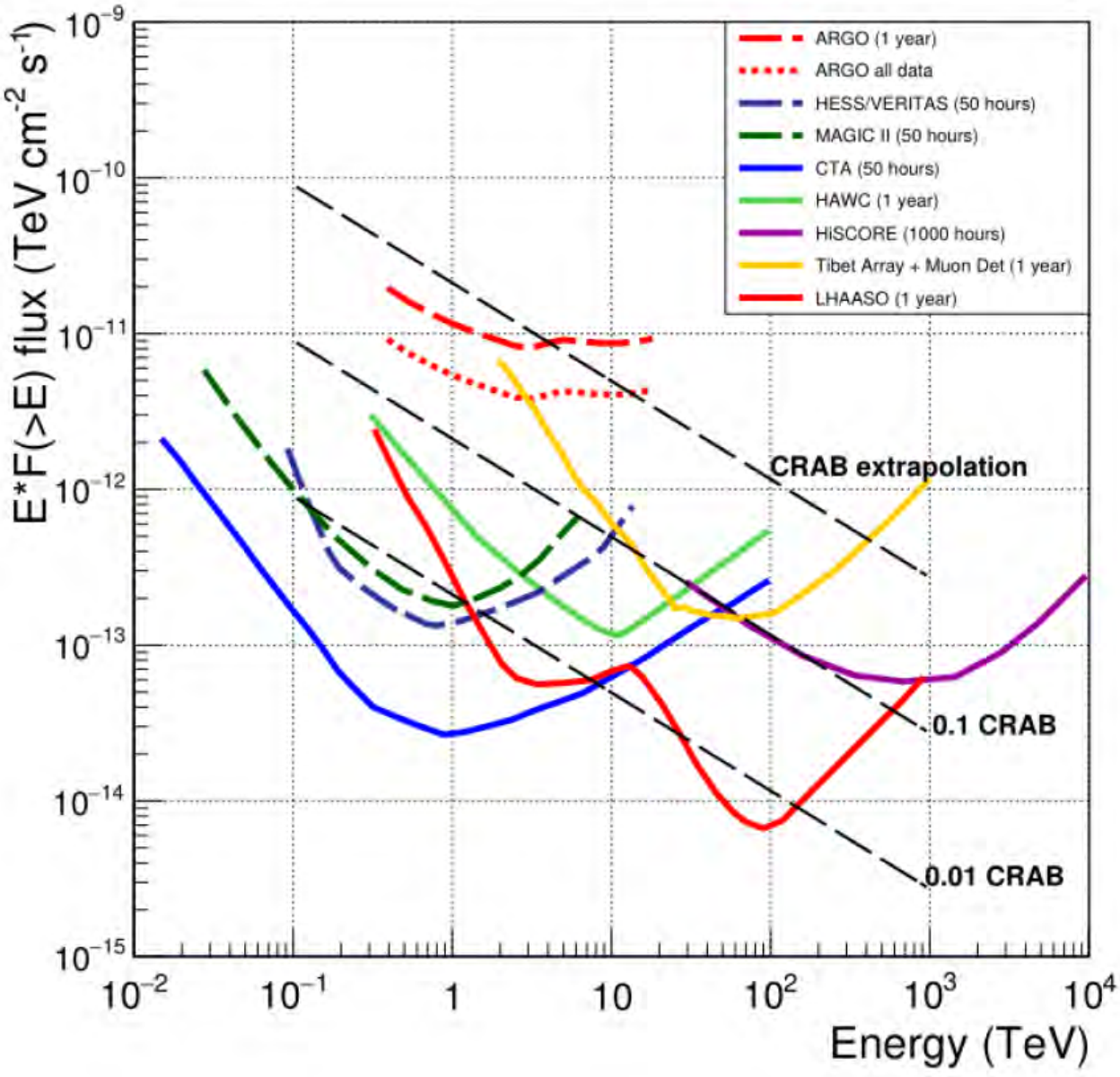

NEUTRINO TELESCOPES

The cosmic neutrino spectrum, from MeV to EeV

- **MeV-GeV:** Solar neutrinos & super Novæ, atmospheric neutrinos: various detectors but mostly a water Cherenkov domain with SuperKamiokande

- **GeV-TeV:** Cherenkov in natural water or ice, neutrinos atmospheric neutrinos and beyond.
  ICECUBE, ANTARES.

- **TeV-PeV:** the same but extended to 1 km^3 size.
  ICECUBE so far the only one.

- **EeV:** arrays foreseen for UHECR detection proved to be very efficient for UHE ν's. Observe quasi horizontal showers with AUGER.

Neutrino cross sections

- ν-matter cross sections:

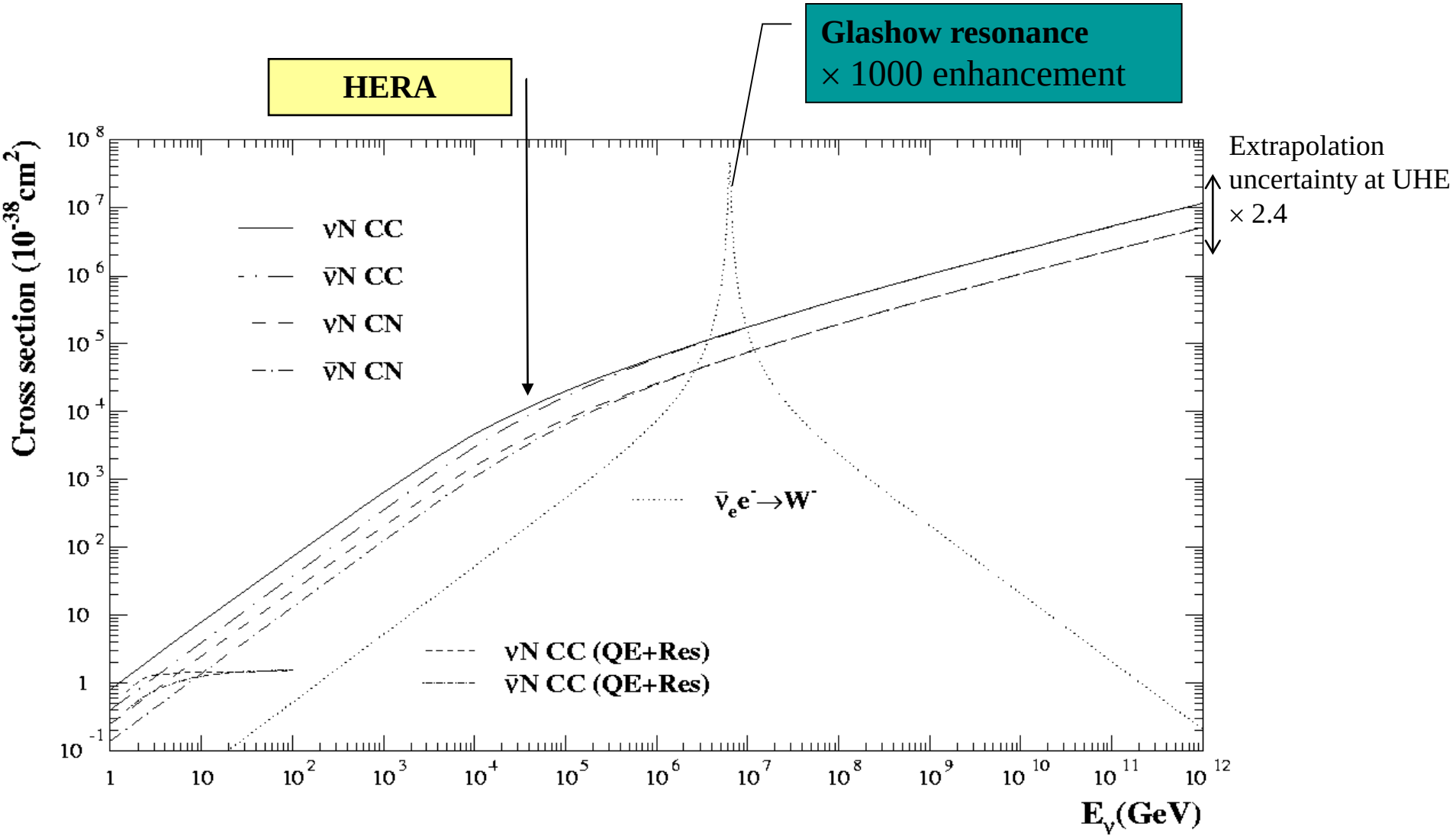

Neutrino detectors

… super heavy weight category !

$$\sigma(\nu N) \sim 0.6\times10^{-38} \times \left(\frac{E_\nu}{1\,\mathrm{GeV}}\right)\ \mathrm{cm}^{-2}$$

ex. the WBB of CERN :

10^{13} 400 GeV protons per extraction

$\Rightarrow \phi_\nu \approx 10^6\ \nu\ \mathrm{cm}^{-2}$ $\quad <E_\nu> \approx 20$ GeV

with:

$\sigma_{\nu,N} = 0.6\times10^{-38}\ (E/\mathrm{GeV})\ \mathrm{cm}^2\ \mathrm{GeV}^{-1}$

$N_A = 6.02\times10^{23}\ \mathrm{mol}^{-1}$

With a 100 tons detector, one gets:

$N_{evt} = N_{nucl} \times \phi_\nu \times \sigma_{\nu,N}$

$= 6.02\times10^{23}\times10^{8}\times10^{6} \times 0.6\times10^{-38}\times20$

$= 7{,}2$ events / extraction

GeV detection with SuperKamiokande

Atmospheric neutrino flux:

$$\phi \sim 2\ cm^{-2} s^{-1} sr^{-1}$$

$$\lambda = \frac{1}{\sigma n}$$

Interaction probability: $P(x) = 1 - \exp\left(\frac{-x}{\lambda}\right) = 1 - \exp(-n\sigma x)$

$$n = \rho\ N_A$$

Interaction length λ: $\lambda \sim \left(6 \times 10^{23} \times 10^{-38}\right)^{-1} \sim 1.7\ \ 10^{14}\ cm$

thus : $P(L) \sim \left(\frac{L}{1m}\right) \times 6\ \ 10^{-13}$

Number of events per day in a detector of volume V=S×L

$$N = \phi\ \Omega S\ P(L)$$
$$\approx \left(2.10^4\, m^{-2} sr^{-1} s^{-1}\right) \times \left(4\pi\, sr\right) \times \left(8.10^4\, s\right) \times 6.10^{-13} \times V$$
$$\approx 1.2 \times 10^{-2}\ \text{events/day/m}^3\ \text{of water}$$

Super Kamiokande

- Super-Kamiokande, underground water cherenkov detector in Japan, 50000 tons of ultra pure water, 12000 PM with Ø=50cm.

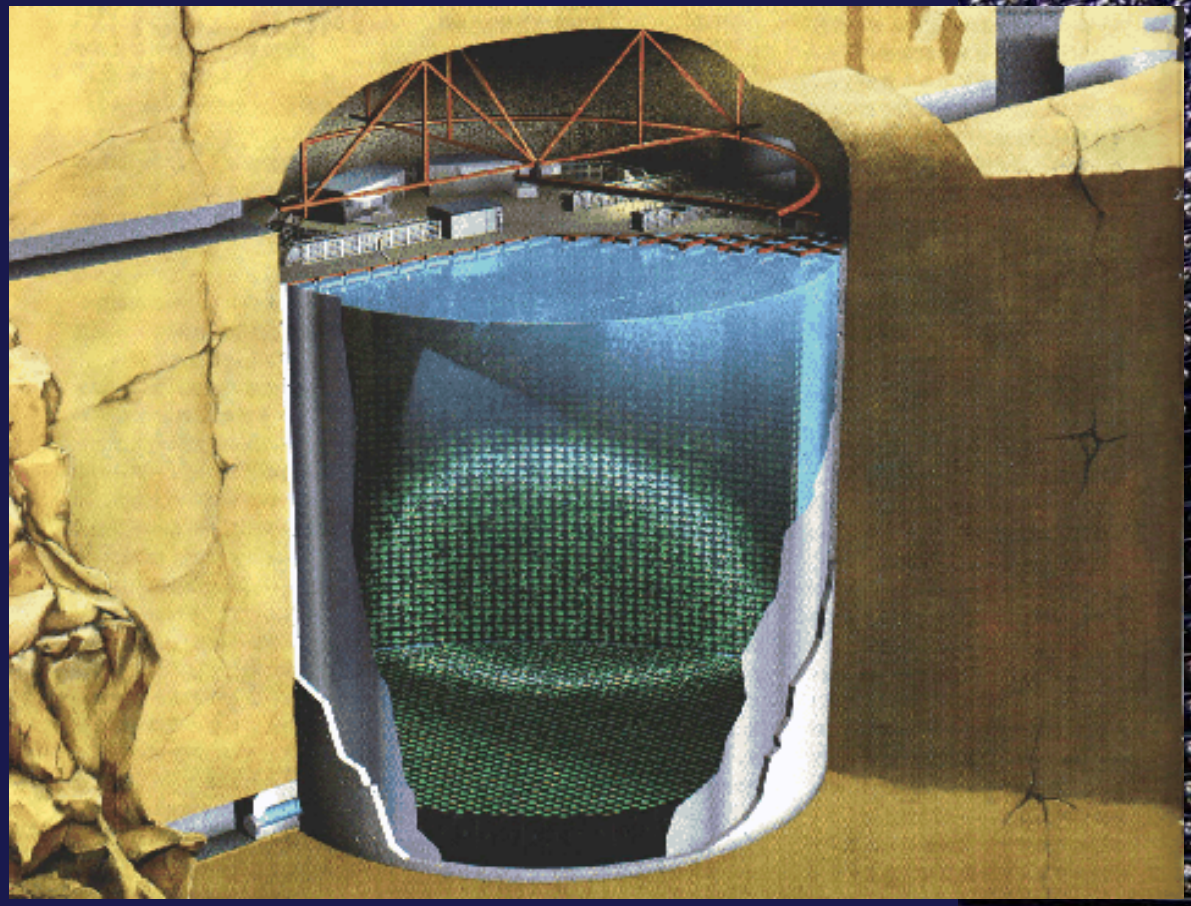

- Water Cherenkov type Detector
- 22.5 kton Fid. Volume
- Concentric Cylindrical Shape
- 11146 PMTs for Inner Detector
- 1885 PMTs for Outer Detector
- Run from Apr. 1996 to Jul. 2001

Super Kamiokande

Super Kamiokande

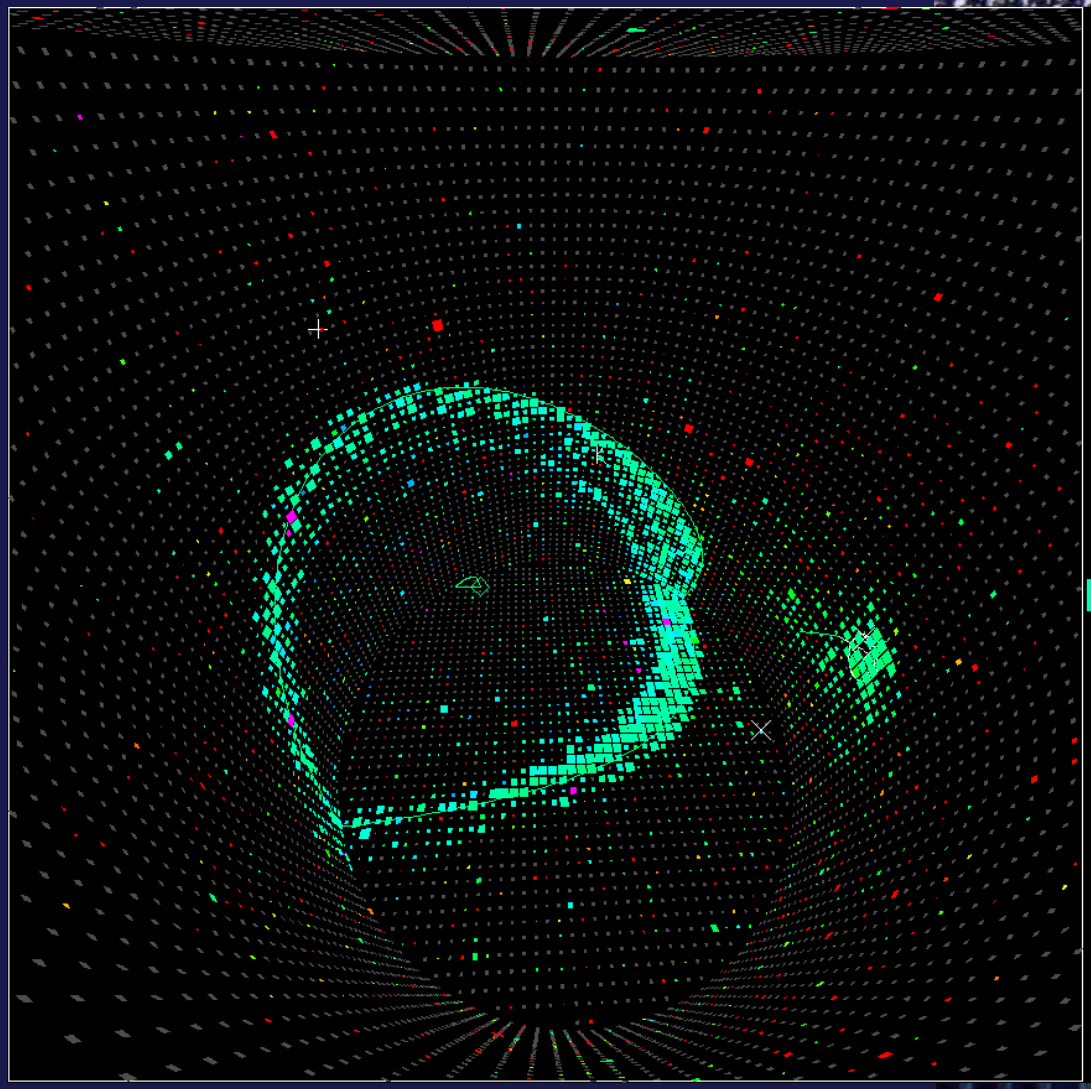

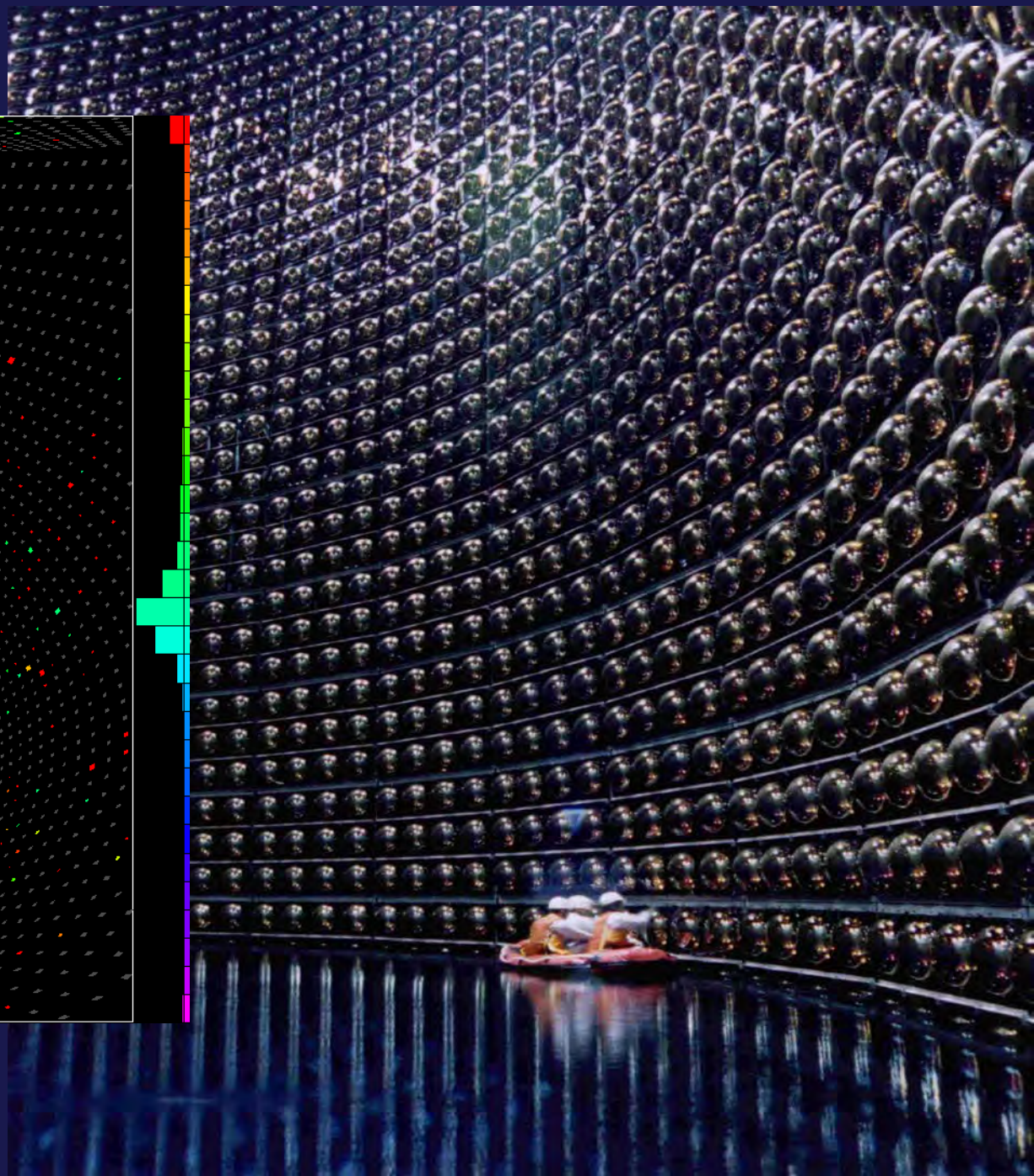

Super Kamiokande

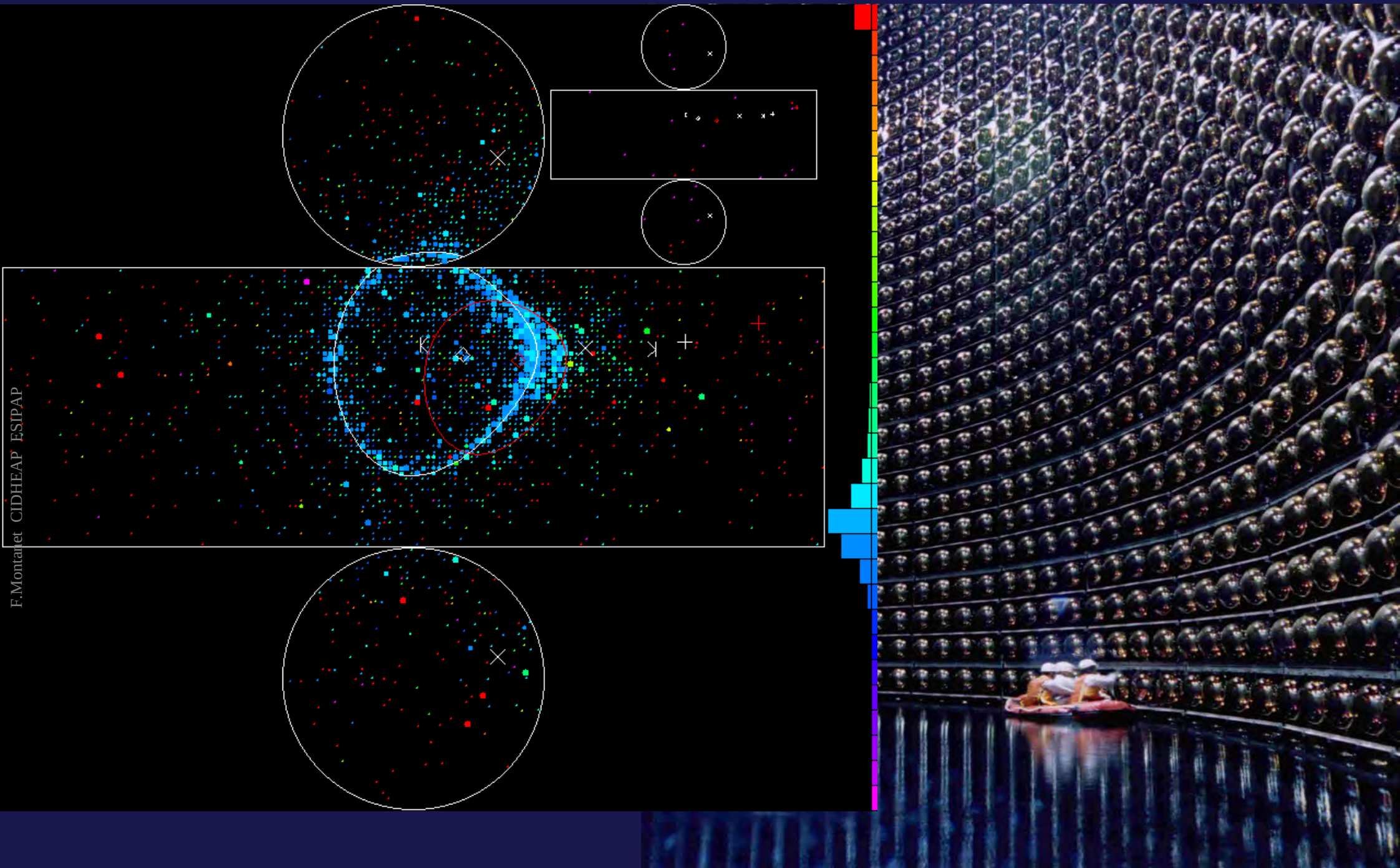

Event patterns in Super-Kamiokande

Fully Contained (FC) event

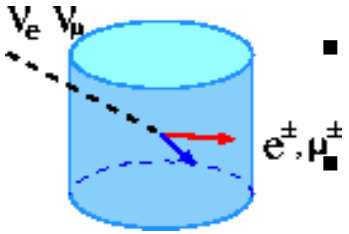

- All visible particles are contained in the detector
- both ν_μ、ν_e via NC or CC interaction
- Typically E_ν = 1 GeV
- Particle ID

Partially Contained (PC) event

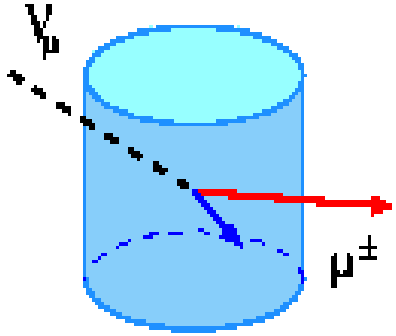

- At least 1 charged particle escapes from detector
- ν_μCC (97%)
- Typically E_ν=10 GeV

Upward-going muons (Up-mu)

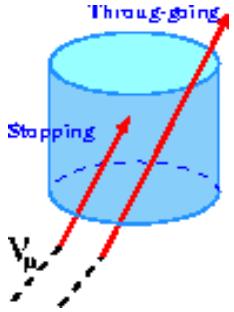

- Entering muon from below
- ν_μ CC only
- E_ν= 10 GeV(stopping),
- 100 GeV(through-going)

Super-Kamiokande covers E_ν = 100 MeV ~ over 1 TeV

Atmospheric neutrinos

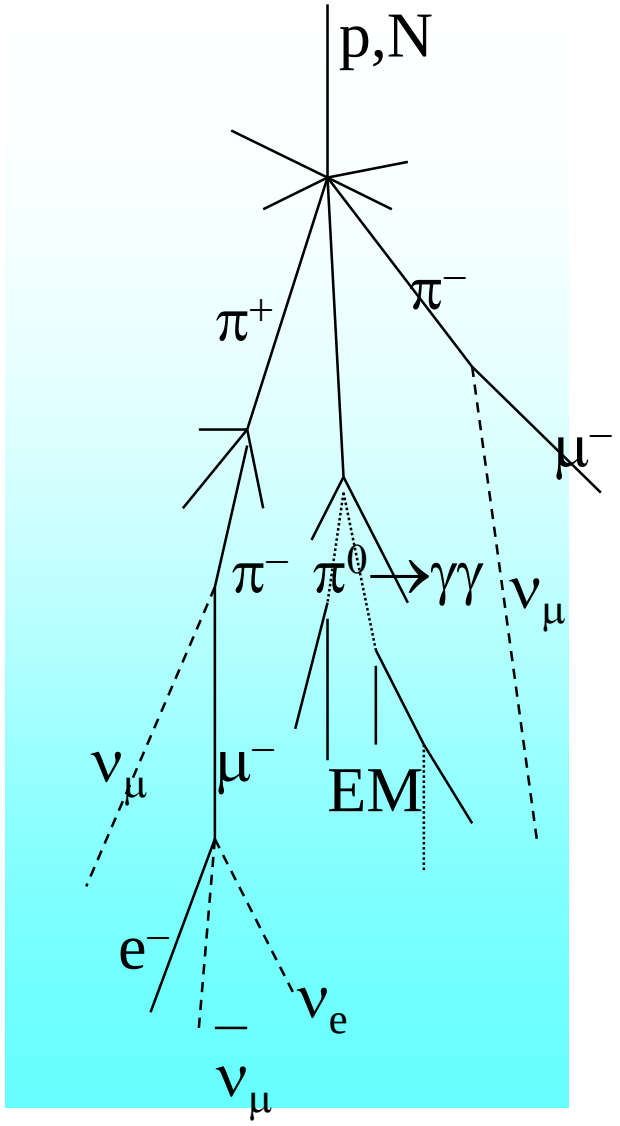

- Atmosphere :
  - ~1000 g/cm²
  - ~20 km
  - 11 nuclear λ_{int}
- ν dominated by :

$$\left.\begin{array}{rcll} \pi^+ & \rightarrow & \mu^+ & + \nu_\mu \\ & & \hookrightarrow & e^+ + \bar{\nu}_\mu + \nu_e \\ \pi^- & \rightarrow & \mu^- & + \bar{\nu}_\mu \\ & & \hookrightarrow & e^- + \nu_\mu + \bar{\nu}_e \end{array}\right\} \Rightarrow 2\nu_\mu \text{ for } 1\nu_e$$

- Kinematics :

$$\pi^+ \rightarrow \mu^+ + \nu_\mu \qquad \mu^+ \rightarrow e^+ + \nu_e + \bar{\nu}_\mu$$
$$\langle E_\mu \rangle = 0.787 E_\pi \qquad \langle E_\nu \rangle = 1/3 E_\mu$$
$$\langle E_\nu \rangle = 0.213 E_\pi$$

$$\Rightarrow \left\langle E_{\nu_\mu} \right\rangle : \langle E_{\nu_e} \rangle : \left\langle E_{\bar{\nu}_\mu} \right\rangle \approx 1 : 1 : 1$$

- 1 GeV sea level neutrino fux:

$$\phi \approx 2 \text{cm}^{-2} \text{s}^{-1} \text{sr}^{-1}$$

Atmospheric neutrinos

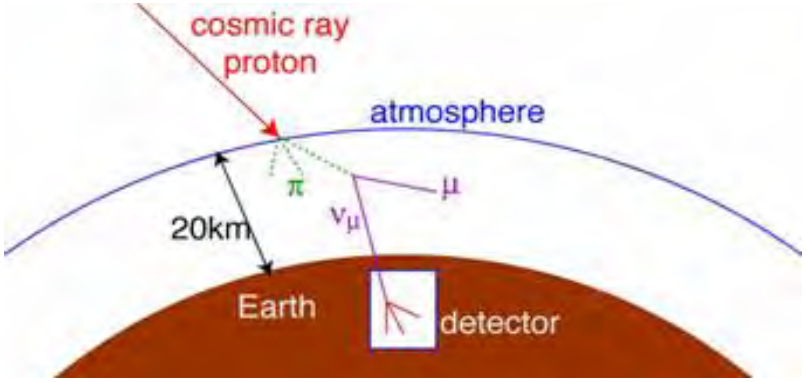

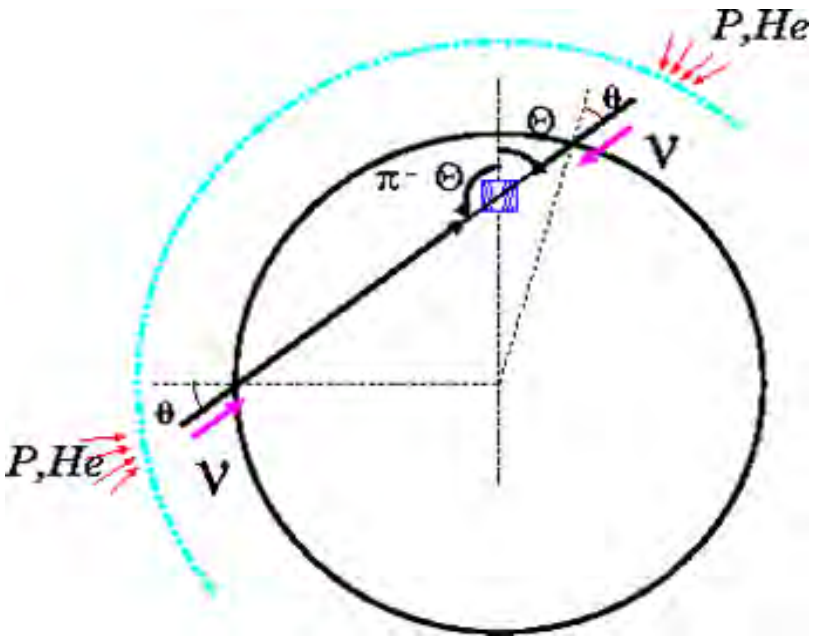

- **Flavor ratio**

$$\frac{\nu_\mu + \bar{\nu}_\mu}{\nu_e + \bar{\nu}_e} \approx 2 \text{ for } E_\nu \leq \text{qq GeV}$$
$$> 2 \text{ for } E_\nu > \text{qq GeV}$$

- **top down symmetry**

for $E_\nu >$ qq GeV

Distance traveled : $L_\nu = 10$ to 13000 km

Survival probability

$p = 1\,\mathrm{GeV/c}\ ,\ \sin^2 2\theta = 1$

$\Delta m^2 = 3 \times 10^{-3}\ (\mathrm{eV/c^2})^2$

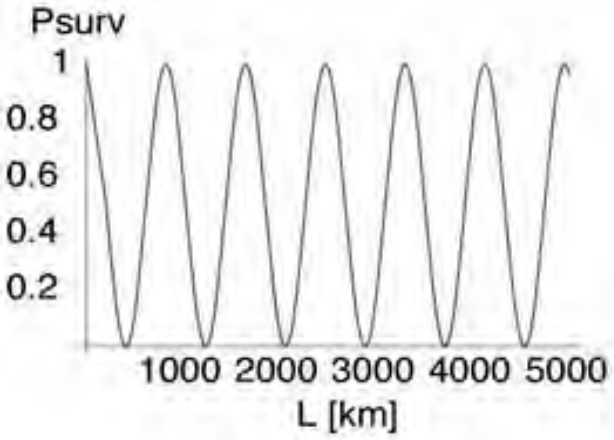

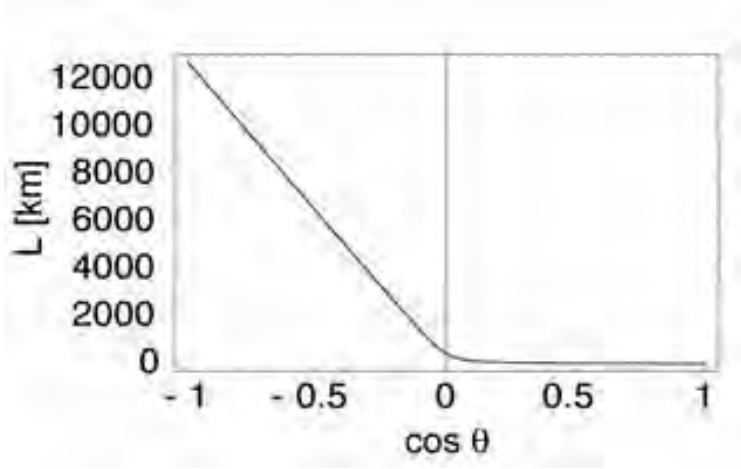

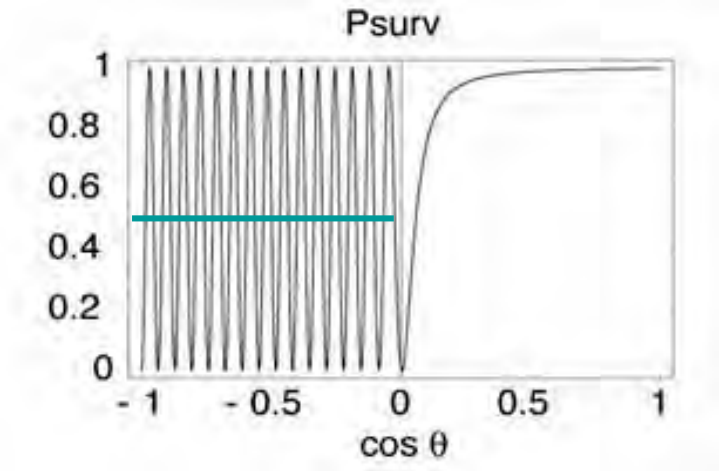

Half of upgoing ν_μ are lost.

Half of ν_μ disappeared !

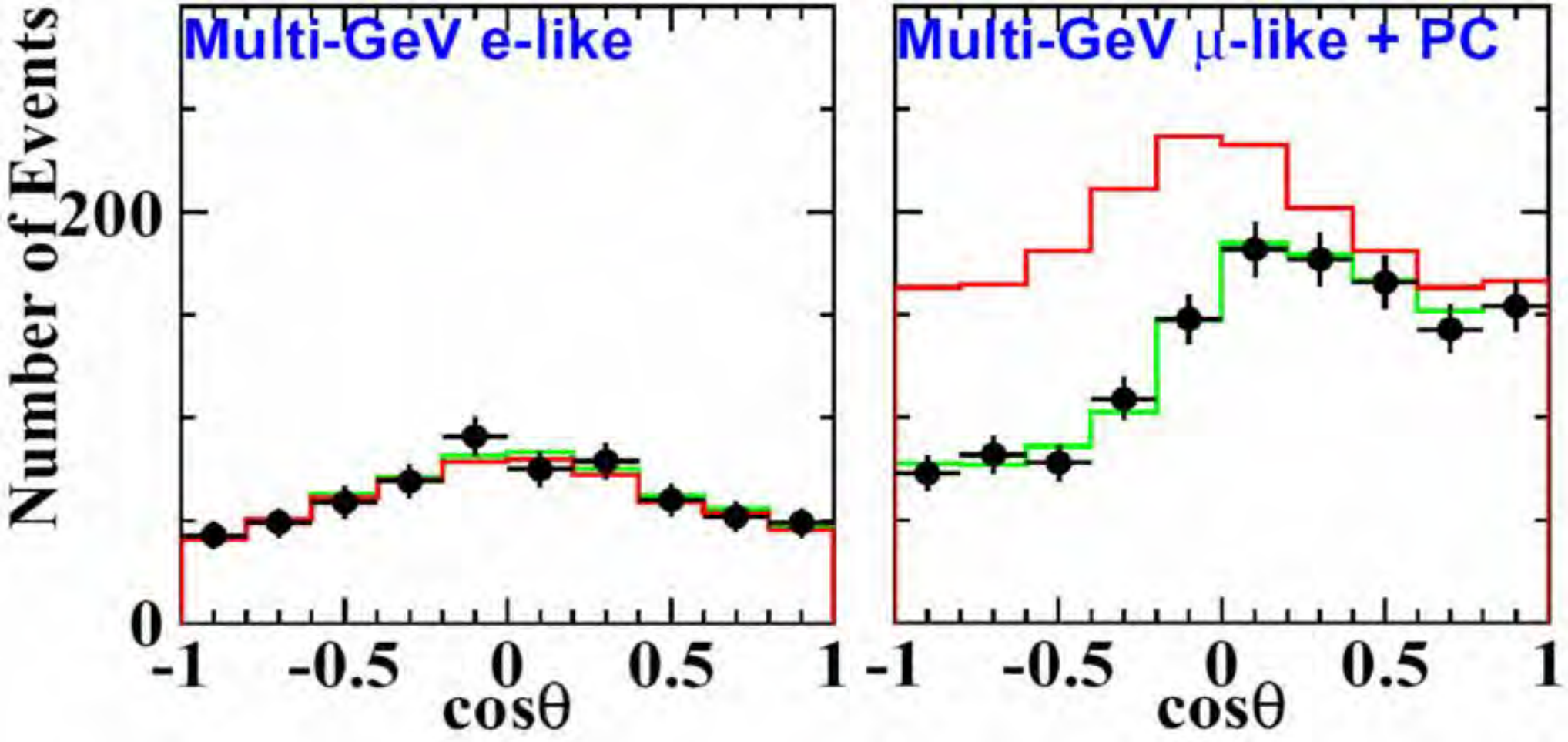

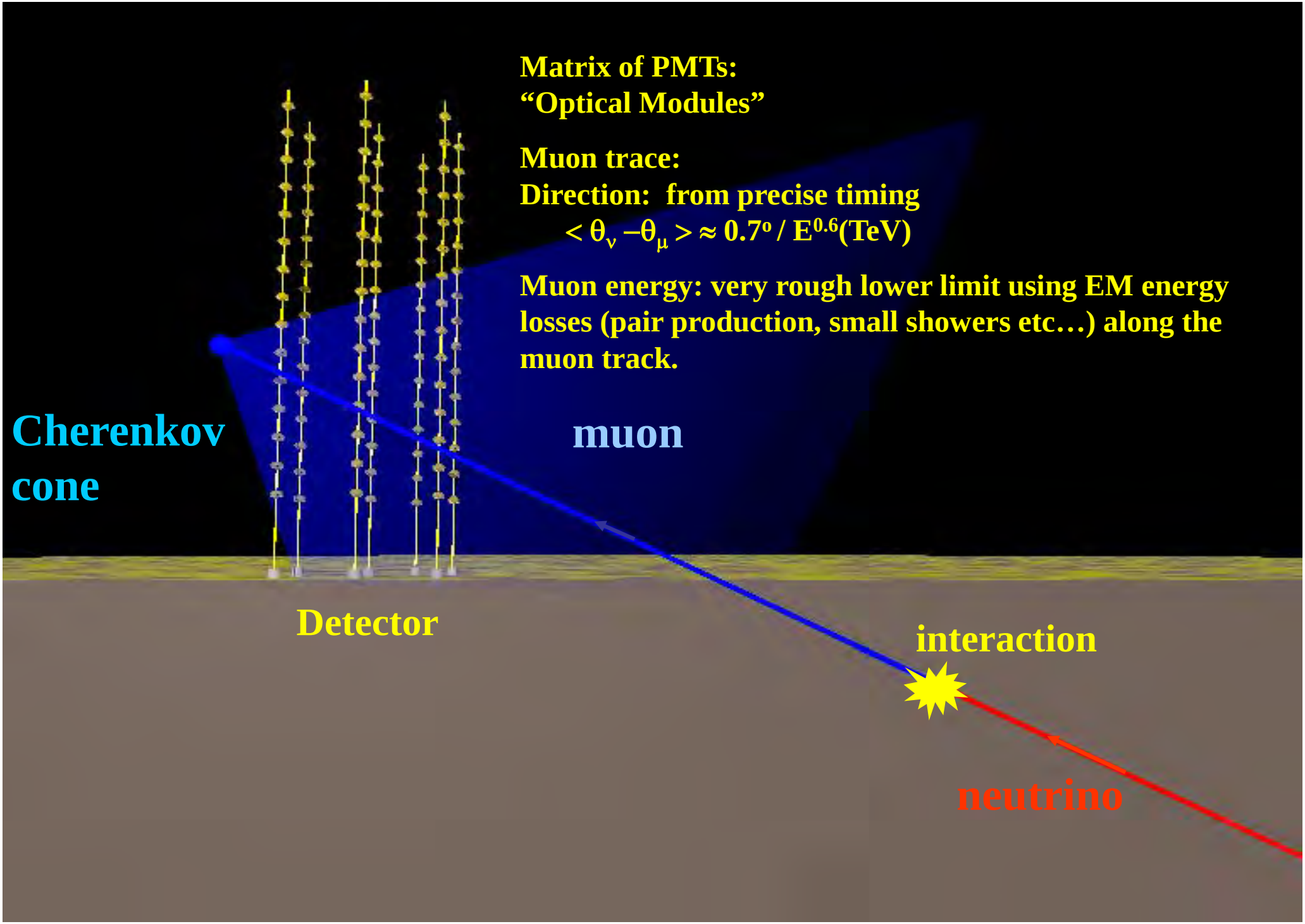
Matrix of PMTs:
"Optical Modules"
Muon trace:
Direction: from precise timing
$< \theta_\nu - \theta_\mu > \approx 0.7^o / E^{0.6}(TeV)$
Muon energy: very rough lower limit using EM energy losses (pair production, small showers etc…) along the muon track.
Cherenkov cone
muon
Detector
interaction
neutrino

Neutrino cross sections

- ν-matter cross sections:

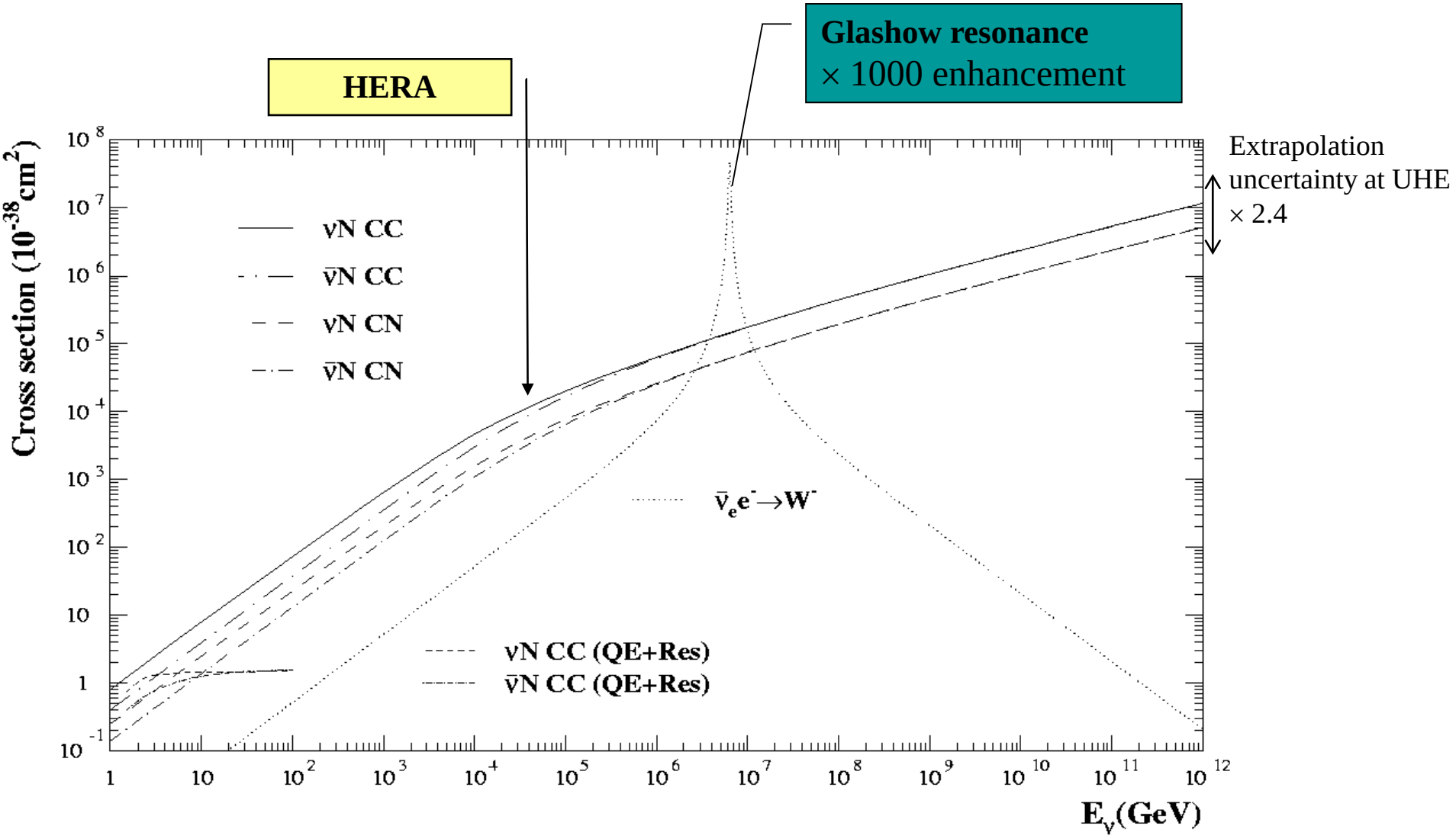

Particle Ranges

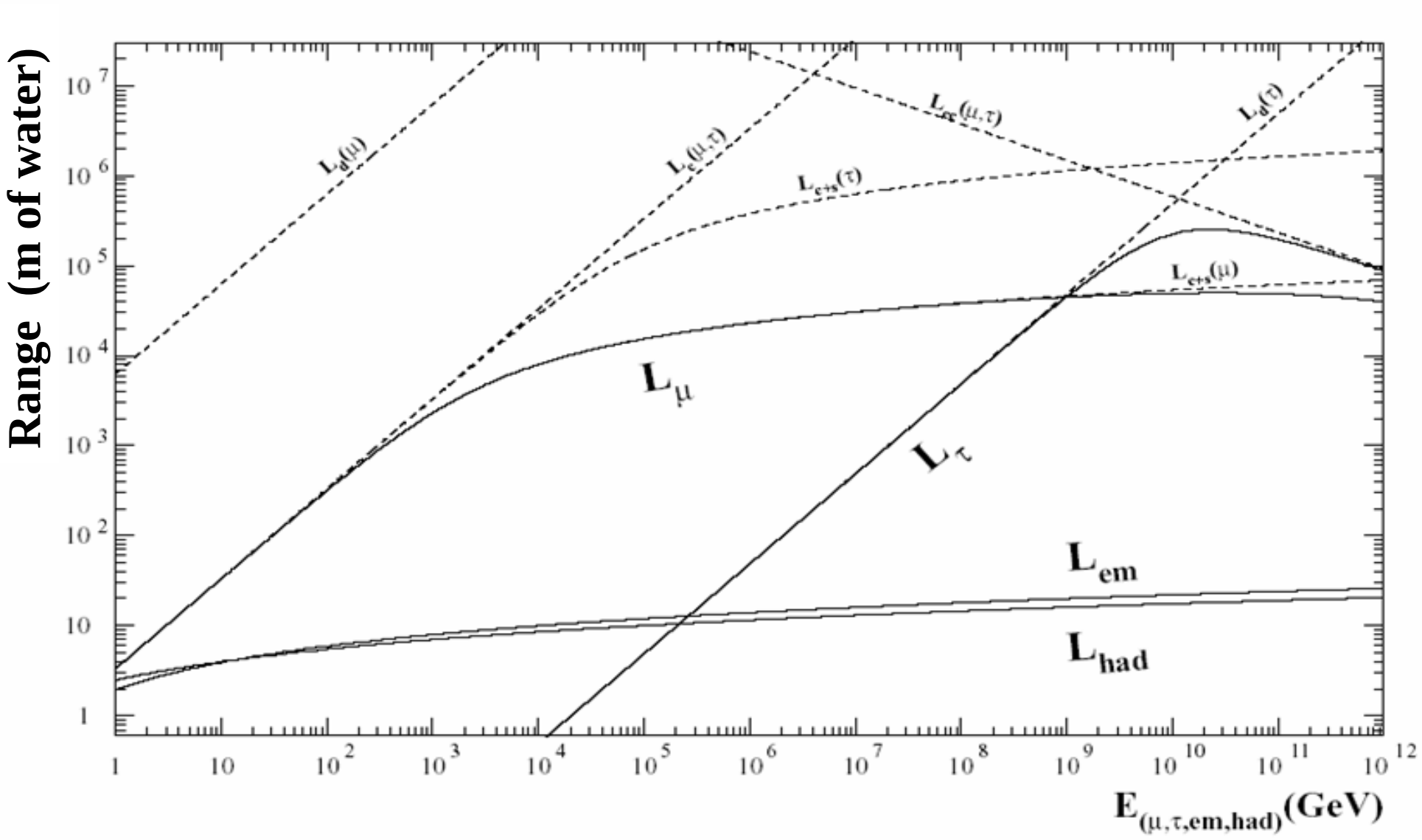

Earth opacity

The earth is transparent to ν_μ < 100 TeV

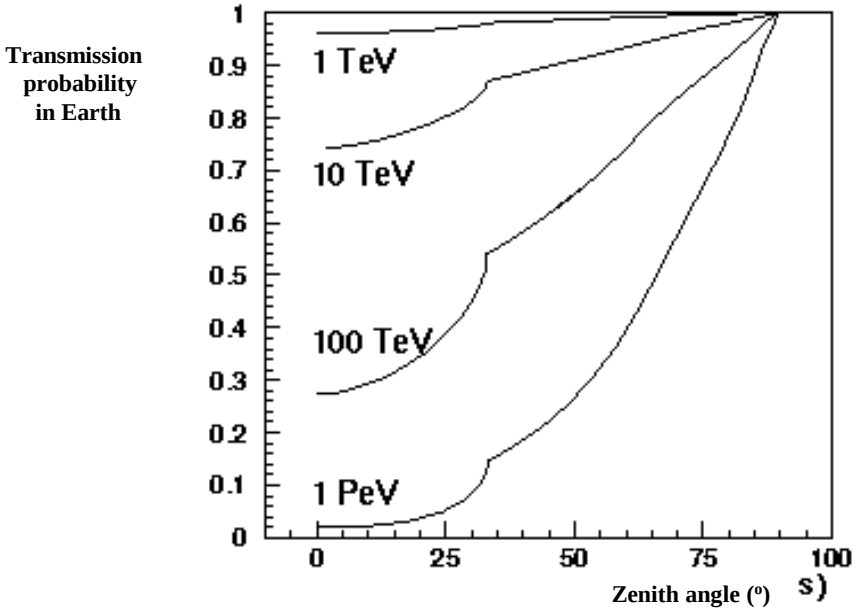

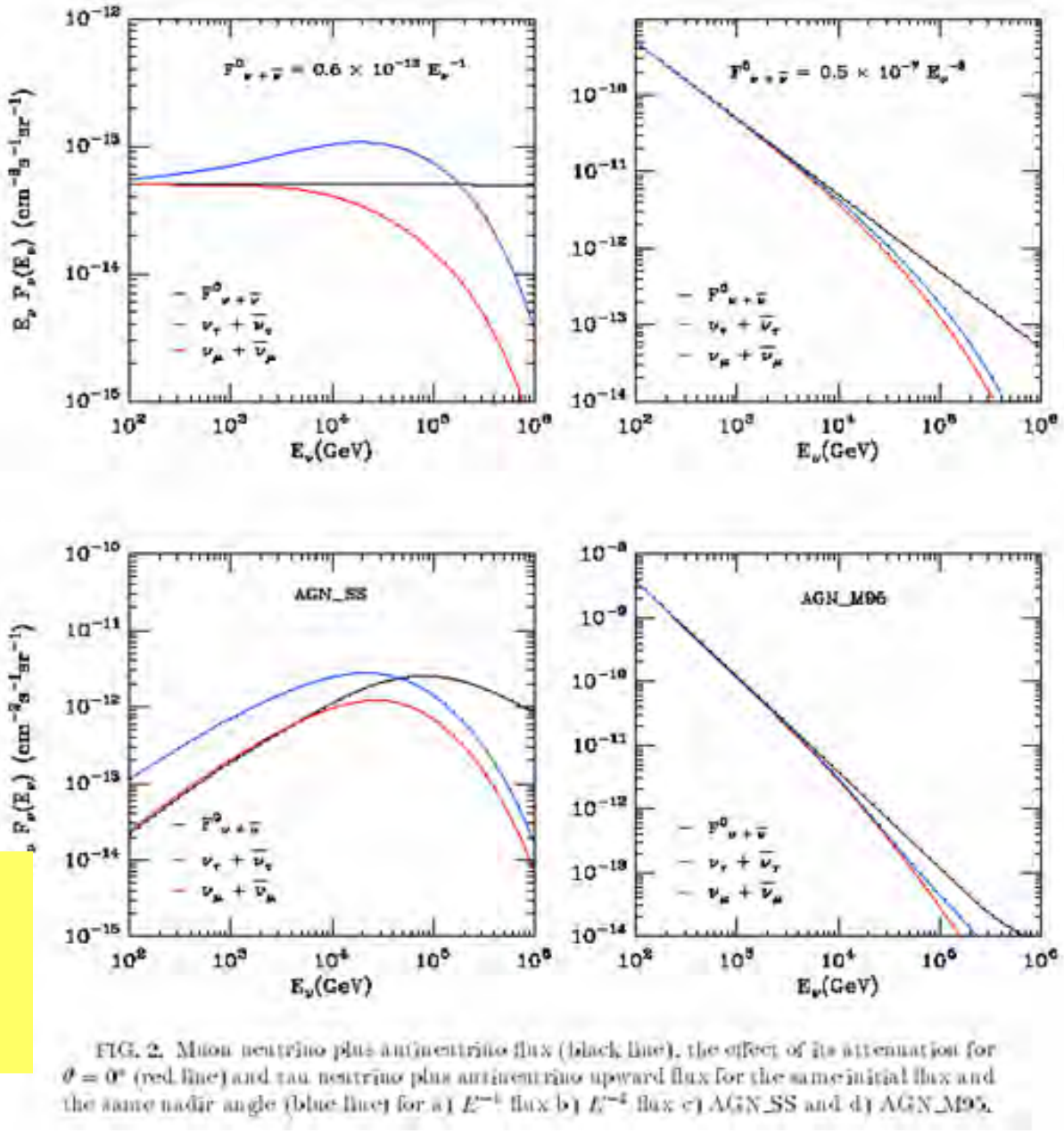

FIG. 2. Muon neutrino plus antineutrino flux (black line), the effect of its attenuation for $\theta = 0°$ (red line) and tau neutrino plus antineutrino upward flux for the same initial flux and the same nadir angle (blue line) for a) E^{-1} flux b) E^{-2} flux c) AGN_SS and d) AGN_M95.

ν_μ absorbed via cc, or regenerated via nc

ν_τ regenerated via cc because $\tau \rightarrow \nu_\tau$ before interacting or losing significant energy.

Detection principles

– **The effective target volume is / the muon range**

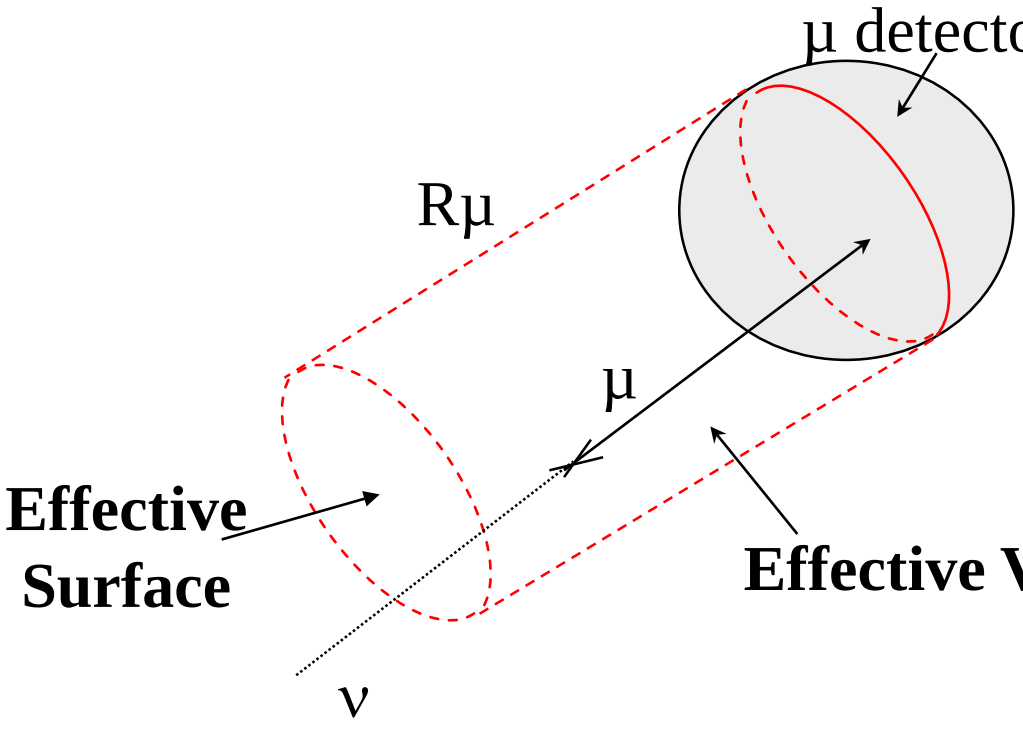

Effective Volume >> Detection Volume

$$V_{eff}(E_\mu) = A_{eff}(E_\mu) \cdot R_\mu(E_\mu)$$

R_μ = 2 km @ 1 TeV

R_μ = 10 km @ 100 TeV

R_μ^{max} = 50 km @ 1 EeV

PeV ν_μ in IceCube

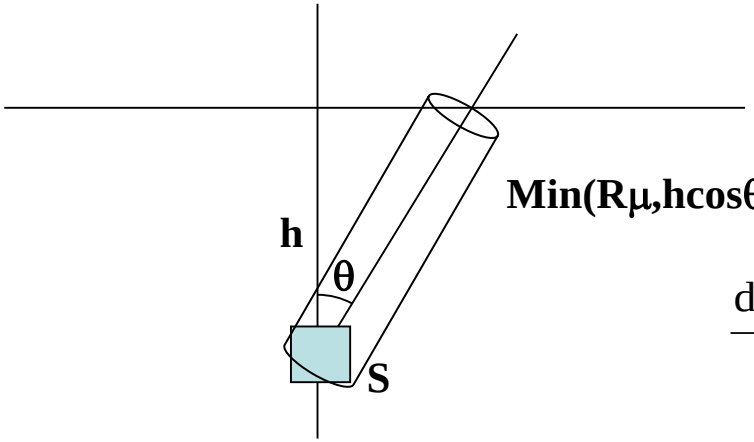

$$\frac{\partial \phi_i(E,z)}{\partial z} = -\frac{\partial P^i_{loss}(E,z)\partial z}{\partial z}\phi_i(E,t) + \sum_j \int_E^\infty \frac{\partial P_{j\to i}(E',E,z)}{\partial E \partial z}\phi_i(E',z)\,dE'$$

$$\frac{dN_{\mu\ E>1PeV}}{dE} = 2\pi\, S \int_{-1}^{1} \frac{\partial \phi_i(E,z(\cos\theta))}{\partial z}\,\sigma_{cc}(E)\,\frac{\rho_{det}}{m_p}\,\mathrm{Min}(R_\mu, z(\cos\theta))\,d(\cos\theta)$$

Target volume accounting for E_μ>1 PeV range and an ν initial energy of 1EeV ~ 10^{13} tons of ice.

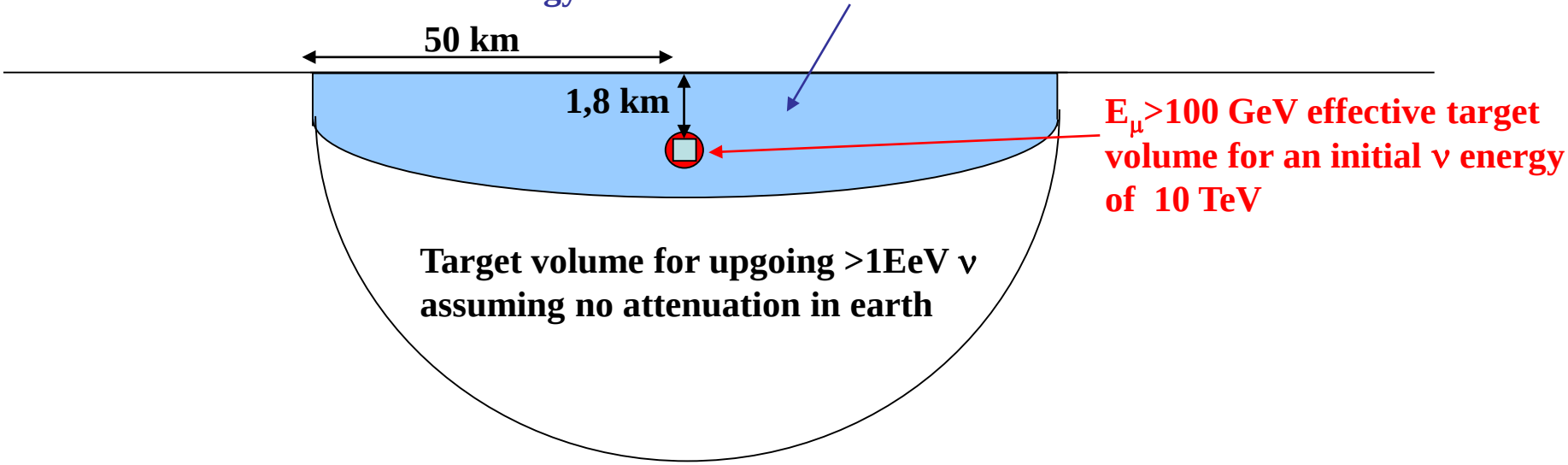

Neutrino Telescope Projects

ANTARES La-Seyne-sur-Mer, France
NEMO Catania, Italy, KM3NET ?

BAIKAL:
Lake Baikal, Siberia

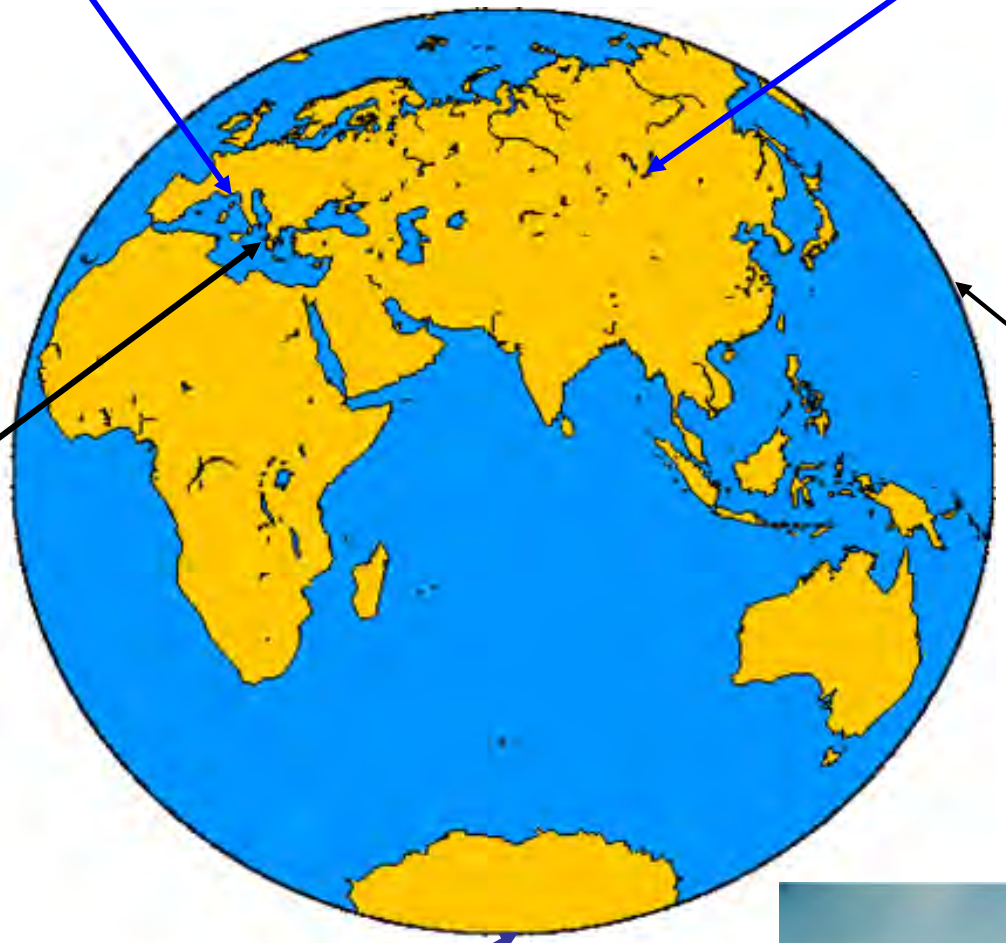

NESTOR : Pylos, Greece

DUMAND, Hawaii
(cancelled 1995)

AMANDA, ICECUBE
South Pole, Antarctica

AMANDA

South Pole: glacial ice

1993 First strings AMANDA A
1998 AMANDA B10 ~ 300 Optical Modules

2000 ~ 700 Optical Modules

→ ICECUBE 8000 Optical Modules

AMANDA
ν > 50GeV

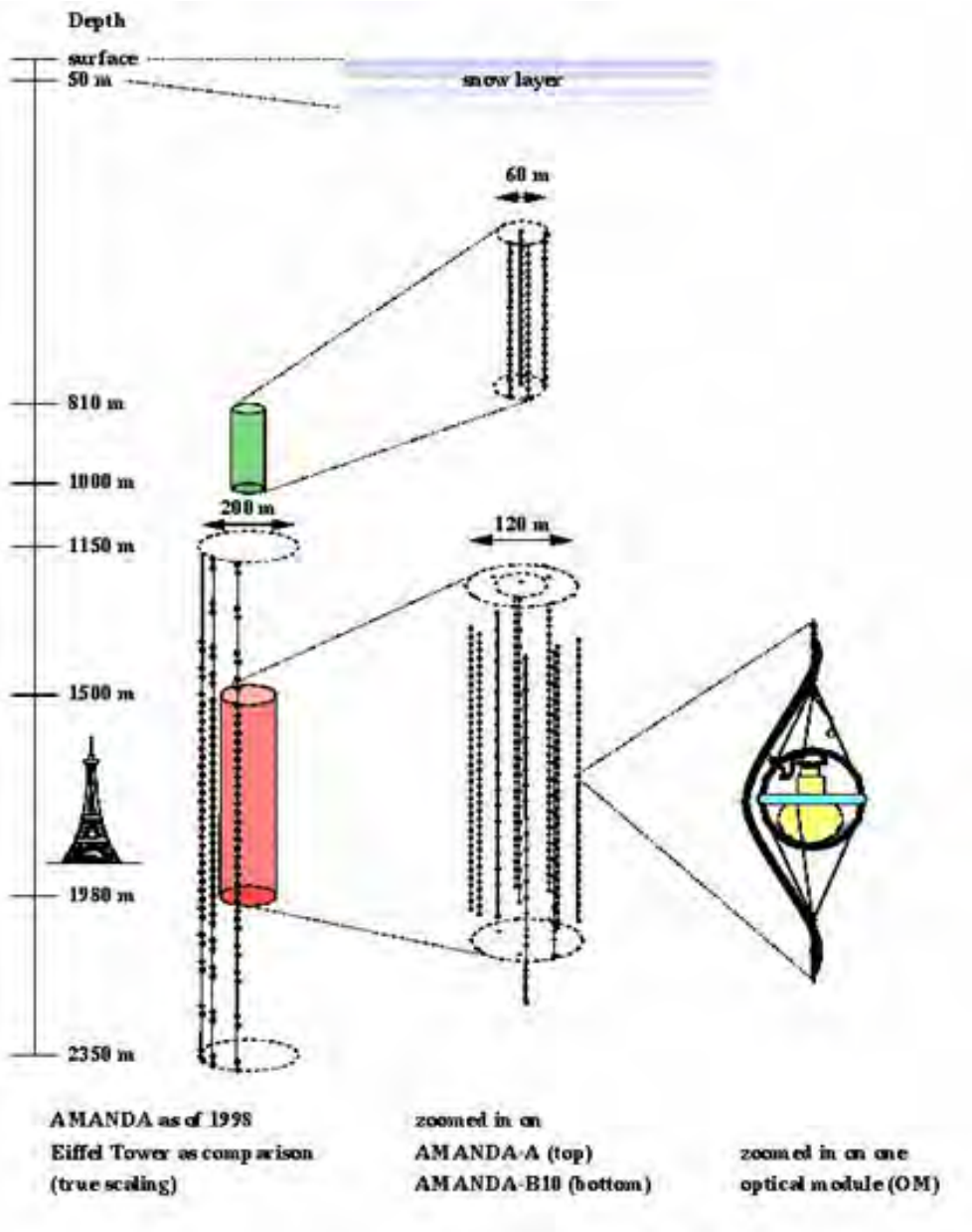

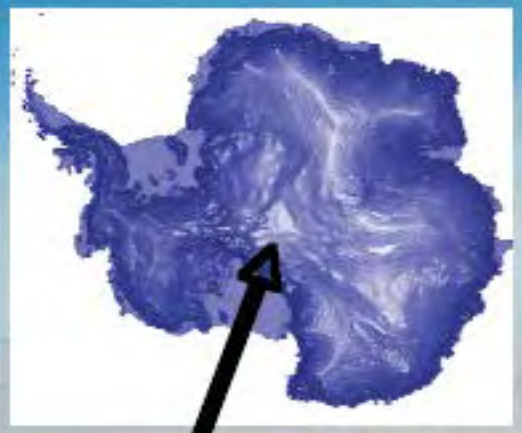

Geographic South Pole

Skiway

IceCube

Drill Site

Counting House

AMANDA

Amundsen-Scott
South Pole Station
(NSF)

AMANDA: Drill Holes in ice with Hot Water

Event reconstruction in Amanda

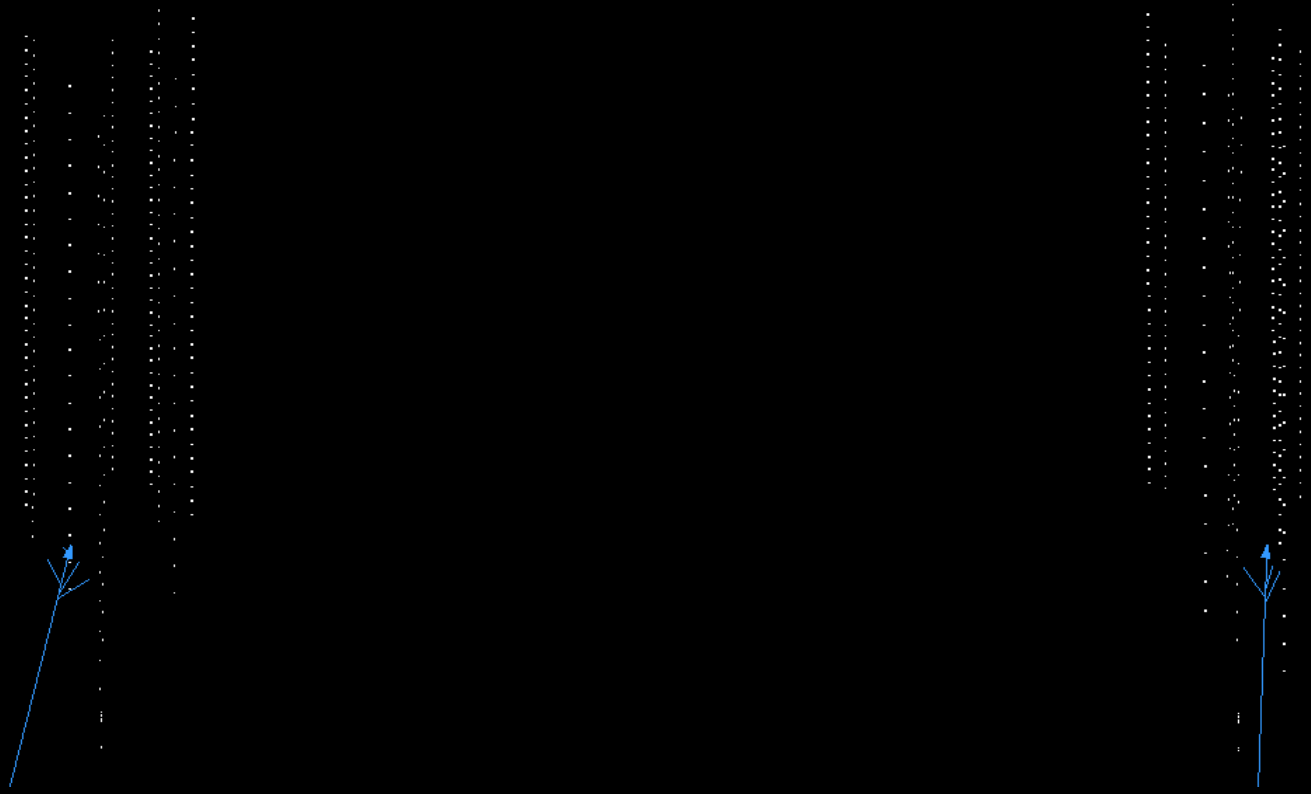

The IceCube detector

instrumenting 1 km³ of ice

IceTop :
Surface air shower array
Frozen tanks - 2DOMs

InIce :
80 strings each with 60 digital optical modules (DOM)

125m spacing between strings
17m between DOMs

Detect **ν** *of all flavors*
E range : 10^{11} to 10^{20} eV

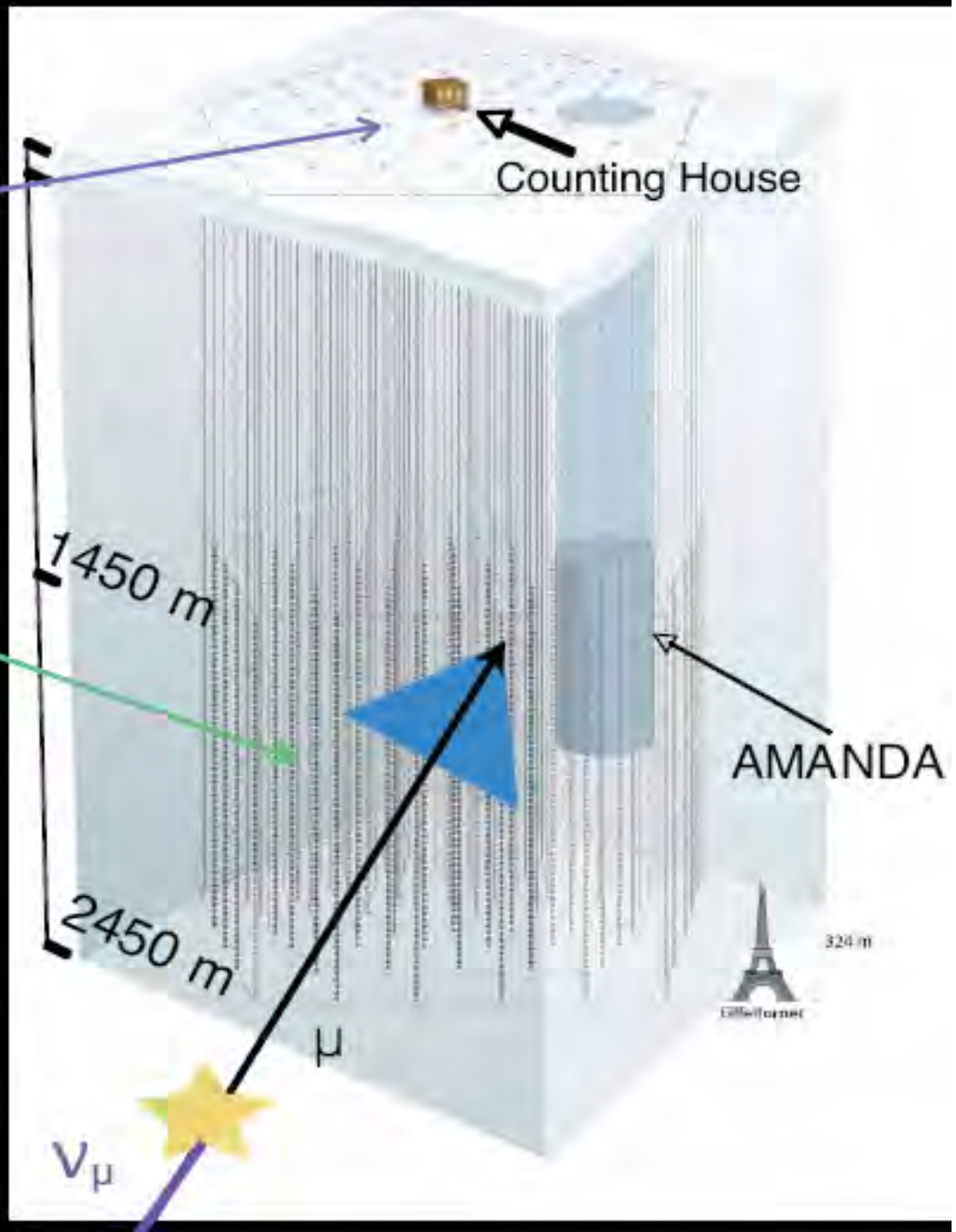

Current ν telescope in the sea: ANTARES

1996	Started
1996 - 2000	Site exploration and demonstrator line
2001 - 2004	Construction of 10 line detector, area ~0.1km^2 on Toulon site
future	1 km^3 in Mediterranean

Angular resolution <0.4° for E>10 TeV

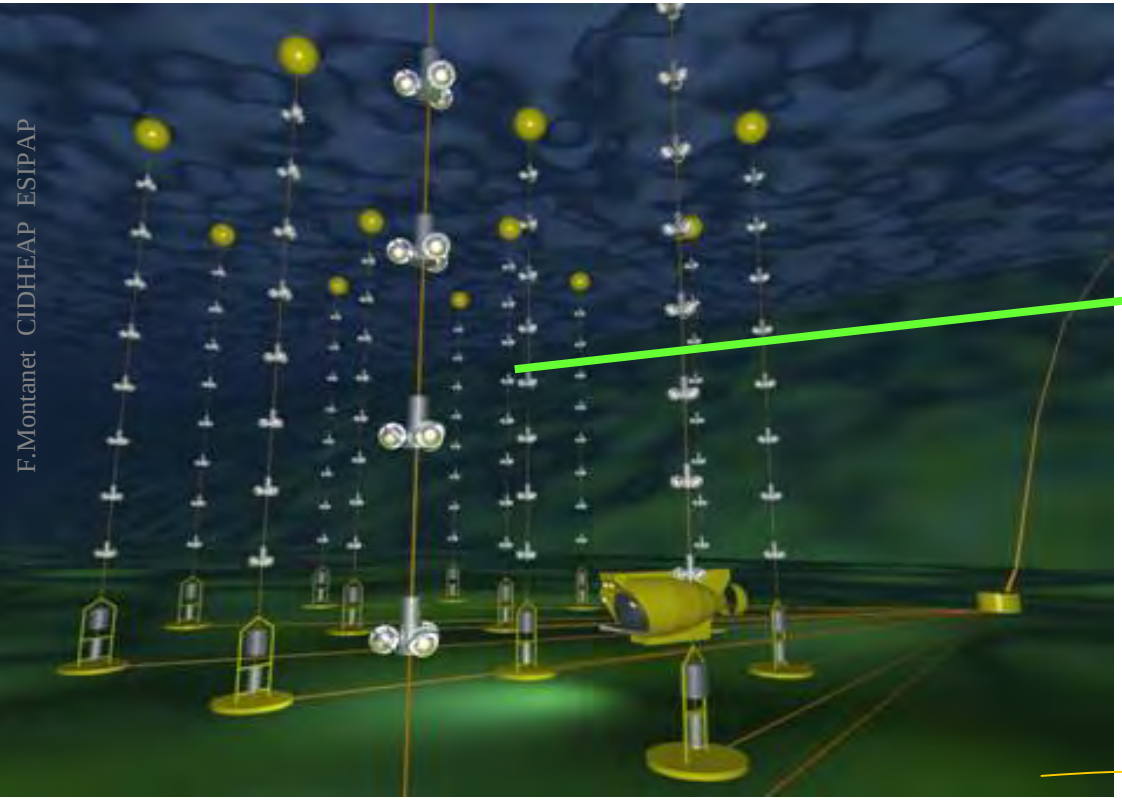

F.Montanet CIDHEAP ESIPAP

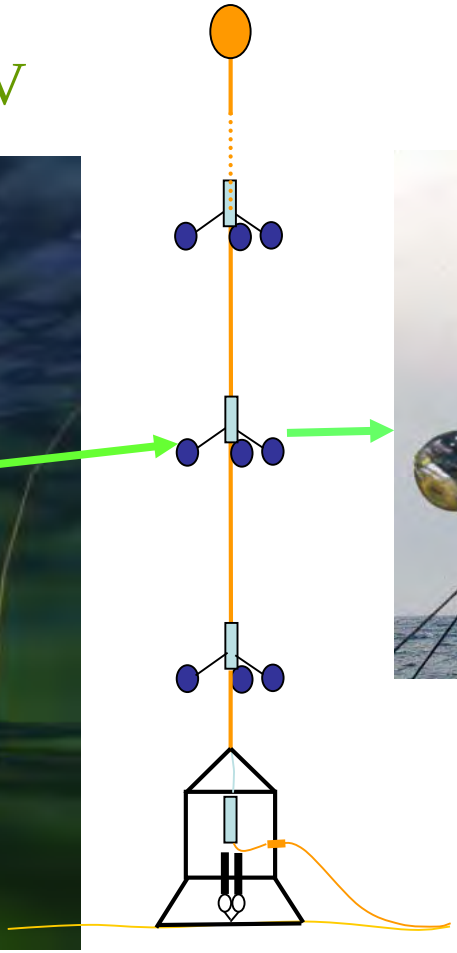

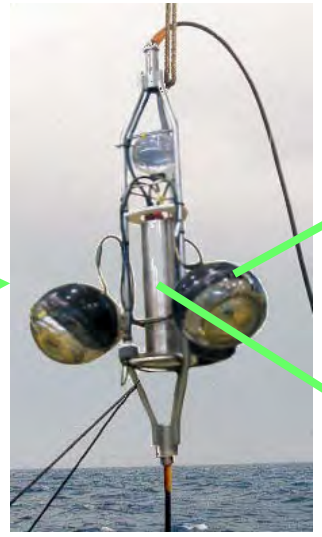

ANTARES 0.1km^2 Detector

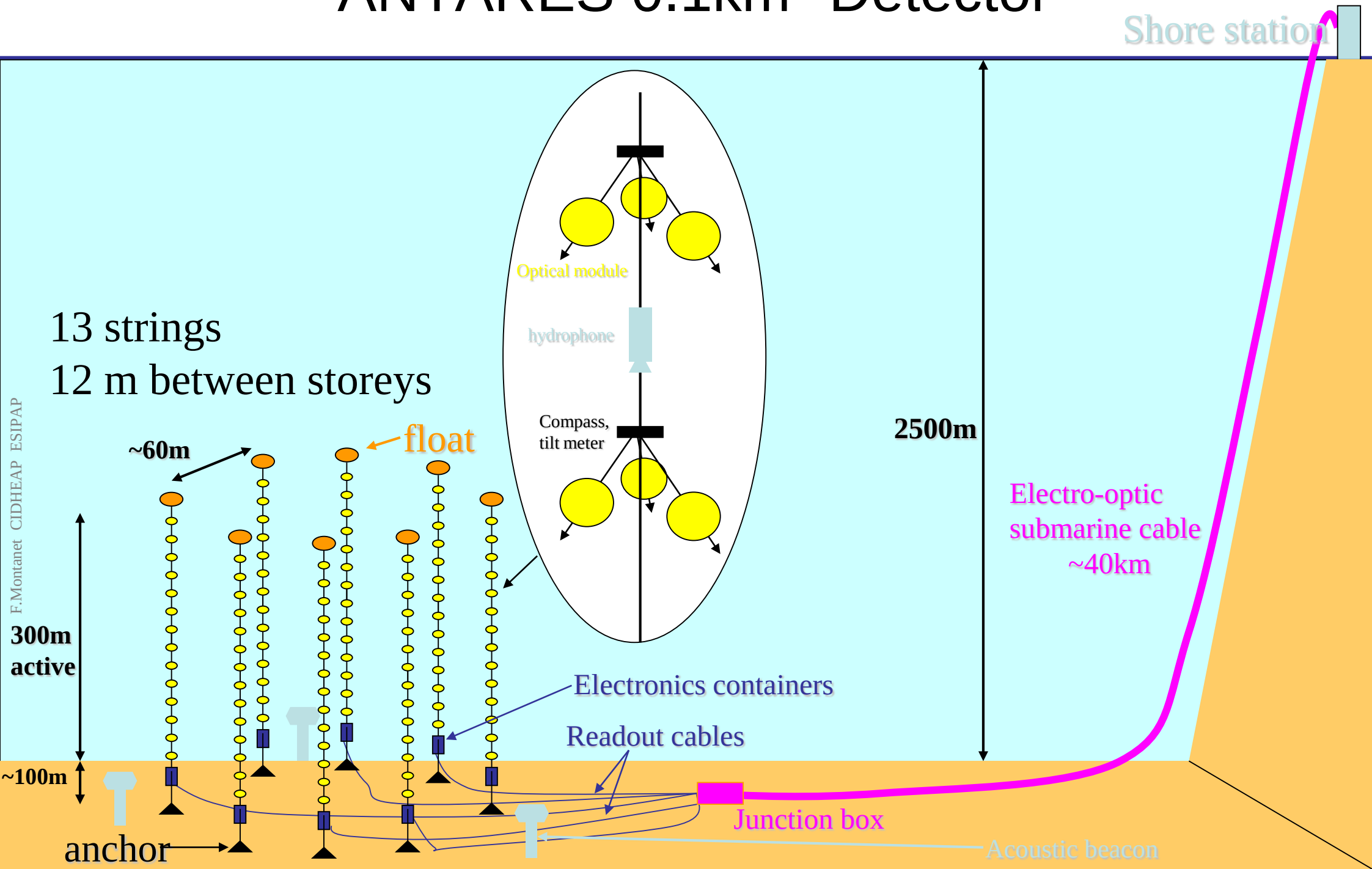

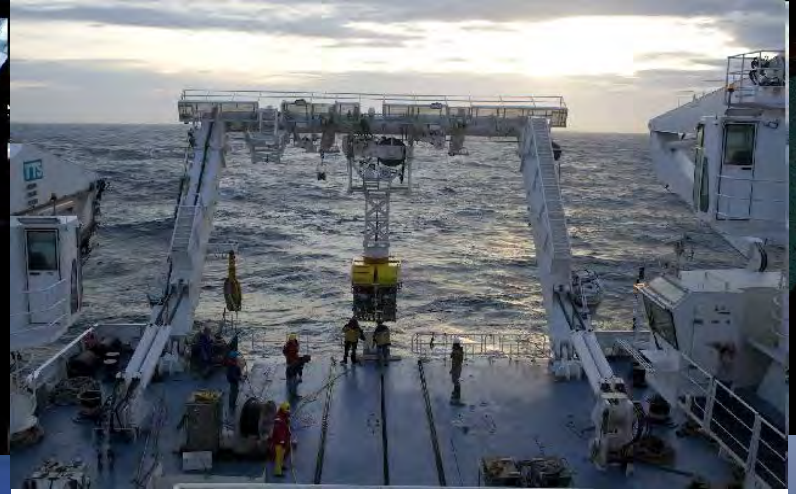

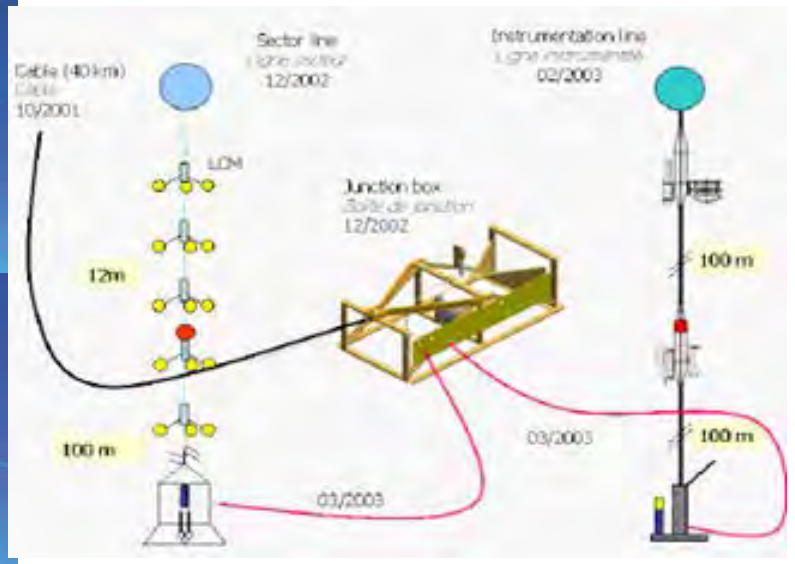

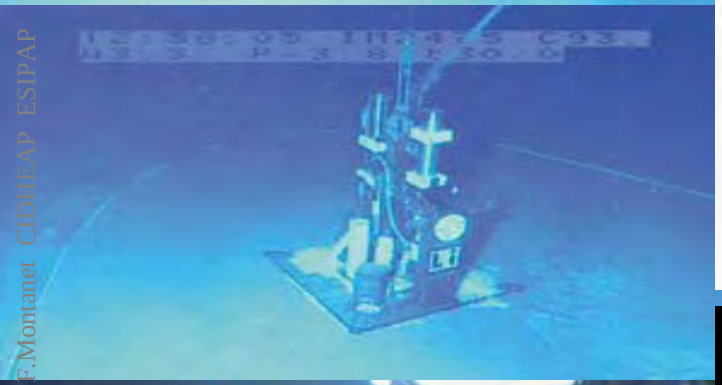

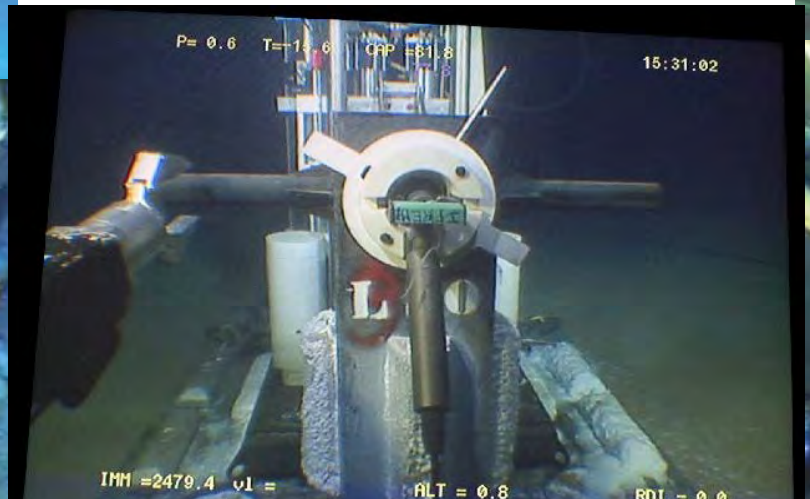

Detection principle

Production energy of μ's reaching the detector

Mean Eμ/Eν ratio versus Eν

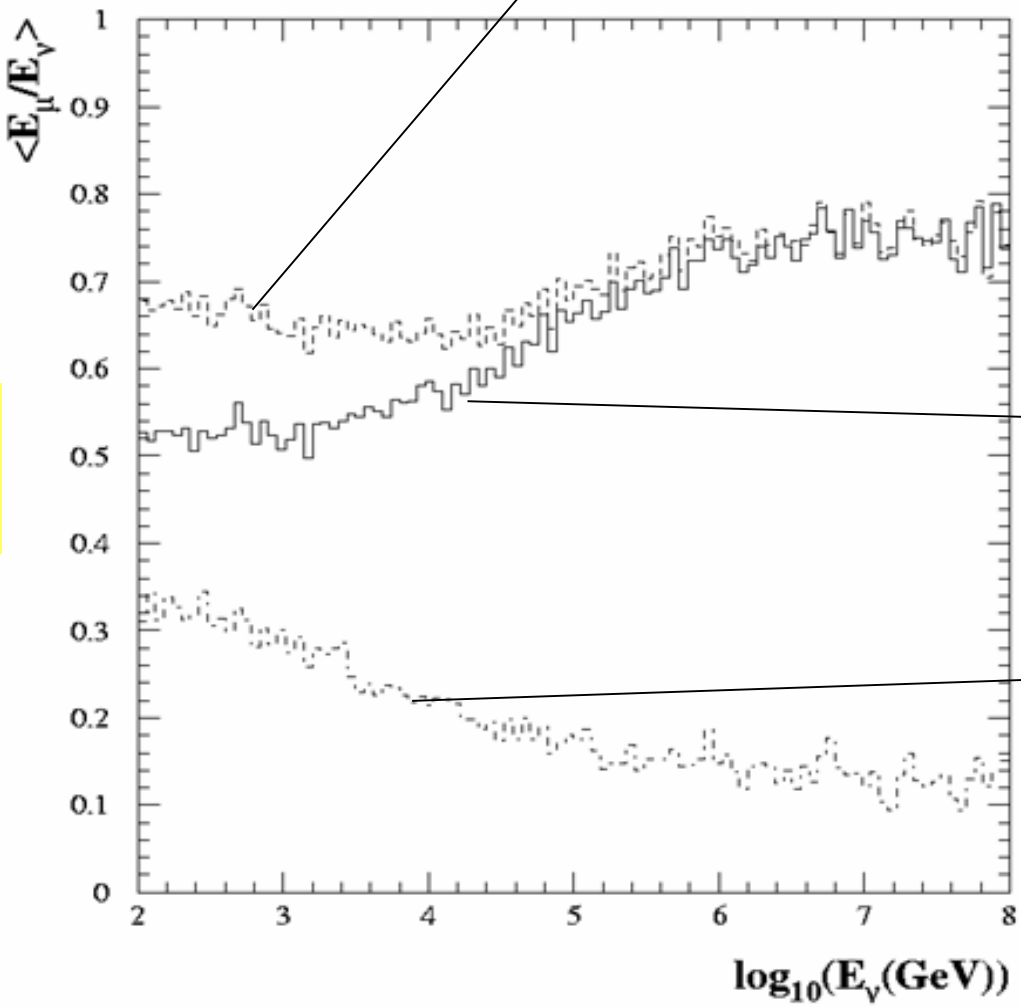

Energy of all μ's as produced

Energy of μ's as they reach the detector

Energy measurement

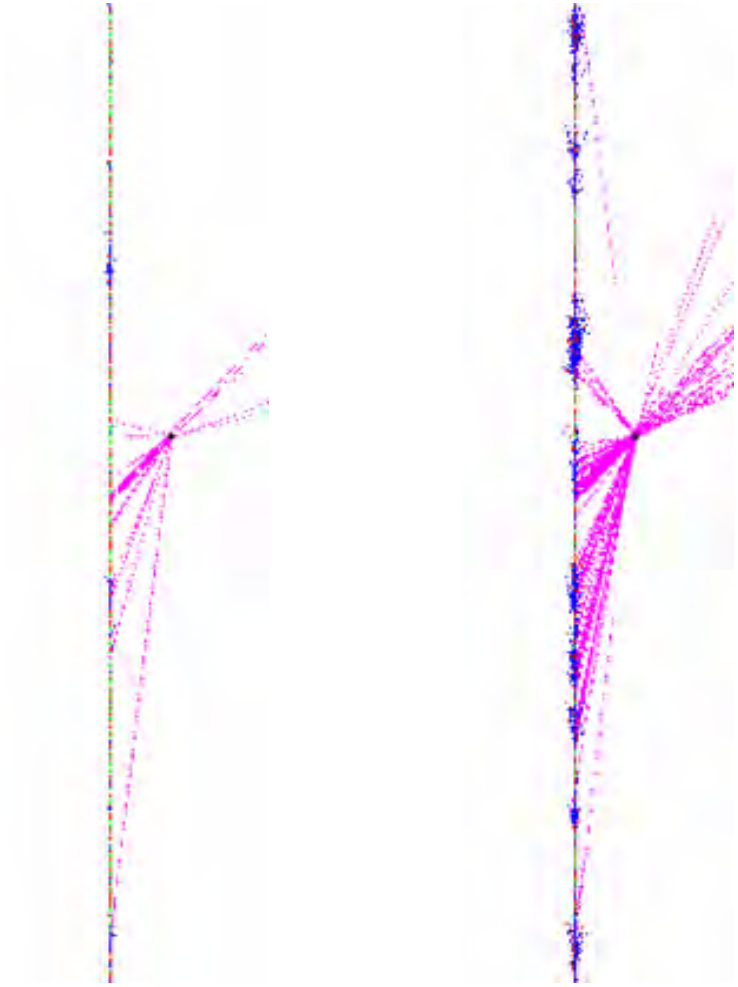

100 GeV μ 10 TeV μ

(Seuls les photons atteignant un PM sont dessinés)

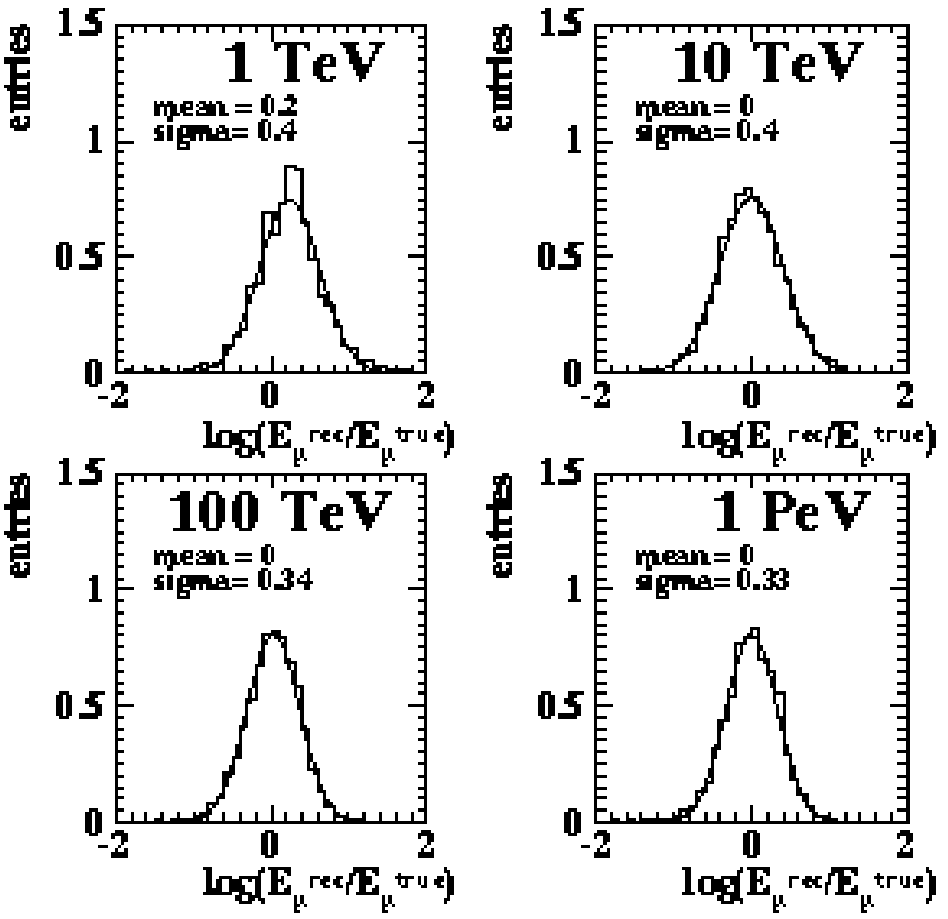

$\Delta E/E = 3$ (< 10TeV)

$= 2$ (> 10TeV)

No real neutrino energy measurement, instead possibility to cut on the muon deposited energy hence on the muon energy (for ex: 1 PeV) and hence to reject muon neutrinos with lower energy.

ν_μ	ν_e	ν_τ
6×10^{15} eV (6 PeV) ~1000 DOMs hit ~ 20 km	E = 375 TeV "spherical" shell	E = 10 PeV 2 bangs separated by ~ $50*(E_\tau/\text{PeV})$
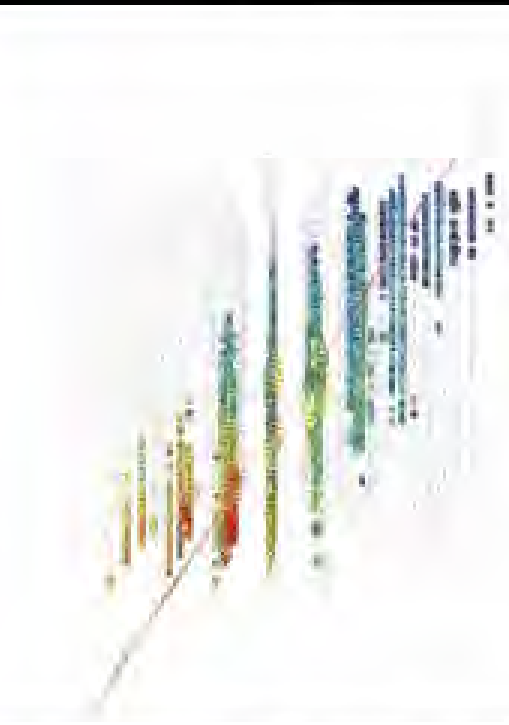		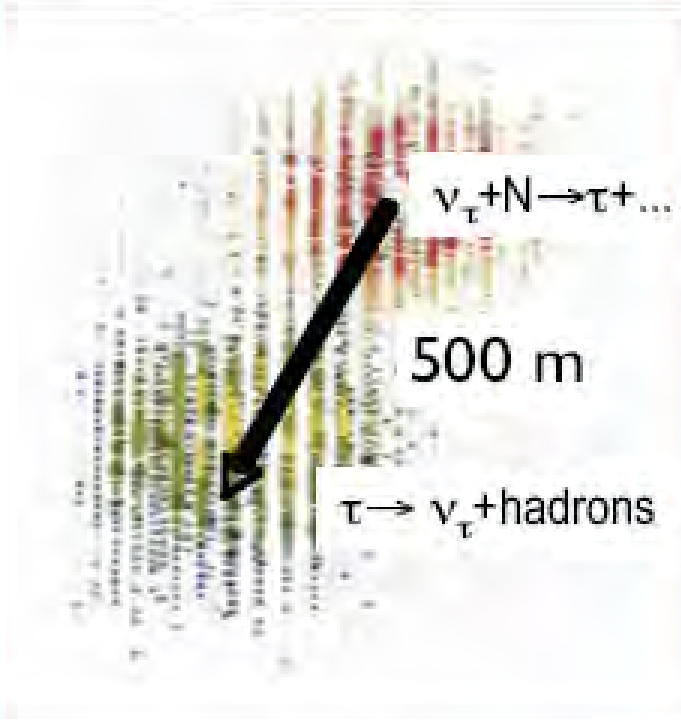
E~dE/dx , e> 1TeV E res. : Δlog(E)~0.3 ang res : 0.8-2 deg	poor angular resolution E res : Δlog(E)~0.1-0.2	very low background pointing capability good E measurement

ICECUBE atmospheric flux

Atmospheric neutrino flux and diffuse limit

- high-energy atmospheric ν_μ/ν_e-spectrum as seen by **IC-40** & **IC-79/DC**
  [IceCube'11,'12]
- diffuse ν_μ limit from **IC-59** (90% C.L.) (**preliminary**)
- predicted prompt atmospheric ν-fluxes (charmed meson decay)
  [Enberg *et al.*'08]
- **theoretical limit** on diffuse astrophysical ν_μ's
  [Waxman&Bahcall '98]

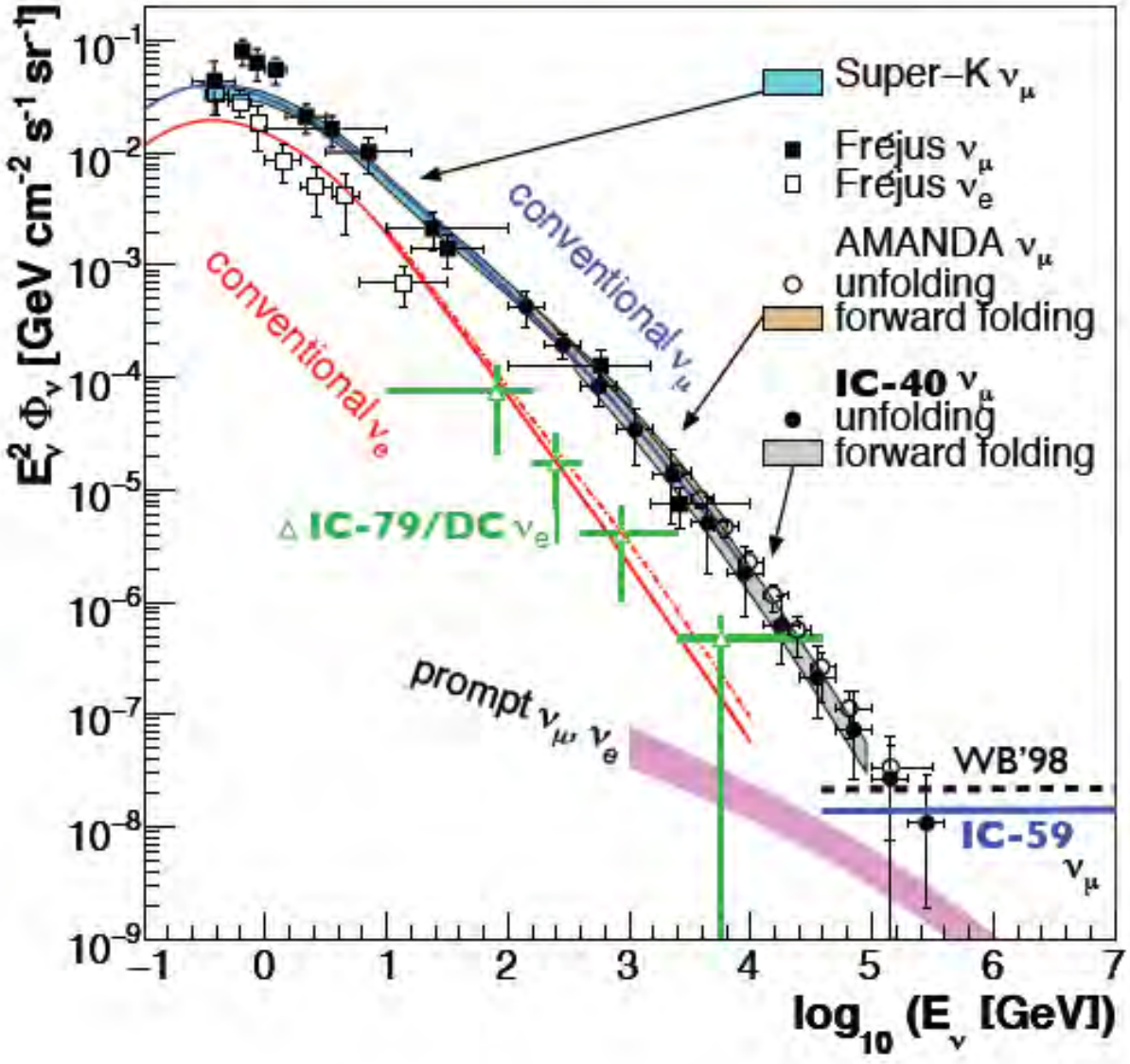

ICECUBE atmospheric flux

Steady point-source search

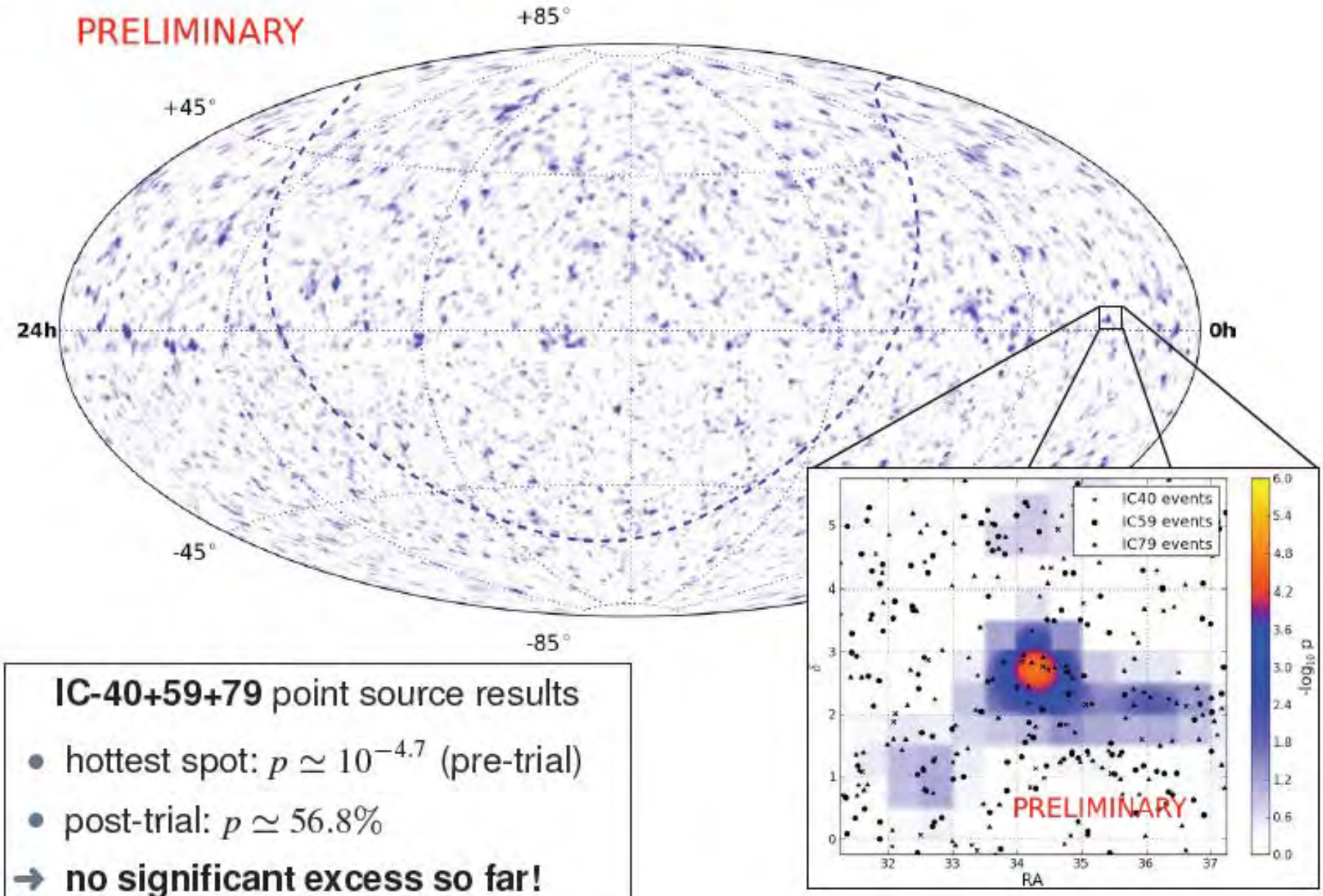

IC-40+59+79 point source results

- hottest spot: $p \simeq 10^{-4.7}$ (pre-trial)
- post-trial: $p \simeq 56.8\%$

➜ **no significant excess so far!**

ICECUBE atmospheric flux

Extremely-high energy analysis

Follow-up studies of background events:
energy, **orientation**,...
➜ Are there more contained events?

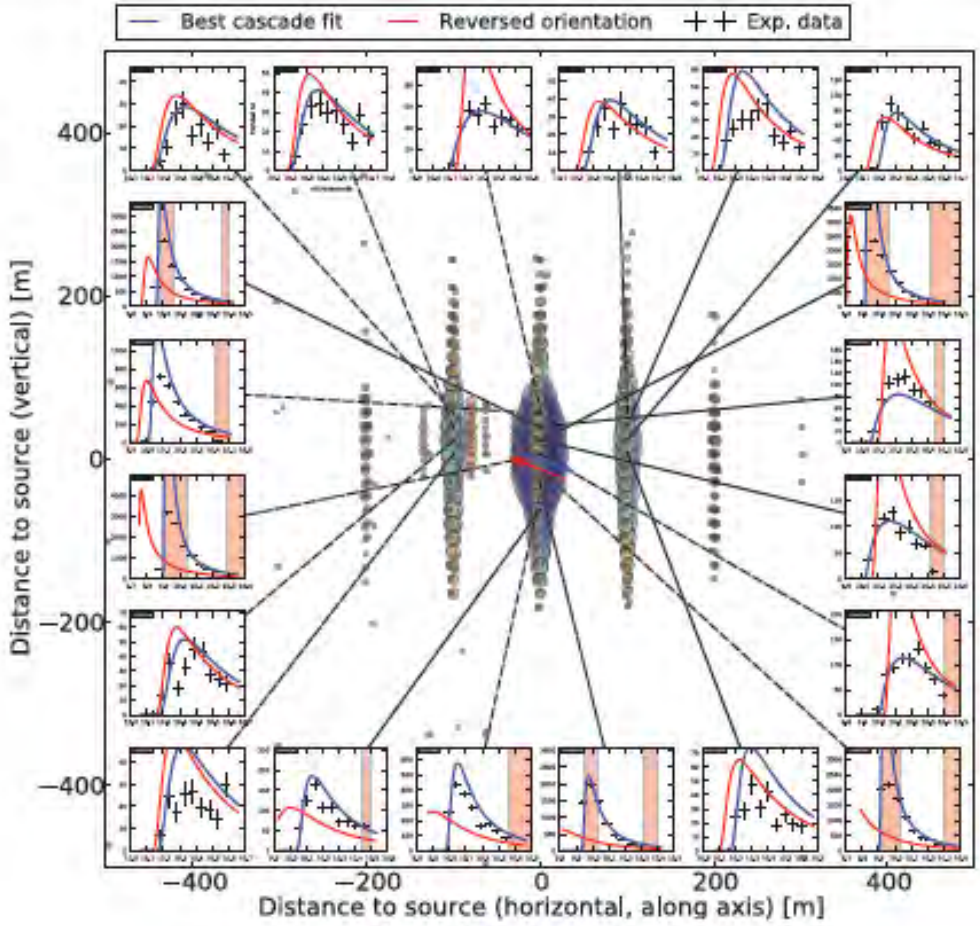

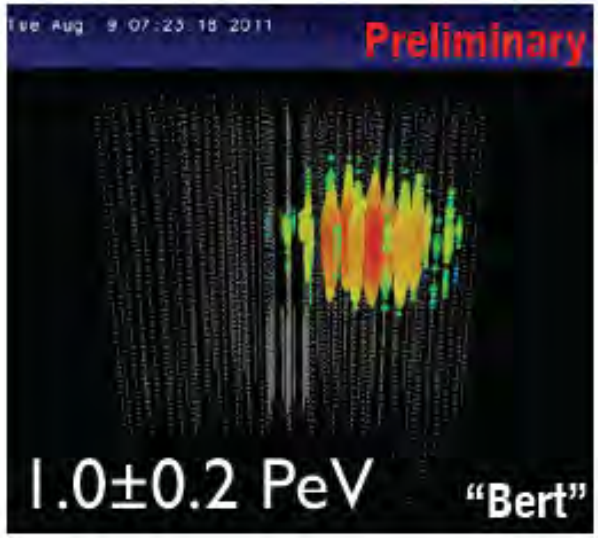

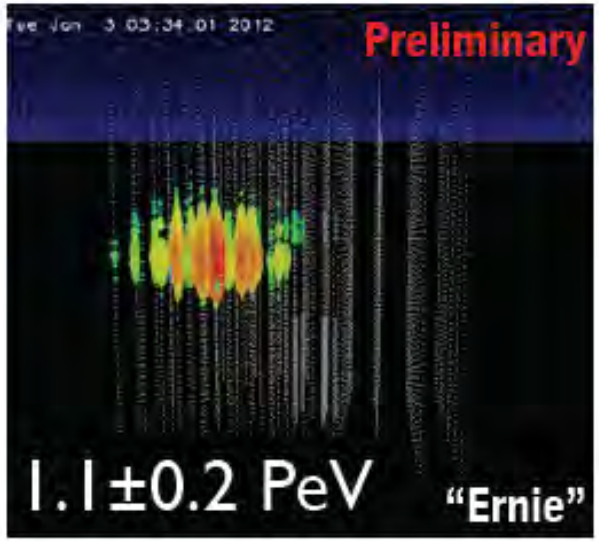

ICECUBE atmospheric flux

Extremely-high energy analysis

- Study for cosmogenic neutrino fluxes in **IC-79+86**
- optimized cuts on zenith angle and "brightness" (NPE: number of photo-electons)

➜ two "background" events above NPE threshold

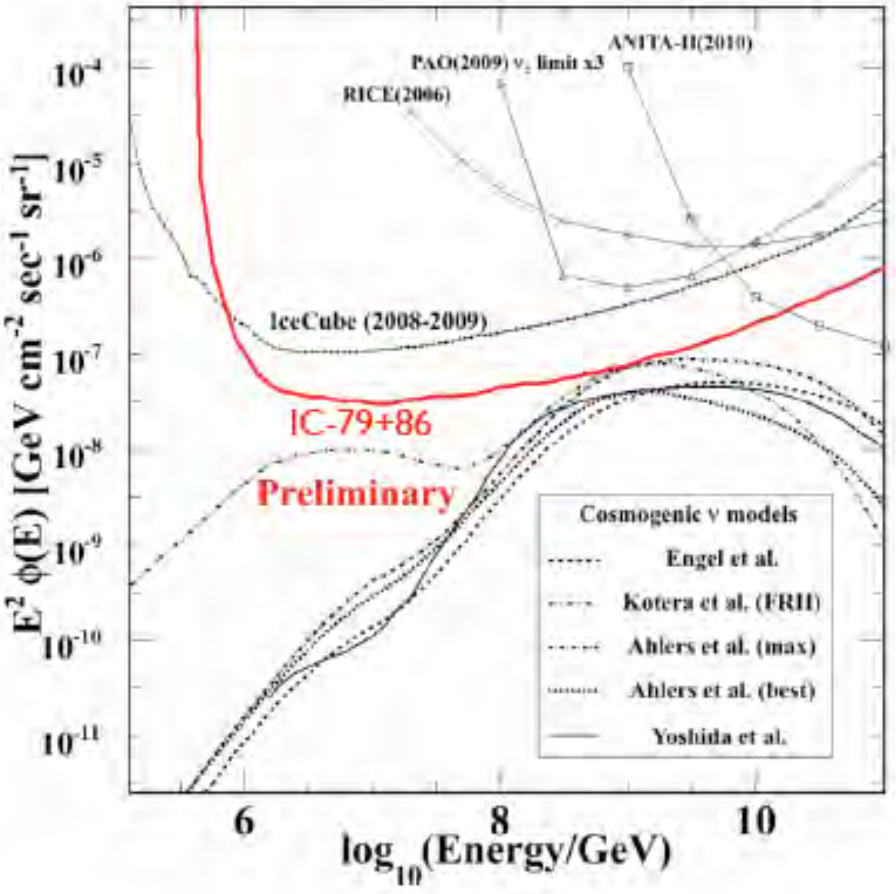

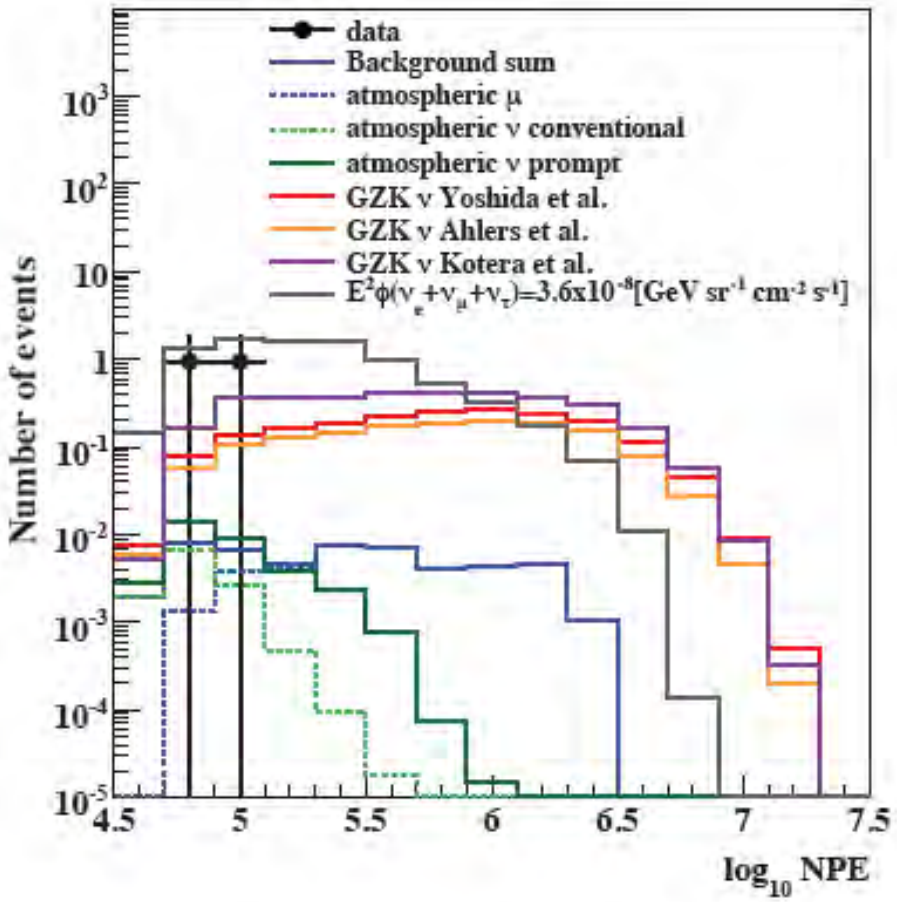

KM3NET (ORCA & ASCA)

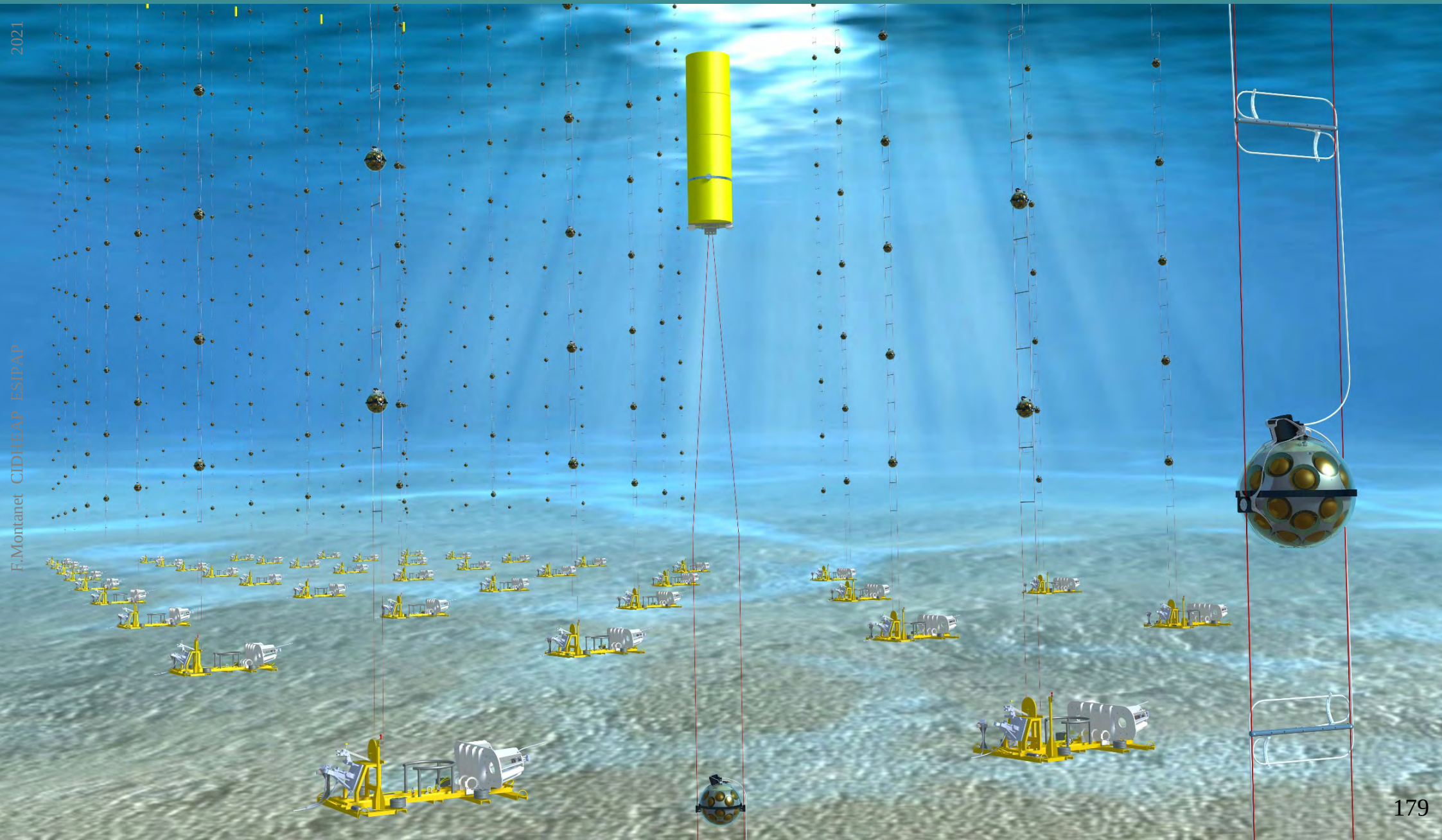

KM3NeT ARCA & ORCA

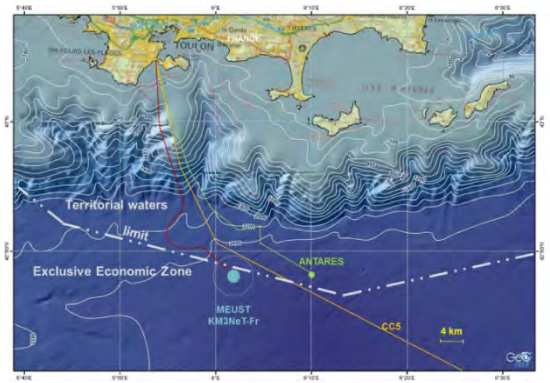

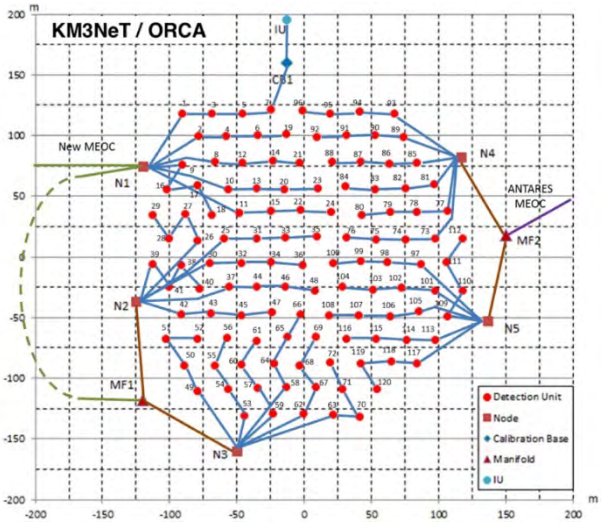

F.Montanet CIDHEAP ESIPAP

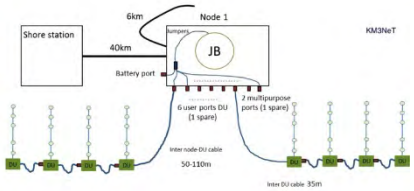

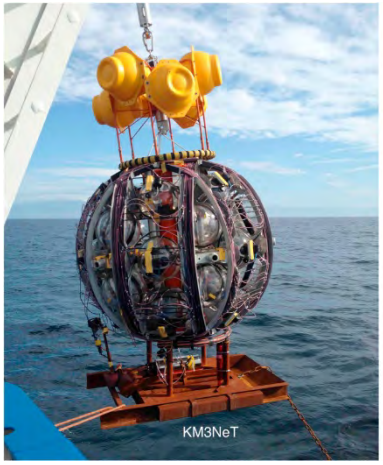

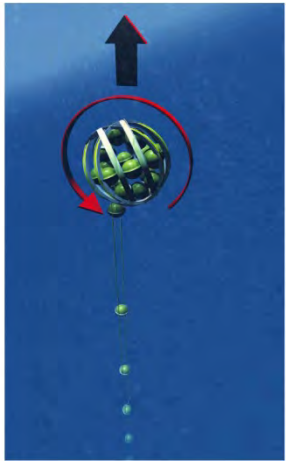

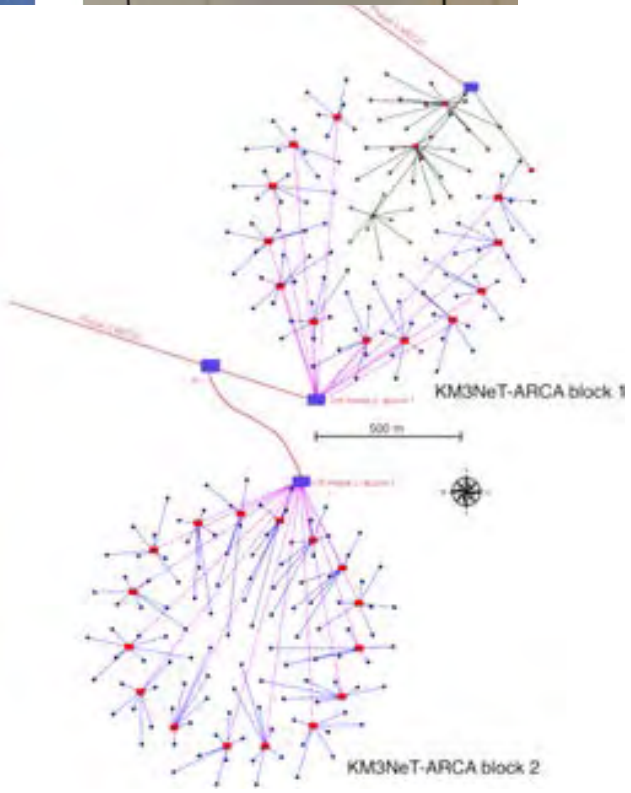

KM3NET deployment

Km3NET ORCA line deployment

Km3NET ORCA line unfurling

Neutrinos in Auger

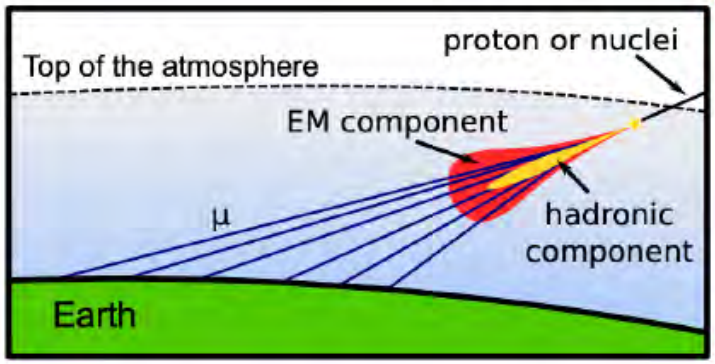

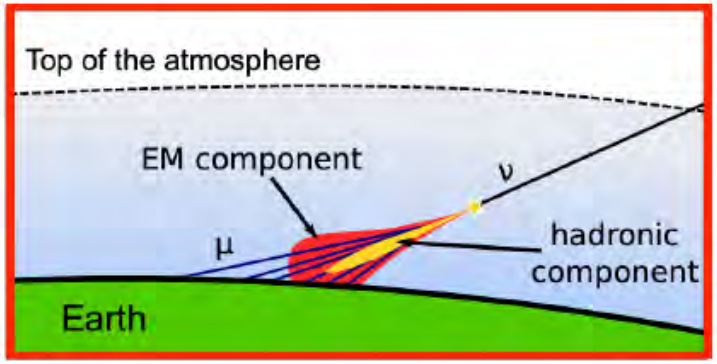

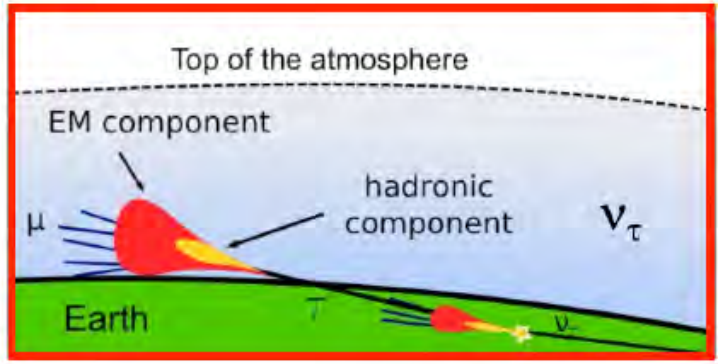

Searching for neutrinos = look for inclined showers with em component

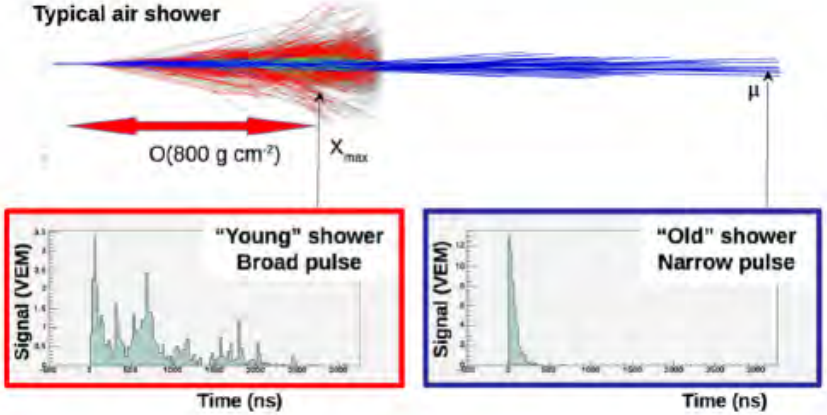

extended in time

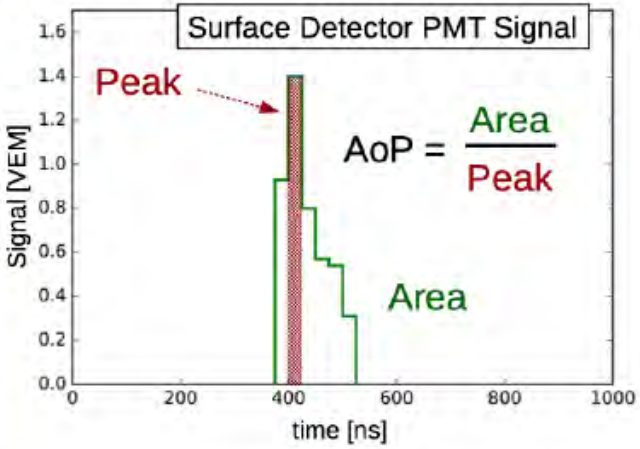

with large area/peak
(A/P~1 for muons)

Complementary properties to other neutrino telescopes

- largest exposure at EeV energies
- different flavour response wrt under-water or under-ice telescopes: higher sensitivity to ν_τ , lowest to ν_μ

Neutrino diffuse flux

$$p + \gamma \rightarrow n + \pi^+$$
$$\rightarrow \mu^+ + \nu_\mu$$
$$\rightarrow e^+ + \overline{\nu}_\mu + \nu_e$$

$$k = \frac{N_{up}}{\int_{E_\nu} E_\nu^{-2} \epsilon_{tot}(E_\nu) dE_\nu}$$

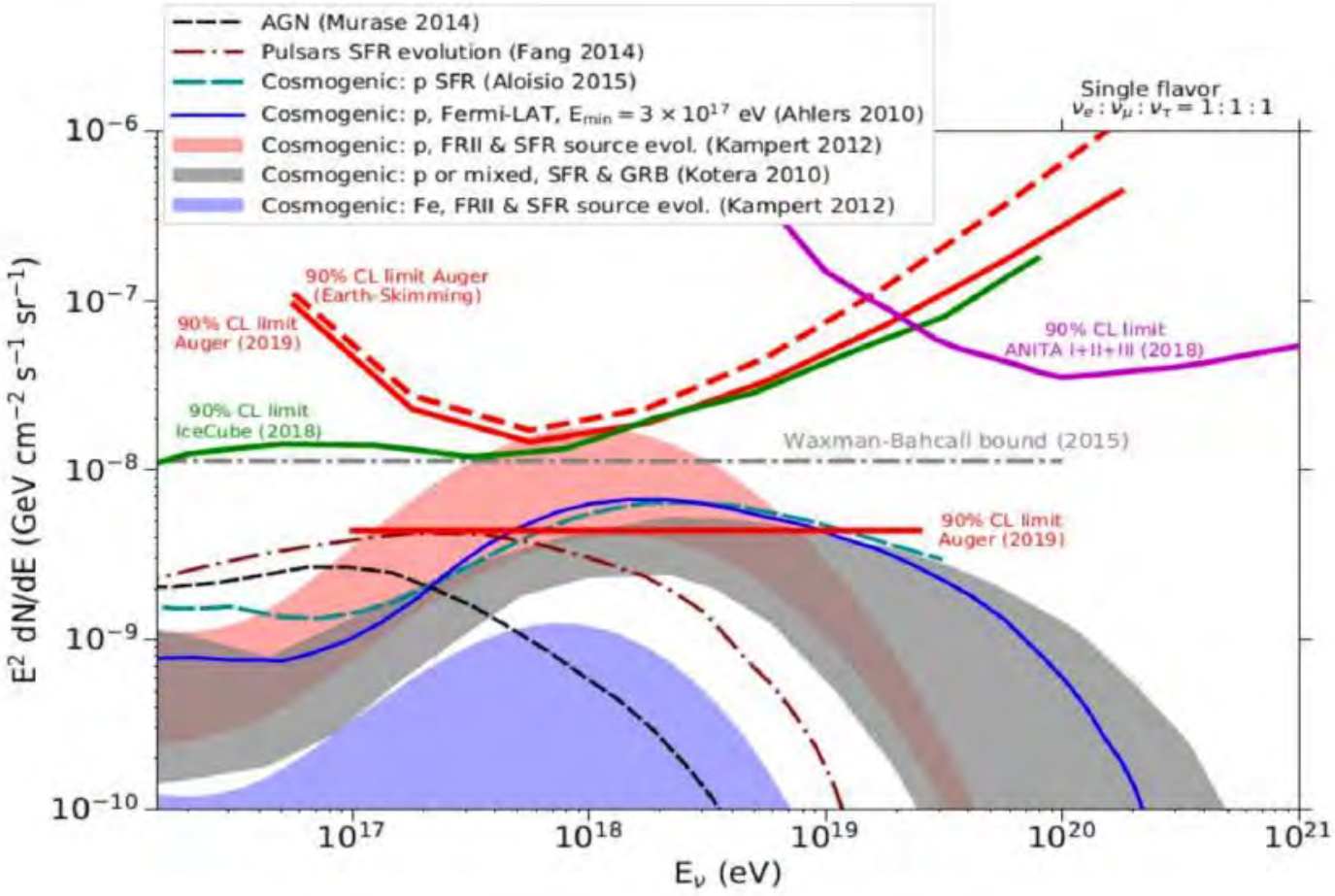

Maximum sensitivity around EeV

k (90% CL) < 4.4. 10^{-9} GeV cm^{-2} s^{-1} sr^{-1}

Constraints on sources

From the expected event rates in Auger, different models of cosmogenic and astrophysical neutrino production are

- excluded (red)
- disfavoured (orange)

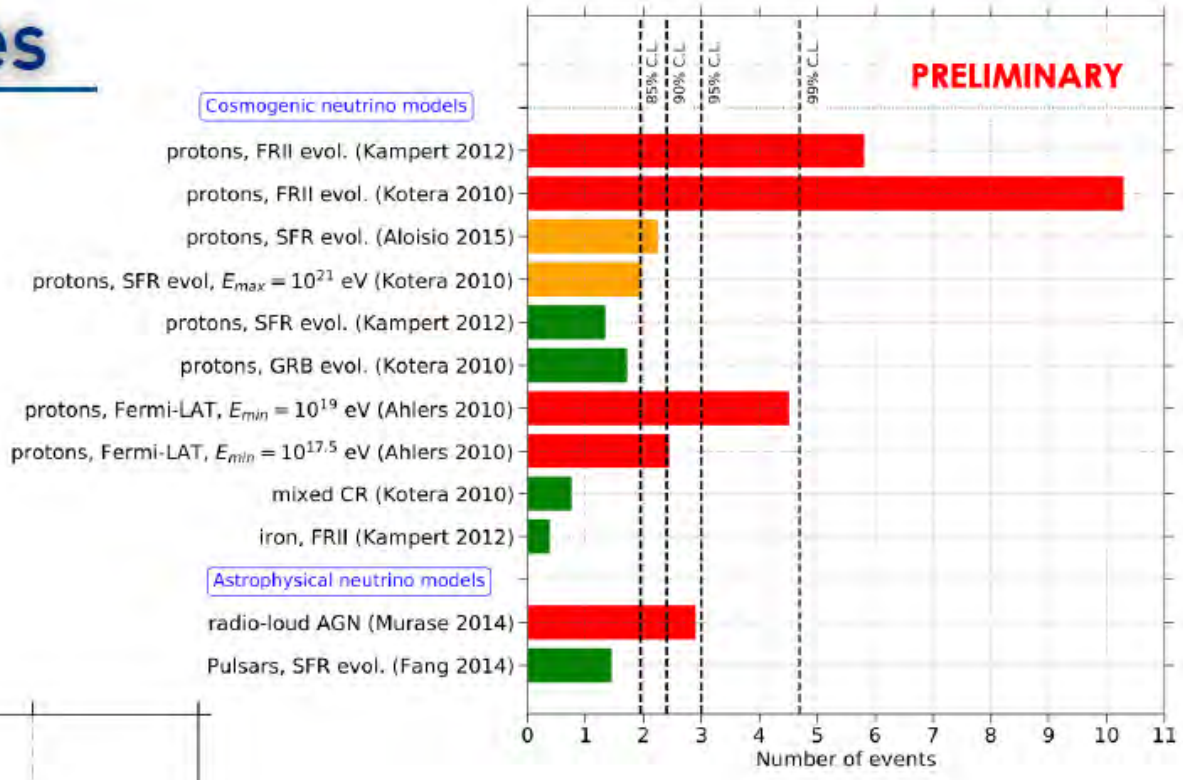

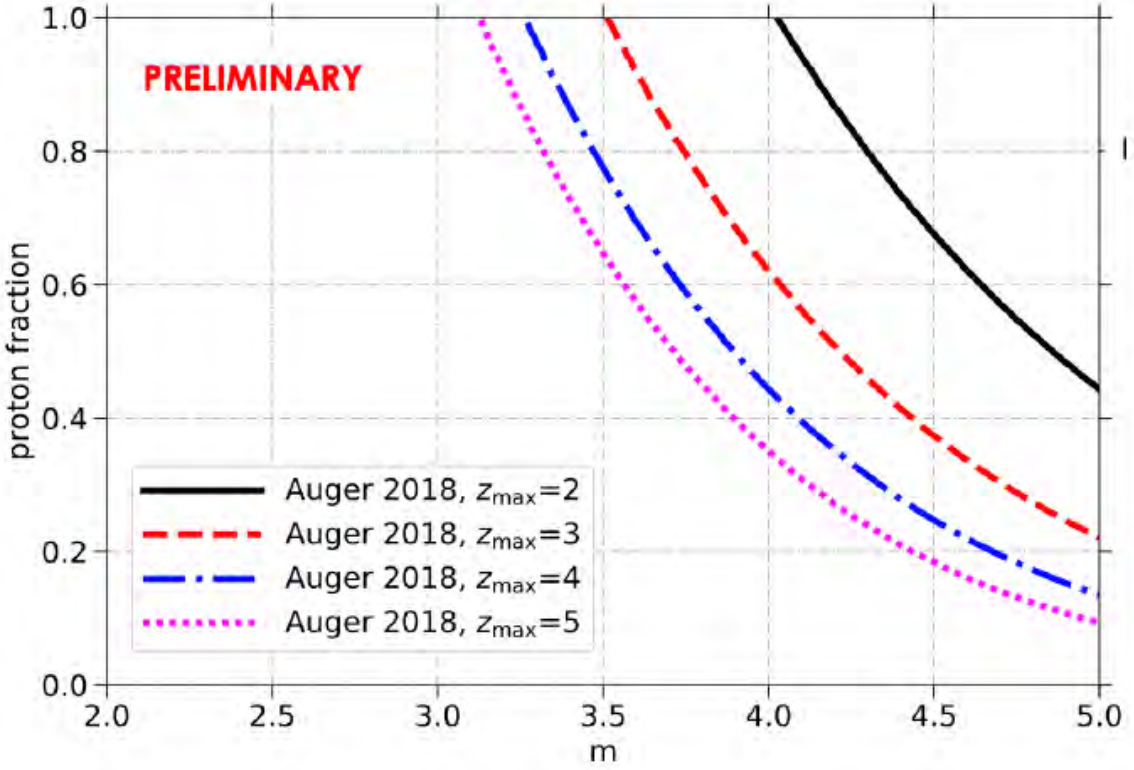

Large proton fractions and strong evolution of sources are disfavoured at 90% C.L.
[assuming sources evolving as $(1+z)^m$]

Follow up of the GW170817 event

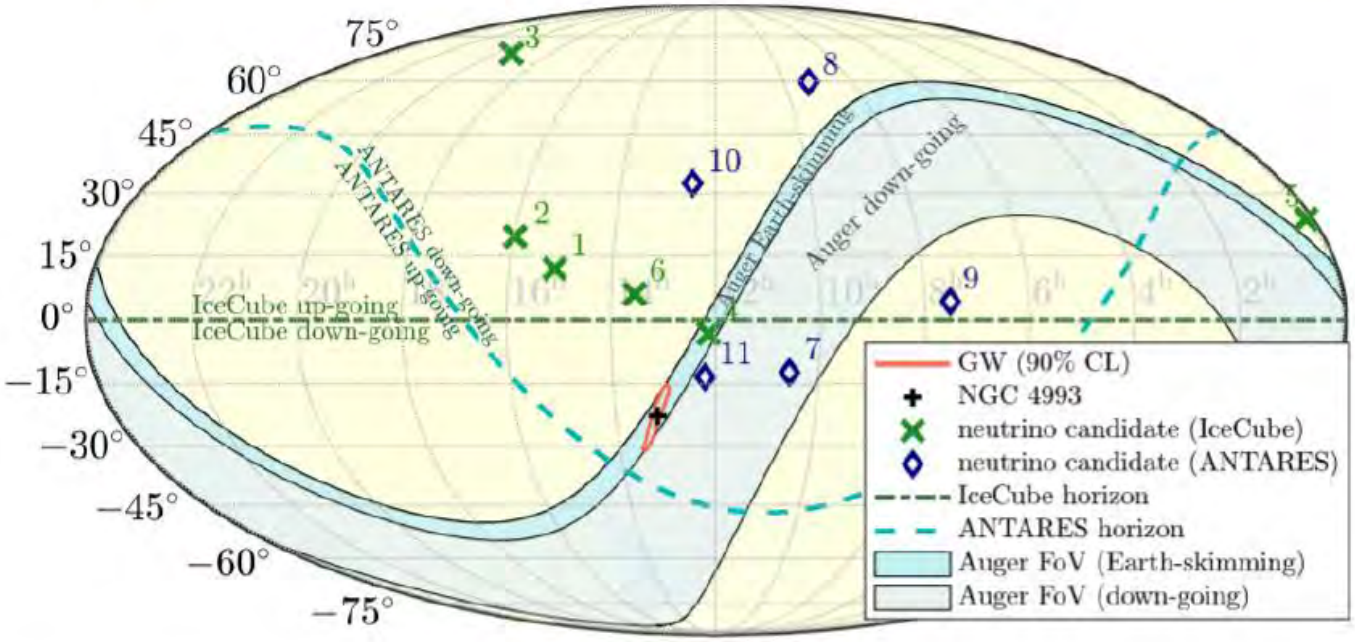

No UHE neutrino candidate found
either in the coincidence window ±500 s around the GW events
or in the 14-days search period after it

In the energy range 10^{17} - 2.5 10^{19} eV, the total energy emitted in $\nu\tau$ is

±500 s : $< 6.9\ 10^{-4}\ M_\odot$
+14 days : $< 2.3\ 10^{-2}\ M_\odot$

LIGO,Virgo,Auger,IceCube, Antares Coll., ApJ 848 (2017)

Constraints to models

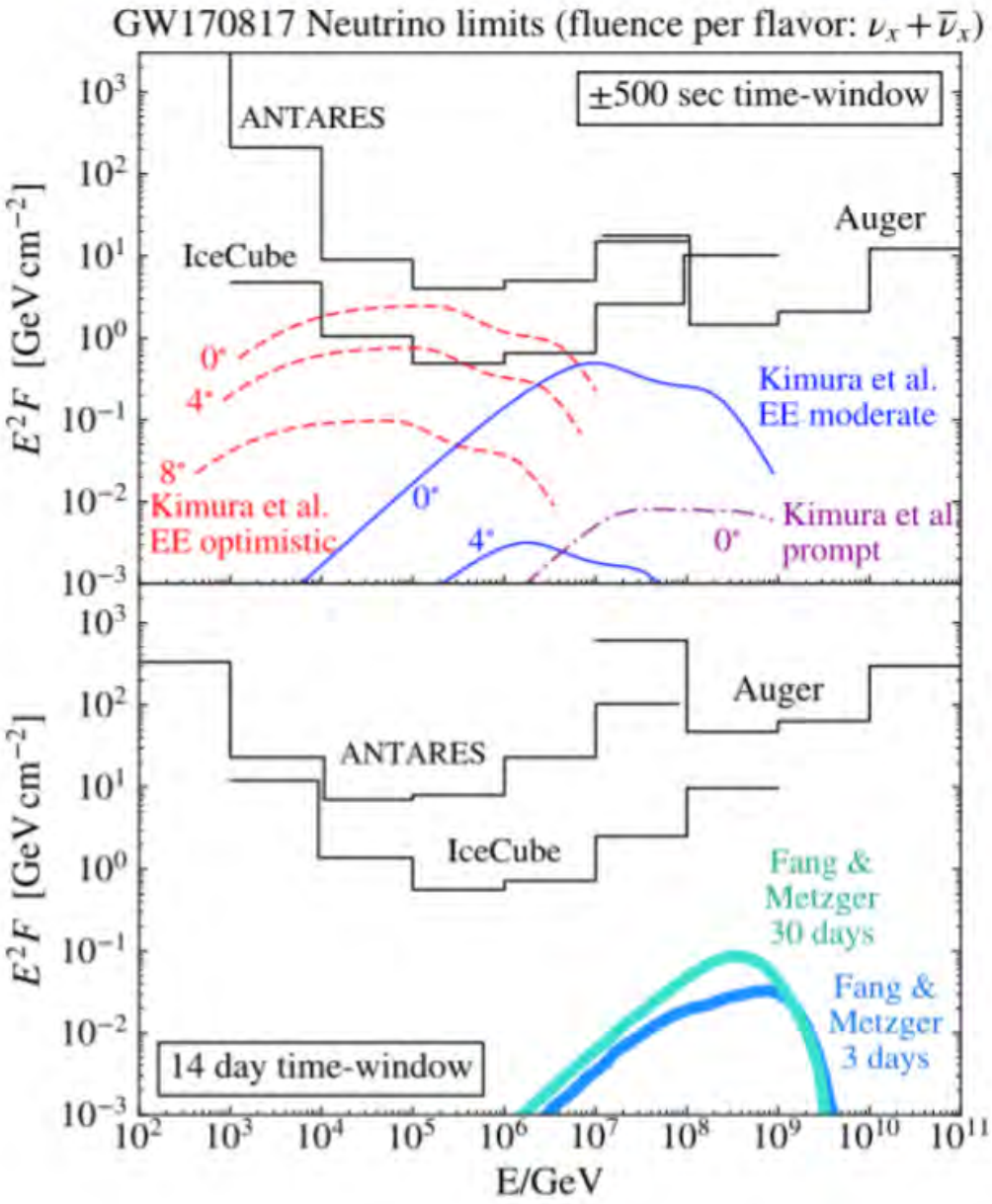

sGRBs

- prompt emission (due to internal energy dissipation in the jet), extended emission (afterglow due to forward shocks around the burst)
- viewed on-axis or off-axis
- neutrinos can arise from closely GRBs or EE

S.Kimura et al., ApJ Lett.848: L4 (2017)

msec Magnetar remnants

- promising site for accelerating particles to UHE
- neutrino late production from UHECRs interactions with ambient photons and baryons
- strong neutrino signal at 10^{18} eV if large contribution of magnetars to the bulk of UHECRs (light nuclei at $10^{17.5}$-10^{18} eV)

K.Fang, B.Metzger, ApJ 849 (2017) 153